On the Reactivity of Pnictinidene-Bridged Complexes

Dissertation

zur Erlangung des

DOKTORGRADES DER NATURWISSENSCHAFTEN

(Dr. rer. nat.)

der Naturwissenschaftlichen Fakultät Chemie und Pharmazie

der Universität Regensburg

vorgelegt von

Lena Rummel

aus Großberg

Regensburg 2021

Die vorliegende Arbeit wurde in der Zeit vom Dezember 2017 bis September 2021 am Institut für Anorganische Chemie der Universität Regensburg unter Anleitung von Herrn Prof. Dr. Manfred Scheer angefertigt.

Promotionsgesuch eingereicht am:	06.09.2021
Tag der mündlichen Prüfung:	08.10.2021

Prüfungskommission:

Vorsitzender:	Prof. Dr. Alkwin Slenczka
1. Gutachter:	Prof. Dr. Manfred Scheer
2. Gutachter:	Prof. Dr. Henri Brunner
3. Gutachter:	Prof. Dr. Frank-Michael Matysik

Universität Regensburg

Affidavit

I hereby declare that I have completed the dissertation presented without the impermissible help of third parties, without the use of resources other than those indicated, and that any data and concepts stemming directly or indirectly from other sources are indicated with citations to the literature.

No further persons were involved with the creation of the contents of the dissertation presented. In particular, I have not made use of the assistance of a doctoral consultant or other person in return for payment. No-one has received payment in kind either directly or indirectly for work which is associated with the content of the dissertation submitted.

The dissertation has not been submitted in the same or similar form to another examining authority, neither in Germany nor abroad.

Eidesstattliche Erklärung

Ich erkläre hiermit an Eides statt, dass ich die vorliegende Arbeit ohne unzulässige Hilfe Dritter und ohne Benutzung anderer als der angegebenen Hilfsmittel angefertigt habe. Die aus anderen Quellen direkt oder indirekt übernommenen Daten und Konzepte sind unter Angabe des Literaturzitats gekennzeichnet.

Weitere Personen waren an der inhaltlich-materiellen Herstellung der vorliegenden Arbeit nicht beteiligt. Insbesondere habe ich hierfür nicht die entgeltliche Hilfe eines Promotionsberaters oder anderer Personen in Anspruch genommen. Niemand hat von mir weder unmittelbar noch mittelbar geldwerte Leistungen für Arbeiten erhalten, die im Zusammenhang mit dem Inhalt der vorgelegten Dissertation stehen.

Die Arbeit wurde bisher weder im In- noch im Ausland in gleicher oder ähnlicher Form einer anderen Prüfungsbehörde vorgelegt.

_____

Lena Rummel

To Ludwig

Preface

In the beginning of this thesis, a general introduction discussing the state of research concerning pnictinidene complexes is given. Subsequently, the research objectives outlined in this work are presented.

The chapters in this thesis are suitable for publication either in the future or are already being published. Therefore, each chapter starts with a short introduction to the specific topic discussed highlighting the current state of research. A short list of contributions is given at the beginning of each chapter to avoid accusations of plagiarism, although a strict separation is not always possible. Additionally, a graphical abstract has been created for each chapter.

The layout of all chapters has been matched so that a uniform design of this work is accomplished. Nonetheless, the numbering of compounds, figures, tables and sources starts anew each time for reasons of future publishing.

Lastly, a summary containing all results from the chapters discussed is given at the end of this work.

One chapter of this thesis is already published:

L. Rummel, G. Lassandro, M. Seidl, A. Y. Timoshkin, M. Scheer. Reactivity of the pentelidene complexes [Cp*E{W(CO)$_5$}$_2$] (E = P, As) towards dichalcogenides and chalcogenols – synthesis of novel chalcogenopentelidene complexes. *Dalton Trans.* **2021**, 50, 12648. **DOI**: 10.1039/D1DT01866C

TABLE OF CONTENTS

1 INTRODUCTION

1.1 Low-valent main group compounds

The research revolving around low-valent main group compounds is one of the fastest growing fields in modern chemistry. Especially since the first stable carbene was synthesized in the group of Bertrand in 1988[1] and the subsequent discovery of N-heterocyclic carbenes (NHCs) in the group of Arduengo a few years later,[2] these compounds have been studied extensively. Lots of different types of stable carbenes have been synthesized over the years,[3] benefitting the field of organocatalysis, which is one of the main applications of carbene compounds.[4] Cyclic Alkyl-Amino-Carbenes (CAACs) have been found to activate small molecules like CO,[5] H_2[6] and NH_3,[6] with the latter being a "difficult task, even for transition-metal centers", according to Bertrand et al.[7] However, there are a few other main-group compounds, for example silylenes, that are able to activate small molecules too, including CO,[8] NH_3,[9] P_4[10] and H_2.[11] Another versatile class of low-valent main group compounds are pnictinidene (or pentelidene) compounds with the general formula R-E (E = pnictogen atom), where E possesses six valence electrons and are isolobal to carbenes. In this group, the first carbene-analogous compounds are nitrenes (R-N), which have been spectroscopically characterized at low temperatures[12] or isolated as metallonitrenes,[13] before the first 'free' nitrene stable at room temperature was finally synthesized in 2012.[14] Their heavier homologs, phosphinidenes (R-P), arsinidenes (R-As) and stibinidenes (R-Sb) have been of similar interest to the scientific community. An in-depth explanation of their properties is given in the following chapters.

Phosphinidenes

As briefly mentioned above, in contrast to carbenes, phosphinidenes (IUPAC: *phosphanylidenes*) contain only one substituent at the phosphorus atom. Similarly to carbenes, phosphinidenes can also exist in a singlet or triplet spin state (cf. Figure 1.1) with the triplet state being the usual ground state. Theoretical calculations, however, have shown an energy difference of only 28 kcal·mol^{-1} between the two for the parent phosphinidene H-P,[15] but attempts to isolate a stable singlet phosphinidene have long been unsuccessful.

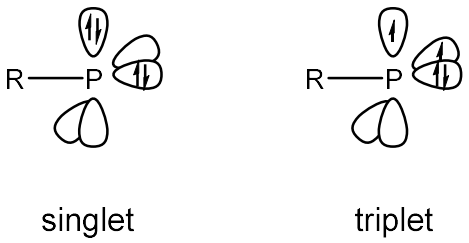

***Figure 1.1**: Possible spin states of phosphinidenes.*

‘Free’ phosphinidenes

The reason why singlet phosphinidenes are of interest is that they are predicted to be less reactive than their triplet counterparts and therefore should be “bottle-able”. The first efforts in characterizing these ‘free’ phosphinidenes have been made as early as the 1960s, when they were mentioned as intermediates in the reactions of organochlorophosphines with Mg or Li,[16] the thermolytic decomposition of cyclopolyphosphanes $(R\text{-}P)_n$[17] or the formation of cyclophosphanes from P_1 compounds, although there was no definite proof at that time.[18] Over the years, numerous attempts in synthesizing ‘free’ phosphinidenes have been made, such as by irradiation of suitable starting materials like diphosphenes,[19] phosphiranes,[20] phosphordiazides[21] and phosphanylidenephosphoranes.[22] The unstable Mes*-P (Mes* = 2,4,6-tri-*tert*-butylphenyl) is obtained in all these reactions, which then forms a phosphaindane via intramolecular CH activation. The first spectroscopic evidence of a ‘free’ phosphinidene was given in 1994 by Gaspar and co-workers, who irradiated a mesitylphosphirane at 77 K in a solvent matrix. The resulting mesitylphosphinidene was then characterized via EPR spectroscopy, which confirmed it to be in a triplet state.[23] Other groups succeeded in characterizing triplet phosphinidenes by electron paramagnetic resonance, infrared and UV-spectroscopy.[24] At last, in 2016, Bertrand and co-workers managed to synthesize a singlet phosphinidene stable at room temperature by the UV induced elimination of carbon monoxide from a (phosphino)phosphaketene. Nonetheless, in order to prevent the singlet phosphinidene from dimerizing, it has to be substituted with extremely bulky ligands (cf. Figure 1.2).[25]

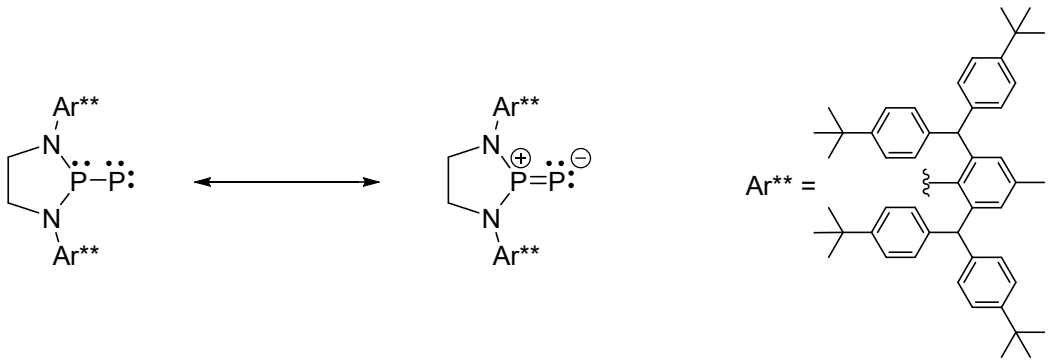

***Figure 1.2**: Singlet phosphinidene by Bertrand and co-workers.*

As mentioned above, triplet phosphinidenes are highly reactive species and therefore have to be stabilized to use them for synthetic purposes. This can be achieved by coordination of the phosphorus atom to transition metal fragments, which favors the singlet spin state and makes the phosphinidene more stable. The coordination modes can be differentiated into terminal phosphinidenes and bridging phosphinidenes with up to four transition metal fragments being coordinated by the phosphinidene moiety (cf. Figure 1.3).[26]

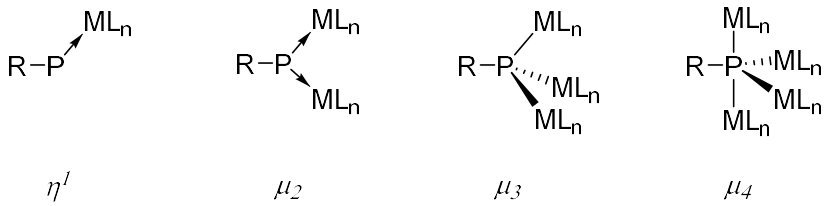

***Figure 1.3**: Selected coordination modes of phosphinidenes towards transition metal fragments.*

Terminal phosphinidenes

There are numerous review articles about terminal phosphinidenes, which proves them to be an extensively investigated class of compounds.[26,27,28] The first terminal phosphinidene complex has been synthesized in 1984 by *Mathey et al*. via thermolysis of $M(CO)_5$-substituted 7-phosphanorbornadiene complexes (M = Cr, Mo, W). Because of their instability, the group had to trap the terminal phosphinidenes R-P-$M(CO)_5$ as phosphiranes or phosphirenes in the presence of alkenes and alkynes, respectively.[29] Their similarity to carbenes is once again expressed for terminal phosphinidenes in their divisibility into nucleophilic ('Schrock-type') and electrophilic ('Fischer-type') terminal phosphinidenes based on the reactivity that has been observed for them. A theoretical study[30] confirms this classification and therefore, electrophilic terminal phosphinidenes can be described as singlet phosphinidenes forming dative bonds with singlet transition metal fragments while also receiving π-backbonding from an occupied d-orbital of the metal atom into the empty phosphorus p orbital. The abovementioned reaction by Mathey and co-workers is a characteristic example for the reaction behavior of electrophilic phosphinidenes. Nucleophilic terminal phosphinidene complexes, on the other hand, can be described as a triplet phosphinidene and a triplet transition metal fragment connected through a P=M double bond.[28] Lappert and co-workers synthesized the first nucleophilic terminal phosphinidene complex [Cp_2M=P-Mes*] (M = Mo, W) in 1987 via salt elimination from [{Cp_2MHLi}$_4$] with Mes*PCl_2.[31] A typical reaction of a nucleophilic terminal phosphinidene is the formation of a phosphaalkene through the reaction with an aldehyde or ketone. Conveniently, the reaction behavior of terminal phosphinidene complexes can be tuned via the ligands at the transition metal. By using π-acceptor ligands, the phosphorus atom gets more electron deficient and thus the electrophilic character increases. On the contrary, σ-donor ligands at the transition metal increase the electron density at the phosphorus atom and therefore the nucleophilicity also increases.[32]

Bridging phosphinidenes

Comparing μ-phosphinidene complexes to their terminal analogs, the former turn out to be more stable. Thus, the first bridging phosphinidene complex, $[(C_6H_5)P\{(CO)_2MnCp\}_2]$, has already been synthesized in 1975 by Huttner.[33] Additionally, in the case of bridging phosphinidene complexes, complexes of their higher homologs, namely arsinidenes (As), stibinidenes (Sb) and bismuthinidenes (Bi), are known.[34] In general, there are three types of bridging phosphinidene complexes (cf. Figure 1.4): symmetric (**A**), asymmetric (**B**) and pyramidal (**C**) complexes. They all show high reactivity due to either a chemically active lone pair at the phosphorus (**C**-type) or multiple P-M bonds (**A**- and **B**-type).

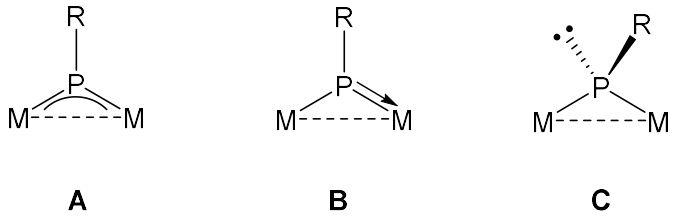

Figure 1.4*: Types of bridging phosphinidene complexes.*

Generally speaking, pyramidal phosphinidene complexes **C** consist of a formally double metallated phosphine, which results in a pseudo-pyramidal geometry of the sp^3 hybridized P atom. Due to the lone pair located at the P atom, type **C** phosphinidene complexes typically exhibit a nucleophilic reactivity. These types of complexes, however, are very rare. Another bonding possibility for phosphinidene complexes arises when the phosphorus lone pair takes part in P-M π-bonding, resulting in a trigonal planar environment at the P atom. Type **A** and type **B** complexes are in this case differentiated based on the electron count of the metal fragments. Type **A** phosphinidene complexes use metal fragments with the same electron count while phosphinidenes of the type **B** are substituted with metal fragments using different electron counts, mostly 15 and 17 valence electron metal fragments. It should be noted that while the formal P-M bond order is increased to 1.5 (**A**) and up to 2 (**B**) due to the π-bonding interaction of the empty p orbital of P with filled d orbitals of M, the corresponding P-M bond lengths are usually shortened in the respective complexes.[35] In contrast to pyramidal and asymmetric phosphinidene complexes, symmetric phosphinidene complexes react as electrophiles.[36] The bonding properties of type **A** phosphinidene complexes are described further on the basis of $[Cp^*P\{W(CO)_5\}_2]$ (**1a**; Cp* = $C_5(CH_3)_5$) in chapter 1.2.

Arsinidenes

The chemistry of arsinidene complexes, much like the chemistry of stibinidene and bismuthinidene complexes, is significantly less developed than phosphinidene chemistry. Even more reactive than their lighter homologs, 'free' arsinidenes tend to dimerize, resulting in the corresponding diarsenes,[37,38] or – depending on the sterical demand of their substituents – oligomerize, giving cycloarsines.[39] Nevertheless, arsinidenes can be stabilized analogously to phosphinidenes by coordination to transition metal fragments or Lewis acids. Another similarity to phosphinidene complexes is the stability of bridging arsinidene complexes as compared to their terminal analoga. The synthesis of the first trigonal planar arsinidene complex $[(C_6H_5)As\{Cr(CO)_5\}_2]$ happened in the group of Huttner as early as 1975,[40] while the first stable terminal arsinidene complex has only been described in 2019 by Ghadwal et al.[41] The bonding situation of bridging arsinidene complexes is similar to that of type **A** phosphinidene complexes, which are described in chapter 1.2. Type **B** and **C** arsinidene complexes are also known, in addition to $L_nM(R)As{=}As(R)ML_n$-type complexes, which can be generated from type **A** and **C** arsinidenes and vice versa. It is worth noting that in the reaction of $RAsCl_2$ with $Na_2[M_2(CO)_{10}]$ (M = Cr, Mo, W), which is often used to synthesize arsinidene complexes, type **A**, **C** and $L_nM(R)As{=}As(R)ML_n$-type complexes are generated alongside each other. By tuning the reaction conditions, however, the arsinidene complexes can be synthesized more selectively.[38] Other than transition metal-coordinated arsinidenes, the NHC-stabilized parent arsinidenes (^{R}NHC)AsH (R = Dipp, Mes, Ar*; Dipp = 2,6-diisopropylphenyl; Ar* = 2,6-bis-(diphenylmethyl)-4-methylphenyl) have to be mentioned as a remarkable class of pnictinidene compounds. Synthesized via desilylation of trimethylsilyl substituted precursors (^{R}NHC)$AsSiMe_3$ or salt metathesis of $[Na(diox)_x][AsCO]$ with imidazolium salts of the desired NHC, the resulting compounds have been proven to be adducts of the parent arsinidene with NHCs.[42] Just recently, Bertrand and co-workers tried to synthesize a 'free' singlet phosphino-arsinidene analogously to their singlet phosphino-phosphinidene, but due to its high reactivity, the arsinidene could only be trapped with phosphines and had to be complexed subsequently to be characterized.[43]

Stibinidenes and Bismuthinidenes

As expected, Stibinidenes and Bismuthinidenes are rare classes of compounds due to their high reactivity and general instability towards air, moisture and light. Therefore, most resources available in regards to these complexes focus on their preparation and properties rather than their reactivities. While transition metal-coordinated stibinidenes have been known since the late 1970s,[44,45] base-stabilized stibinidenes were only reported quite recently. In 2010, Dostál and co-workers were able to prepare stable monomeric stibinidene and bismuthinidene compounds via salt elimination reactions with *N,C,N* pincer-type ligands,[46] which has been the start of further research activities regarding base-stabilized pnictinidenes.[47] As mentioned above, transition metal-coordinated stibinidene complexes have been a research interest for a long time. In 1978, Huttner et al. synthesized $[PhSb\{Mn(CO)_2Cp\}_2]$ from a diiodostibane and described its trigonal planar geometry with its unusual bond lengths and angles.[44,45] To this date, trigonal planar stibinidene complexes of the type $[XSb(ML_n)_2]$ (X = Cl, Br, R; ML_n = 16 valence electron metal fragments) are the most investigated group of stibinidene complexes. The properties of the stibinidene complex $[ClSb\{Cr(CO)_5\}_2(thf)]$ (**1c**) are discussed in chapter 1.3. In regards to bismuthinidenes, it has recently been shown that *N,C,N*-chelated bismuthinidenes are able to activate N_2O under very mild conditions,[48] which underlines the potential of pictinidenes being used in the catalytic activation of small molecules in the future.

1.2 Properties of [Cp*E{W(CO)$_5$}$_2$] (1a: E = P, 1b: E = As)

The pnictinidene complexes [Cp*E{W(CO)$_5$}$_2$] (**1a**: E = P, **1b**: E = As) have first been synthesized via a salt elimination reaction between $Na_2[W_2(CO)_{10}]$ and Cp^*ECl_2 in the group of Jutzi in 1990.[49] As mentioned before, both compounds are symmetric A-type μ-pnictinidene complexes. According to Huttner,[34] the bonding situation can be described as follows: The pnictinidene moiety (R-E) coordinates to two 16 valence electron transition metal fragments, resulting in a trigonal planar environment at the pnictogen atom. The E lone pairs form σ bonds with both transition metals, which in turn donate electron density from the occupied d orbitals into the empty p orbital of the sp^2 hybridized pnictogen atom (π backdonation). Figure 1.5 shows the resulting 3 center 4 π electron interaction with the help of the MO model.

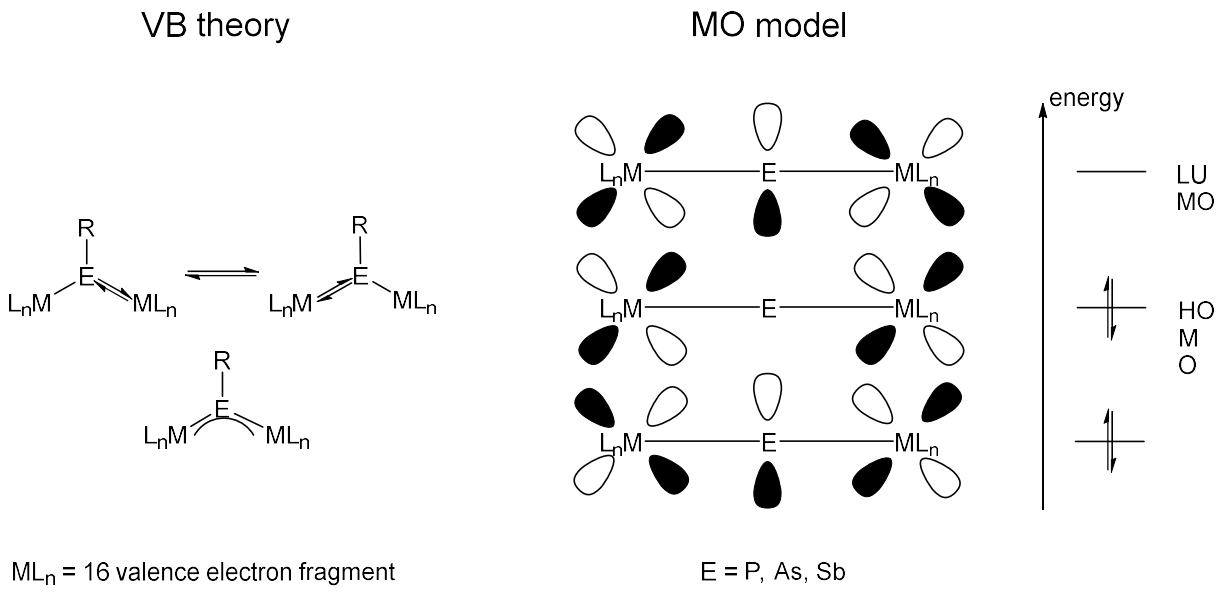

***Figure 1.5**: bonding situation in type **A** pnictinidene complexes.*

This interaction also results in a relatively small HOMO-LUMO gap, which is the cause of various spectroscopic characteristics of **1a** and **1b**. One of these characteristics is the large low field shift of type **A** phosphinidene complexes in the ^{31}P NMR spectrum (**1a**: δ = 1076 ppm; [^{t}BuP{Cr(CO)$_5$}$_2$]: δ = 1362 ppm[36]). The paramagnetic contribution of the 3 center 4 π electron interaction of the M-P-M moiety to its ^{31}P NMR shift can be correlated to the energy of the π-π^* transition, which, in turn, corresponds to the HOMO-LUMO gap.[50] Another characteristic of type **A** pnictinidene complexes is the intense color of their solutions. Both **1a** and **1b**, when dissolved in organic solvents, have a deep blue color which is present even in low concentrated solutions. This is because of an electron transfer taking place from the non-bonding into the antibonding π^* orbital of the 3 center 4 π electron system, as shown previously for the arsinidene complex [PhAs{Cr(CO)$_5$}$_2$].[51] The frontier orbitals of **1a** are displayed in Figure 1.6. According to DFT calculations, the HOMO is mainly localized at the Cp* diene system, making it the preferred position for the attacks of electrophiles. The LUMO, however, is located at the pnictogen

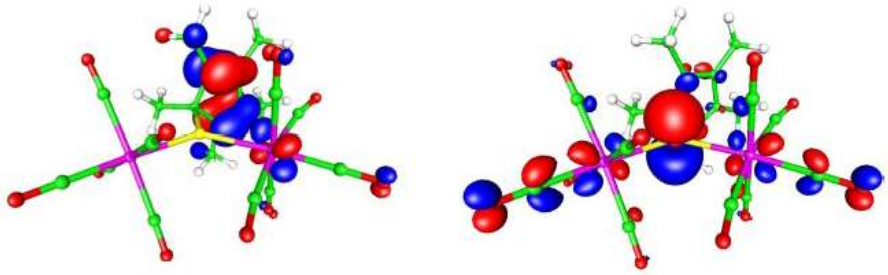

HOMO LUMO

***Figure 1.6**: Graphic representation of the frontier orbitals of **1a**.*

atom, representing its empty p orbital, suitable for the generation of Lewis acid/base adducts via nucleophilic attacks.[52] Hence, the phosphinidene **1a** and its heavier analog, the arsinidene **1b**, show a versatile reaction behavior. In our group, it has been shown that both **1a** and **1b** react with ionic Nucleophiles Nu^-X^+ (Nu = CN, ^{n}Bu, N_3, NH_2, OH, F, Cl, Br, I; X = Li, Na, K, $HNEt_3$, NBu_4, PPh_4) to form Lewis acid-base adducts $[Cp^*E\{W(CO)_5\}_2Nu]^-X^+$, which can be isolated.[53]

As mentioned above, the Cp* substituent is partly responsible for **1a** and **1b**'s versatile reactivity. Being a popular substituent in transition metal organometallic as well as main group chemistry, it both increases the solubility and stability of complexes, compared to the Cp derivatives. In addition, it is able to coordinate to the central pnictogen atom or metal in different modes ranging from η^1 to η^5. The $\eta^1(\sigma)$ bound Cp* substituent in **1a** and **1b** is characterized by a weak E-C bond, which can be cleaved off easily either thermally or photolytically or by electrophiles, nucleophiles and reducing agents.[54] Other examples for the rich reactivity of the $\eta^1(\sigma)$ bound Cp* substituent are migration reactions[55] and rearrangement reactions,[56] which can be monitored by ^{1}H NMR spectroscopy. While the Cp* substituent can be cleaved off photolytically in **1a**, another pathway that occurs in this reaction is the generation of the reactive intermediate **D** containing a W≡P triple bond (cf. Scheme 1.1) via elimination of three CO ligands. It then reacts with the $\bullet P\{W(CO)_5\}_2$ radical **E** which is the product of the homolytical cleavage of the Cp* substituent to form the tetrahedran complex **F**.[57] Radical **E** can be trapped in the presence of the diphosphene $(Mes^*P)_2$ to yield the isolable triphosphaallyl radical **G** stabilized by $W(CO)_n$ (n = 4,5) fragments.[58] Heating a solution of **1a** to 110 °C results in a Cp* migration reaction. After two CO ligands are eliminated from **1a**, the $\eta^1(\sigma)$ bound Cp* substituent migrates to the tungsten atom, changing its coordination mode to η^5. The resulting intermediate **H** then either forms compound **I** via CH activation or loses another CO ligand to give again reactive intermediate $[Cp^*(CO)_2W{\equiv}P{\rightarrow}W(CO)_5]$ (**D**). Since **D** is not stable, it dimerizes and after $W(CO)_5$ elimination and subsequent rearrangements the tetrahedran complex **K** is formed. A way to form isolable products from **D** is to trap it with suitable reaction partners such as alkynes[59] and phosphaalkynes.[60]

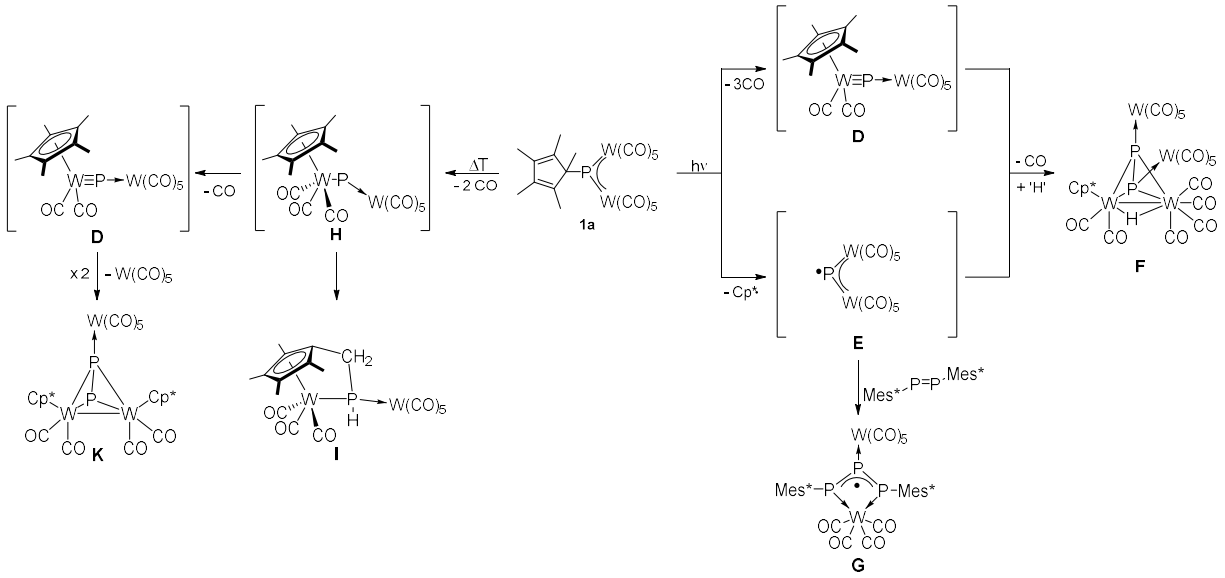

***Scheme 1.1**: Reaction pathways of the thermolysis (left) and photolysis (right) of **1a**.*

Another class of nucleophiles, which have been extensively studied in the reactions with **1a** and **b**, are group 15 nucleophiles. Though the original intent was to generate novel E-E (E = pnictogen atom) bonds, a variety of remarkable results have additionally been obtained (cf. Scheme 1.2). The reaction of **1a** with aniline or other primary amines leads to the aminophosphinidene complex **L** upon elimination of the Cp* substituent as Cp*H.[61] In addition to the formation of N-P bonds, reacting **1a** with nitriles results in heterocycle formation via insertion of the nitrile into the P-C bond with the ring size dependent

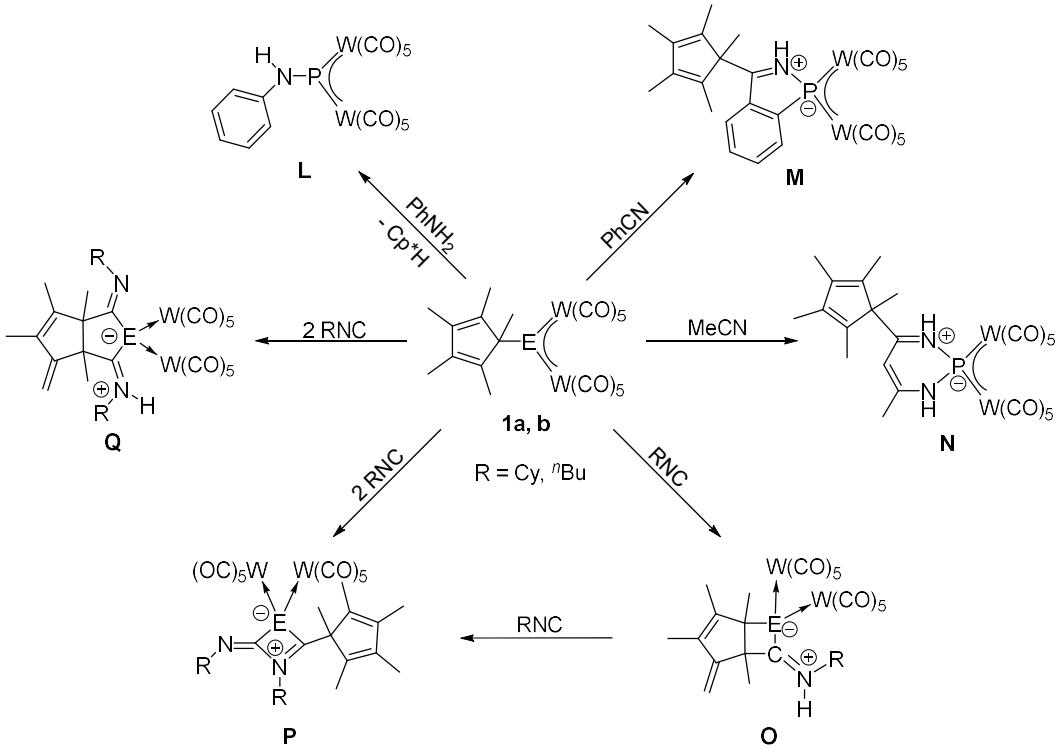

***Scheme 1.2**: Selected reactions of **1a**, **b** with N and C centered nucleophiles.*

on the substituent bound to the nitrile moiety. The five-membered heterocycle **M** is formed using benzonitrile as a reagent, while the use of acetonitrile leads to a six-membered heterocycle of type **N**.[62] Additionally, isonitriles have been investigated as nucleophilic reaction partners of **1a** and **1b**. Their reactions are highly dependent on the steric demand of the substituent R at the isonitrile RNC (R = Cy, ^{n}Bu) as well as the stoichiometry of the reagents. In the reaction of **1a** and **1b** with one equivalent of isonitrile, the bicyclic complex **O** is formed. **O** can then further react with another equivalent of CyNC to the 2,3-dihydro-1,3-azaphosphete complex **P** if E = P or, in the case of E = As, to the bicyclic compound **Q**. Using two equivalents of ^{n}BuNC, on the other hand, both **O** and **Q** are formed. It is worth mentioning that in the case of R = ^{n}Bu, only the adduct is formed.[63]

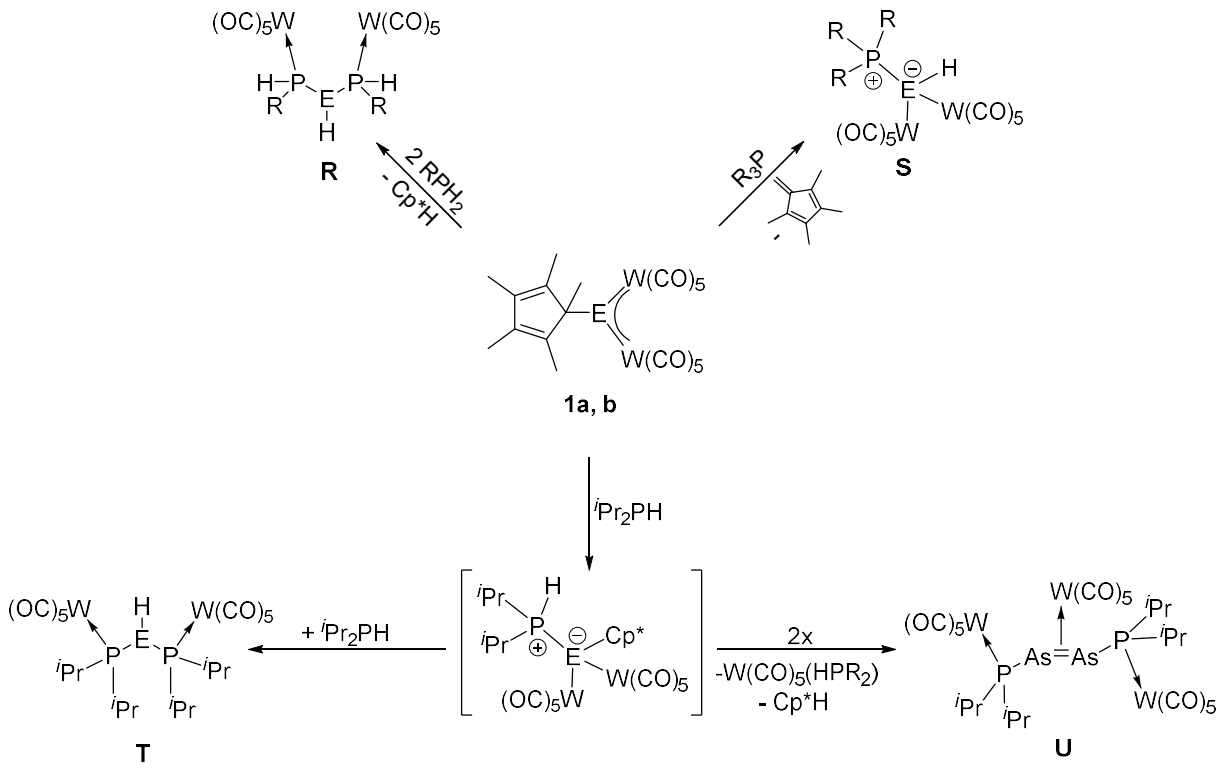

***Scheme 1.3**: Selected reactions of **1a, b** with phosphines.*

The reactions of **1a** and **1b** with phosphines are also well-studied (cf. Scheme 1.3). Treating the pnictinidene complexes with primary phosphines, arsadiphosphines or triphosphines coordinated to two $W(CO)_5$ moieties (**R**) are generated.[64] There is, however, one exception: If the primary phosphine used is Cp^*PH_2, the reaction does not stop at **R** but instead a Cp*H elimination with a subsequent cycloaddition and rearrangement follows, yielding phosphorus/arsenic-carbon cage compounds.[65] In the reactions of **1a** and **1b** with tertiary phosphines, an elimination of 1,2,3,4-tetramethylfulvene occurs and product **S** is formed in both cases. The reaction of **1a** additionally yields $[R_3P\text{-}PW(CO)_5Cp^*]$ as a second product through overall elimination of $W(CO)_5(PR_3)$. Using two equivalents of the secondary phosphine $^{i}Pr_2PH$ in the reaction with **1a**, triphosphine **T** is formed, among others. The outcome of the

reaction of $^{i}Pr_2PH$ with **1b** is dependent on the solvent. An arsanylidenephosphine is formed conducting the reaction in toluene, while the use of the polar CH_2Cl_2 as a solvent results on the formation of compound **U** containing a side-on coordinated As=As double bond.[66]

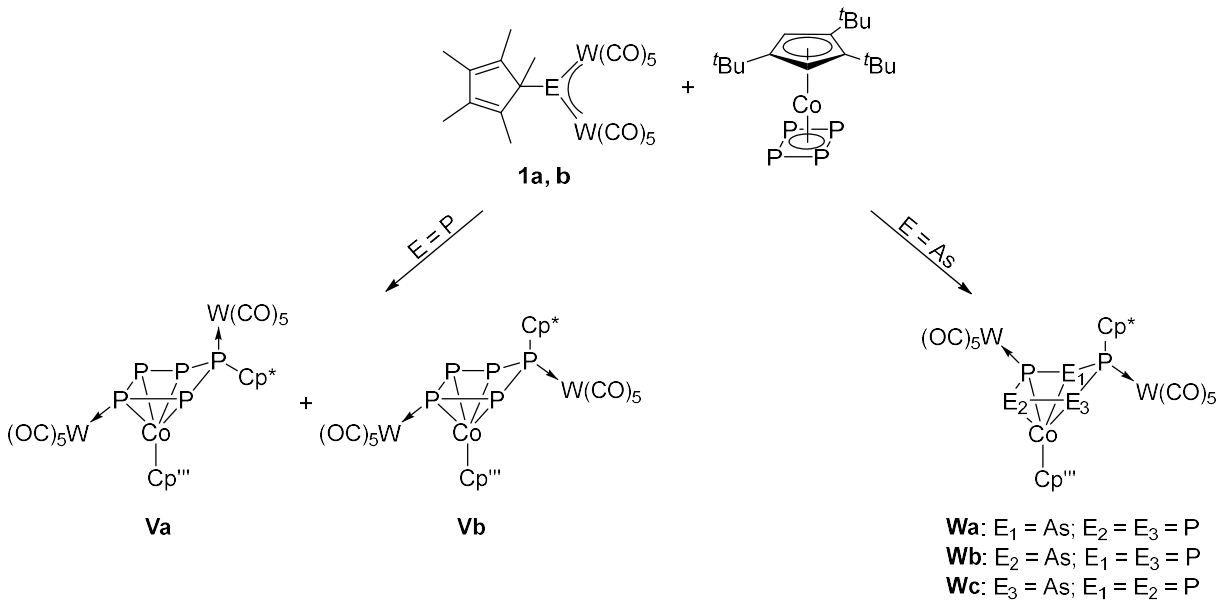

***Scheme 1.4**: Reactions of **1a**, **b** with [Cp'''Co(η⁴-P₄)].*

The last example mentioned to highlight the versatile reactivity of pnictinidene complexes **1a** and **1b** in this chapter is their ability to expand P_n heterocycles. The reaction of **1a** with $[Na(thf)_3][(\eta^3\text{-}P_3)Nb(ODipp)_3]$ for example, leads to the corresponding $W(CO)_5$-coordinated P_4 complex via insertion of **1a** into the P_3 ring of the starting material. This ring expansion does also work with the neutral P_4-ligand complex $[Cp'''Co(\eta^4\text{-}P_4)]$ (Cp''' = 1,2,4-tri-*tert*-butyl-cyclopentadienyl) as a reagent (cf. Scheme 1.4). The reaction with **1a** gives two isomeric P_5 complexes **Va** and **Vb**, while the reaction with **1b** yields isomers **Wa**, **b** and **c**, which are examples of compounds containing a rare *cyclo*-P_4As ligand.[67]

1.3 Properties of [ClSb{Cr(CO)$_5$}$_2$(thf)] (1c)

A few years after the discovery of the first trigonal planar stibinidene complex [PhSb{Mn(CO)$_2$Cp}$_2$] by Huttner et al.,[44,45] the group reported the synthesis of the chlorosubstituted homoleptic stibinidene complex [ClSb{Cr(CO)$_5$}$_2$] (**X**). Upon dissolving the stibinidene in thf, it forms the isolable adduct [ClSb{Cr(CO)$_5$}$_2$(thf)] (**1c**), which is stable enough to be used for synthetic purposes.[68,69] It is poorly soluble in unpolar organic solvents like n-hexane and dissolves very well in polar solvents like CH_2Cl_2. Furthermore, **1c** exhibits solvato- as well as thermochromic properties due to the diverse nature of interactions between the Sb atom with Lewis-basic substituents at adjacent molecules in different solvents as well as different temperatures, resulting in a variety of intensely colored solutions, which is also emphasized to be the "most striking feature of stibinidene complexes" by Huttner et al.[68]

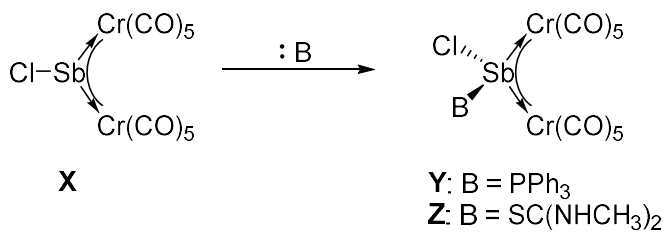

***Scheme 1.5**: Trapping of the reactive **X** by Lewis bases.*

As can be seen in Scheme 1.5, the reactive trigonal planar stibinidene complex **X**, generated from the reaction of $Na_2[Cr_2(CO)_{10}]$ and $SbCl_3$, can also be trapped using Lewis bases such as PPh_3 or N,N'-dimethylthiourea to yield tetrahedral complexes **Y** and **Z**.[69] Apart from these reactions, the reaction behavior of **1c** has not been explored so far, which is one of the purposes of this work.

1.4 References

[1] A. Igau, H. Grutzmacher, A. Baceiredo, G. Bertrand, *J. Am. Chem. Soc.* **1988**, *110*, 6463.

[2] A. J. Arduengo, R. L. Harlow, M. Kline, *J. Am. Chem. Soc.* **1991**, *113*, 361.

[3] a) D. Martin, M. Melaimi, M. Soleilhavoup, G. Bertrand, *Organometallics* **2011**, *30*, 5304; b) M. N. Hopkinson, C. Richter, M. Schedler, F. Glorius, *Nature* **2014**, *510*, 485.

[4] D. Enders, O. Niemeier, A. Henseler, *Chem. Rev.* **2007**, *107*, 5606.

[5] a) V. Lavallo, Y. Canac, B. Donnadieu, W. W. Schoeller, G. Bertrand, *Angew. Chem.* **2006**, *118*, 3568; b) V. Lavallo, Y. Canac, B. Donnadieu, W. W. Schoeller, G. Bertrand, *Angew. Chem. Int. Ed. Engl.* **2006**, *45*, 3488.

[6] G. D. Frey, V. Lavallo, B. Donnadieu, W. W. Schoeller, G. Bertrand, *Science* **2007**, *316*, 439.

[7] M. Melaimi, R. Jazzar, M. Soleilhavoup, G. Bertrand, *Angew. Chem. Int. Ed.* **2017**, *56*, 10046.

[8] a) C. Ganesamoorthy, J. Schoening, C. Wölper, L. Song, P. R. Schreiner, S. Schulz, *Nat. Chem.* **2020**, *12*, 608; b) A. V. Protchenko, P. Vasko, D. C. H. Do, J. Hicks, M. Á. Fuentes, C. Jones, S. Aldridge, *Angew. Chem.* **2019**, *131*, 1822; c) A. V. Protchenko, P. Vasko, D. C. H. Do, J. Hicks, M. Á. Fuentes, C. Jones, S. Aldridge, *Angew. Chem. Int. Ed.* **2019**, *58*, 1808.

[9] a) T. J. Hadlington, J. A. B. Abdalla, R. Tirfoin, S. Aldridge, C. Jones, *Chem. Comm.* **2016**, *52*, 1717; b) D. Reiter, P. Frisch, D. Wendel, F. M. Hörmann, S. Inoue, *Dalton Trans.* **2020**, *49*, 7060.

[10] a) M. M. D. Roy, M. J. Ferguson, R. McDonald, Y. Zhou, E. Rivard, *Chem. Sci.* **2019**, *10*, 6476; b) M. Scheer, G. Balázs, A. Seitz, *Chem. Rev.* **2010**, *110*, 4236; c) M. Driess, A. D. Fanta, D. R. Powell, R. West, *Angew. Chem. Int. Ed.* **1989**, *28*, 1038; d) M. Driess, A. D. Fanta, D. Powell, R. West, *Angew. Chem.* **1989**, *101*, 1087; e) Y. Xiong, S. Yao, M. Brym, M. Driess, *Angew. Chem. Int. Ed.* **2007**, *46*, 4511; f) Y. Xiong, S. Yao, M. Brym, M. Driess, *Angew. Chem.* **2007**, *119*, 4595; g) S. S. Sen, S. Khan, H. W. Roesky, D. Kratzert, K. Meindl, J. Henn, D. Stalke, J.-P. Demers, A. Lange, *Angew. Chem. Int. Ed.* **2011**, *50*, 2322; h) S. S. Sen, S. Khan, H. W. Roesky, D. Kratzert, K. Meindl, J. Henn, D. Stalke, J.-P. Demers, A. Lange, *Angew. Chem.* **2011**, *123*, 2370.

[11] a) A. V. Protchenko, A. D. Schwarz, M. P. Blake, C. Jones, N. Kaltsoyannis, P. Mountford, S. Aldridge, *Angew. Chem. Int. Ed.* **2013**, *52*, 568; b) A. V. Protchenko, A. D. Schwarz, M. P. Blake, C. Jones, N. Kaltsoyannis, P. Mountford, S. Aldridge, *Angew. Chem.* **2013**, *125*, 596; c) A. V. Protchenko, K. H. Birjkumar, D. Dange, A. D. Schwarz, D. Vidovic, C. Jones, N. Kaltsoyannis, P. Mountford, S. Aldridge, *J. Am. Chem. Soc.* **2012**, *134*, 6500; d) D. Wendel, A. Porzelt, F. A. D. Herz, D. Sarkar, C. Jandl, S. Inoue, B. Rieger, *J. Am. Chem. Soc.* **2017**, *139*, 8134; e) D. Reiter, R. Holzner, A. Porzelt, P. J. Altmann, P. Frisch, S. Inoue, *J. Am. Chem. Soc.* **2019**, *141*, 13536.

[12] G. Smolinsky, E. Wasserman, W. A. Yager, *J. Am. Chem. Soc.* **1962**, *84*, 3220.

[13] C. T. Saouma, J. C. Peters, *Coord. Chem. Rev.* **2011**, *255*, 920.

[14] F. Dielmann, O. Back, M. Henry-Ellinger, P. Jerabek, G. Frenking, G. Bertrand, *Science* **2012**, *337*, 1526.

[15] M. T. Nguyen, A. van Keer, L. G. Vanquickenborne, *J. Org. Chem.* **1996**, *61*, 7077.

[16] O. M. Nefedov, M. N. Manakov, *Angew. Chem. Int. Ed. Engl.* **1966**, *5*, 1021.

[17] U. Schmidt, I. Boie, C. Osterroht, R. Schröer, H.-F. Grützmacher, *Chem. Ber.* **1968**, *101*, 1381.

[18] a) U. Schmidt, *Angew. Chem. Int. Ed. Engl.* **1975**, *14*, 523; b) U. Schmidt, *Angew. Chem.* **1975**, *87*, 535; c) H.-F. Grützmacher, W. Silhan, U. Schmidt, *Chem. Ber.* **1969**, *102*, 3230.

[19] M. Yoshifuji, T. Sato, N. Inamoto, *Chem. Lett.* **1988**, *17*, 1735.

[20] X. Li, D. Lei, M. Y. Chiang, P. P. Gaspar, *J. Am. Chem. Soc.* **1992**, *114*, 8526.

[21] A. H. Cowley, F. Gabbai, R. Schluter, D. Atwood, *J. Am. Chem. Soc.* **1992**, 3142.

[22] S. Shah, M. C. Simpson, R. C. Smith, J. D. Protasiewicz, *J. Am. Chem. Soc.* **2001**, *123*, 6925.

[23] X. Li, S. I. Weissman, T.-S. Lin, P. P. Gaspar, A. H. Cowley, A. I. Smirnov, *J. Am. Chem. Soc.* **1994**, *116*, 7899.

[24] a) J. J. Harrison, B. E. Williamson, *J. Phys. Chem. A* **2005**, *109*, 1343; b) J. Glatthaar, G. Maier, *Angew. Chem. Int. Ed. Engl.* **2004**, *43*, 1294; c) G. Bucher, M. L. G. Borst, A. W. Ehlers, K. Lammertsma, S. Ceola, M. Huber, D. Grote, W. Sander, *Angew. Chem. Int. Ed. Engl.* **2005**, *44*, 3289.

[25] L. Liu, D. A. Ruiz, D. Munz, G. Bertrand, *Chem* **2016**, *1*, 147.

[26] K. Lammertsma in *Topics in Current Chemistry*, *Vol. 229* (Eds.: J.-P. Majoral, T. Chivers), Springer, Berlin, **2003**, pp. 95–119.

[27] a) F. Mathey, *Angew. Chem.* **1987**, *99*, 285; b) F. Mathey, *Angew. Chem. Int. Ed.* **1987**, *26*, 275; c) K. Lammertsma, M. J. M. Vlaar, *Eur. J. Org. Chem.* **2002**, 1127; d) H. Aktaş, J. C. Slootweg, K. Lammertsma, *Angew. Chem. Int. Ed.* **2010**, *49*, 2102.

[28] F. Mathey, *Dalton Trans.* **2007**, 1861.

[29] A. Marinetti, F. Mathey, *Organometallics* **1984**, *3*, 456.

[30] G. Frison, F. Mathey, A. Sevin, *J. Organomet. Chem.* **1998**, *570*, 225.

[31] P. B. Hitchcock, M. F. Lappert, W.-P. Leung, *J. Chem. Soc., Chem. Commun.* **1987**, 1282.

[32] A. W. Ehlers, E. J. Baerends, K. Lammertsma, *Eur. J. Org. Chem.* **2002**, *124*, 2831.

[33] G. Huttner, H.-D. Müller, A. Frank, H. Lorenz, *Angew. Chem. Int. Ed. Engl.* **1975**, *14*, 705.

[34] K. E. G. Huttner, *Acc. Chem. Res.* **1986**, *19*, 406.

[35] M. E. García, D. García-Vivó, A. Ramos, M. A. Ruiz, *Coord. Chem. Rev.* **2017**, *330*, 1.

[36] G. Huttner, J. Borm, L. Zsolnai, *J. Organomet. Chem.* **1984**, *263*, c33-c36.

[37] B. Twamley, C. D. Sofield, M. M. Olmstead, P. P. Power, *J. Am. Chem. Soc.* **1999**, *121*, 3357.

[38] H. Lang, G. Hüttner, B. Sigwarth, U. Weber, L. Zsolnai, I. Jibril, O. Orama, *Z. Naturforsch. B* **1986**, *41*, 191.

[39] E. Röttinger, H. Vahrenkamp, *J. Organomet. Chem.* **1981**, *213*, 1.

[40] a) G. Huttner, H.-G. Schmid, *Angew. Chem.* **1975**, *87*, 454; b) G. Huttner, H.-G. Schmid, *Angew. Chem. Int. Ed. Engl.* **1975**, *14*, 433.

[41] M. K. Sharma, B. Neumann, H.-G. Stammler, D. M. Andrada, R. S. Ghadwal, *Chem. Comm.* **2019**, *55*, 14669.

[42] a) A. Doddi, M. Weinhart, A. Hinz, D. Bockfeld, J. M. Goicoechea, M. Scheer, M. Tamm, *Chem. Comm.* **2017**, *53*, 6069; b) L. Dostál, *Coord. Chem. Rev.* **2017**, *353*, 142.

[43] a) A. Hinz, M. M. Hansmann, G. Bertrand, J. M. Goicoechea, *Chem. Eur. J* **2018**, *24*, 9514; b) R. Kretschmer, D. A. Ruiz, C. E. Moore, A. L. Rheingold, G. Bertrand, *Angew. Chem. Int. Ed.* **2014**, *53*, 8176.

[44] J. von Seyerl, G. Huttner, *Angew. Chem. Int. Ed. Engl.* **1978**, *17*, 843.

[45] J. von Seyerl, G. Huttner, *Angew. Chem.* **1978**, *90*, 911.

[46] a) P. Simon, F. de Proft, R. Jambor, A. Růzicka, L. Dostál, *Angew. Chem. Int. Ed.* **2010**, *49*, 5468; b) P. Šimon, F. de Proft, R. Jambor, A. Růžička, L. Dostál, *Angew. Chem.* **2010**, *122*, 5600.

[47] a) I. Vránová, M. Alonso, R. Jambor, A. Růžička, J. Turek, L. Dostál, *Chem. Eur. J* **2017**, *23*, 2340; b) R. Kretschmer, D. A. Ruiz, C. E. Moore, A. L. Rheingold, G. Bertrand, *Angew. Chem.* **2014**, *126*, 8315; c) C. L. Dorsey, R. M. Mushinski, T. W. Hudnall, *Chem. Eur. J* **2014**, *20*, 8914; d) J. Krüger, C. Wölper, L. John, L. Song, P. R. Schreiner, S. Schulz, *Eur. J. Inorg. Chem.* **2019**, *2019*, 1669; e) I. Vránová, M. Alonso, R. Lo, R. Sedlák, R. Jambor, A. Růžička, F. de Proft, P. Hobza, L. Dostál, *Chem. Eur. J* **2015**, *21*, 16917.

[48] Y. Pang, M. Leutzsch, N. Nöthling, J. Cornella, *J. Am. Chem. Soc.* **2020**, *142*, 19473.

[49] P. Jutzi, R. Kroos, *J. Organomet. Chem.* **1990**, *390*, 317.

[50] G. Huttner, *J. Organomet. Chem.* **1986**, *308*, C11-C13.

[51] a) G. Huttner, J. von Seyerl, M. Marsili, H.-G. Schmid, *Angew. Chem. Int. Ed. Engl.* **1975**, *14*, 434; b) G. Huttner, J. von Seyerl, M. Marsili, H.-G. Schmid, *Angew. Chem.* **1975**, *87*, 455.

[52] D. Himmel, *Dissertation*, Regensburg, Universität, **2004**.

[53] M. Stubenhofer, *Dissertation*, Regensburg, Universität, Regensburg, **2012**.

[54] a) P. Jutzi, *Pure Appl. Chem.* **2003**, *75*, 483; b) P. Jutzi, N. Burford, *Chem. Rev.* **1999**, *99*, 969.

[55] P. Jutzi, R. Kroos, *Chem. Ber.* **1988**, *121*, 1399.

[56] P. Jutzi, G. Reumann, *Dalton Trans.* **2000**, 2237.

[57] M. Schiffer, E. Leiner, M. Scheer, *Eur. J. Inorg. Chem.* **2001**, *2001*, 1661.

[58] M. Scheer, C. Kuntz, M. Stubenhofer, M. Linseis, R. F. Winter, M. Sierka, *Angew. Chem. Int. Ed.* **2009**, *48*, 2600.

[59] M. Schiffer, M. Scheer, *Chem. Eur. J.* **2001**, *7*, 1855.

[60] a) M. Scheer, D. Himmel, B. P. Johnson, C. Kuntz, M. Schiffer, *Angew. Chem. Int. Ed.* **2007**, *46*, 3971; b) M. Scheer, D. Himmel, B. P. Johnson, C. Kuntz, M. Schiffer, *Angew. Chem.* **2007**, *119*, 4045; c) M. Scheer, E. Leiner, P. Kramkowski, M. Schiffer, G. Baum, *Chem. Eur. J.* **1998**, *4*, 1917.

[61] M. Seidl, R. Weinzierl, A. Y. Timoshkin, M. Scheer, *Chem. Eur. J* **2016**, *22*, 5484.

[62] M. Schiffer, M. Scheer, *Angew. Chem. Int. Ed.* **2001**, *40*, 3413.

[63] M. Seidl, M. Schiffer, M. Bodensteiner, A. Y. Timoshkin, M. Scheer, *Chem. Eur. J.* **2013**, *19*, 13783.

[64] M. Scheer, C. Kuntz, M. Stubenhofer, M. Zabel, A. Y. Timoshkin, *Angew. Chem. Int. Ed. Engl.* **2010**, *49*, 188.

[65] M. Stubenhofer, G. Lassandro, G. Balázs, A. Y. Timoshkin, M. Scheer, *Chem. Comm.* **2012**, *48*, 7262.

[66] M. Stubenhofer, C. Kuntz, M. Bodensteiner, A. Y. Timoshkin, M. Scheer, *Organometallics* **2013**, *32*, 3521.

[67] M. Piesch, M. Seidl, M. Stubenhofer, M. Scheer, *Chem. Eur. J* **2019**, *25*, 6311.

[68] U. Weber, L. Zsolnai, G. Huttner, *J. Organomet. Chem.* **1984**, *260*, 281.

[69] B. Sigwarth, U. Weber, L. Zsolnai, G. Huttner, *Chem. Ber.* **1985**, *118*, 3114.

2 RESEARCH OBJECTIVES

The reactivity of pnictinidene complexes has been a subject of interest in the scientific community for quite some time now. A plethora of results was obtained with a few small gaps in between. Aiming to close these gaps and looking at the current state of research, the following research objectives could be derived:

1 – Chalcogenopnictinidenes

There are some compounds coined in the literature as "chalcogenopnictinidenes". However, these examples cannot be considered true chalcogenopnictinidenes due to different reasons (vide infra). As mentioned in chapter 1.2, **1a** and **1b** can generate radicals upon irradiation. Another class of compounds which are known to generate radicals are dichalcogenides. So naturally, the question arises whether the two of them can be combined to form true terminal chalcogenopnictinidene complexes. An in-depth investigation of this question has been conducted within this work.

2 – Aminopnictinidenes

Albeit aminopnictinidene complexes having been investigated since the 1980s, no consistent pattern of reactivity could be derived from these analyses. Hence, systematic syntheses of different novel aminopnictinidene compounds have been conducted and subsequently, their reactivity has been examined.

3 – Stibinidenes

In contrast to their lighter homologs and due to the extremely high reactivity and sensitivity of these compounds and the resulting challenge of handling them properly, there are only a few publications about stibinidene complexes. In this work, an attempt has been made to fill this gap by exploring the reactivity of **1c**.

3 THE REACTIVITY OF THE PENTELIDENE COMPLEXES [Cp*E{W(CO)$_5$}$_2$] (E = P, As) TOWARDS DICHALCOGENIDES AND CHALCOGENOLS

Lena Rummel, Giuliano Lassandro, Michael Seidl, Alexey Y. Timoshkin and Manfred Scheer

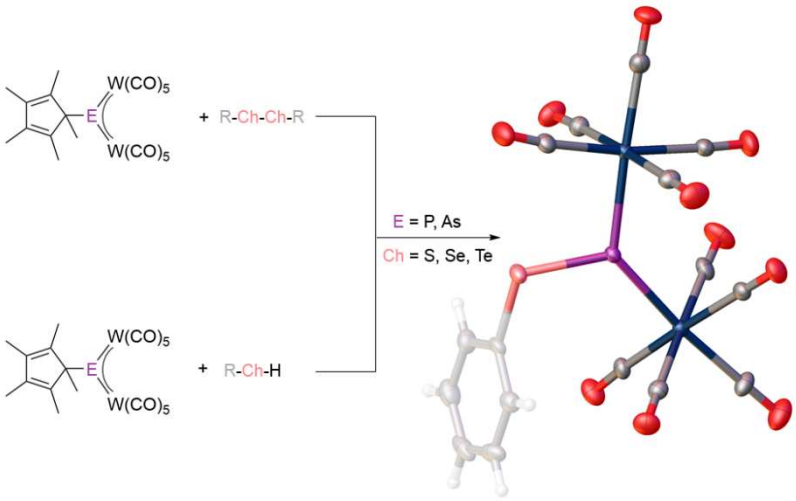

- ⇨ Synthesis and characterization of compounds **2a**, **2b**, **3a-II**, **3b**, **5**, **6a** was carried out by Giuliano Lassandro
- ⇨ Synthesis and characterization of compounds **3a-I**, **4a-I**, **4a-II** and **6b** was carried out by Lena Rummel
- ⇨ X-ray measurements were finalized by Michael Seidl
- ⇨ DFT calculations were performed by Alexey Y. Timoshkin
- ⇨ Figures and manuscript were prepared by Lena Rummel, except DFT calculation part: Alexey Y. Timoshkin

Acknowledgements: The Deutsche Forschungsgemeinschaft is acknowledged for support within the project Sche 384/28-2.

This chapter is already published in *Dalton Trans.* **2021**. DOI: 10.1039/D1DT01866C

3.1 Introduction

Pentelidene complexes of the type [Cp*E{W(CO)$_5$}$_2$] (Cp* = C_5Me_5; **1a**: E = P, **1b**: E = As) were reacted with the dichalcogenides R_2Ch_2 (R = Ph, Mes, Tipp; Ch = S, Se, Te; Mes = 2,4,6-trimethylphenyl; Tipp = 2,4,6-triisopropylphenyl) and the chalcogenols PhChH (Ch = S, Se). It has been shown that the formation of new E–Ch bonds proceeds under elimination of the Cp* substituent. The resulting chalcogenopentelidene complexes, which have been isolated and fully characterised, represent a novel class of phosphinidene complexes which can be synthesised through this general synthetic route.

Phosphinidene complexes exhibit a variety of interesting properties and reaction behaviors due to their unique electronic structure and bonding.[1] The first phosphinidene was described by Schmidt *et al.* in 1975 as a possible intermediate in the formation of cyclophosphines from P_1 compounds or the thermolytic decomposition products of cyclopolyphosphines $(RP)_n$, but its existence could not be confirmed doubtlessly.[2] It was only in 1994 that Gaspar succeeded in detecting a 'free' triplet mesitylphosphinidene *via* EPR spectroscopy generated by UV irradiation of a mesitylphosphirane at 77 K in a solvent matrix.[3] The ground state of the parent phosphinidene H–P is the triplet state, which, according to theoretical calculations, is favored over the singlet state by 28 kcal mol^{-1}. By introducing suitable substituents, the energy difference can be reduced further and the stabilization of the singlet ground state species should therefore also be possible.[4] Just recently, Bertrand *et al.* succeeded in generating a singlet phosphinidene that is stable at room temperature by the UV-induced elimination of carbon monoxide from a (phosphino)phosphaketene. Nonetheless, in order to prevent dimerization, the P atom must carry an extremely bulky substituent.[5] A different way to stabilize reactive phosphinidene species is their coordination to transition metals where coordination modes ranging from η^1 to μ_4 are known.[6] In our group, we focus on the pentelidene complexes [Cp*E{W(CO)$_5$}$_2$] (**1a**: E = P, **1b**: E = As; Cp* = C_5Me_5) with an $\eta^1(\sigma)$-bound Cp* substituent. The η^1-bound Cp* group does not only increase the solubility and stability of the complexes but can also undergo various reactions. Many examples were reported for the Cp* substituent undergoing migration reactions,[7,8] rearrangement reactions,[9] ring expansions[10] or substitution reactions,[11] among others. The Cp* substituent can also be cleaved off homolytically by irradiating the phosphinidene complex with UV light, leaving a ·P{W(CO)$_5$}$_2$ radical as an intermediate which can be trapped *e.g.* with Mes*P=PMes* (Mes* = 2,4,6-tri-tert-butylphenyl) to give a W(CO)$_n$ (n = 4, 5) stabilised triphosphaallyl radical.[12,13] Another class of compounds, commonly known to form radical species and act as radical scavengers, are dichalcogenides. While there are only hints of a radical formation of dichalcogen compounds in solution,[14] upon irradiation with UV light, organosubstituted disulfides do generate monovalent sulfur radicals.[15] Combining these two classes of compounds would open up the possibility for the synthesis of RCh-substituted phosphinidene complexes (Ch = chalcogen).

Different types of chalcogenopentelidene complexes have been reported and are summarized in Chart 3.1. Types **A** and **B** are generated *via* formal [2 + 1] addition of S or Se from S_8 or grey selenium to the P═M double bond (M = Mo, W) of the respective starting material, resulting in a chalcogen-bridged P–M bond.[16] However, due to the side-on coordination of the P–Ch bond, the chalcogenophosphinidene character is limited. The base-stabilised phosphinidene sulfide Ar*(NHC)PS (**C**) also features a P═S moiety, however, the phosphorus(III) atom is described as "significantly pyramidal" with Σ_{ang} = 310.5°.[17] In the area of arsinidene complexes, a thio- and a selenoarsinidene complex of type **D** were synthesised by the reaction of the arsinidene complex [ClAs{Cp′Mn(CO)$_2$}$_2$]

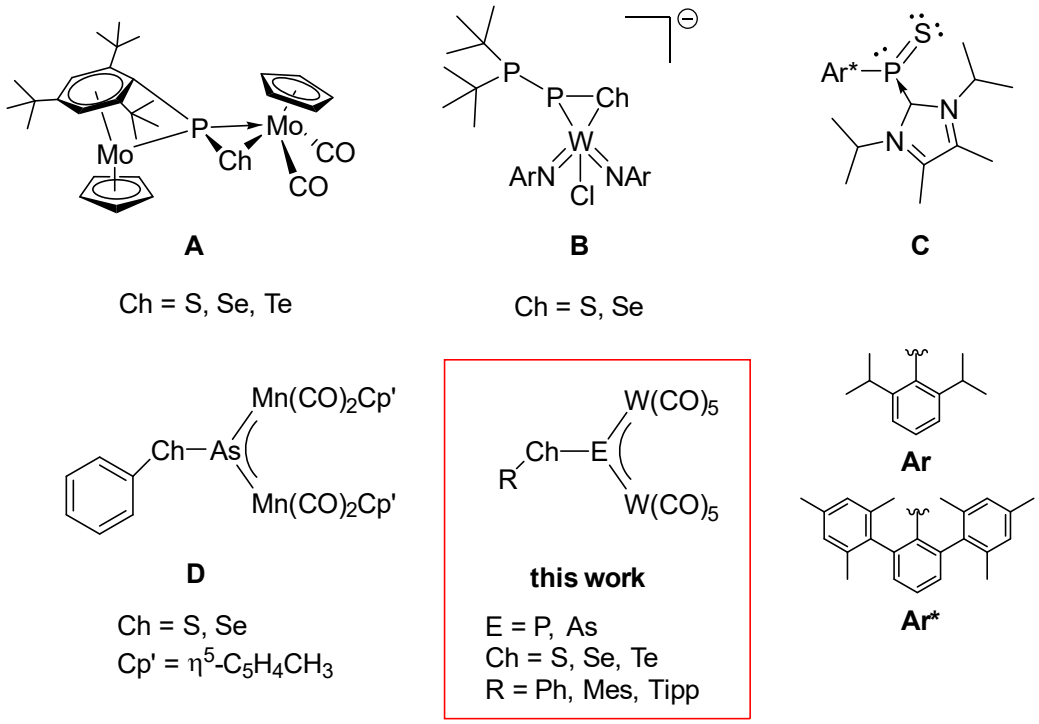

***Chart 3.1**: Previously reported chalcogenopentelidene complexes.*

(Cp′ = η^5-C_5H_4Me) with thiophenol and thioselenol, respectively.[18] Other than these, to the best of our knowledge, no chalcogenopentelidene complexes have been synthesized so far. In view of these examples, the question arises if a general pathway to terminal substituted RCh compounds can be developed. Herein we report the reactions of the pentelidene complexes [Cp*E{W(CO)$_5$}$_2$] (E = P, As) with dichalcogenides and chalcogenols, giving general access to this novel class of compounds and the characterisation of the resulting chalcogenopentelidene complexes [RChE{W(CO)$_5$}$_2$] (E = P, As; R = Ph, Mes, Tipp; Ch = S, Se, Te).

3.2 Results and Discussion

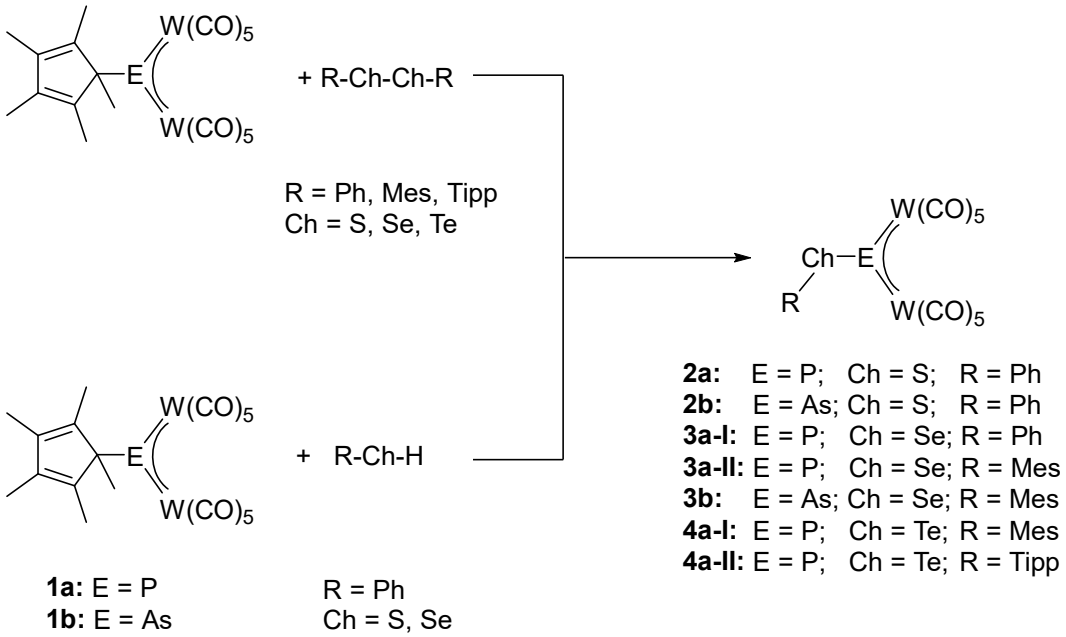

***Figure 3.1**: Reaction of **1a**,**b** with dichalcogenides and chalcogenols.*

The reaction of the pentelidene complexes [Cp*E{W(CO)$_5$}$_2$] (**1a**: E = P, **1b**: E = As) with dichalcogenides R_2Ch_2 (Ch = S, Se; R = Ph, Mes) leads to the thiopentelidene and selenopentelidene compounds **2a,b** and **3a-II,b** in 10–15% isolated crystalline yields (cf. Figure 3.1). These relatively low yields are probably a result of the thermal instability of the chalcogenopentelidene complexes in solution. Additionally, the reaction conditions, *i.e.* the long reaction time that is needed, favour the decomposition of the products. The reactions were started at low temperatures, warmed up to room temperature and stirred until a colour change from deep blue to violet could be observed. However, as the reactions of **1a**,**b** with Ph_2S_2 take a few days to be completed under these conditions and since some unidentified side products can be distinguished in the ^{31}P NMR spectrum, we tried to find an alternative way to conduct a faster reaction. Heating the reaction mixtures to 90 °C reduced the reaction times to a maximum of 2 h, with, however, significantly more side products being formed. This did not come unexpected, since **1a**,**b** decomposes at elevated temperatures or under photochemical conditions.[13,19]

When **1b** was reacted with Ph_2S_2 and heated to 90 °C, two different side products could be identified: [PhS{W(CO)$_4$}]$_2$ and (PhS)$_3$As and had already been reported in literature.[20–22] Of both compounds, only a few crystals were obtained from the reaction solution. Due to a missing suitable NMR-active nucleus to monitor this reaction, it is as of yet unclear whether **2b** is formed in this reaction at all or if it could just not be isolated. Since the reaction of **1** with R_2Ch_2 proceeds probably *via* a radical mechanism and because it is known that R_2Ch_2 dissociates into RCh· radicals upon irradiation with UV light, we reacted **1** with R_2Ch_2 under photolytic reaction conditions at room temperature. By irradiating the

reaction mixture with a mercury lamp (λ_{max} = 254 nm), the reaction time could be reduced significantly to between 30 and 120 min. From comparing the $^{31}P\{^{1}H\}$ NMR spectra of the reaction mixtures of **1a** with Ph_2S_2 it can be concluded that irradiating the solution with UV light results in fewer side products than stirring the mixture for a few days at room temperature or even heating it to 90 °C (cf. chapter 3.4). Since the isolation of these compounds proved to be difficult, yields for the reaction of **1a** with R_2S_2 were also determined *via* $^{31}P\{^{1}H\}$ NMR spectroscopy. The ^{31}P NMR spectroscopic yield is 12% in the photolytic reaction, which is, however, still comparable to the yield in the long-term reaction at room temperature (13% yield of **2a**). Furthermore, in the photolytic reaction of **1a** with Ph_2Se_2, $[PhSe\{W(CO)_4\}]_2$ (**5**) was obtained after column chromatographic workup in 2% yield. The respective chalcogenopentelidene complex, $[PhSeP\{W(CO)_5\}_2]$ (**3a-I**), could not be identified in this reaction. Compound **5** was first mentioned by Ziegler *et al.*,[22] but its crystal structure was not reported. Therefore, an X-ray diffraction study was carried out for this compound. The molecular structure is depicted in Figure 3.2.

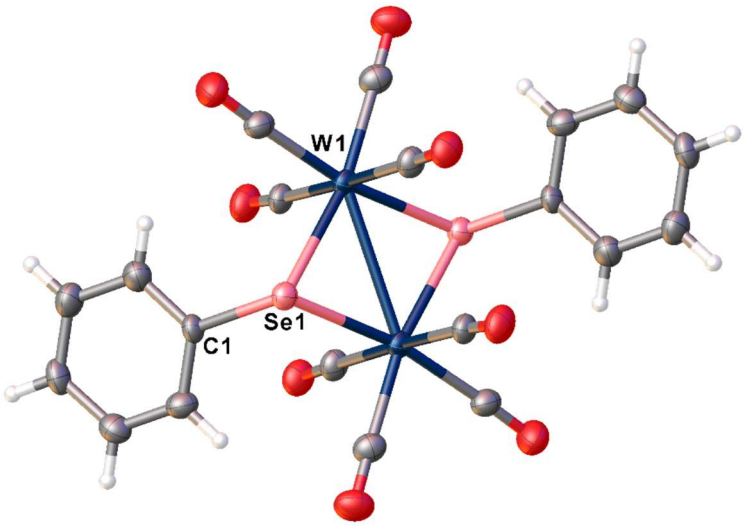

***Figure 3.2**: Molecular structure of **5**. Anisotropic displacement parameters are set to 50% probability level. Selected distances (Å) and angles (°): W1–W1: 3.0247(6), W1–Se1: 2.5891(8)–2.5929(8), Se1–C1: 1.953(7); Se1–W1–W1: 54.231(19)–54.347(19), Se1–W1–Se1: 108.58(2), W1–Se1–W1: 74.42(2), C1–Se1–W1: 107.8(2)–110.1(2).*

Comparing **5** to its sulfur analogon, $[(PhS)_2\{W(CO)_4\}_2]^{2-}$,[21] the W–W distance in **5** (3.0247(6) Å) is shorter by approx. 1 Å, but longer than the single bond covalent radii ($\Sigma_{r.cov.}$ = 2.74 Å) resulting in a slightly elongated W–W bond.[23,24] The W–Se distances also show a slightly elongated single bond, which was also found in $[Et_4N]_2[(PhS)_2\{W(CO)_4\}_2]$.[21] In order to augment the stability of the chalcogenopentelidene complexes, we increased the steric bulk of the organic substituent on the chalcogen atom. To that effect, we used mesityl- and 2,4,6-triisopropylphenyl(Tipp)-substituted diselenides and ditellurides in the reactions with **1a,b**, respectively. The reactions of **1a** with Ph_2Se_2 did not result in the formation of the desired chalcogenophosphinidene complex, whereas, by the reaction

of **1a** with Mes_2Se_2, [MesSeP{W(CO)$_5$}$_2$] (**3a-II**) could be isolated in 15% yield. In the reaction of R_2Te_2 (R = Mes, Tipp; Tipp = 2,4,6-triisopropylphenyl) with the pentelidene complexes **1a** and **1b**, the desired products [RTeP{W(CO)$_5$}$_2$] (**4a-I**: R = Mes, **4a-II**: R = Tipp) could not be isolated as crystalline material, however their formation was indicated via ^{31}P NMR spectroscopy. For compound **4a-I**, a singlet at 841 ppm and, for compound **4a-II**, a singlet at 839 ppm, each with a $^1J_{P,W}$ coupling constant of 174 Hz, were detected in the ^{31}P NMR spectra of the reaction solutions. The high downfield shift is in accordance with the ^{31}P NMR chemical shifts of the compounds **2a**, **3a-I** and **3a-II** all of which lie in between 822 and 854 ppm with $^1J_{P,W}$ coupling constants in the range 184 to 192 Hz. For **3a-I** and **3a-II**, the $^1J_{P,Se}$ coupling constants are 488 and 507 Hz, respectively. Despite numerous attempts, the ^{125}Te satellites of **4a-I** and **4a-II** could not be detected in their ^{31}P NMR spectra due to the relatively low signal-to-noise ratio. Long-term measurements turned out to be problematic due to the sensitivity of the tellurophosphinidene complexes towards air.

***Table 3.1**: Experimental and calculated ^{31}P NMR chemical shifts (ppm). All computed chemical shifts are scaled according to Sinyashin et al.[25]*

		PBE0/def2-SVPD	
	Experimental	**On optimized geom.**	**On exp. geom.**
2a	822.9	866.2	809.7
3a-I	835.0	898.3	869.1
3a-II	854.3	911.9	873.5
4a-I	840.4	958.8	-

In order to test the validity of the ^{31}P NMR shifts of **4a-I** and **4a-II**, DFT calculations were carried out at the PBE0/def2-SVPD level of theory. The calculated ^{31}P NMR chemical shifts show a downfield shift of the chalcogenophosphinidene complex with increasing atomic number of the chalcogen atom, which compares well with the experimental trend (cf. Table 3.1). The calculated ^{31}P NMR shift of **4a-I** and **4a-II** compares reasonably well with the experimental values and therefore strengthen the assumption that the complexes **4a-I** and **4a-II** were formed. The validity of the method is demonstrated by the calculated chemical shifts of **2a**, **3a-I** and **3a-II**, which are in agreement with the experimental data (cf. Table 3.1). In the reactions of Mes_2Te_2 with **1a** and **1b**, two side products could be isolated: [{W(CO)$_5$}$_2$(μ,η^1:η^1-Mes_2Te_2)] (**6a**) and [W(CO)$_5$(η^1-Mes_2Te_2)] (**6b**). Both compounds consist of a diorgano-ditellurane ligand which coordinates to two and one W(CO)$_5$ fragment(s), respectively.[24] **6a** shows inversion symmetry, while **6b** does not possess an inversion center in the solid state. The respective phenyl-substituted derivatives [{W(CO)$_5$}$_2$(μ,η^1:η^1-Ph_2Te_2)] and [W(CO)$_5$(η^1-Ph_2Te_2)] were reported before.[26] The molecular structures of the compounds **2a,b**; **3a-I**, **3a-II**, **3b** as determined by single crystal X-ray

diffractions are all isostructural and show a trigonal planar configurated pentel atom, which is bound to a Ch-R moiety. Figure 3.3 displays the molecular structures of [PhSP{W(CO)$_5$}$_2$] (**2a**), [PhSAs{W(CO)$_5$}$_2$] (**2b**), [MesSeP{W(CO)$_5$}$_2$] (**3a-II**) and [MesSeAs{W(CO)$_5$}$_2$] (**3b**).

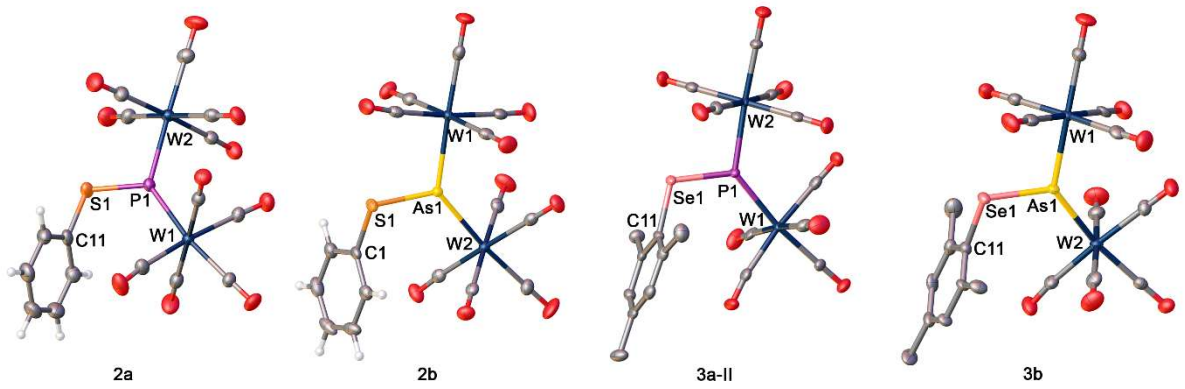

***Figure 3.3**: Molecular structures of the chalcogenopentelidene compounds **2a**, **2b**, **3a-II** and **3b**. Anisotropic displacement parameters are set to 50% probability level. Selected distances (Å) and angles (°): **2a**: S1–P1: 2.0703(13), P1–W1: 2.4065(9), P1–W2: 2.4239(9); C11–S1–P1: 109.59(13), S1–P1–W1: 123.17(5), S1–P1–W2: 104.68(4), W1–P1–W2: 132.12(4). **2b**: W1–As1 2.5024(3), W2–As1 2.5043(3), As1–S1 2.1958(8), S1–C1 1.776(3); W1–As1–W2 133.550(14), S1–As1–W1 104.62(2), S1–As1–W2 121.82(2), C1–S1–As1 108.61(10). **3a-II**: W1–P1 2.4134(11), W2–P1 2.4360(11), Se1–P1 2.1974(13), Se1–C11 1.924(4); W1–P1–W2 133.23(5), Se1–P1–W2 103.50(5), Se1–P1–W1 123.27(5). **3b**: W1–As1 2.5192(6), W2–As1 2.5024(6), As1–Se1 2.3193(8), Se1–C11 1.910(6); W2–As1–W1 133.83(3), Se1–As1–W1 103.28(2), Se1–As1–W2 122.86(3), C11–Se1–As1 108.23(16).*

When looking at the Ch–E bond lengths, the bonding situation is not immediately obvious. All the Ch–E bond lengths – as well as the E–W distances – are in between single and double bonds.[24,27] The shortening of these bonds can be explained by the donation of electron density from a lone pair at the chalcogen or from the d orbitals of the W atoms into the empty p orbital at the pentel atom, respectively. Such a shortening has also been described for the aminophosphinidene complex [(Ph)N(H)P{W(CO)$_5$}$_2$].[11] As–Se bond lengths similar to that found in **3b** (2.3193(8) Å) have been reported for [(η^5-C$_5$H$_4$CH$_3$)(CO)$_2$Mn]$_2$AsSePh (2.381(1) Å).[18] No thio-phosphinidene complex has been characterised by single crystal X-ray analysis so far. Due to the divergent conditions, it is very probable that the reaction proceeds *via* different reaction pathways. In the photolytic reactions of [Cp*E{W(CO)$_5$}$_2$] (**1a,b**) with R$_2$Ch$_2$, one possible reaction pathway could start with the formation of the ·[E{W(CO)$_5$}$_2$] radical (**E**),[13] by cleaving the Cp* substituent off homolytically (cf. Figure 3.4). The radical **E** then attacks the dichalcogenide under chalcogen–chalcogen bond cleavage, leading to the chalkogenopentelidene complex. The Cp*· radical formed in the first step reacts further, for example to 1,2,3,4-tetramethyl-5-methylenefulvene as well as different products generated through an unspecific recombination of the radical species. A second possible reaction pathway is the homolytic cleavage of the Ch–Ch bond in the dichalkogenide, in the first step leading to the ·ChR radical, which then reacts with **1a,b** to form intermediate **F**. After elimination of a ·Cp* radical from **F**, the chalkogenopentelidene complex is generated (cf. Figure 3.4). The formed RCh· and ·Cp* radicals in solution can recombine and be stabilised in many different ways, leading to a plethora of side products as observed

experimentally within the ^{31}P NMR spectra. Nevertheless, the question arises which pathway is more likely to occur. To answer it, DFT computations were carried out at the B3LYP/def2-SVPD level of theory (for details see chapter 3.4). The results show that the formation of the radical species E· and ·Cp* is endergonic by 54 kJ mol^{-1}, while generation of two PhS· radicals from Ph_2S_2 is endergonic by 137 kJ mol^{-1}. The subsequent reaction of **E** with Ph_2S_2 (cf. Figure 3.4) is exergonic by 23 kJ mol^{-1}. The process of formation of **F** from **1a** and PhS· is exergonic by 17 kJ mol^{-1}, and subsequent ·Cp* elimination from **F** is exergonic by 88 kJ mol^{-1}. Thus, the pathway via intermediate E is less energetically demanding than generation of PhS· radicals, but once PhS· is generated, its reaction with **1a** is thermodynamically allowed. In contrast, for the Se derivative, computations predict that the reaction of **E** with Ph_2Se_2 is endergonic by 21 kJ mol^{-1}, and the generation of PhSe· from Ph_2Se_2 is much more endergonic (199 kJ mol^{-1}), which may explain the experimentally observed absence of **3a-I** in the reaction of **1a** with Ph_2Se_2. Notably, in case of bulkier Mes substituents, reactions of **E** with Mes_2Ch_2 are predicted to be exergonic by 48, 10, and 12 kJ mol^{-1} for Ch = S, Se, and Te, respectively. This, along with the smaller energetic demand to generate MesCh· from Mes_2Ch_2, is in agreement with the experimentally observed formation of **3a-II** and **4a-I**.

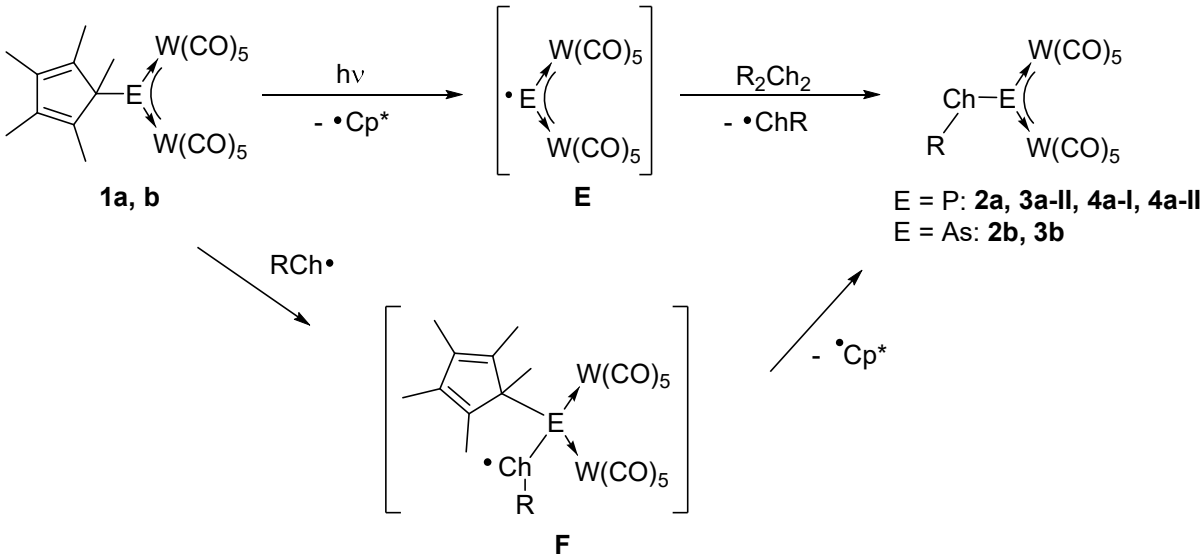

***Figure 3.4**: Possible reaction pathways in the reaction of **1a,b** with R_2Ch_2.*

Since the reactions with the dichalcogenides did not result in high yields and because the products could not always be isolated successfully, we tried a different synthetic route using chalcogenols PhChH (Ch = S, Se) as nucleophiles (cf. Figure 3.1). Since tellurols are unstable at room temperature,[28] reactions of **1a,b** with tellurols were not conducted. Comparing dichalcogenides with chalcogenols as starting materials in these reactions, the chalcogenols PhSH and PhSeH result in cleaner reactions by revealing less phosphorus-containing side products in the ^{31}P NMR spectra of the respective reaction mixtures. This indicates that the reaction might not proceed via a radical mechanism. The NMR yields of **2a** could

also be increased to 19 %. Further, the reaction time was decreased significantly from a few days in the reactions with R_2Ch_2 at room temperature to a few hours using chalcogenols as starting materials. However, **3a-I** and **2b** seem to decompose or react further at elevated temperatures in solution, since the reaction solutions turn brownish red when warmed up to room temperature. In the reaction of **1a** with PhSeH, **3a-I** could be isolated at -30 °C (cf. Figure 3.5).

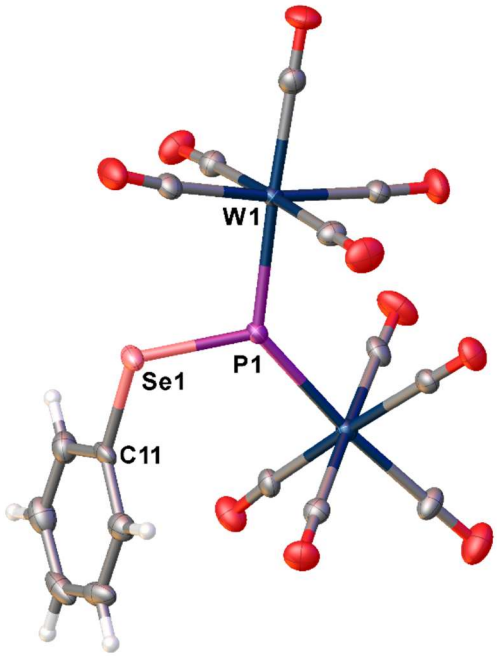

***Figure 3.5**: Molecular structure of **3a-I**. Anisotropic displacement parameters are set to 50% probability level. Selected distances (Å) and angles (°): W1–P1 2.4232(11), W2–P1 2.4141(11), Se1–P1 2.2060(13), Se1–C11 1.925(5); W2–P1–W1 132.95(5), Se1–P1–W1 104.19(4), Se1–P1–W2 122.84(5), C11–Se1–P1 107.95(14).*

In contrast to the reaction solution, the isolated crystals are stable at room temperature. A possible reaction pathway for the reactions of **1a** with PhChH is depicted in Figure 3.6. The chalcogenol attacks the phosphinidene complex at the pentel atom, forming an adduct (**G**). After the Cp*H elimination, the chalcogenophosphinidene complex is formed.

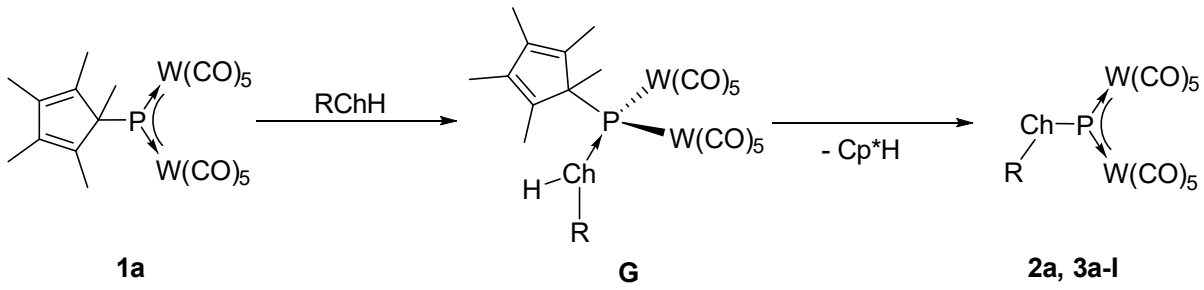

***Figure 3.6**: Proposed reaction pathway for the reaction of **1a** with chalcogenols.*

This kind of mechanism – the formation of an adduct and subsequent Cp*H elimination – was already observed in the reactions of **1a** with nucleophiles such as e.g. amines[11] or phosphines.[29] Additionally, in contrast to the radical mechanism, this reaction pathway should be more selective, which can also be seen in the ^{31}P NMR spectra of the respective reaction mixtures (cf. chapter 3.4), because in the chalkogenol reactions, there are fewer side products present. DFT computations indicate that formation of the intermediate **1a**·PhChH (**G**) is endergonic by 83, 81, and 75 kJ mol^{-1} for Ch = S, Se, and Te, respectively. However, subsequent elimination of Cp*H and formation of **2a** and **3a-I** is highly exergonic (by 170 and 175 kJ mol^{-1}, respectively) and the overall reaction of **1a** with PhChH is thermodynamically allowed for all Ch, in line with experimental findings

3.3 Conclusion

We herein report a general pathway for the synthesis of chalcogenopentelidene complexes. Through the reaction of **1a** and **1b** with the dichalcogenides R_2Ch_2, the chalcogenophosphinidene complexes **2a** and **3a-II** as well as the chalcogenoarsinidene complexes **2b** and **3b** were isolated and fully characterised. Additionally, the formation of the tellurophosphinidene complexes **4a-I** and **4a-II** can be assumed as indicated by the ^{31}P NMR spectra of the reaction solutions. This assumption is further supported because of the calculated ^{31}P NMR shifts of **4a-I** and **4a-II** compare well with the experimental values. As products of the reaction of **1a** with the chalcogenols PhChH, the chalcogenophosphinidene complexes **2a** and **3a-I** were obtained and characterized as well. The approach via chalcogenols seems to be a preferable synthetic route, due to smoother reaction conditions by shorter reaction times and lower conversion temperatures.

These novel compounds exhibit interesting bonding properties such as the partial double bond character of the E-Ch bonds and the shortened E-W distances. In order to elucidate the reaction pathways, DFT calculations were carried out to find the most probable reaction pathway for these reactions.

3.4 Supporting Information

3.4.1 Working techniques

The following reactions were carried out under an atmosphere of dry Nitrogen or Argon using standard Schlenk techniques. Traces of O_2 were eliminated by leading the inert gas (N_2 or Ar) through a copper catalyst heated to 145 °C, subsequently washing it with concentrated sulphuric acid and drying it with orange gel and phosphorous pentoxide. Solvents were either collected from a solvent purification system (MBraun SPS 800) or dried, degassed and distilled according to standard techniques. Before use, the diatomaceous earth required for filtration was stored at 110 °C. The silica gel 60 required for column chromatography (particle size 0.063-0.2 mm) was dried at 150 °C in vacuo for 3 d prior to use. For photolytical reactions, a mercury vapor lamp from the Hanau company (type TQ 150) was used.

The **NMR spectra** were recorded on a BRUKER Avance 300 (^{1}H: 300.13 MHz, ^{13}C: 75.48 MHz, ^{31}P: 121.49 MHz) or Avance 400 (^{1}H: 400.13 MHz, ^{13}C: 100.61 MHz, ^{31}P: 161.98 MHz) spectrometer at room temperature unless stated otherwise. Chemical shifts δ refer to external standards of tetramethylsilane (^{1}H, ^{13}C NMR) and 85 % phosphoric acid (^{31}P NMR, ^{31}P{^{1}H} NMR), respectively, and are given in ppm. Coupling constants J are given in Hz without consideration of absolute signs. Analysis, Simulations and graphic representations of the spectra were prepared with *TopSpin 3.0*[30]. **Infrared spectra** were recorded in solution (CH_2Cl_2) with a ThermoScientific Nicolet iS5 spectrometer using the iD5 Transmission element or an ATR element equipped with a Ge crystal. **Mass spectra** were recorded on a Jeol AccuTOF GCX (FD) spectrometer by the mass spectrometry department of the University of Regensburg or a ThermoQuest Finnigan MAT 95 spectrometer. **Elemental analysis** was conducted by the microanalytics laboratory of the University of Regensburg with the Elementar Vario MICRO cube**.**

The following substances were bought or synthesized according to standard techniques: [Cp*P{W(CO)$_5$}$_2$] (**1a**)[8], [Cp*As{W(CO)$_5$}$_2$] (**1b**)[8], Ph_2S_2, PhSH, Ph_2Se_2, Mes_2Se_2[31], PhSeH, Mes_2Te_2[1], $Tipp_2Te_2$[32].

[1] Mes_2Te_2 was synthesized analogously to Mes_2Se_2.

3.4.2 Experimental Data with NMR details

3.4.2.1 Synthesis of 2a

A solution of Ph_2S_2 (44 mg, 0.2 mmol) in 20 mL of toluene was added dropwise to a solution of **1a** (163 mg, 0.2 mmol) in 30 mL of toluene at room temperature. The mixture was stirred for two days, whereupon the blue solution turned violet. The solvent was removed in vacuo and the residue recrystallized from hexane at -28 °C, to give green, shiny crystals of [PhSP{W(CO)$_5$}$_2$] (**2a**). NMR yield: 21 mg (13 %)

Photolytical reaction: A mixture of **1a** (163 mg, 0.2 mmol) and Ph_2S_2 (44 mg, 0.2 mmol) in 50 mL of toluene was irradiated for 2 h with a TQ 150 Hg lamp until the reaction solution turned violet. The solution was then concentrated and stored at -28 °C, where a dark green powder of [PhSP{W(CO)$_5$}$_2$] (**2a**) could be obtained. NMR yield: 19 mg (12 %)

Chalkogenol reaction: A solution of PhSH (22 mg, 0.02 mL, 0.2 mmol) in 20 mL of toluene was added dropwise to a solution of **1a** (163 mg, 0.2 mmol) at -80 °C. The mixture was stirred and warmed to room temperature, whereupon the blue solution turned violet. After extraction of the dried reaction mixture with hexane, a few crystals of **2a** could be obtained by storing the concentrated hexane solution at -28 °C. NMR yield: 30 mg (19 %)

Analytical data for **2a**:

^{1}H NMR (CD_2Cl_2, 400 MHz):	δ [ppm] = 7.55 (m, 3H), 7.65 (m, 2H).
^{31}P{^{1}H} NMR (CD_2Cl_2, 162 MHz):	δ [ppm] = 822.9 (s, $^1J_{P,W}$ = 192 Hz).
^{31}P NMR (CD_2Cl_2, 162 MHz):	δ [ppm] = 822.9 (s, $^1J_{P,W}$ = 192 Hz).
IR (KBr):	ν_{max}/cm^{-1} = 2962 w (CH), 2922 w (CH), 2852 w (CH), 2093 m (CO), 2055 s (CO), 1956 sh (CO), 1937 vs br (CO).
MS (EI, 70eV):	m/z (%): 787.7 (11) [M$^+$], 703.8 (9) [M$^+$-3CO], 678.7 (19) [P{W(CO)$_5$}$_2^+$], 650.7 (17) [P{W(CO)$_5$}$_2^+$-CO], 619.9 (29) [M$^+$-6CO], 591.8 (37) [M$^+$-7CO], 563.9 (29) [M$^+$-8CO], 535.9 (28) [M$^+$-9CO], 507.9 (60) [M$^+$-10CO], 481.9 (22) [P{W(CO)$_5$}$_2^+$-7CO], 352.0 (14) [W(CO)$_6^+$], 295.9 (12) [W(CO)$_6^+$-2CO], 268.0 (23) [W(CO)$_6^+$-3CO], 240.0 (9) [W(CO)$_6^+$-4CO], 212.0 (8) [W(CO)$_6^+$-5CO], 186.0 (12) [W(CO)$_6^+$-6CO], 110.0 (33) [PhSH$^+$], 78.1 (100) [Ph$^+$].
elemental analysis:	calcd (%) for $C_{16}H_5O_{10}PSW_2$: C 24.39, H 0.64, S 4.07; found: C 25.65, H 0.89, S 4.04

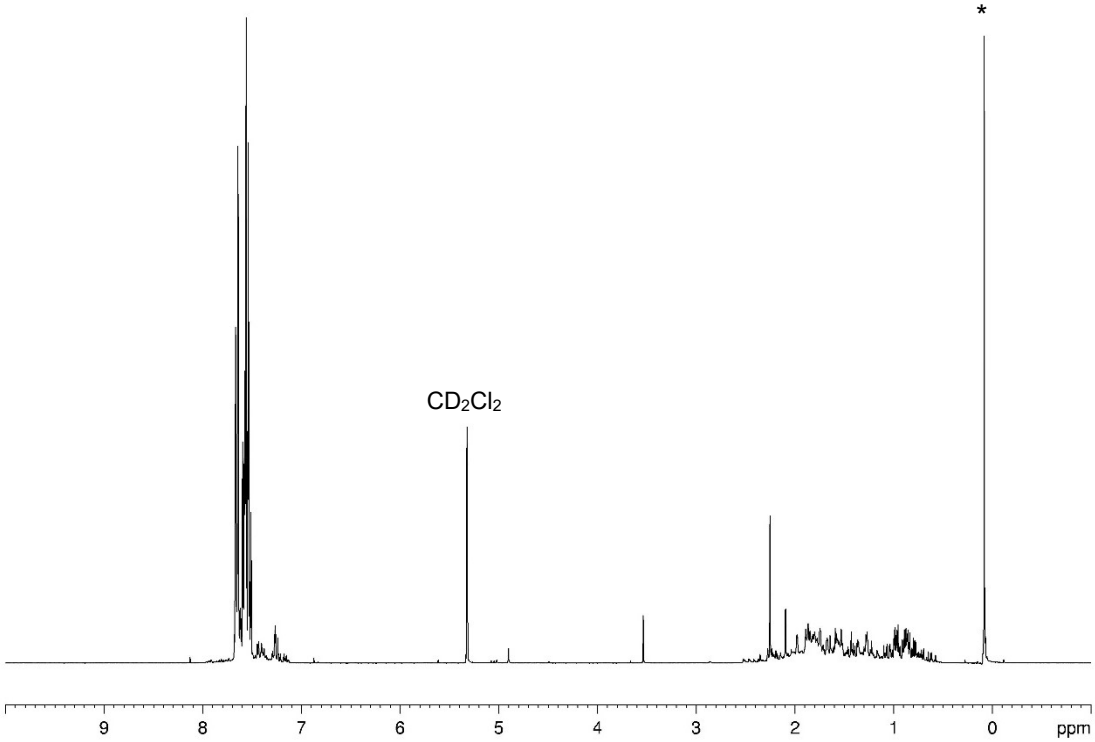

***Figure 3.7**: ^{1}H NMR spectrum of **2a** in CD_2Cl_2. * = grease*

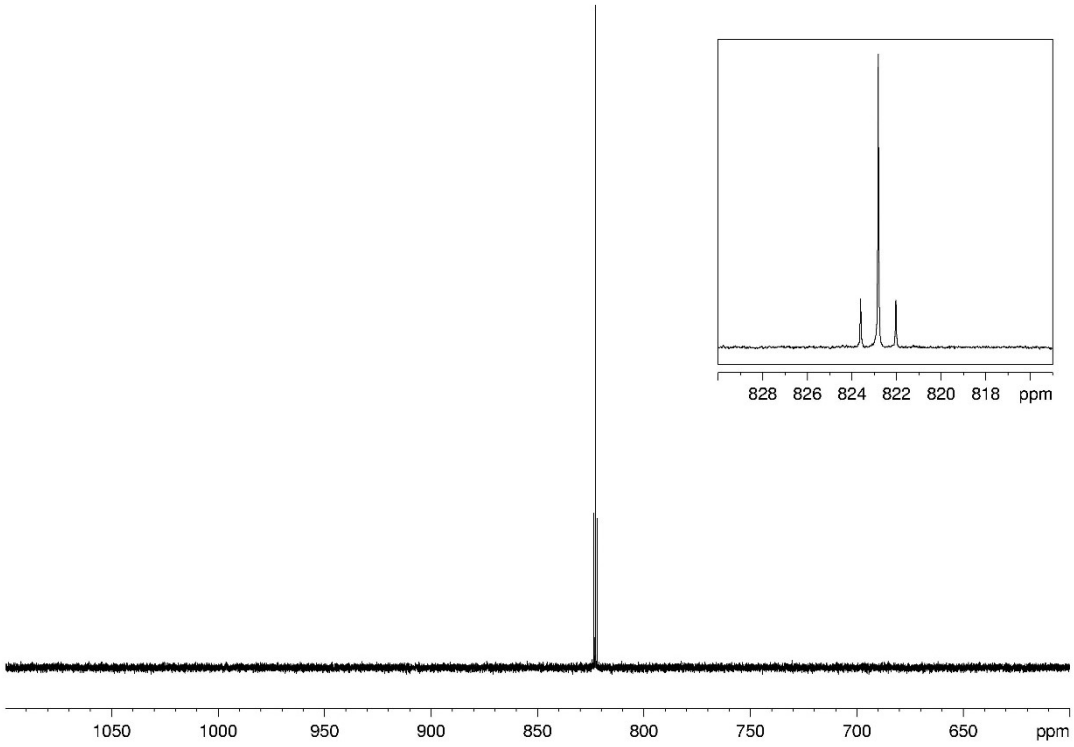

***Figure 3.8**: $^{31}P\{^{1}H\}$ NMR spectrum of **2a** in CD_2Cl_2.*

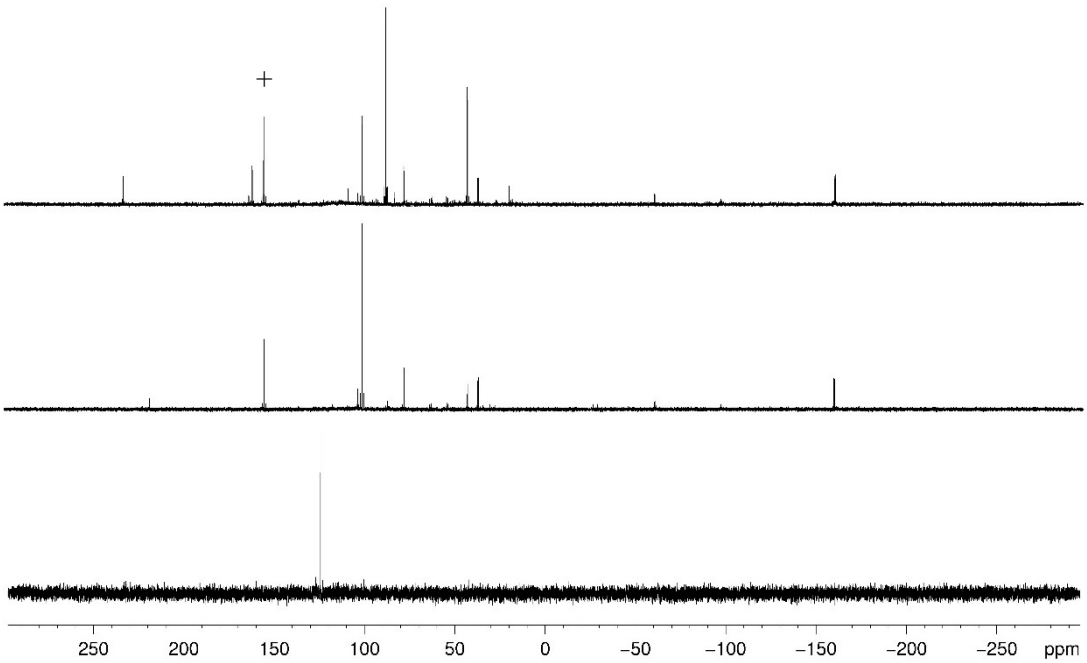

Figure 3.9: *Part of the $^{31}P\{^{1}H\}$ NMR spectra of the reaction mixtures of* ***1a*** *+ Ph_2S_2 in CD_2Cl_2. Bottom to top: Irradiation, stirring at room temp., heating to 90 °C. + = impurity in* ***1a****. Rest of the products could not be identified.*

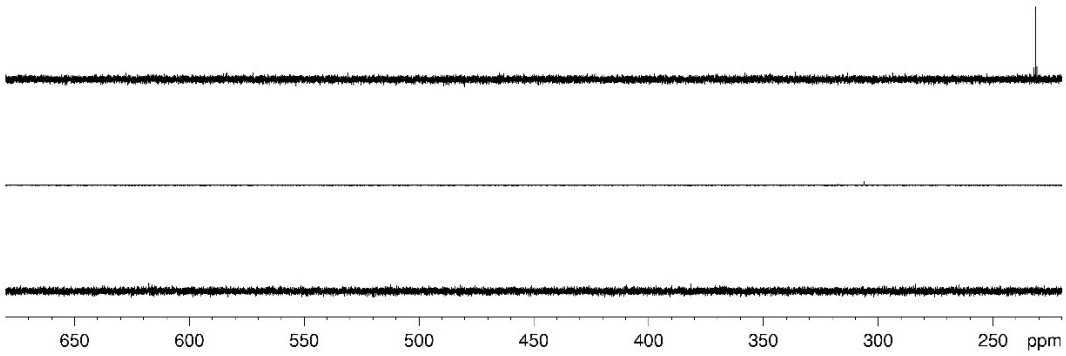

Figure 3.10: *Part of the $^{31}P\{^{1}H\}$ NMR spectra of the reaction mixtures of* ***1a*** *with Ph_2S_2 in CD_2Cl_2. Bottom to top: Irradiation, stirring at room temp., heating to 90 °C.*

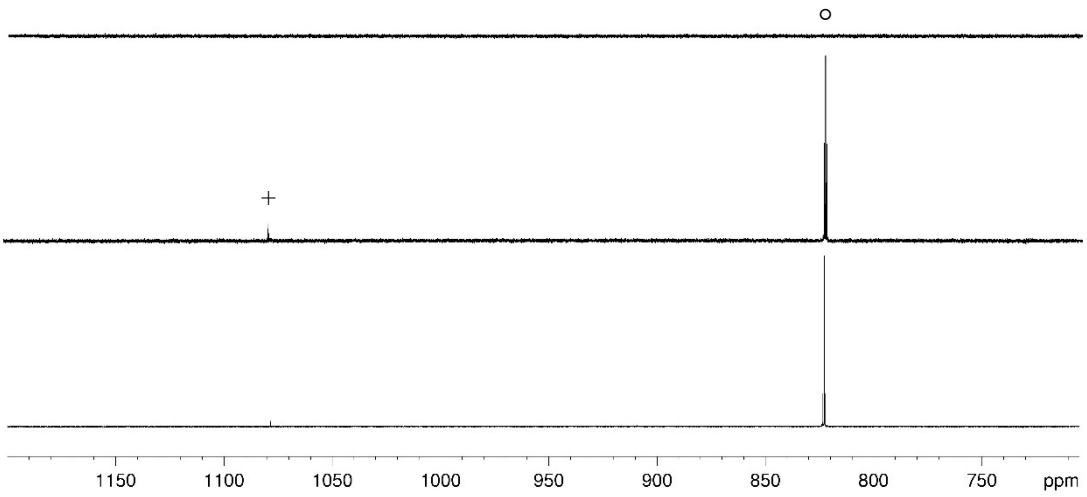

Figure 3.11: *Part of the $^{31}P\{^1H\}$ NMR spectra of the reaction mixtures of* ***1a*** *+ Ph_2S_2 in CD_2Cl_2. Bottom to top: Irradiation, stirring at room temp., heating to 90 °C. + =* ***1a****, ° =* ***2a****.*

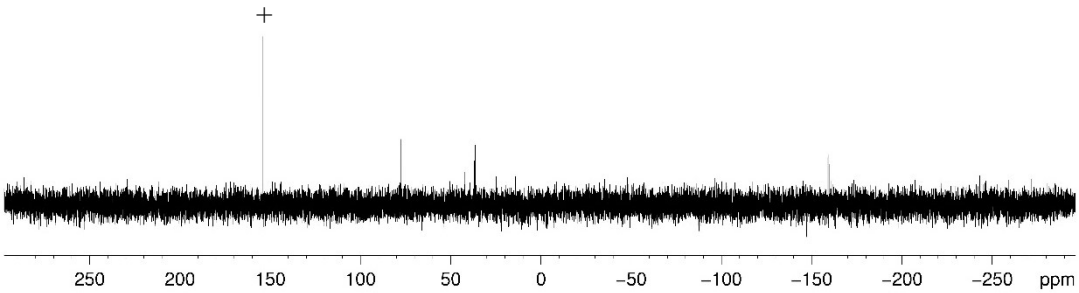

Figure 3.12: *Part of the $^{31}P\{^1H\}$ NMR spectrum of the reaction mixture of* ***1a*** *+ PhSH in in CD_2Cl_2. + = impurity in* ***1a****.*

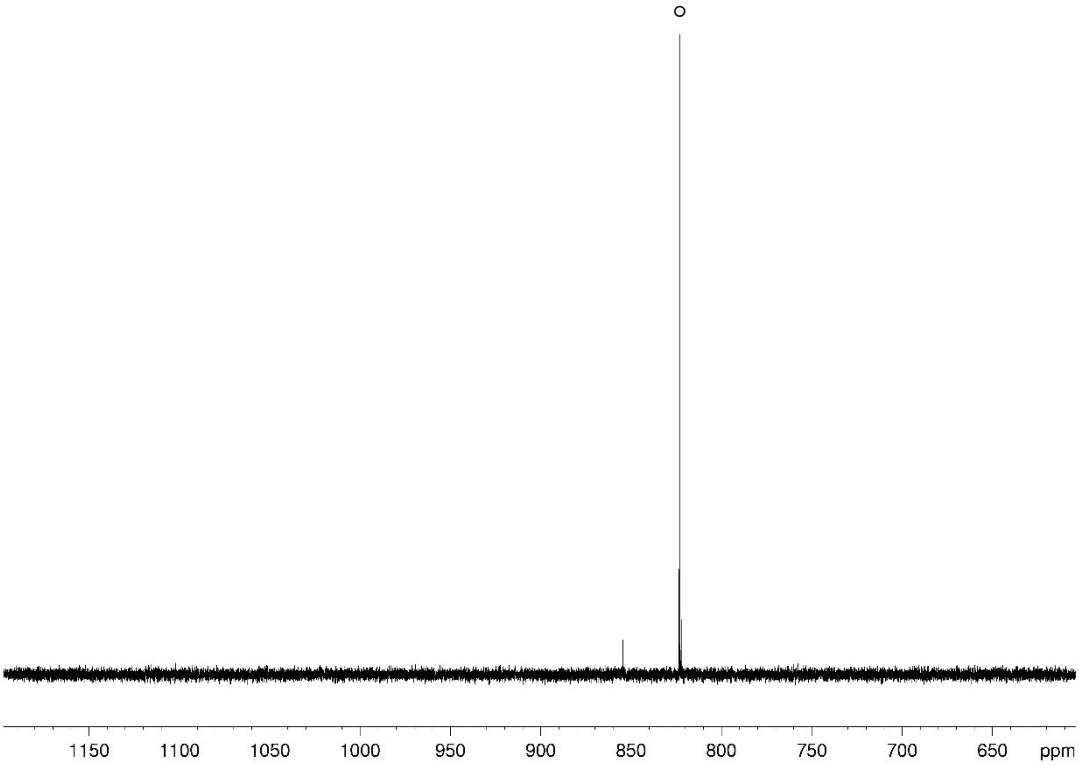

***Figure 3.13**: Part of the $^{31}P\{^{1}H\}$ NMR spectrum of the reaction mixture of **1a** + PhSH in CD_2Cl_2. ° = **2a**.*

3.4.2.2 Reaction of 1b with Ph_2S_2

A solution of Ph_2S_2 (44 mg, 0.2 mmol) in 20 mL of toluene was added dropwise to a solution of **1b** (172 mg, 0.2 mmol) in 30 mL of toluene at room temperature. The mixture was stirred for two days, whereupon the blue solution turned violet. The solvent was removed in vacuo and the residue was dissolved again in hexane. After storing the solution at -28 °C, green shiny crystals of **2b** could be obtained. **Yield**: 17 mg (10 %).

Heating the reaction solution to 90 °C for 2h results in a brownish green solution. After removing the solvent and extracting the residue with hexane, the known compounds $[PhS\{W(CO)_4\}]_2$ (green blocks) and $(PhS)_3As$ (brown plates) were obtained as a few crystals each at – 28 °C from the hexane phase. Since there is no suitable NMR active nucleus present in the desired compound $[PhSAs\{W(CO)_5\}_2]$ (**2b**), we cannot say whether **2b** is formed or not in this reaction.

<u>Chalkogenol reaction:</u> A solution of PhSH (0.02 mL, 22 mg, 0.2 mmol) in 5 mL of toluene was added dropwise to a solution of **1b** (172 mg, 0.2 mmol) in 20 mL of toluene at – 80 °C. The solution was then warmed to -10 °C, where the blue solution turned violet. The solvent was removed in vacuo and the residue was extracted with hexane. Storing the violet hexane solution at -28 °C gave a few green shiny crystals of **2b**.

Analytical data for **2b**:

^{1}H NMR (C_6D_6, 400 MHz):	δ [ppm] = 7.01 (m, 3H), 7.19 (m, 2H).
IR (KBr):	ν_{max}/cm^{-1} = 2965 w (CH), 2918 w (CH), 2851 w (CH), 2091 m (CO), 2058 s (CO), 2017 sh (CO), 1970 sh (CO), 1933 vs (CO).
MS (EI, 70eV):	m/z (%): 831.5 (1) [M$^+$], 803.6 (1) [M$^+$-CO], 775.6 (1) [M$^+$-2CO], 722.6 (1) [M$^+$-PhS], 694.6 (1) [M$^+$-PhS-CO], 666.6 (1) [M$^+$-PhS-2CO], 635.7 (1) [M$^+$-7CO], 607.8 (1) [M$^+$-8CO], 579.7 (1) [M$^+$-9CO], 551.8 (1) [M$^+$-10CO], 442.8 (1) [M$^+$-PhS-10CO], 351.9 (1) [W(CO)$_6^+$], 295.9 (1) [W(CO)$_6^+$-2CO], 268.0 (2) [W(CO)$_6^+$-3CO], 239.9 (1) [W(CO)$_6^+$-4CO], 212.0 (1) [W(CO)$_6^+$-5CO].
elemental analysis:	calcd. (%) for $C_{16}H_5AsO_{10}SW_2$: C 23.10, H 0.61, S 3.85; found: C 23.33, H 0.70, S 3.82.

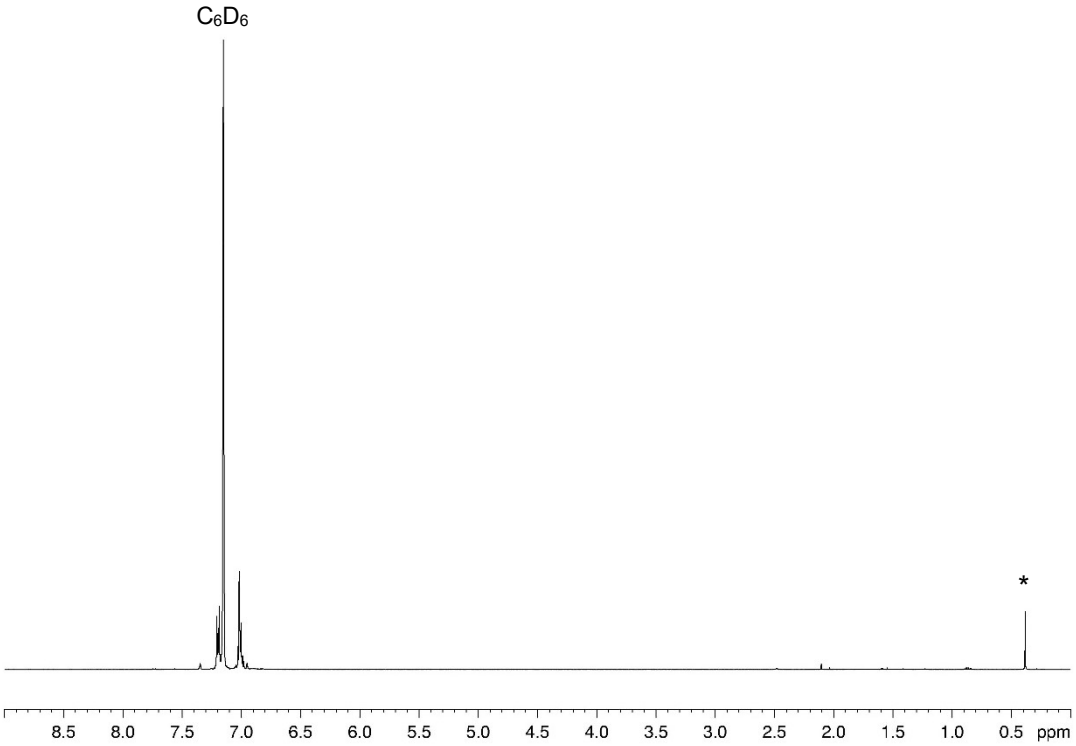

Figure 3.14: *^{1}H NMR spectrum of **2b** in C_6D_6. * = grease*

3.4.2.3 Synthesis of 3a-I

A solution of PhSeH (0,02 mL, 31 mg, 0.2 mmol) in 20 mL of toluene was added dropwise to a solution of **1a** (163 mg, 0.2 mmol) in 30 mL of toluene at -80 °C. The mixture was stirred until the cooling bath reached –30 °C and the solution turned violet. After analyzing the reaction solution spectroscopically, it was stored at -28 °C and a few dark red plates of [PhSeP{W(CO)$_5$}$_2$] (**3a-I**) could be obtained. The rest of the solution was then spectroscopically characterized.

Analytical data for **3a-I**:

Yield:	27 mg (15 %).
^{31}P{^{1}H} NMR (C_6D_6, 162 MHz):	δ [ppm] = 835.0 (s, $^1J_{P,W}$ = 186 Hz, $^1J_{P,Se}$ = 488 Hz).
^{31}P NMR (C_6D_6, 162 MHz):	δ [ppm] = 835.0 (s, $^1J_{P,W}$ = 186 Hz, $^1J_{P,Se}$ = 488 Hz).

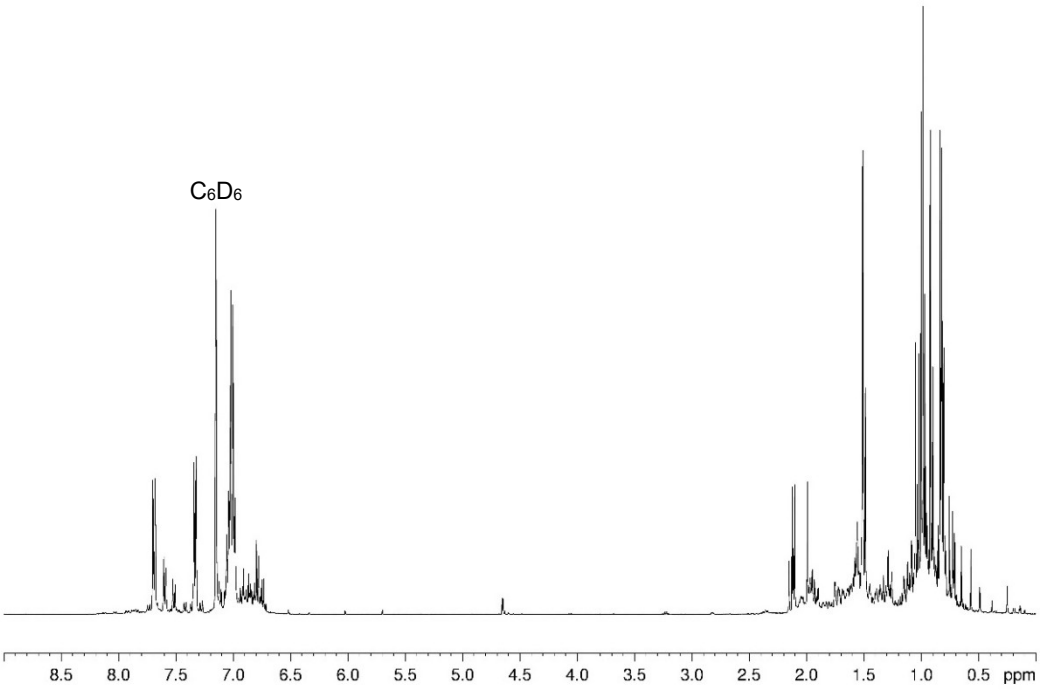

Figure 3.15: *^{1}H NMR spectrum of the reaction mixture of **1a** + PhSeH in C_6D_6.*

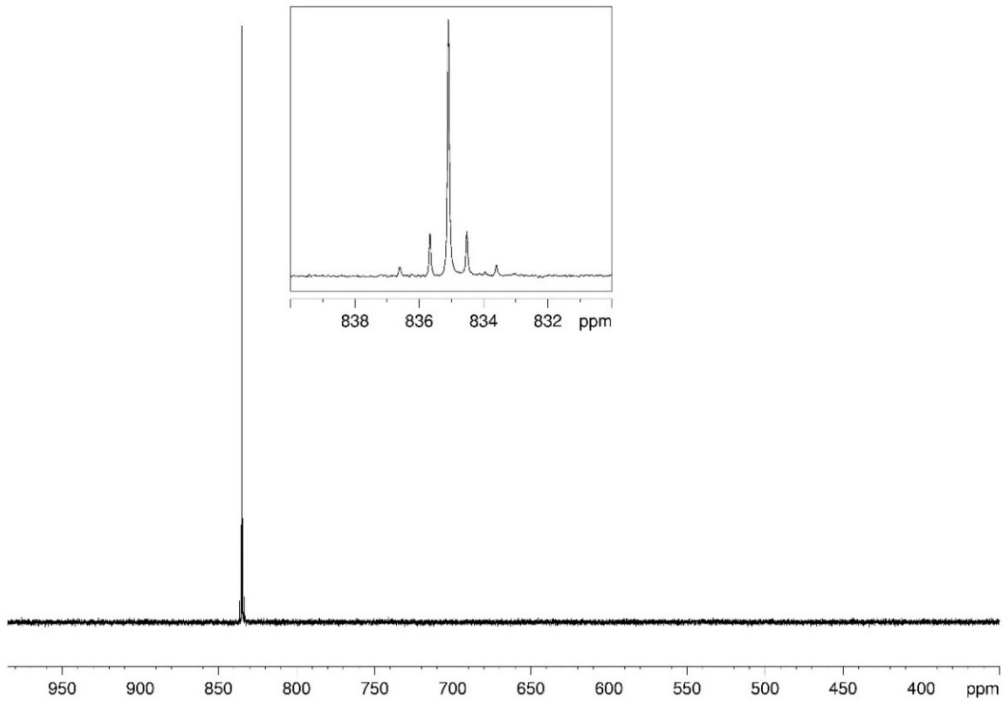

Figure 3.16: *$^{31}P\{^1H\}$ NMR spectrum of* ***3a-I*** *in C_6D_6.*

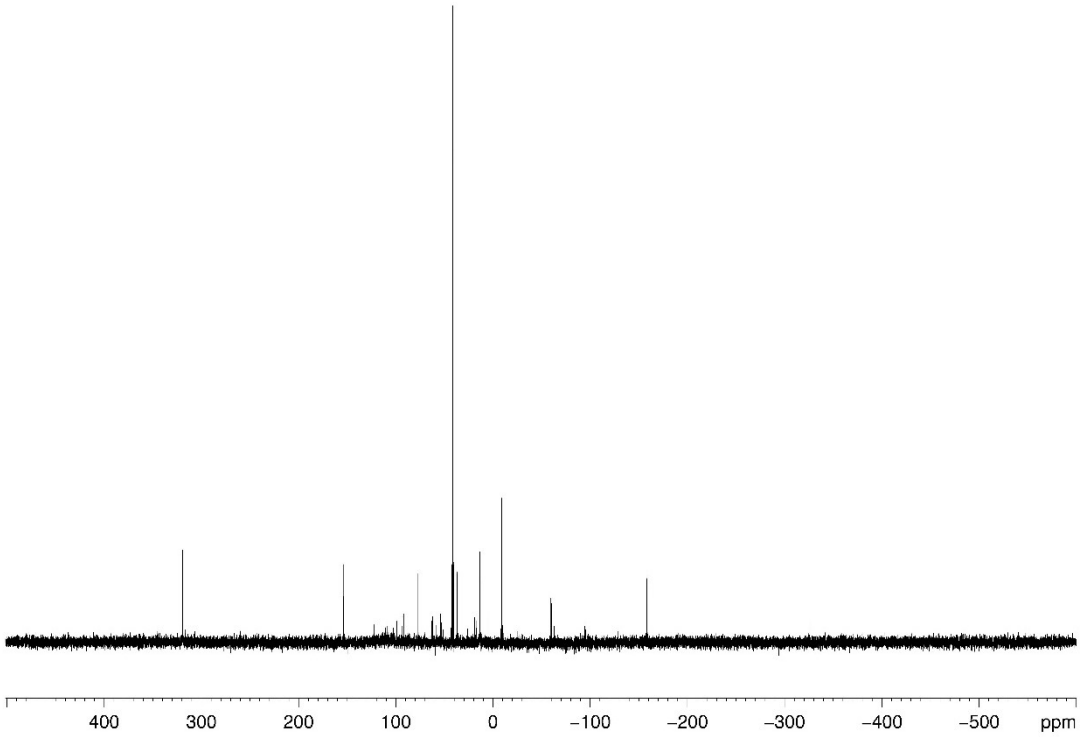

Figure 3.17: *$^{31}P\{^1H\}$ NMR spectrum of the reaction mixture of* ***1a*** *+ PhSeH in C_6D_6.*

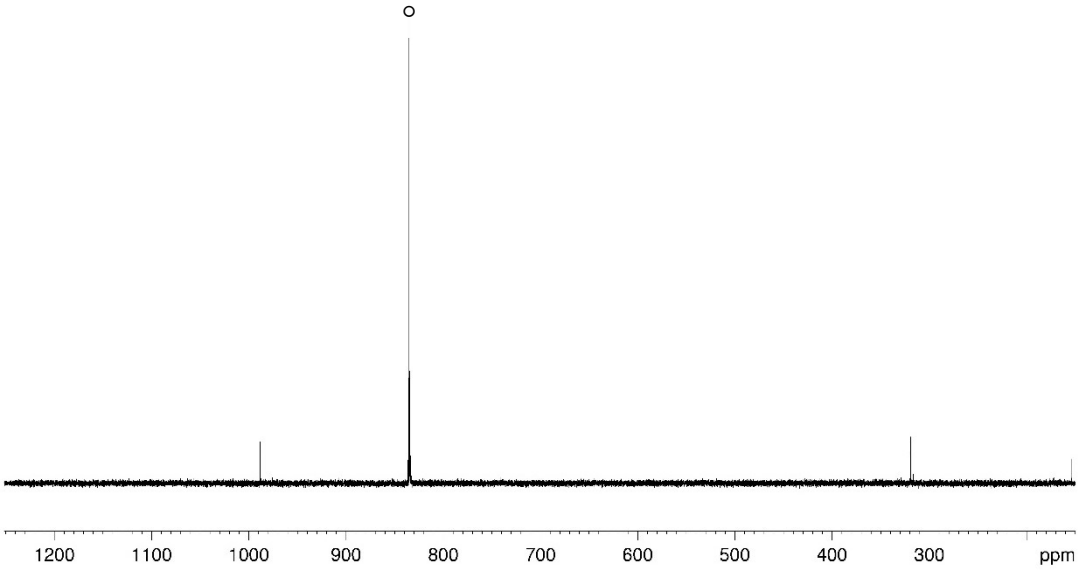

***Figure 3.18**: $^{31}P\{^1H\}$ NMR spectra of the reaction mixture of **1a** + PhSeH in C_6D_6. ° = **3a-I**.*

3.4.2.4 Synthesis of 3a-II

A solution of Mes_2Se_2 (160 mg, 0.4 mmol) in 20 mL of toluene was added dropwise to a solution of **1a** (326 mg, 0.4 mmol) in 30 mL of toluene at room temperature. The mixture was stirred for two days, whereupon the blue solution turned violet. After removing the solvent and recrystallizing from CH_2Cl_2 at -28 °C, green, shiny crystals of [MesSeP{W(CO)$_5$}$_2$] (**3a-II**) could be obtained.

Analytical data for **3a-II**:

Yield:	57 mg (15 %).
^{1}H NMR (CD_2Cl_2, 400 MHz):	δ [ppm] = 2.32 (s, 3H, *p*-CH_3), 2.44 (s, 6H, *o*-CH_3), 7.10 (s, 2H, Mes).
$^{31}P\{^1H\}$ NMR (CD_2Cl_2, 162 MHz):	δ [ppm] = 854.3 (s, $^1J_{P,W}$ = 184 Hz, $^1J_{P,Se}$ = 507 Hz).
^{31}P NMR (CD_2Cl_2, 162 MHz):	δ [ppm] = 854.3 (s, $^1J_{P,W}$ = 184 Hz, $^1J_{P,Se}$ = 507 Hz).
IR (KBr):	ν_{max}/cm^{-1} = 2957 w (CH), 2919 w (CH), 2850 w (CH), 2090 m (CO), 2053 s (CO), 2015 sh (CO), 1956 vs (CO), 1936 vs (CO).
MS (EI, 70eV):	m/z (%): 877.8 (2) [M$^+$], 678.9 (16) [P{W(CO)$_5$}$_2^+$], 651.0 (15) [P{W(CO)$_5$}$_2^+$-CO], 622.9 (8) [P{W(CO)$_5$}$_2^+$-2CO], 595.9 (17) [P{W(CO)$_5$}$_2^+$-3CO], 567.0 (4) [P{W(CO)$_5$}$_2^+$-4CO], 538.9 (3) [P{W(CO)5}2$^+$-5CO].
elemental analysis:	calcd. (%) for $C_{19}H_{11}O_{10}PSeW_2$: C 26.02, H 1.26; found: C 24.63, H 1.28.

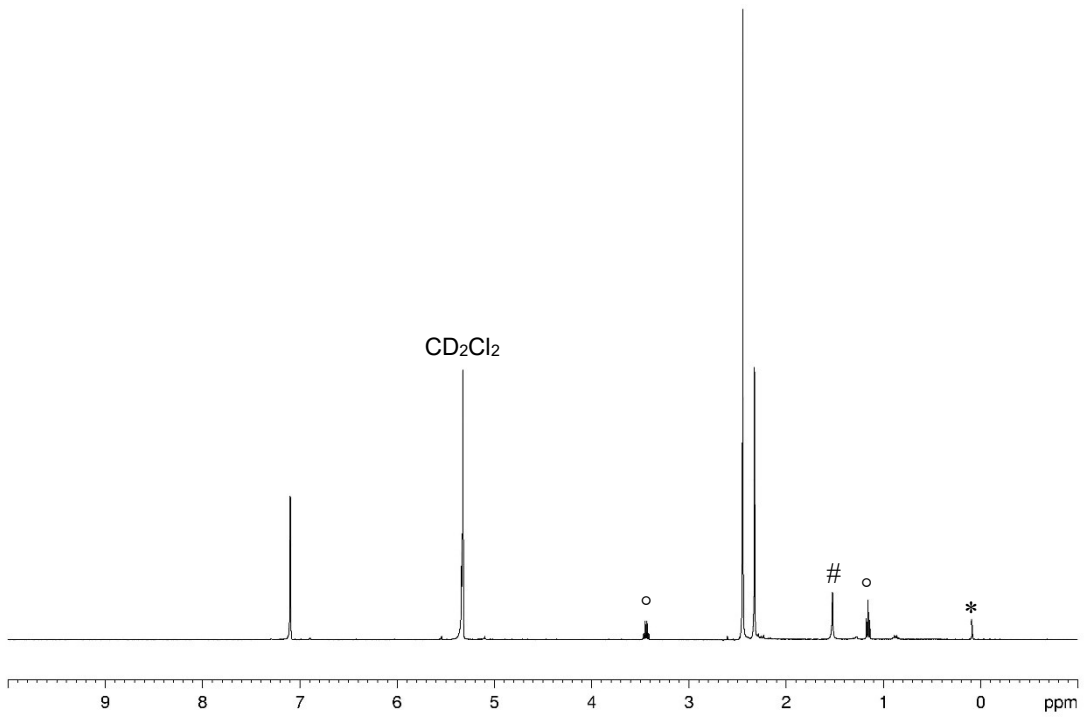

Figure 3.19: *^{1}H NMR spectrum of* ***3a-II*** *in CD_2Cl_2. ° = Et_2O, # = H_2O, * = grease*

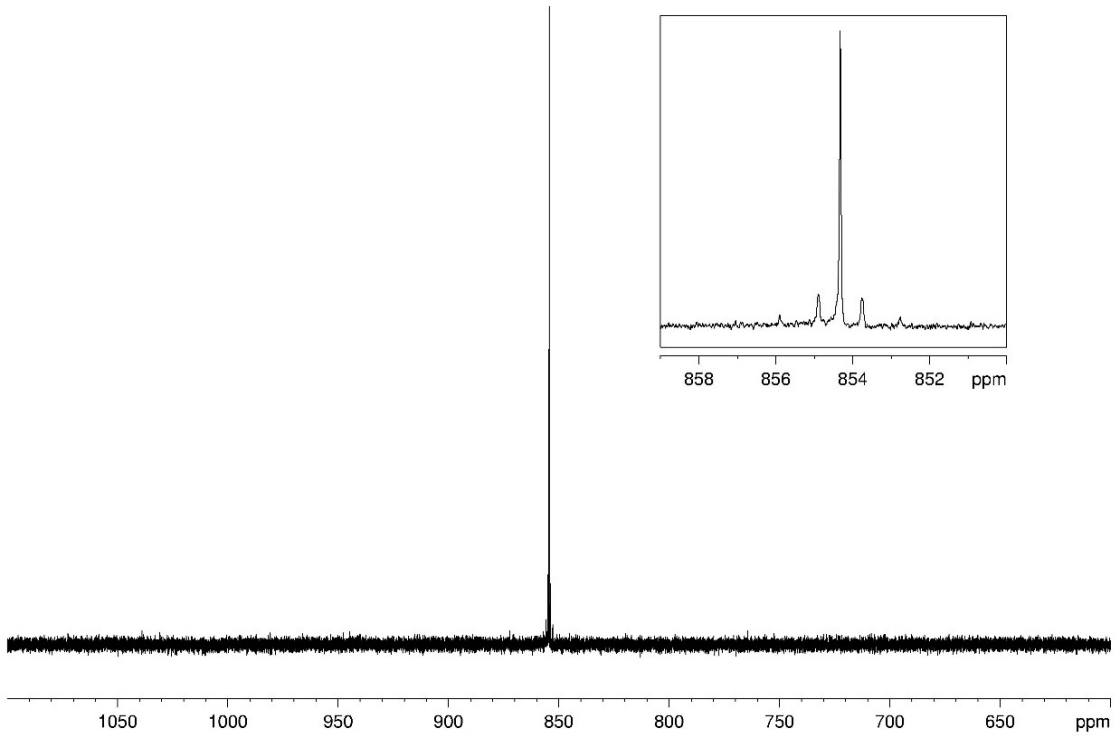

Figure 3.20: *$^{31}P\{^{1}H\}$ NMR spectrum of* ***3a-II*** *in CD_2Cl_2.*

3.4.2.5 Synthesis of 3b

A solution of Mes_2Se_2 (80 mg, 0.2 mmol) in 20 mL of toluene was added dropwise to a solution of **1b** (172 mg, 0.2 mmol) in 30 mL of toluene at room temperature. The mixture was stirred for two days, whereupon the blue solution turned violet. After recrystallizing from CH_2Cl_2 at -28 °C, green, shiny crystals of [MesSeAs{W(CO)$_5$}$_2$] (**3b**) could be obtained.

Analytical data for **3b**:

Yield:	20 mg (11 %).
^{1}H NMR ($CDCl_3$, 400 MHz):	δ [ppm] = 2.37 (s, 3H, *p*-CH_3), 2.43 (s, 6H, *o*-CH_3), 7.10 (s, 2H, Mes).
IR (KBr):	ν_{max}/cm^{-1} = 2964 w (CH), 2919 w (CH), 2850 w (CH), 2088 m (CO), 2051 s (CO), 2014 sh (CO), 1998 sh (CO), 1954 vs (CO), 1935 vs (CO).
MS (EI, 70eV):	m/z (%): 922.0 (2) [M$^+$], 722.9 (48) [As{W(CO)$_5$}$_2^+$], 694.8 (25) [As{W(CO)$_5$}$_2^+$-CO], 666.8 (48) [As{W(CO)$_5$}$_2^+$-2CO], 639.9 (87) [As{W(CO)$_5$}$_2^+$-3CO].
elemental analysis:	calcd. (%) for $C_{16}H_5AsO_{10}SW_2$: C 24.78, H 1.20; found: C 25.77, H 1.31.

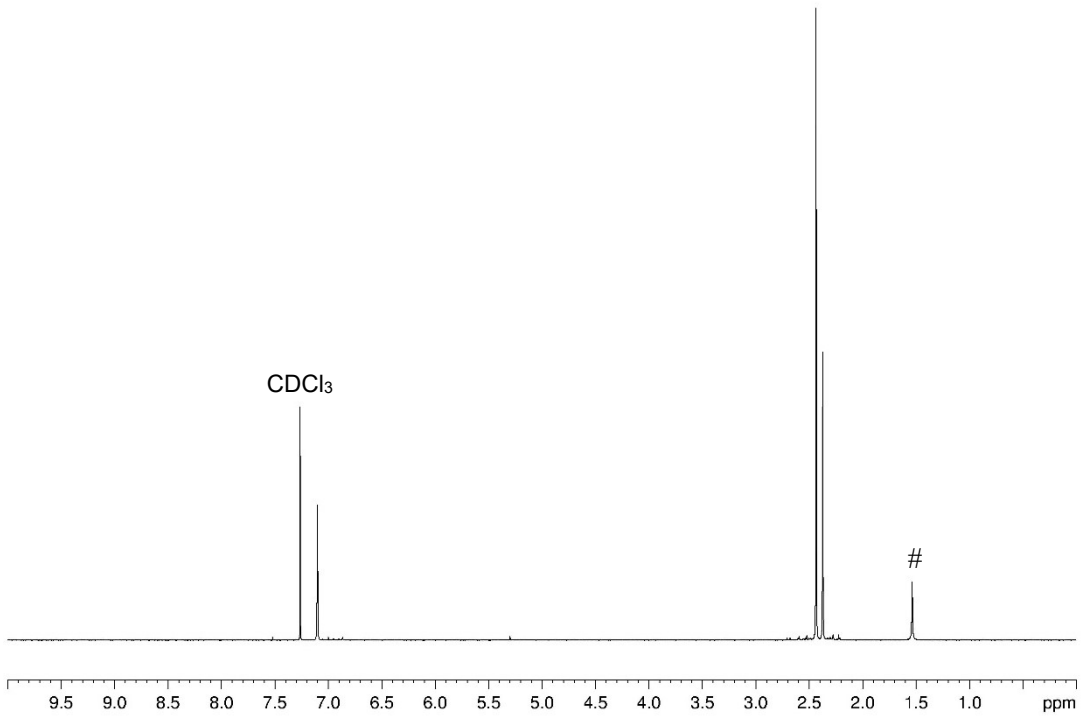

Figure 3.21: *^{1}H NMR spectrum of **3b** in $CDCl_3$. # = H_2O*

3.4.2.6 Reaction of 1a with Ph_2Se_2

A solution of Ph_2Se_2 (36 mg, 0.2 mmol) in 10 mL toluene was added dropwise to a solution of **1a** (163 mg, 0.2 mmol) in 20 mL toluene at -80 °C. The solution is warmed to room temperature and stirred for 3 d, whereupon the blue solution turns brown. After analyzing the reaction solution via $^{31}P\{^1H\}$ NMR spectroscopy, it was purified via column chromatography (ø = 2.5 cm, l = 10 cm) using hexane/toluene in a 2:1 ratio. $[PhSeW(CO)_4]_2$ (**5**) crystallizes from the first of three fractions as green needles.

Analytical data for **5**:

Yield:	4 mg (2 %).
^1H NMR (CD_2Cl_2, 400 MHz):	δ [ppm] = 7.31 (m, 6*H*, CH), 7.46 (m, 4*H*, CH).

Reaction solution:

$^{31}P\{^1H\}$ NMR ($CDCl_3$, 162 MHz):	δ [ppm] = 41.0 (s, $^1J_{P,W}$ = 275 Hz, 305 Hz $^1J_{P,Se}$ = 580 Hz, 607 Hz).
^{31}P NMR ($CDCl_3$, 162 MHz):	δ [ppm] = 41.0 (s, $^1J_{P,W}$ = 277 Hz, 303 Hz $^1J_{P,Se}$ = 582 Hz, 610 Hz).

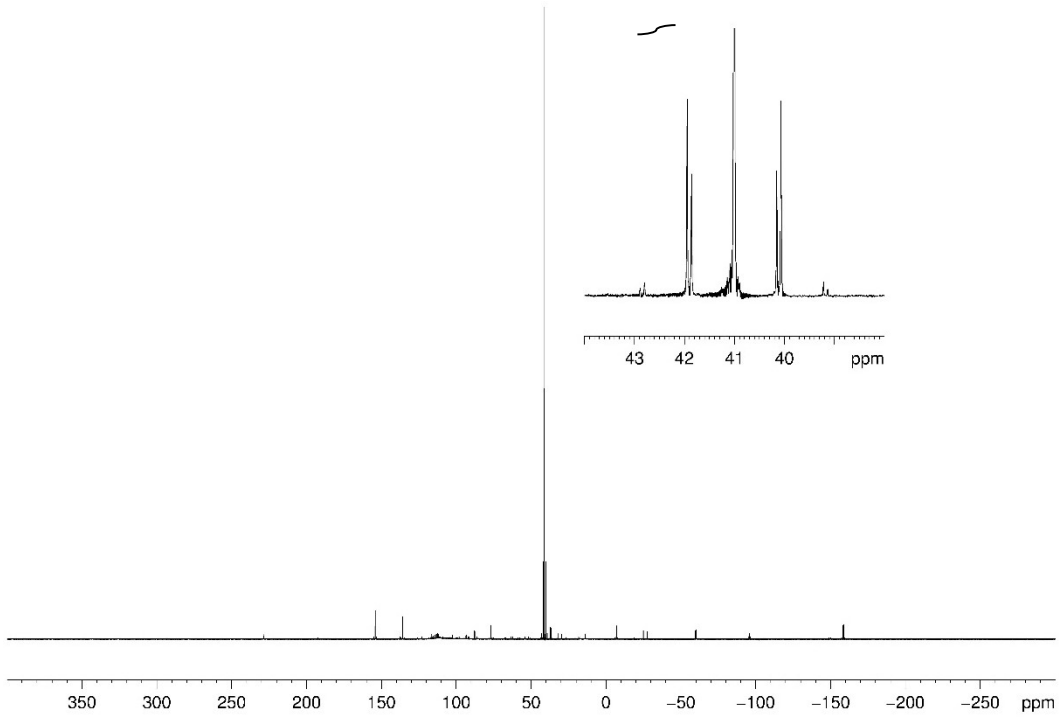

***Figure 3.22**: $^{31}P\{^1H\}$ NMR spectrum of the reaction solution of **1a** + Ph_2Se_2 in $CDCl_3$.*

3.4.2.7 Reaction of 1a with Mes_2Te_2

A solution of Mes_2Te_2 (50 mg, 0.1 mmol) in 10 mL of toluene is added dropwise to a solution of **1a** (82 mg, 0.1 mmol) in 20 mL of toluene at -80 °C. The reaction mixture is stirred for 16 h and warmed to room temperature, whereupon the blue solution turns red. Before the solvent is removed in vacuo, the solution is analysed spectroscopically. $[Mes(W\{CO\}_5)Te]_2$ (**6a**) crystallizes from a concentrated CH_2Cl_2 solution at -28 °C as dark red blocks.

Photolytic reaction: A solution of Mes_2Te_2 (100 mg, 0.2 mmol) and **1a** (163 mg, 0.2 mmol) in 50 mL of toluene was irradiated for 20 min at 254 nm. The resulting violet solution was then characterized spectroscopically, wherein $[MesTeP\{W(CO)_5\}_2\}]$ (**4a-I**) could be identified.

Analytical data for **6a**:

Yield:	6 mg (3 %).
^{1}H NMR (CD_2Cl_2, 400 MHz):	δ [ppm] = 2.35 (s, 6*H*, *p*-CH_3), 2.44 (s, 12*H*, *o*-CH_3), 6.97 (s, 4*H*, C_6H_2).

Reaction solution of the photolytic reaction:

$^{31}P\{^1H\}$ NMR (C_6D_6, 162 MHz):	δ [ppm] = 122.2 (s), 840.4 (s, $^1J_{P,W}$ = 174 Hz, **4a-I**).

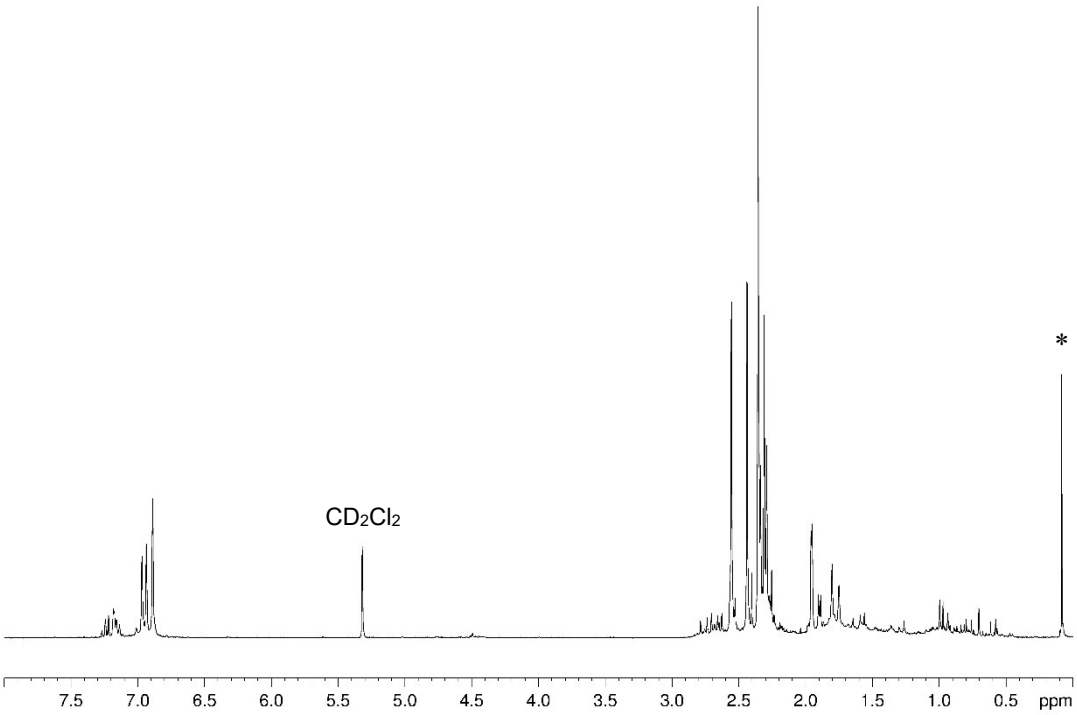

Figure 3.23: *^{1}H NMR spectrum of the reaction solution of the photolytic reaction of **1a** + Mes_2Te_2 in CD_2Cl_2.* * = grease.*

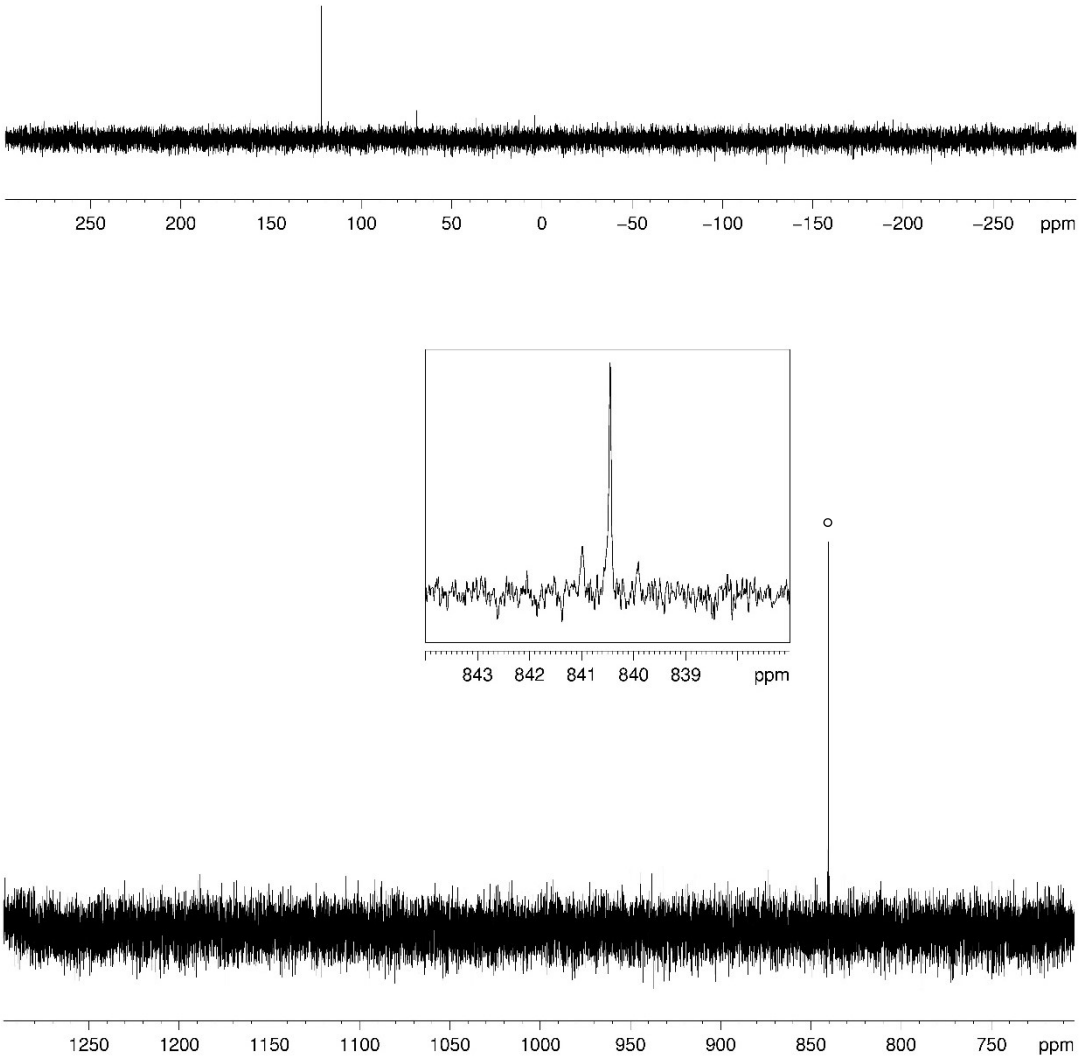

Figure 3.24: *$^{31}P\{^{1}H\}$ NMR spectra of the reaction mixture of the photolytic reaction of* ***1a*** *+ Mes_2Te_2 in CD_2Cl_2.* **° = 4a-I.**

3.4.2.8 Reaction of 1b with Mes_2Te_2

A mixture of **1b** (172 mg, 0.2 mmol) and Mes_2Te_2 (100 mg, 0.2 mmol) in 50 mL of toluene was irradiated for 20 minutes at 254 nm until the reaction solution turned a reddish violet. The solvent was removed and the residue extracted with hexane. [Mes(W{CO}$_5$)TeTeMes] (**6b**) was obtained from a concentrated solution at -28 °C as violet plates.

Analytical data for **6b**:

Yield:	few crystals
^{1}H NMR (CD_2Cl_2, 400 MHz):	δ [ppm] = 2.27 (s, 2H, CH_3), 2.44 (s, 2H, CH_3), 2,56 (s, 1H, CH_3), 2.81 (s, 4H, CH_3), 6.93 (s, 2H, CH).

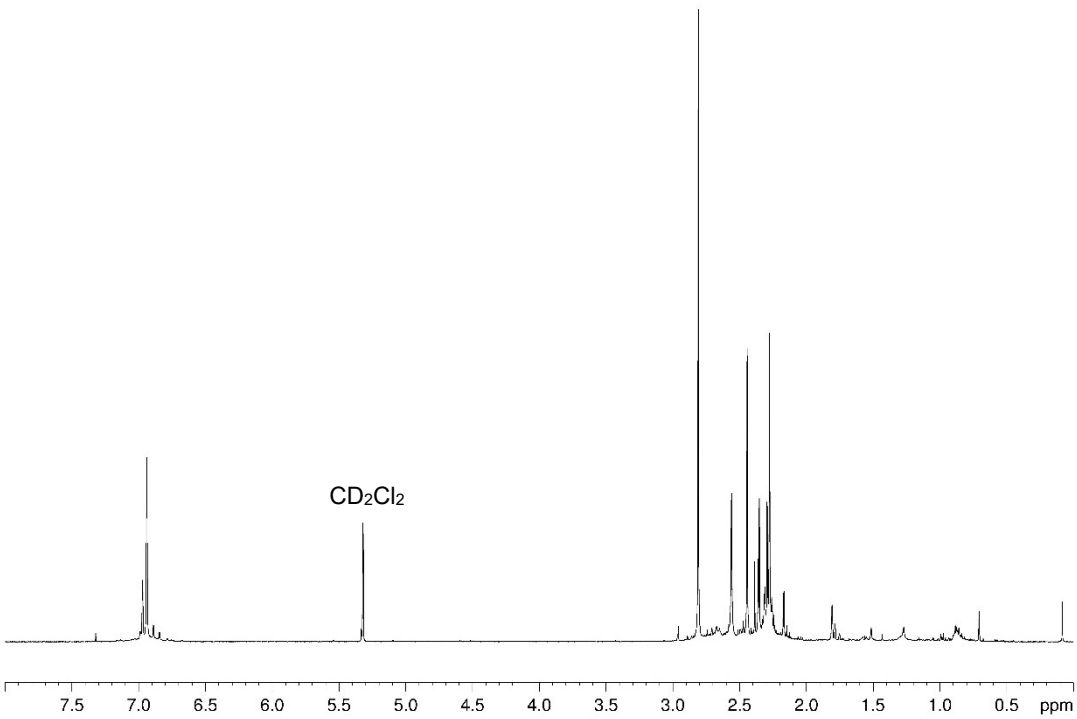

Figure 3.25: *^{1}H NMR spectrum of the reaction mixture of **1b** + Mes_2Te_2 in CD_2Cl_2.*

3.4.2.9 Reaction of 1a with $Tipp_2Te_2$

A solution of $Tipp_2Te_2$ (132 mg, 0.2 mmol) and **1a** (163 mg, 0.2 mmol) in 50 mL of toluene was irradiated for 60 min at 254 nm. The resulting violet solution was then characterized spectroscopically, where [TippTeP{$W(CO)_5$}$_2$] (**4a-II**) could be identified.

Analytical data for **4a-II**:

$^{31}P\{^1H\}$ NMR (CD_2Cl_2, 162 MHz): δ [ppm] = 839 (s, $^1J_{P,W}$ = 174 Hz).

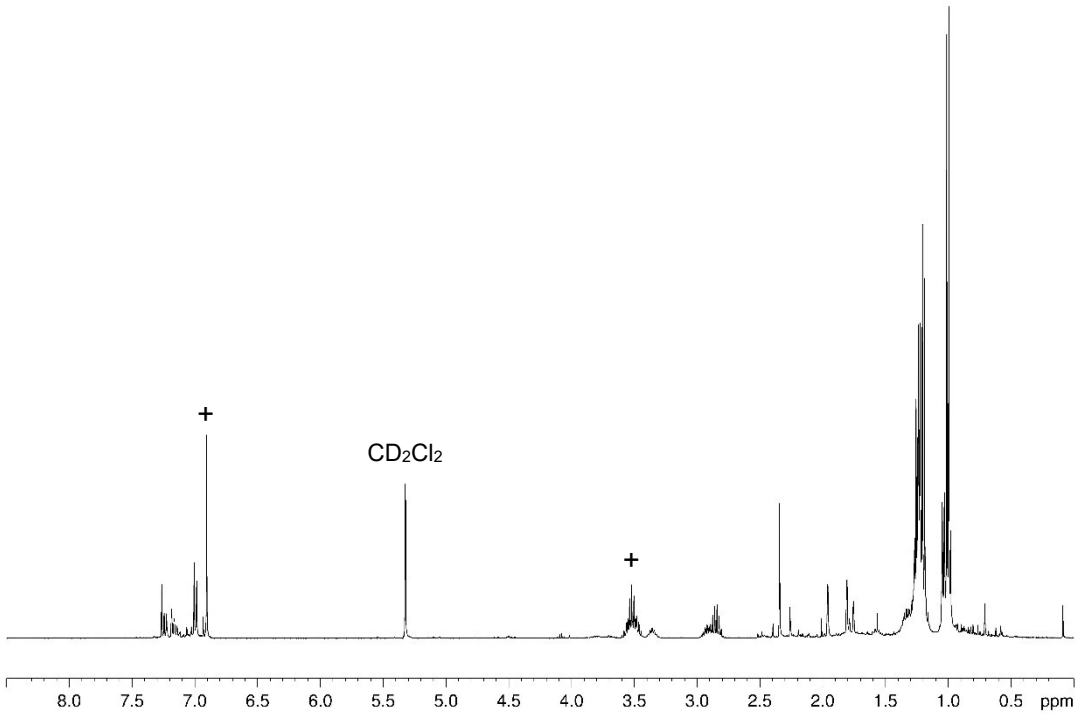

Figure 3.26**: ^1H NMR spectrum of the reaction mixture of **1a** + $Tipp_2Te_2$ in CD_2Cl_2. + = **$Tipp_2Te_2$

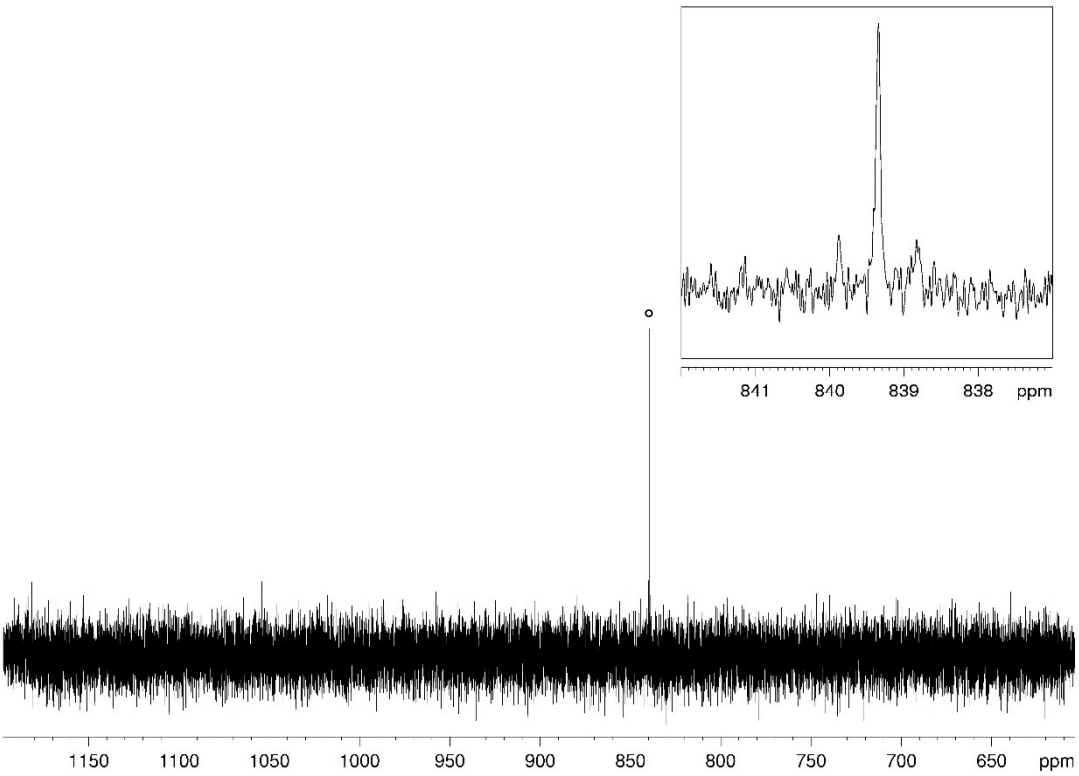

***Figure 3.27**: $^{31}P\{^{1}H\}$ NMR spectrum of the reaction mixture of **1a** + $Tipp_2Te_2$ in CD_2Cl_2.* **° = 4a-II.**

3.4.3 Crystallographic Data

Single crystal X-ray structure analyses were either carried out on a Gemini Ultra Diffractometer (Rigaku Oxford Diffraction, formerly Agilent Technologies) or a GV50 diffractometer (Rigaku Oxford Diffraction). The Gemini Ultra diffractometer was equipped with either a molybdenum X-ray radiation source (Mo-K_α = 0.71072 Å) or a copper X-ray radiation source (Cu-K_α = 1.5406 Å) and an AtlasS2 CCD detector as well as an Oxford Systems CryoJet cooling system. The GV50 diffractometer was equipped with a copper X-ray radiation source and a TitanS2 detector as well as an Oxford Cryosystems CryoStream 700 cooling system. Figures of the molecular structures were prepared with the program *Olex2*[33].

Due to their air and water sensitivity, the crystals were coated with mineral oil (Sigma Aldrich, CAS 8042-47-5). Suitable single crystals were picked under the microscope from the oil and transferred onto a MiTeGen MicroLoop attached to a goniometer head. The goniometer head was then placed onto the goniometer with the loop sitting in a current of cold nitrogen. After collection of the crystal structure data, integration and data reduction were carried out with the program *CrysAlis Pro.*[34] Structure elucidation was carried out with the program *SHELXT*[35] using direct methods. Refinement occurred with the least squares method with the program *SHELXL*[36]. Both were used within *Olex2*[33] as the platform.

CIF files with comprehensive information on the details of the diffraction experiments and full tables of bond lengths and angles for **2a**, **2b**, **3a-I**, **3a-II**, **3b**, **5**, **6a**, and **6b** are deposited in Cambridge Crystallographic Data Centre under the deposition codes CCDC-2083565, CCDC-2083566, CCDC-2083567, CCDC-2083568, CCDC-2083569, CCDC-2083570, CCDC-2083571, CCDC-2083572, respectively.

3.4.3.1 Crystal Structure Data for 2a

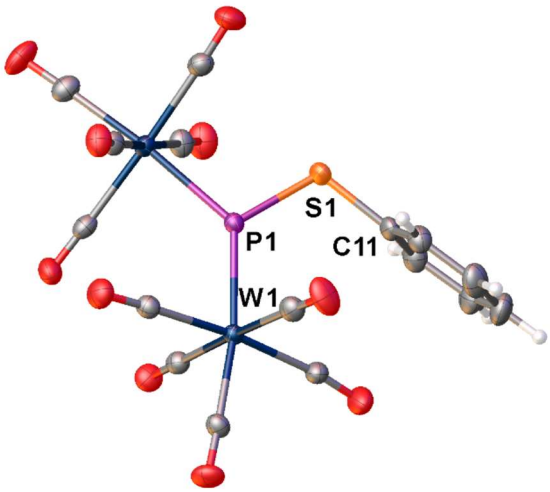

Molecular structure of **2a**. Anisotropic displacement parameters are set to 50% probability level. Selected bond lengths [Å] and angles [°]: W1-P1 2.4065(9), W2-P1 2.4239(9), P1-S1 2.0703(13), S1-C11 1.787(4); W1-P1-W2 132.12(4), S1-P1-W2 104.68(4), S1-P1-W1 123.17(5), C11-S1-P1 109.59(13).

Compound	**2a**
Formula	$C_{16}H_5O_{10}PSW_2$
$D_{calc.}$/ g cm^{-3}	2.486
μ/mm^{-1}	22.032
Formula Weight	787.93
Colour	green
Shape	block
Size/mm^3	0.18×0.07×0.06
T/K	123(1)
Crystal System	triclinic
Space Group	P-1
a/Å	6.59340(10)
b/Å	17.2561(4)
c/Å	19.7432(4)
α/°	109.413(2)
β/°	91.241(2)
γ/°	95.635(2)
V/Å^3	2104.83(8)
Z	4
Z'	2
Wavelength/Å	1.54184
Radiation type	Cu K_a
Θ_{min}/°	2.958
Θ_{max}/°	73.827
Measured Refl's.	13300
Indep't Refl's	7859
Refl's I≥2 s(I)	7270
R_{int}	0.0284
Parameters	541
Restraints	0
Largest Peak	0.704
Deepest Hole	-0.800
GooF	1.005
wR_2 (all data)	0.0499
wR_2	0.0486
R_1 (all data)	0.0245
R_1	0.0220
Molecules in asymm. unit	1

3.4.3.2 Crystal Structure Data for 2b

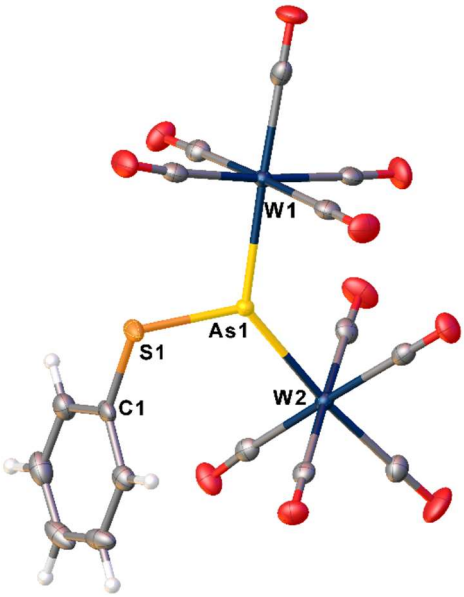

Molecular structure of **2b**. Anisotropic displacement parameters are set to 50% probability level. Selected bond lengths [Å] and angles [°]: W1-As1 2.5024(3), W2-As1 2.5043(3), As1-S1 2.1958(8), S1-C1 1.776(3); W1-As1-W2 133.550(14), S1-As1-W1 104.62(2), S1-As1-W2 121.82(2), C1-S1-As1 108.61(10).

Compound	**2b**
Formula	$C_{16}H_5AsO_{10}SW_2$
$D_{calc.}$/ g cm^{-3}	2.632
μ/mm^{-1}	23.124
Formula Weight	831.88
Colour	violet
Shape	needle
Size/mm^3	0.21×0.04×0.02
T/K	123.00(14)
Crystal System	monoclinic
Space Group	$P2_1/c$
a/Å	6.97820(10)
b/Å	16.3547(2)
c/Å	18.6493(3)
α/°	90
β/°	99.533(2)
γ/°	90
V/Å^3	2098.98(5)
Z	4
Z'	1
Wavelength/Å	1.54184
Radiation type	Cu K_α
Θ_{min}/°	3.617
Θ_{max}/°	66.815
Measured Refl's.	16040
Indep't Refl's	3697
Refl's I≥2 s(I)	3472
R_{int}	0.0295
Parameters	271
Restraints	0
Largest Peak	0.568
Deepest Hole	-0.595
GooF	1.053
wR_2 (all data)	0.0360
wR_2	0.0352
R_1 (all data)	0.0184
R_1	0.0163
Molecules in asymm. unit	1

3.4.3.3 Crystal Structure Data for 3a-I

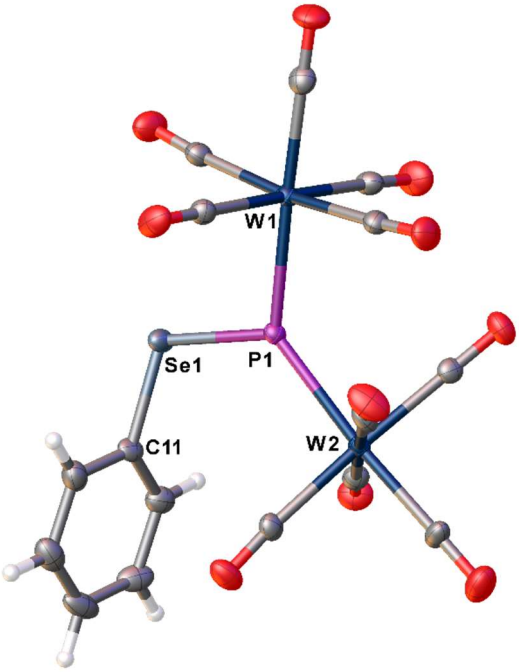

Molecular structure of **3a-I**. Anisotropic displacement parameters are set to 50% probability level. Selected bond lengths [Å] and angles [°]: W1-P1 2.4232(11), W2-P1 2.4141(11), Se1-P1 2.2060(13), Se1-C11 1.925(5); W2-P1-W1 132.95(5), Se1-P1-W1 104.19(4), Se1-P1-W2 122.84(5), C11-Se1-P1 107.95(14).

Compound	**3a-I**
Formula	$C_{16}H_5O_{10}PSeW_2$
$D_{calc.}$/ g cm^{-3}	2.637
μ/mm^{-1}	23.108
Formula Weight	834.83
Colour	dark red
Shape	plate
Size/mm^3	0.14×0.11×0.03
T/K	123(2)
Crystal System	monoclinic
Space Group	$P2_1/c$
a/Å	7.01510(10)
b/Å	16.4460(2)
c/Å	18.4907(2)
α/°	90
β/°	99.7400(10)
γ/°	90
V/Å^3	2102.53(5)
Z	4
Z'	1
Wavelength/Å	1.54184
Radiation type	Cu K_α
Θ_{min}/°	3.620
Θ_{max}/°	72.061
Measured Refl's.	22306
Indep't Refl's	4109
Refl's I≥2 s(I)	3879
R_{int}	0.0454
Parameters	271
Restraints	0
Largest Peak	2.537
Deepest Hole	-1.009
GooF	1.096
wR_2 (all data)	0.0735
wR_2	0.0720
R_1 (all data)	0.0294
R_1	0.0275
Molecules in asymm. unit	1

3.4.3.4 Crystal Structure Data for 3a-II

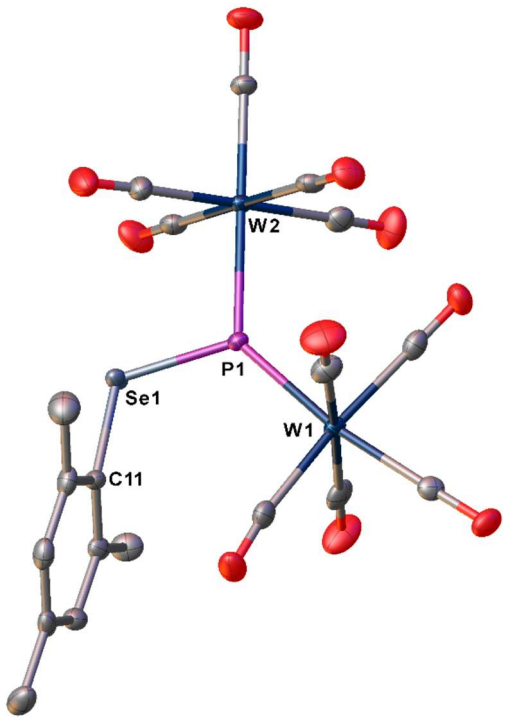

Molecular structure of **3a-II**. Anisotropic displacement parameters are set to 50% probability level. H atoms are omitted for clarity. Selected bond lengths [Å] and angles [°]: W1-P1 2.4134(11), W2-P1 2.4360(11), Se1-P1 2.1974(13), Se1-C11 1.924(4); W1-P1-W2 133.23(5), Se1-P1-W2 103.50(5), Se1-P1-W1 123.27(5).

Compound	**3a-II**
Formula	$C_{38}H_{22}O_{20}P_2Se_2W_4$
$D_{calc.}$/ g cm^{-3}	2.436
μ/mm^{-1}	20.365
Formula Weight	1753.81
Colour	metallic dark green
Shape	block
Size/mm^3	0.60×0.33×0.28
T/K	123.00(14)
Crystal System	triclinic
Space Group	P-1
a/Å	9.61900(10)
b/Å	15.3701(2)
c/Å	18.5803(3)
α/°	66.5430(10)
β/°	78.3160(10)
γ/°	72.3750(10)
V/Å^3	2391.12(6)
Z	2
Z'	1
Wavelength/Å	1.54184
Radiation type	Cu K$_\alpha$
Θ_{min}/°	3.235
Θ_{max}/°	66.589
Measured Refl's.	29701
Indep't Refl's	8372
Refl's I≥2 s(I)	8226
R_{int}	0.0438
Parameters	602
Restraints	0
Largest Peak	1.330
Deepest Hole	-2.630
GooF	1.224
wR_2 (all data)	0.0842
wR_2	0.0837
R_1 (all data)	0.0323
R_1	0.0316
Molecules in asymm. unit	2

3.4.3.5 Crystal Structure Data for 3b

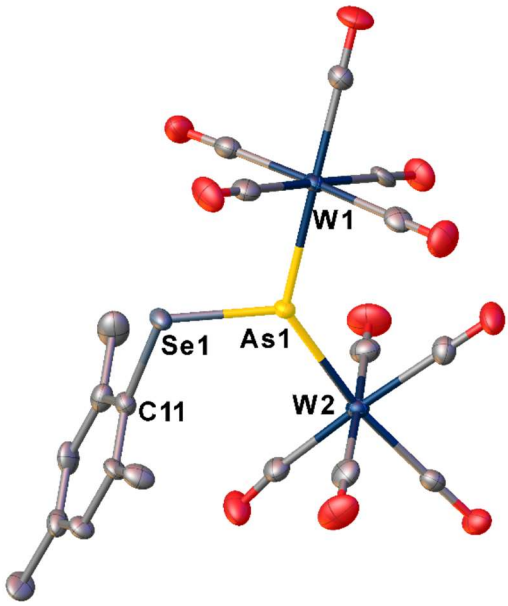

Molecular structure of **3b**. Anisotropic displacement parameters are set to 50% probability level. H atoms are omitted for clarity. Selected bond lengths [Å] and angles [°]: W1-As1 2.5192(6), W2-As1 2.5024(6), As1-Se1 2.3193(8), Se1-C11 1.910(6); W2-As1-W1 133.83(3), Se1-As1-W1 103.28(2), Se1-As1-W2 122.86(3), C11-Se1-As1 108.23(16).

Compound	**3b**
Formula	$C_{38}H_{22}As_2O_{20}Se_2W_4$
$D_{calc.}$/ g cm^{-3}	2.520
μ/mm^{-1}	20.952
Formula Weight	1841.71
Colour	metallic dark green
Shape	block
Size/mm^3	0.49×0.33×0.19
T/K	123.2(4)
Crystal System	triclinic
Space Group	P-1
a/Å	9.7509(2)
b/Å	15.2808(5)
c/Å	18.6934(7)
α/°	66.459(3)
β/°	78.315(2)
γ/°	72.751(2)
V/Å^3	2427.41(14)
Z	2
Z'	1
Wavelength/Å	1.54184
Radiation type	Cu K_α
Θ_{min}/°	3.250
Θ_{max}/°	74.127
Measured Refl's.	24588
Indep't Refl's	9207
Refl's I≥2 s(I)	8822
R_{int}	0.0475
Parameters	602
Restraints	0
Largest Peak	1.655
Deepest Hole	-2.108
GooF	1.193
wR_2 (all data)	0.0935
wR_2	0.0924
R_1 (all data)	0.0384
R_1	0.0366
Molecules in asymm. unit	2

3.4.3.6 Crystal Structure Data for 5

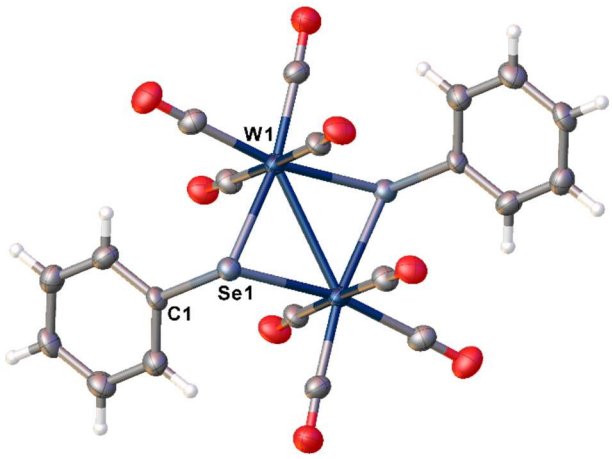

Molecular structure of **5**. Anisotropic displacement parameters are set to 50% probability level. Selected bond lengths [Å] and angles [°]: W1-W1[2] 3.0247(6), W1-Se1 2.5891(8), W1-Se1[2] 2.5929(8), Se1-C1 1.953(7); Se1[2]-W1-W1[2] 54.231(19), Se1-W1-W1[2] 54.347(19), Se1-W1-Se1[2] 108.58(2), W1-Se1-W1[2] 74.42(2), C1-Se1-W1[2] 107.8(2), C1-Se1-W1 110.1(2).

Compound	**5**
Formula	$C_{20}H_{10}O_8Se_2W_2$
$D_{calc.}$/ g cm^{-3}	2.718
μ/mm^{-1}	23.147
Formula Weight	903.90
Colour	green
Shape	needle
Size/mm^3	0.13×0.04×0.03
T/K	123.00(14)
Crystal System	monoclinic
Space Group	$C2/c$
a/Å	18.3332(5)
b/Å	7.2060(2)
c/Å	17.1601(5)
α/°	90
β/°	102.976(4)
γ/°	90
V/Å^3	2209.11(11)
Z	4
Z'	0.5
Wavelength/Å	1.54184
Radiation type	Cu K_α
Θ_{min}/°	4.951
Θ_{max}/°	73.958
Measured Refl's.	4009
Indep't Refl's	2077
Refl's I≥2 s(I)	1852
R_{int}	0.0573
Parameters	145
Restraints	0
Largest Peak	1.626
Deepest Hole	-1.469
GooF	1.054
wR_2 (all data)	0.1019
wR_2	0.0978
R_1 (all data)	0.0392
R_1	0.0351
Molecules in asymm. unit	1

[2] 1-x, 1-y, 1-z

3.4.3.7 Crystal Structure Data for 6a

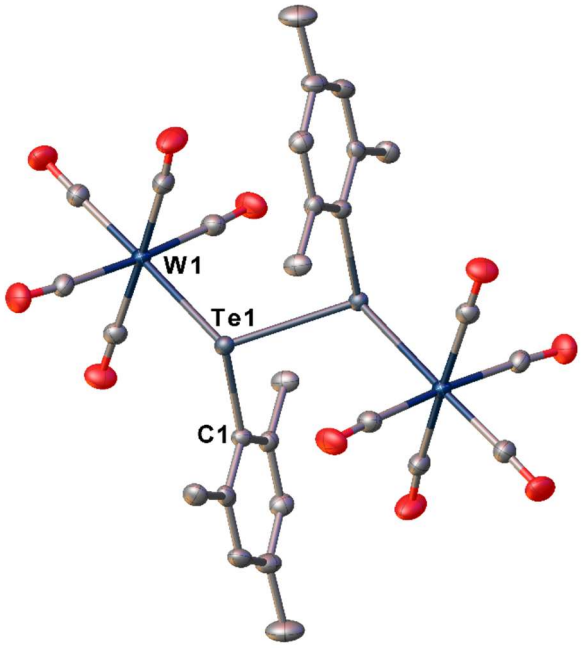

Molecular structure of **6a**. Anisotropic displacement parameters are set to 50% probability level. H atoms are omitted for clarity. Selected bond lengths [Å] and angles [°]: W1-Te1 2.79539(17), Te1-Te1[3] 2.8186(3), Te1-C1 2.139(2); W1-Te1-Te1[3] 108.710(8), C1-Te1-W1 112.93(6), C1-Te1-Te1[3] 94.27(7).

Compound	**6a**
Formula	$C_{28}H_{22}O_{10}Te_2W_2$
$D_{calc.}$/ g cm^{-3}	2.342
μ/mm^{-1}	8.918
Formula Weight	1141.35
Colour	clear dark red
Shape	block
Size/mm^3	0.22×0.17×0.12
T/K	123.00(14)
Crystal System	monoclinic
Space Group	$P2_1/c$
a/Å	9.9217(2)
b/Å	12.1683(2)
c/Å	13.7521(2)
α/°	90
β/°	102.838(2)
γ/°	90
V/Å^3	1618.79(5)
Z	2
Z'	0.5
Wavelength/Å	0.71073
Radiation type	Mo K_α
Θ_{min}/°	2.850
Θ_{max}/°	29.431
Measured Refl's.	30810
Indep't Refl's	4243
Refl's I≥2 s(I)	4027
R_{int}	0.0309
Parameters	193
Restraints	0
Largest Peak	0.897
Deepest Hole	-0.590
GooF	1.071
wR_2 (all data)	0.0374
wR_2	0.0367
R_1 (all data)	0.0192
R_1	0.0175
Molecules in asymm. unit	1

[3] 1-x, 1-y, 1-z

3.4.3.8 Crystal Structure Data for 6b

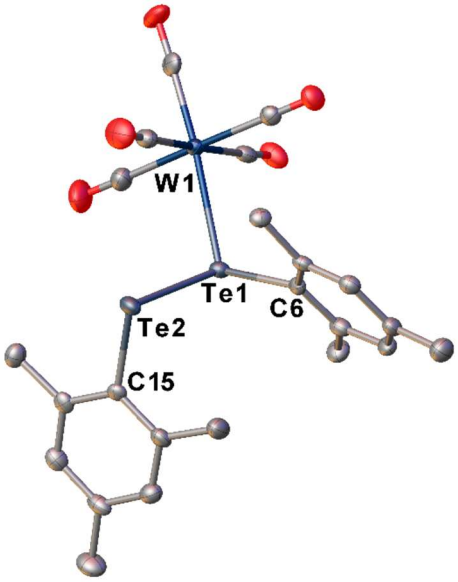

Molecular structure of **6b**. Anisotropic displacement parameters are set to 50% probability level. H atoms are omitted for clarity. Selected bond lengths [Å] and angles [°]: W1-Te1 2.8145(5), Te1-Te2 2.7574(11), Te1-C6 2.145(4), Te2-C15 2.126; Te2-Te1-W1 105.09(2), C6-Te1-W1 115.23(11), C6-Te1-Te2 99.57(11), C15-Te2-Te1 95.63(11).

Compound	**6b**
Formula	$C_{23}H_{22}O_5Te_2W$
$D_{calc.}$/ g cm^{-3}	2.143
μ/mm^{-1}	26.511
Formula Weight	817.45
Colour	light violet
Shape	plate
Size/mm^3	0.32×0.21×0.05
T/K	123
Crystal System	monoclinic
Space Group	$P2_1/c$
a/Å	16.5396(12)
b/Å	18.5800(3)
c/Å	28.924(2)
α/°	90
β/°	145.249(17)
γ/°	90
V/Å^3	5066.6(13)
Z	8
Z'	2
Wavelength/Å	1.54184
Radiation type	Cu K_α
Θ_{min}/°	3.584
Θ_{max}/°	72.941
Measured Refl's.	27607
Indep't Refl's	9821
Refl's I≥2 s(I)	9047
R_{int}	0.0351
Parameters	571
Restraints	0
Largest Peak	1.427
Deepest Hole	-1.143
GooF	1.097
wR_2 (all data)	0.0776
wR_2	0.0756
R_1 (all data)	0.0337
R_1	0.0296
Molecules in asymm. unit	2

3.4.4 Computational Details

The geometries of the compounds have been fully optimized with gradient-corrected density functional theory (DFT) in form of Becke's three-parameter hybrid method B3LYP[37] with def2-SVPD all electron basis set (ECP on W).[38] Gaussian 16 program package[39] was used throughout. All structures correspond to minima on their respective potential energy surfaces as verified by computation of second derivatives. Basis sets were obtained from the EMSL basis set exchange database.[40]

Gas phase chemical shifts were calculated at PBE0[41] level of theory both on experimental and optimized geometries using GIAO approach[42]. Chemical shifts of phosphorus nuclei are given relative to the H_3PO_4 optimized in the gas phase. Values are scaled by the linear equation recommended by *Sinyashin et al.*[25]: $\delta_{scaled}=(\delta_{unscaled}-a)/k$, where values of a=14.4 and k=1.073 were obtained at PBE/6-311G(2d,2p) level of theory by fitting known ^{31}P chemical shifts of 34 organophosphorus compounds.

Standard entropies of the reactions in solution were estimated by taking into account the entropy of the solvation of one gaseous mole in the inert solvent (90 J mol^{-1} K^{-1}).[25]

Table 3.2: *Experimental and computed ^{31}P NMR chemical shifts, on gas phase optimized and on experimental geometries (ppm). All computed chemical shifts are scaled according to [25].*

	Exp.	PBE0/def2-SVPD		PBE0/6-311++G(2d,2p)// PBE0/def2-SVPD
Compound		on optimized geom.	on exp. geom.	on optimized geom.
PhSP{W(CO)$_5$}	822.9	866.2	809.7	927.6
PhSeP{W(CO)$_5$}	835.0	898.3	869.1	966.9
MesSeP{W(CO)$_5$}	854.3	911.9	873.5	991.5
MesTeP{W(CO)$_5$}	840.4	958.8		1044.9

Table 3.3: *Gas phase reaction energies ΔE^o_0, enthalpiesΔH^o_{298}, Gibbs energies ΔG^o_{298} in kJ mol^{-1}, and reaction entropies ΔS^o_{298}, J mol^{-1} K^{-1}. B3LYP/def2-SVPD (ECP on W) level of theory. Reaction entropies and Gibbs energies in solution were estimated according to [26].*

Reaction	ΔE^o_0	ΔH^o_{298}	ΔS^o_{298}	ΔG^o_{298}	ΔS^o_{298} solvent	ΔG^o_{298} solvent
Cp*P{W(CO)$_5$}$_2$ = Cp* +P{W(CO)$_5$}$_2$	128.7	114.6	293.0	27.3	203.0	54.1
(Cp*)$_2$ = 2 Cp*	111.4	87.3	300.6	-2.3	210.6	24.6
Ph$_2$S$_2$ = 2 PhS	165.0	157.6	159.9	109.9	69.9	136.7
Ph$_2$Se$_2$ = 2 PhSe	225.4	219.2	159.2	171.7	69.2	198.6
Ph$_2$Te$_2$ = 2 PhTe	164.3	158.8	152.9	113.2	62.9	140.1
Mes$_2$S$_2$ = 2 MesS	130.9	123.7	156.8	76.9	66.8	103.8
Mes$_2$Se$_2$ = 2 MesSe	189.6	182.6	153.9	136.7	63.9	163.5
Mes$_2$Te$_2$ = 2 MesTe	144.9	138.8	158.1	91.7	68.1	118.5
Cp*P{W(CO)$_5$}$_2$ + ½ Ph$_2$S$_2$ = Cp* + PhSP{W(CO)$_5$}$_2$	1.4	-8.9	139.9	-50.6	94.9	-37.2
Cp*P{W(CO)$_5$}$_2$ + ½ Ph$_2$Se$_2$ = Cp* + PhSeP{W(CO)$_5$}$_2$	15.2	4.6	142.8	-38.0	97.8	-24.6
Cp*P{W(CO)$_5$}$_2$ + ½ Ph$_2$Te$_2$ = Cp* + PhTeP{W(CO)$_5$}$_2$	34.0	22.8	148.7	-21.5	103.7	-8.1
Cp*P{W(CO)$_5$}$_2$ + ½ Mes$_2$S$_2$ = Cp* + MesSP{W(CO)$_5$}$_2$	-9.9	-20.0	132.3	-59.4	87.3	-46.0
Cp*P{W(CO)$_5$}$_2$ + ½ Mes$_2$Se$_2$ = Cp* + MesSeP{W(CO)$_5$}$_2$	5.0	-5.6	152.5	-51.0	107.5	-37.6
Cp*P{W(CO)$_5$}$_2$ + ½ Mes$_2$Te$_2$ = Cp* + MesTeP{W(CO)$_5$}$_2$	24.3	13.3	146.0	-30.3	101.0	-16.9
P{W(CO)$_5$}$_2$ + Ph$_2$S$_2$ = PhS + PhSP{W(CO)$_5$}$_2$	-44.8	-44.7	-73.1	-22.9	-73.1	-22.9
P{W(CO)$_5$}$_2$ + Ph$_2$Se$_2$ = PhSe + PhSeP{W(CO)$_5$}$_2$	-0.8	-0.4	-70.6	20.6	-70.6	20.6
P{W(CO)$_5$}$_2$ + Ph$_2$Te$_2$ = PhTe + PhTeP{W(CO)$_5$}$_2$	-12.6	-12.4	-67.8	7.8	-67.8	7.8
P{W(CO)$_5$}$_2$ + Mes$_2$S$_2$ = MesS + MesSP{W(CO)$_5$}$_2$	-73.2	-72.8	-82.3	-48.2	-82.3	-48.2
P{W(CO)$_5$}$_2$ + Mes$_2$Se$_2$ = MesSe + MesSeP{W(CO)$_5$}$_2$	-28.9	-28.9	-63.5	-9.9	-63.5	-9.9
P{W(CO)$_5$}$_2$ + Mes$_2$Te$_2$ = MesTe + MesTeP{W(CO)$_5$}$_2$	-32.0	-31.9	-67.9	-11.7	-67.9	-11.7
Cp*P{W(CO)$_5$}$_2$ + PhSH = HCp* + PhSP{W(CO)$_5$}$_2$	-84.5	-79.4	25.6	-87.0	25.6	-87.0
Cp*P{W(CO)$_5$}$_2$ + PhSeH = HCp* + PhSeP{W(CO)$_5$}$_2$	-96.2	-89.7	14.7	-94.0	14.7	-94.0
Cp*P{W(CO)$_5$}$_2$ + PhTeH = HCp* + PhTeP{W(CO)$_5$}$_2$	-106.3	-97.7	30.0	-106.7	30.0	-106.7
Cp*P{W(CO)$_5$}$_2$ + MesSH = HCp* + MesSP{W(CO)$_5$}$_2$	-86.7	-81.8	22.0	-88.4	22.0	-88.4
Cp*P{W(CO)$_5$}$_2$ + MesSeH = HCp* + MesSeP{W(CO)$_5$}$_2$	-95.3	-88.9	38.9	-100.5	38.9	-100.5
Cp*P{W(CO)$_5$}$_2$ + MesTeH = HCp* + MesTeP{W(CO)$_5$}$_2$	-104.1	-95.5	27.5	-103.7	27.5	-103.7
Cp*P{W(CO)$_5$}$_2$ + PhSH = Cp*P{W(CO)$_5$}$_2$·PhSH	37.7	44.2	-220.0	109.8	-130.0	83.0
Cp*P{W(CO)$_5$}$_2$ + PhSeH = Cp*P{W(CO)$_5$}$_2$·PhSeH	34.9	40.5	-227.0	108.2	-137.0	81.4
Cp*P{W(CO)$_5$}$_2$ + PhTeH = Cp*P{W(CO)$_5$}$_2$·PhTeH	33.2	38.8	-212.4	102.1	-122.4	75.3
Cp*P{W(CO)$_5$}$_2$ + PhS = Cp*P{W(CO)$_5$}$_2$·PhS	-55.7	-48.7	-194.4	9.3	-104.4	-17.5
Cp*P{W(CO)$_5$}$_2$ + PhSe = Cp*P{W(CO)$_5$}$_2$·PhSe	-76.7	-70.4	-197.6	-11.5	-107.6	-38.3
Cp*P{W(CO)$_5$}$_2$ + PhTe = Cp*P{W(CO)$_5$}$_2$·PhTe	-35.7	-30.2	-199.3	29.2	-109.3	2.4
Cp*P{W(CO)$_5$}$_2$·PhSH = Cp*H + PhSP{W(CO)$_5$}$_2$	-122.2	-123.6	245.5	-196.8	155.5	-170.0
Cp*P{W(CO)$_5$}$_2$·PhSeH = Cp*H + PhSeP{W(CO)$_5$}$_2$	-131.1	-130.2	241.7	-202.2	151.7	-175.4
Cp*P{W(CO)$_5$}$_2$·PhTeH = Cp*H + PhTeP{W(CO)$_5$}$_2$	-139.5	-136.5	242.3	-208.8	152.3	-181.9
Cp*P{W(CO)$_5$}$_2$·PhS = Cp* + PhSP{W(CO)$_5$}$_2$	-25.4	-39.0	254.4	-114.8	164.4	-88.0
Cp*P{W(CO)$_5$}$_2$·PhSe = Cp* + PhSeP{W(CO)$_5$}$_2$	-20.8	-34.6	260.7	-112.4	170.7	-85.5
Cp*P{W(CO)$_5$}$_2$·PhTe = Cp* + PhTeP{W(CO)$_5$}$_2$	-12.4	-26.4	271.5	-107.4	181.5	-80.5
Cp*P{W(CO)$_5$}$_2$ + Ph$_2$S$_2$ = Cp* + PhS + PhSP{W(CO)$_5$}$_2$	83.9	69.9	219.9	4.4	129.9	31.2
Cp *P{W(CO)$_5$}$_2$ + Ph$_2$Se$_2$ = Cp* + PhSe + PhSeP{W(CO)$_5$}$_2$	127.9	114.2	222.4	47.9	132.4	74.7
Cp *P{W(CO)$_5$}$_2$ + Ph$_2$Te$_2$ = Cp* + PhTe + PhTeP{W(CO)$_5$}$_2$	116.1	102.2	225.2	35.1	135.2	61.9

Table 3.4: *Total energies E^o_0, sum of electronic and thermal enthalpies H^o_{298} (Hartree) and standard entropies S^o_{298} (cal mol^{-1}K^{-1}) for studied compounds. B3LYP/def2-SVPD (ECP on W) level of theory.*

Compound	E^o_0	H^o_{298}	S^o_{298}
$Cp^*P\{W(CO)_5\}_2$	-1998.074106	-1997.726543	255.279
$P\{W(CO)_5\}_2$	-1608.222862	-1608.110192	211.186
Cp^*	-389.8022192	-389.572698	114.119
HCp^*	-390.4336937	-390.190214	107.606
$(Cp^*)_2$	-779.646884	-779.178663	156.397
Ph_2S_2	-1259.167212	-1258.970067	116.934
Ph_2Se_2	-5265.593876	-5265.397772	123.375
Ph_2Te_2	-999.2120126	-999.016188	128.912
PhS	-629.5521767	-629.455028	77.571
PhSe	-2632.754012	-2632.657141	80.716
PhTe	-499.5747193	-499.477846	82.729
PhSH	-630.1823598	-630.075681	79.286
PhSeH	-2633.385984	-2633.28051	85.794
PhTeH	-500.1840423	-500.079707	86.315
$PhSP\{W(CO)_5\}_2$	-2237.854952	-2237.642255	233.07
$PhSeP\{W(CO)_5\}_2$	-4241.063034	-4240.85099	236.973
$PhTeP\{W(CO)_5\}_2$	-2107.864944	-2107.653253	241.156
Mes_2S_2	-1494.906249	-1494.535302	165.612
Mes_2Se_2	-5501.330759	-5500.960724	172.102
Mes_2Te_2	-1234.945736	-1234.576189	175.936
MesS	-747.4281989	-747.244098	101.543
MesSe	-2750.629273	-2750.445586	104.447
MesTe	-617.4452823	-617.261661	106.867
MesSH	-748.0553572	-747.861612	102.642
MesSeH	-2751.258643	-2751.066128	106.682
MesTeH	-618.0554551	-617.864192	109.791
$MesSP\{W(CO)_5\}_2$	-2355.728791	-2355.429107	255.58
$MesSeP\{W(CO)_5\}_2$	-4358.935359	-4358.636331	263.659
$MesTeP\{W(CO)_5\}_2$	-2225.735511	-2225.436889	264.029
$Cp^*P\{W(CO)_5\}_2\cdot SHPh$	-2628.242112	-2627.785385	281.995
$Cp^*P\{W(CO)_5\}_2\cdot SeHPh$	-4631.446804	-4630.991622	286.816
$Cp^*P\{W(CO)_5\}_2\cdot TeHPh$	-2498.245498	-2497.791476	290.839
$Cp^*P\{W(CO)_5\}_2\cdot SPh$	-2627.647488	-2627.200101	286.392
$Cp^*P\{W(CO)_5\}_2\cdot SePh$	-4630.857325	-4630.410494	288.774
$Cp^*P\{W(CO)_5\}_2\cdot TePh$	-2497.662422	-2497.215882	290.386

Table 3.5: *Optimized xyz coordinates (in Angstroms) for studied compounds. B3LYP/def2-SVPD (ECP on W) level of theory.*

Cp*P{W(CO)$_5$}$_2$

6	-0.684066000	3.352063000	0.405450000
6	0.455018000	2.350011000	0.173394000
6	1.205780000	2.632434000	-1.115337000
6	2.494840000	2.955701000	-0.797879000
6	2.681578000	2.870798000	0.658657000
6	1.509752000	2.493206000	1.245988000
15	-0.070974000	0.500883000	0.081462000
6	0.550896000	2.655382000	-2.464336000
6	3.585967000	3.394954000	-1.725439000
6	3.969872000	3.222748000	1.337205000
6	1.204918000	2.376195000	2.711046000
74	-2.544971000	0.032645000	0.007398000
74	1.741468000	-1.265582000	-0.013645000
6	3.066616000	-2.834546000	-0.087398000
6	0.335759000	-2.767304000	0.232249000
6	3.424322000	-0.076212000	-0.291847000
6	2.025151000	-1.116145000	2.050011000
6	1.511031000	-1.343155000	-2.090133000
6	-4.528145000	-0.534170000	-0.105257000
6	-2.295059000	-1.319178000	1.582690000
6	-2.904988000	1.415951000	-1.502734000
6	-2.156655000	-1.436581000	-1.419931000
6	-3.122014000	1.461029000	1.405651000
8	-1.997799000	-2.240242000	-2.221657000
8	-3.519321000	2.214129000	2.176212000
8	-2.195130000	-2.033321000	2.472675000
8	-5.628361000	-0.857756000	-0.173134000
8	-3.145537000	2.177432000	-2.328015000
8	1.405672000	-1.373897000	-3.231366000
8	2.203637000	-1.031328000	3.179758000
8	-0.344045000	-3.685179000	0.357139000
8	4.460328000	0.395027000	-0.458966000
8	3.801853000	-3.717996000	-0.127909000
1	-1.464532000	3.281238000	-0.357511000
1	-0.265869000	4.367993000	0.368317000
1	-1.147447000	3.216567000	1.387721000
1	0.815916000	3.325743000	3.115616000
1	2.097417000	2.119169000	3.293952000
1	0.446925000	1.609427000	2.918918000
1	4.229633000	4.279101000	1.162822000
1	4.804523000	2.623719000	0.943617000
1	3.920631000	3.068056000	2.420894000
1	3.261097000	3.412905000	-2.771328000
1	4.456462000	2.725775000	-1.654253000
1	3.941720000	4.403917000	-1.463497000
1	0.257277000	1.653562000	-2.812952000
1	1.219998000	3.075312000	-3.223942000
1	-0.363775000	3.267594000	-2.458204000

$P\{W(CO)_5\}_2$

15	-0.000291000	0.440461000	0.001411000
74	-2.375095000	0.028871000	0.000826000
74	2.375440000	0.032232000	-0.000617000
6	4.418928000	-0.382960000	-0.002740000
6	1.951982000	-2.001753000	0.197169000
6	2.744614000	2.081994000	-0.196856000
6	2.467487000	0.227637000	2.084027000
6	2.384524000	-0.170695000	-2.086176000
6	-4.418157000	-0.389951000	-0.000240000
6	-2.133963000	-1.290198000	1.606384000
6	-2.655038000	1.350622000	-1.599687000
6	-2.065288000	-1.558196000	-1.323738000
6	-2.693794000	1.623085000	1.320113000
8	-1.892230000	-2.430618000	-2.044964000
8	-2.878196000	2.499341000	2.033692000
8	-2.001785000	-2.017025000	2.481061000
8	-5.537516000	-0.643481000	-0.000911000
8	-2.820051000	2.078899000	-2.467495000
8	2.398496000	-0.283784000	-3.224987000
8	2.529025000	0.335434000	3.221772000
8	1.709403000	-3.116021000	0.304961000
8	2.950452000	3.203592000	-0.302407000
8	5.538786000	-0.634591000	-0.003986000

Cp*

6	-1.534586000	-2.230810000	0.004225000
6	-0.641235000	-1.031938000	0.001323000
6	0.733231000	-0.983291000	-0.001020000
6	1.113315000	0.422084000	-0.006617000
6	-0.070567000	1.233629000	-0.005963000
6	-1.153633000	0.366660000	-0.000709000
6	1.715034000	-2.116985000	-0.007538000
6	2.521708000	0.913690000	0.010339000
6	-0.082186000	2.735618000	-0.005754000
6	-2.609473000	0.700005000	0.003494000
1	3.007883000	0.688489000	0.976385000
1	2.586039000	1.996857000	-0.148504000
1	3.131210000	0.414022000	-0.760112000
1	2.417823000	-2.054420000	0.839967000
1	2.329373000	-2.123382000	-0.923943000
1	1.213030000	-3.090226000	0.055339000
1	-2.195395000	-2.241133000	0.887637000
1	-0.964956000	-3.167721000	0.003264000
1	-2.198143000	-2.242727000	-0.877149000
1	-3.121484000	0.273851000	-0.876119000
1	-2.787596000	1.781661000	0.003073000
1	-3.115679000	0.275937000	0.887437000
1	0.446788000	3.152568000	-0.878580000
1	0.406530000	3.152913000	0.890307000
1	-1.105072000	3.131339000	-0.029681000

HCp*

6	-2.177334000	-0.168840000	1.547676000
6	-0.923028000	0.001191000	0.742513000
6	0.344451000	0.181032000	1.192198000
6	1.273091000	0.313096000	0.000000000
6	0.344451000	0.181032000	-1.192198000
6	-0.923028000	0.001191000	-0.742513000
6	0.841861000	0.264817000	2.601407000
1	1.701531000	1.335008000	0.000000000
6	2.438872000	-0.691345000	0.000000000
6	0.841861000	0.264817000	-2.601407000
6	-2.177334000	-0.168840000	-1.547676000
1	1.377636000	1.211700000	2.783623000
1	1.554775000	-0.544834000	2.832533000
1	0.025770000	0.200756000	3.331617000
1	-2.912900000	0.618375000	1.315248000
1	-1.983169000	-0.135925000	2.626031000
1	-2.668275000	-1.130241000	1.325314000
1	-2.912900000	0.618375000	-1.315248000
1	-2.668275000	-1.130241000	-1.325314000
1	-1.983169000	-0.135925000	-2.626031000
1	1.377636000	1.211700000	-2.783623000
1	0.025770000	0.200756000	-3.331617000
1	1.554775000	-0.544834000	-2.832533000
1	3.075102000	-0.560540000	0.886175000
1	3.075102000	-0.560540000	-0.886175000
1	2.057408000	-1.722478000	0.000000000

$(Cp^*)_2$

6	1.356004000	-2.356278000	1.978081000
6	0.458520000	-1.959929000	0.839164000
6	-1.197375000	-0.881196000	-0.503635000
6	-0.859820000	-2.069481000	-1.064910000
6	0.150225000	-2.741141000	-0.225972000
6	-1.399645000	-0.807460000	1.984816000
6	-2.233831000	0.079542000	-0.998517000
6	-1.399645000	-2.688347000	-2.321151000
6	0.687709000	-4.103514000	-0.552470000
1	-1.783839000	0.985943000	-1.426268000
1	-2.897817000	0.414819000	-0.187456000
1	-2.864728000	-0.379911000	-1.769238000
1	-2.213833000	-0.081301000	1.915756000
1	-0.903643000	-0.666046000	2.953609000
1	-1.843873000	-1.810799000	1.980039000
1	1.376622000	-3.446794000	2.101693000
1	1.023441000	-1.927181000	2.932467000
1	2.400456000	-2.035875000	1.835499000
1	1.384053000	-4.470233000	0.210056000
1	1.226022000	-4.097848000	-1.514077000
1	-0.123211000	-4.842001000	-0.654732000
1	-2.163754000	-2.063640000	-2.796732000
1	-1.847447000	-3.675409000	-2.123111000
1	-0.599319000	-2.851821000	-3.060753000
6	-0.407291000	-0.688546000	0.798469000
6	0.407291000	0.688546000	0.798469000
6	1.197375000	0.881196000	-0.503635000
6	0.859820000	2.069481000	-1.064910000
6	-0.150225000	2.741141000	-0.225972000
6	-0.458520000	1.959929000	0.839164000
6	1.399645000	0.807460000	1.984816000
6	2.233831000	-0.079542000	-0.998517000
6	1.399645000	2.688347000	-2.321151000
6	-0.687709000	4.103514000	-0.552470000
6	-1.356004000	2.356278000	1.978081000
1	2.213833000	0.081301000	1.915756000
1	0.903643000	0.666046000	2.953609000
1	1.843873000	1.810799000	1.980039000
1	-1.023441000	1.927181000	2.932467000
1	-2.400456000	2.035875000	1.835499000
1	-1.376622000	3.446794000	2.101693000
1	-1.226022000	4.097848000	-1.514077000
1	0.123211000	4.842001000	-0.654732000
1	-1.384053000	4.470233000	0.210056000
1	0.599319000	2.851821000	-3.060753000
1	2.163754000	2.063640000	-2.796732000
1	1.847447000	3.675409000	-2.123111000
1	2.864728000	0.379911000	-1.769238000
1	1.783839000	-0.985943000	-1.426268000
1	2.897817000	-0.414819000	-0.187456000

Ph_2S_2

16	-0.806978000	0.686853000	-1.723953000
16	0.806978000	-0.686853000	-1.723953000
6	-0.393188000	1.825574000	-0.399160000
6	-1.038835000	1.705072000	0.840537000
1	-1.755478000	0.898761000	0.996491000
6	0.528612000	2.863220000	-0.608959000
1	1.021589000	2.956567000	-1.576940000
6	0.806978000	3.765405000	0.419008000
1	1.523936000	4.571122000	0.251939000
6	-0.759567000	2.615740000	1.864036000
1	-1.264769000	2.518779000	2.826521000
6	0.163457000	3.644157000	1.656103000
1	0.380116000	4.354074000	2.455849000
6	0.393188000	-1.825574000	-0.399160000
6	-0.528612000	-2.863220000	-0.608959000
6	1.038835000	-1.705072000	0.840537000
6	-0.806978000	-3.765405000	0.419008000
6	0.759567000	-2.615740000	1.864036000
6	-0.163457000	-3.644157000	1.656103000
1	-1.021589000	-2.956567000	-1.576940000
1	1.755478000	-0.898761000	0.996491000
1	-1.523936000	-4.571122000	0.251939000
1	1.264769000	-2.518779000	2.826521000
1	-0.380116000	-4.354074000	2.455849000

Ph_2Se_2

34	-0.727755000	0.942261000	-1.365313000
34	0.727755000	-0.942261000	-1.365313000
6	0.021788000	2.019635000	0.060967000
6	-0.531160000	1.948897000	1.348248000
1	-1.355819000	1.264344000	1.547340000
6	1.081632000	2.901828000	-0.197091000
1	1.508393000	2.958054000	-1.198821000
6	1.586842000	3.702931000	0.829903000
1	2.411226000	4.388177000	0.624633000
6	-0.021788000	2.755258000	2.370937000
1	-0.455457000	2.697393000	3.370864000
6	1.036965000	3.630952000	2.114205000
1	1.432575000	4.259548000	2.913621000
6	-0.021788000	-2.019635000	0.060967000
6	-1.081632000	-2.901828000	-0.197091000
6	0.531160000	-1.948897000	1.348248000
6	-1.586842000	-3.702931000	0.829903000
6	0.021788000	-2.755258000	2.370937000
6	-1.036965000	-3.630952000	2.114205000
1	-1.508393000	-2.958054000	-1.198821000
1	1.355819000	-1.264344000	1.547340000
1	-2.411226000	-4.388177000	0.624633000
1	0.455457000	-2.697393000	3.370864000
1	-1.432575000	-4.259548000	2.913621000

Ph_2Te_2

52	-0.978743000	0.973672000	-1.168712000
52	0.978743000	-0.973672000	-1.168712000
6	-0.250169000	2.247027000	0.410156000
6	-0.697644000	2.054598000	1.726042000
1	-1.392631000	1.246247000	1.955902000
6	0.642403000	3.291410000	0.126115000
1	0.993964000	3.449662000	-0.894053000
6	1.086070000	4.131496000	1.152140000
1	1.780934000	4.941726000	0.923677000
6	-0.250169000	2.898426000	2.748045000
1	-0.602514000	2.742618000	3.769373000
6	0.641956000	3.936223000	2.463481000
1	0.989477000	4.593523000	3.262259000
6	0.250169000	-2.247027000	0.410156000
6	-0.642403000	-3.291410000	0.126115000
6	0.697644000	-2.054598000	1.726042000
6	-1.086070000	-4.131496000	1.152140000
6	0.250169000	-2.898426000	2.748045000
6	-0.641956000	-3.936223000	2.463481000
1	-0.993964000	-3.449662000	-0.894053000
1	1.392631000	-1.246247000	1.955902000
1	-1.780934000	-4.941726000	0.923677000
1	0.602514000	-2.742618000	3.769373000
1	-0.989477000	-4.593523000	3.262259000

PhS

16	2.308057000	0.000003000	-0.000053000
6	0.578722000	-0.000098000	-0.000099000
6	-0.149486000	1.221261000	0.000102000
6	-0.149630000	-1.221353000	0.000013000
6	-1.539695000	1.216046000	0.000143000
6	-1.539811000	-1.215966000	0.000247000
6	-2.239235000	0.000082000	-0.000423000
1	0.405338000	2.159542000	0.000374000
1	0.405076000	-2.159710000	0.000273000
1	-2.086928000	2.160103000	0.000390000
1	-2.087104000	-2.159990000	0.000439000
1	-3.330492000	0.000174000	-0.000536000

PhSe

34	1.849360000	0.000008000	0.000066000
6	-0.068859000	0.000512000	-0.000273000
6	-0.774297000	1.214463000	-0.000016000
6	-0.773596000	-1.214001000	0.000022000
6	-2.171587000	1.206494000	-0.000236000
6	-2.170825000	-1.206963000	-0.000279000
6	-2.876372000	-0.000418000	0.000601000
1	-0.240012000	2.165810000	-0.000546000
1	-0.238799000	-2.165068000	-0.000513000
1	-2.710266000	2.155879000	-0.000492000
1	-2.708874000	-2.156705000	-0.000512000
1	-3.967063000	-0.000692000	0.000894000

PhTe

52	0.000000000	1.582989000	0.000000000
6	0.000687000	-0.536708000	0.000000000
6	0.000085000	-1.251056000	-1.215626000
6	0.000085000	-1.251056000	1.215626000
6	-0.000253000	-2.646780000	-1.211577000
6	-0.000253000	-2.646780000	1.211577000
6	-0.000147000	-3.347331000	0.000000000
1	0.000233000	-0.709185000	-2.161777000
1	0.000233000	-0.709185000	2.161777000
1	-0.000515000	-3.190132000	-2.158156000
1	-0.000515000	-3.190132000	2.158156000
1	-0.000675000	-4.438619000	0.000000000

PhSH

16	2.294009000	-0.083877000	-0.000136000
6	0.509367000	-0.000593000	0.000250000
6	-0.194841000	1.212531000	0.000052000
6	-0.201001000	-1.211357000	0.000200000
6	-1.591754000	1.209938000	-0.000006000
6	-1.597181000	-1.202968000	0.000017000
6	-2.300433000	0.005265000	0.000112000
1	0.342752000	2.161891000	0.000433000
1	0.338236000	-2.160351000	0.000005000
1	-2.127237000	2.160909000	-0.000613000
1	-2.137066000	-2.151478000	-0.000609000
1	-3.391094000	0.007001000	-0.000918000
1	2.525319000	1.247168000	0.000117000

PhSeH

34	1.835756000	0.000000000	-0.044442000
6	-0.110180000	0.000000000	0.007659000
6	-0.811855000	1.212753000	0.001799000
6	-0.811855000	-1.212753000	0.001798000
6	-2.210322000	1.209418000	0.000905000
6	-2.210322000	-1.209418000	0.000904000
6	-2.910992000	0.000000000	0.002892000
1	-0.265232000	2.156056000	-0.002846000
1	-0.265232000	-2.156056000	-0.002849000
1	-2.751833000	2.157042000	-0.001765000
1	-2.751834000	-2.157042000	-0.001766000
1	-4.002164000	0.000000000	0.001480000
1	2.013746000	-0.000016000	1.423044000

PhTeH

52	1.577813000	0.000003000	-0.033200000
6	-0.579504000	0.000003000	0.008651000
6	-1.283150000	1.212402000	0.002638000
6	-1.283146000	-1.212400000	0.002623000
6	-2.682224000	1.209058000	0.000473000
6	-2.682220000	-1.209060000	0.000464000
6	-3.383161000	-0.000002000	0.001071000
1	-0.743433000	2.159854000	0.000823000
1	-0.743427000	-2.159850000	0.000789000
1	-3.223314000	2.157033000	-0.001901000
1	-3.223308000	-2.157037000	-0.001920000
1	-4.474416000	-0.000003000	-0.001273000
1	1.722086000	-0.000169000	1.634385000

PhSP{W(CO)$_5$}$_2$

74	-1.684585000	-1.292988000	0.017100000
74	2.611640000	0.302252000	-0.001551000
15	0.113853000	0.438468000	-0.035059000
16	-0.305474000	2.500839000	-0.138782000
8	0.421780000	-3.369349000	-1.261216000
8	-0.754840000	-2.124417000	3.004472000
8	2.421941000	-2.519181000	1.547949000
8	-3.719802000	-3.774238000	-0.003934000
8	5.803794000	-0.013636000	0.166204000
8	2.635930000	1.949297000	2.781335000
8	-2.742964000	-0.455520000	-2.919640000
8	3.044040000	3.087180000	-1.584864000
8	2.626901000	-1.221571000	-2.856657000
8	-4.109054000	0.356253000	1.374222000
6	-2.997412000	-2.881356000	0.007548000
6	-1.068795000	-1.831750000	1.942612000
6	-0.301463000	-2.602518000	-0.808418000
6	2.464846000	-1.513393000	0.996884000
6	2.612413000	-0.693998000	-1.839581000
6	4.662698000	0.101567000	0.101631000
6	-2.863828000	2.697361000	-1.221402000
1	-2.430800000	2.313634000	-2.144243000
6	-3.209116000	-0.152391000	0.878999000
6	-2.360292000	-0.746148000	-1.878080000
6	2.858400000	2.107725000	-1.018515000
6	-4.209276000	3.068723000	-1.174527000
1	-4.829551000	2.957552000	-2.064994000
6	2.628018000	1.356080000	1.800643000
6	-2.066690000	2.837045000	-0.076279000
6	-3.954057000	3.739054000	1.138295000
1	-4.377220000	4.144130000	2.058425000
6	-4.756059000	3.586964000	0.003358000
1	-5.807099000	3.876636000	0.035275000
6	-2.609326000	3.365284000	1.103902000
1	-1.979806000	3.484003000	1.985958000

PhSeP{W(CO)$_5$}$_2$

74	-2.643765000	0.272444000	0.010464000
74	1.592646000	-1.490039000	0.012786000
34	0.404737000	2.490060000	-0.144332000
15	-0.135385000	0.314997000	-0.023677000
8	2.752677000	-0.594816000	-2.867451000
8	-0.556394000	-3.434284000	-1.397711000
8	-2.619772000	1.772280000	2.875899000
8	-2.559099000	-2.627393000	1.418255000
8	-5.840391000	0.028050000	0.173926000
8	-3.053898000	3.132188000	-1.437069000
8	4.014879000	0.041532000	1.506678000
8	0.550089000	-2.397473000	2.939916000
8	-2.698118000	-1.106701000	-2.917513000
8	3.541488000	-4.038306000	-0.044209000
6	0.184894000	-2.715965000	-0.897227000
6	-2.558813000	-1.594692000	0.917976000
6	2.335777000	-0.904013000	-1.844470000
6	2.327211000	2.706533000	-0.052249000
6	3.123414000	-0.428628000	0.960988000
6	-2.627859000	1.231960000	1.865113000
6	2.849800000	-3.121410000	-0.019524000
6	-2.865992000	2.126682000	-0.917621000
6	2.893446000	3.184447000	1.137473000
1	2.269017000	3.347027000	2.016366000
6	3.124604000	2.506551000	-1.187293000
1	2.679441000	2.157720000	-2.118287000
6	-2.670910000	-0.630581000	-1.875761000
6	-4.696827000	0.119817000	0.111335000
6	4.495785000	2.767883000	-1.120560000
1	5.117256000	2.608798000	-2.003051000
6	0.903705000	-2.076614000	1.898817000
6	4.264140000	3.448502000	1.191420000
1	4.706131000	3.814182000	2.119308000
6	5.066309000	3.237155000	0.066291000
1	6.136858000	3.440933000	0.113507000

PhTeP{W(CO)$_5$}$_2$

74	2.695186000	-0.307131000	0.020707000
74	-1.426712000	1.734483000	0.006200000
52	-0.597122000	-2.515660000	-0.124417000
15	0.176966000	-0.188111000	-0.008821000
8	-2.760767000	0.782374000	-2.778396000
8	0.780082000	3.463210000	-1.588077000
8	2.600246000	-1.617930000	2.976304000
8	2.805549000	2.677537000	1.238234000
8	5.897341000	-0.210992000	0.166558000
8	3.010583000	-3.258300000	-1.250501000
8	-3.814688000	0.365082000	1.700094000
8	-0.204326000	2.726148000	2.834011000
8	2.796759000	0.881225000	-2.989200000
8	-3.236284000	4.381683000	-0.081661000
6	0.012755000	2.824699000	-1.023025000
6	2.728021000	1.616944000	0.807749000
6	-2.284329000	1.110674000	-1.787775000
6	-2.743796000	-2.516603000	-0.023012000
6	-2.948926000	0.788917000	1.080199000
6	2.633691000	-1.144265000	1.933022000
6	-2.593547000	3.429706000	-0.045999000
6	2.845663000	-2.218220000	-0.792136000
6	-3.366183000	-2.907630000	1.171129000
1	-2.772984000	-3.130453000	2.058868000
6	-3.515745000	-2.235946000	-1.159431000
1	-3.040602000	-1.947627000	-2.096829000
6	2.754434000	0.473229000	-1.919527000
6	4.750035000	-0.251931000	0.110663000
6	-4.909218000	-2.330154000	-1.091361000
1	-5.507315000	-2.106899000	-1.976167000
6	-0.619836000	2.372355000	1.826859000
6	-4.759307000	-3.004574000	1.228335000
1	-5.240837000	-3.302308000	2.160969000
6	-5.531464000	-2.712998000	0.100301000
1	-6.618862000	-2.786281000	0.149186000

Mes_2S_2

16	0.212198000	1.074476000	0.000229000
16	-0.212198000	-1.074476000	0.000229000
6	1.999868000	1.015430000	0.001822000
6	4.817402000	1.030674000	0.003807000
6	2.697556000	1.017292000	1.231716000
6	2.700793000	1.010814000	-1.229684000
6	4.098634000	1.020928000	-1.199438000
1	4.644435000	1.019554000	-2.145395000
6	4.098634000	1.027722000	1.203423000
1	4.642570000	1.031664000	2.150032000
6	6.325662000	1.042852000	-0.007274000
1	6.723483000	0.164150000	-0.537784000
1	6.737947000	1.040434000	1.009527000
1	6.709505000	1.933877000	-0.527505000
6	1.983119000	0.991014000	-2.556013000
1	1.328127000	0.112103000	-2.637417000
1	2.701772000	0.967154000	-3.384302000
1	1.341542000	1.875359000	-2.675364000
6	1.980271000	1.004250000	2.558261000
1	1.338883000	1.889235000	2.673808000
1	2.699102000	0.984355000	3.386536000
1	1.325386000	0.125722000	2.644484000
6	-1.999868000	-1.015430000	0.001822000
6	-2.697556000	-1.017292000	1.231716000
6	-2.700793000	-1.010814000	-1.229684000
6	-4.098634000	-1.027722000	1.203423000
6	-4.098634000	-1.020928000	-1.199438000
6	-4.817402000	-1.030674000	0.003807000
1	-4.642570000	-1.031664000	2.150032000
1	-4.644435000	-1.019554000	-2.145395000
6	-1.980271000	-1.004250000	2.558261000
1	-1.338883000	-1.889235000	2.673808000
1	-1.325386000	-0.125722000	2.644484000
1	-2.699102000	-0.984355000	3.386536000
6	-6.325662000	-1.042852000	-0.007274000
1	-6.737947000	-1.040434000	1.009527000
1	-6.723483000	-0.164150000	-0.537784000
1	-6.709505000	-1.933877000	-0.527505000
6	-1.983119000	-0.991014000	-2.556013000
1	-2.701772000	-0.967154000	-3.384302000
1	-1.328127000	-0.112103000	-2.637417000
1	-1.341542000	-1.875359000	-2.675364000

Mes_2Se_2

34	-0.972909000	0.740055000	-0.088262000
34	0.972909000	-0.740055000	-0.088262000
6	0.001835000	2.412526000	-0.008713000
6	1.327748000	4.896299000	0.103549000
6	0.314877000	2.979702000	1.247330000
6	0.355588000	3.070668000	-1.211867000
6	1.010999000	4.303975000	-1.126059000
1	1.286053000	4.817049000	-2.050096000
6	0.972909000	4.217866000	1.273231000
1	1.216616000	4.661539000	2.240562000
6	2.035577000	6.227533000	0.151583000
1	3.012316000	6.173747000	-0.353435000
1	2.205850000	6.558188000	1.183866000
1	1.449949000	7.005228000	-0.362204000
6	0.056993000	2.488637000	-2.572222000
1	0.483145000	1.480912000	-2.675305000
1	0.471692000	3.125490000	-3.363441000
1	-1.025355000	2.390849000	-2.737552000
6	-0.026906000	2.302034000	2.551494000
1	-1.113703000	2.188764000	2.670980000
1	0.355985000	2.882404000	3.400069000
1	0.403037000	1.291716000	2.597520000
6	-0.001835000	-2.412526000	-0.008713000
6	-0.314877000	-2.979702000	1.247330000
6	-0.355588000	-3.070668000	-1.211867000
6	-0.972909000	-4.217866000	1.273231000
6	-1.010999000	-4.303975000	-1.126059000
6	-1.327748000	-4.896299000	0.103549000
1	-1.216616000	-4.661539000	2.240562000
1	-1.286053000	-4.817049000	-2.050096000
6	0.026906000	-2.302034000	2.551494000
1	1.113703000	-2.188764000	2.670980000
1	-0.403037000	-1.291716000	2.597520000
1	-0.355985000	-2.882404000	3.400069000
6	-2.035577000	-6.227533000	0.151583000
1	-2.205850000	-6.558188000	1.183866000
1	-3.012316000	-6.173747000	-0.353435000
1	-1.449949000	-7.005228000	-0.362204000
6	-0.056993000	-2.488637000	-2.572222000
1	-0.471692000	-3.125490000	-3.363441000
1	-0.483145000	-1.480912000	-2.675305000
1	1.025355000	-2.390849000	-2.737552000

Mes_2Te_2

52	-1.100419000	0.881831000	-0.452938000
52	1.100419000	-0.881831000	-0.452938000
6	0.001626000	2.679616000	0.042900000
6	1.353488000	5.078761000	0.668110000
6	0.346728000	2.960121000	1.384163000
6	0.330562000	3.589446000	-0.992112000
6	0.999054000	4.772274000	-0.651264000
1	1.253923000	5.476546000	-1.446272000
6	1.019140000	4.159710000	1.665432000
1	1.287075000	4.377910000	2.701164000
6	2.074636000	6.363895000	0.990379000
1	3.033225000	6.424671000	0.452526000
1	2.282798000	6.452331000	2.064094000
1	1.479026000	7.238538000	0.686785000
6	-0.001626000	3.348606000	-2.446828000
1	0.403759000	2.389980000	-2.799210000
1	0.410295000	4.150740000	-3.072002000
1	-1.087488000	3.309201000	-2.614639000
6	0.038060000	2.024011000	2.525549000
1	-1.036335000	1.800862000	2.583064000
1	0.354718000	2.460385000	3.480874000
1	0.557438000	1.063379000	2.398429000
6	-0.001626000	-2.679616000	0.042900000
6	-0.346728000	-2.960121000	1.384163000
6	-0.330562000	-3.589446000	-0.992112000
6	-1.019140000	-4.159710000	1.665432000
6	-0.999054000	-4.772274000	-0.651264000
6	-1.353488000	-5.078761000	0.668110000
1	-1.287075000	-4.377910000	2.701164000
1	-1.253923000	-5.476546000	-1.446272000
6	-0.038060000	-2.024011000	2.525549000
1	1.036335000	-1.800862000	2.583064000
1	-0.557438000	-1.063379000	2.398429000
1	-0.354718000	-2.460385000	3.480874000
6	-2.074636000	-6.363895000	0.990379000
1	-2.282798000	-6.452331000	2.064094000
1	-3.033225000	-6.424671000	0.452526000
1	-1.479026000	-7.238538000	0.686785000
6	0.001626000	-3.348606000	-2.446828000
1	-0.410295000	-4.150740000	-3.072002000
1	-0.403759000	-2.389980000	-2.799210000
1	1.087488000	-3.309201000	-2.614639000

MesS

16	-2.566098000	-0.009645000	0.000094000
6	-0.845372000	-0.001525000	-0.000037000
6	-0.122390000	1.242316000	-0.000036000
6	-0.109505000	-1.240561000	-0.000056000
6	1.270772000	1.215292000	0.000056000
6	1.279842000	-1.199925000	0.000048000
6	1.994647000	0.012667000	0.000099000
1	1.817356000	2.160221000	0.000142000
1	1.836196000	-2.139586000	0.000087000
6	-0.840379000	2.564672000	-0.000105000
1	-1.493940000	2.660348000	-0.878803000
1	-1.494193000	2.660358000	0.878396000
1	-0.124017000	3.395487000	-0.000028000
6	3.499387000	0.005294000	0.000016000
1	3.912499000	1.021353000	0.002164000
1	3.888814000	-0.525485000	0.882829000
1	3.888642000	-0.521544000	-0.885263000
6	-0.817000000	-2.568871000	-0.000102000
1	-0.093899000	-3.393817000	-0.000376000
1	-1.469760000	-2.669727000	0.878606000
1	-1.470138000	-2.669445000	-0.878555000

MesSe

34	-2.208049000	-0.003295000	0.000039000
6	-0.283790000	0.001549000	-0.000010000
6	0.404609000	1.230088000	-0.000068000
6	0.411149000	-1.226722000	-0.000090000
6	1.805950000	1.203627000	-0.000132000
6	1.809198000	-1.194467000	-0.000192000
6	2.530569000	0.007416000	-0.000245000
1	2.344093000	2.154325000	-0.000236000
1	2.351700000	-2.143045000	-0.000307000
6	-0.340660000	2.539960000	0.000010000
1	-0.988816000	2.630205000	-0.887214000
1	-0.989652000	2.629617000	0.886676000
1	0.349624000	3.392685000	0.000654000
6	4.039864000	-0.001172000	0.000246000
1	4.448184000	1.017548000	-0.005486000
1	4.435063000	-0.517512000	0.888782000
1	4.435688000	-0.527932000	-0.881805000
6	-0.329997000	-2.539088000	0.000036000
1	0.363094000	-3.389486000	-0.000626000
1	-0.977747000	-2.630958000	0.887341000
1	-0.978935000	-2.630555000	-0.886443000

MesTe

52	-2.000477000	-0.002264000	-0.000096000
6	0.125745000	0.001931000	0.000117000
6	2.957982000	0.007676000	-0.000105000
6	0.835531000	1.235316000	0.000127000
6	0.841702000	-1.231106000	0.000087000
6	2.238250000	-1.196051000	-0.000019000
1	2.787353000	-2.140119000	-0.000019000
6	2.235574000	1.205820000	-0.000014000
1	2.780474000	2.151898000	-0.000008000
6	4.464583000	-0.002352000	-0.000221000
1	4.854802000	-0.528890000	0.884504000
1	4.877361000	1.014114000	-0.000652000
1	4.854603000	-0.529578000	-0.884622000
6	0.158886000	-2.577526000	0.000302000
1	-0.487386000	-2.700194000	0.880661000
1	0.901426000	-3.385359000	-0.000063000
1	-0.488301000	-2.700099000	-0.879368000
6	0.149763000	2.580133000	0.000305000
1	-0.496643000	2.701958000	-0.880031000
1	0.890467000	3.389677000	0.000963000
1	-0.497456000	2.701264000	0.880139000

MesSH

16	-2.569373000	0.069146000	0.000063000
6	-0.776412000	-0.015233000	0.000035000
6	-0.096002000	1.220776000	-0.000020000
6	-0.060586000	-1.233872000	0.000021000
6	1.304712000	1.215585000	-0.000084000
6	1.338249000	-1.177912000	-0.000076000
6	2.045870000	0.030510000	-0.000122000
1	1.828477000	2.173934000	-0.000203000
1	1.894338000	-2.118261000	-0.000109000
6	-0.850653000	2.526289000	0.000015000
1	-1.501804000	2.614606000	-0.884401000
1	-1.501597000	2.614660000	0.884575000
1	-0.160515000	3.378452000	-0.000096000
6	3.555215000	0.040772000	0.000087000
1	3.950257000	1.064736000	-0.003146000
1	3.957381000	-0.472602000	0.887234000
1	3.957713000	-0.478435000	-0.883472000
6	-0.746123000	-2.577209000	0.000040000
1	-0.008443000	-3.388455000	0.000190000
1	-1.384997000	-2.709809000	0.888307000
1	-1.384794000	-2.709937000	-0.888359000
1	-2.821669000	-1.253447000	-0.000886000

MesSeH

34	-0.332943000	2.177651000	0.000000000
6	0.000000000	0.266241000	0.000000000
6	-1.144838000	-0.557251000	0.000000000
6	1.296058000	-0.295682000	0.000000000
6	-0.971635000	-1.947894000	0.000000000
6	1.408198000	-1.691989000	0.000000000
6	0.294036000	-2.539969000	0.000000000
1	-1.859746000	-2.583540000	0.000000000
1	2.408525000	-2.130982000	0.000000000
6	-2.535507000	0.026556000	0.000000000
1	-2.706722000	0.659279000	0.885915000
1	-2.706722000	0.659279000	-0.885915000
1	-3.294492000	-0.764835000	0.000000000
6	0.466440000	-4.039397000	0.000000000
1	-0.502056000	-4.555695000	0.000000000
1	1.027853000	-4.375824000	-0.885334000
1	1.027853000	-4.375824000	0.885334000
6	2.552495000	0.538485000	0.000000000
1	3.442223000	-0.102505000	0.000000000
1	2.608900000	1.188274000	-0.887666000
1	2.608900000	1.188274000	0.887666000
1	1.074083000	2.599377000	0.000000000

MesTeH

52	-1.990096000	0.027794000	0.000016000
6	0.169661000	-0.045820000	-0.000015000
6	0.824219000	1.202924000	-0.000017000
6	0.909059000	-1.248994000	0.000006000
6	2.226365000	1.228891000	-0.000019000
6	2.308058000	-1.162837000	-0.000010000
6	2.990597000	0.059520000	-0.000032000
1	2.730821000	2.197636000	-0.000019000
1	2.884284000	-2.091038000	0.000008000
6	0.059416000	2.503442000	0.000003000
1	-0.587802000	2.591019000	-0.888108000
1	-0.587818000	2.590996000	0.888105000
1	0.740417000	3.363014000	0.000033000
6	4.499194000	0.100011000	0.000004000
1	4.874296000	1.131415000	-0.000375000
1	4.910768000	-0.408566000	0.885489000
1	4.910834000	-0.409257000	-0.885049000
6	0.268501000	-2.614448000	0.000056000
1	1.032892000	-3.400862000	0.000221000
1	-0.367263000	-2.762616000	0.886445000
1	-0.367040000	-2.762787000	-0.886467000
1	-2.219818000	-1.620364000	-0.000964000

MesSP{W(CO)$_5$}$_2$

74	2.754850000	-0.648601000	-0.000189000
74	-1.145917000	1.769384000	-0.000317000
16	-0.531493000	-2.232441000	0.001840000
15	0.276404000	-0.289791000	0.000757000
8	-2.599509000	4.627580000	-0.003248000
8	5.946352000	-1.011004000	-0.001484000
8	1.531928000	3.552067000	-0.005361000
8	2.503759000	-2.950858000	-2.254150000
8	3.084401000	1.585806000	2.310159000
8	-4.182475000	0.675431000	0.003334000
8	3.082120000	1.579878000	-2.316598000
8	-1.202200000	1.742926000	3.235341000
8	2.505859000	-2.945161000	2.259819000
8	-1.208072000	1.733722000	-3.235739000
6	2.585873000	-2.130848000	-1.456969000
6	0.609507000	2.868839000	-0.003537000
6	-2.325214000	-2.240036000	0.003345000
6	4.804758000	-0.881268000	-0.000984000
6	-2.088299000	3.598665000	-0.002141000
6	2.955513000	0.803106000	1.481958000
6	-5.116951000	-2.528984000	0.005440000
6	-3.009151000	-2.317607000	1.236274000
6	-3.011918000	-2.322360000	-1.231098000
6	2.587300000	-2.127165000	1.460504000
6	-3.067506000	0.943757000	0.002445000
6	2.954036000	0.799323000	-1.486252000
6	-4.401507000	-2.462986000	-1.198058000
1	-4.944113000	-2.525208000	-2.143439000
6	-4.402026000	-2.457750000	1.205269000
1	-4.942990000	-2.515121000	2.151492000
6	-6.617348000	-2.673050000	-0.006111000
1	-7.087819000	-1.815022000	-0.509714000
1	-7.026514000	-2.735525000	1.009660000
1	-6.923069000	-3.577072000	-0.554103000
6	-1.176822000	1.749353000	-2.089976000
6	-1.172962000	1.755287000	2.089496000
6	-2.293789000	-2.270431000	-2.556698000
1	-1.792783000	-1.303300000	-2.707038000
1	-2.998181000	-2.417201000	-3.383598000
1	-1.514670000	-3.043074000	-2.624439000
6	-2.291806000	-2.261147000	2.562014000
1	-1.508432000	-3.029329000	2.630590000
1	-2.995577000	-2.411434000	3.388826000
1	-1.796455000	-1.291058000	2.712299000

MesSeP{W(CO)$_5$}$_2$

74	2.800527000	-0.632135000	-0.000473000
74	-1.024424000	1.910858000	-0.000284000
34	-0.604449000	-2.239098000	0.003823000
15	0.325632000	-0.201271000	0.001050000
8	-2.368301000	4.820790000	-0.002328000
8	5.984282000	-1.040996000	-0.003575000
8	1.708326000	3.608073000	-0.001750000
8	2.526269000	-2.921021000	-2.264590000
8	3.175834000	1.589912000	2.315757000
8	-4.104077000	0.946471000	-0.000751000
8	3.172083000	1.587992000	-2.319096000
8	-1.084617000	1.867263000	3.235250000
8	2.530713000	-2.919037000	2.266206000
8	-1.084514000	1.863390000	-3.235777000
6	2.613822000	-2.106200000	-1.462267000
6	0.766127000	2.952254000	-0.001095000
6	-2.538993000	-2.106949000	0.003686000
6	4.844213000	-0.896370000	-0.002373000
6	-1.897142000	3.772634000	-0.001552000
6	3.029433000	0.812925000	1.485304000
6	-5.344748000	-2.181635000	0.003509000
6	-3.227111000	-2.128830000	1.235530000
6	-3.228231000	-2.135122000	-1.230777000
6	2.616611000	-2.104939000	1.462971000
6	-2.978098000	1.164274000	-0.000133000
6	3.026982000	0.811670000	-1.487784000
6	-4.625391000	-2.169784000	-1.199021000
1	-5.170416000	-2.188125000	-2.144876000
6	-4.627500000	-2.162885000	1.203533000
1	-5.172184000	-2.175282000	2.149293000
6	-6.851857000	-2.211368000	-0.009114000
1	-7.255675000	-1.319625000	-0.512015000
1	-7.265267000	-2.243711000	1.006371000
1	-7.224906000	-3.089051000	-0.558202000
6	-1.053576000	1.885401000	-2.090100000
6	-1.053631000	1.887986000	2.089549000
6	-2.515328000	-2.128822000	-2.561361000
1	-1.918851000	-1.215137000	-2.695246000
1	-3.235805000	-2.186263000	-3.385601000
1	-1.820580000	-2.976084000	-2.653368000
6	-2.516800000	-2.116232000	2.567370000
1	-1.819103000	-2.960592000	2.663241000
1	-3.238541000	-2.174140000	3.390491000
1	-1.924193000	-1.199868000	2.700164000

MesTeP{W(CO)$_5$}$_2$

74	-2.857325000	-0.668819000	0.032305000
74	0.826299000	2.086314000	-0.001125000
52	0.756377000	-2.267904000	-0.202522000
15	-0.395048000	-0.112256000	-0.036375000
8	2.020341000	5.058437000	-0.053847000
8	-1.944497000	3.586447000	-0.660435000
8	-3.305480000	1.848914000	2.004270000
8	-6.017124000	-1.172842000	0.238654000
8	3.875578000	1.270605000	0.674129000
8	-2.399269000	-2.622484000	2.564330000
8	1.481422000	1.768857000	-3.150904000
8	-2.648954000	-3.226824000	-1.928088000
8	-3.356840000	1.175478000	-2.578788000
6	-0.984044000	3.003521000	-0.425547000
8	0.271538000	2.353987000	3.178031000
6	3.655589000	-1.788206000	-1.207904000
6	3.484692000	-1.987603000	1.241339000
6	2.881707000	-1.934739000	-0.036981000
6	1.601646000	3.987902000	-0.032093000
6	-4.883670000	-0.996252000	0.161427000
6	1.242675000	1.882806000	-2.034801000
6	5.676654000	-1.714311000	0.178258000
6	-3.124762000	0.963989000	1.297398000
6	5.046802000	-1.675084000	-1.068657000
1	5.654327000	-1.556327000	-1.967765000
6	-2.559315000	-1.922191000	1.670084000
6	2.768850000	1.448957000	0.432291000
6	3.057841000	-1.752900000	-2.594760000
1	2.483701000	-2.665199000	-2.813094000
1	3.845203000	-1.661493000	-3.352366000
1	2.370390000	-0.905345000	-2.720826000
6	0.456988000	2.259812000	2.051223000
6	4.876816000	-1.874849000	1.316948000
1	5.352211000	-1.907874000	2.299345000
6	-3.170099000	0.537887000	-1.645015000
6	2.695529000	-2.147753000	2.519547000
1	1.978487000	-1.325739000	2.657350000
1	3.365147000	-2.161293000	3.387669000
1	2.113804000	-3.081212000	2.526133000
6	-2.694868000	-2.317230000	-1.229198000
6	7.173212000	-1.587129000	0.307139000
1	7.656429000	-1.476715000	-0.671435000
1	7.603189000	-2.470900000	0.802433000
1	7.440003000	-0.712126000	0.918962000

Cp*P{W(CO)$_5$}$_2$·SHPh

16	0.210895000	1.918311000	1.409102000
15	-0.128548000	0.401365000	-0.402783000
74	-2.562710000	-0.505106000	0.465790000
74	1.732394000	-1.520606000	-0.646159000
6	-0.034543000	1.893325000	-1.760914000
6	2.775151000	-3.243440000	-0.795692000
6	2.644114000	-0.969415000	-2.416023000
6	1.056411000	-2.247906000	1.182939000
6	0.276561000	-2.446638000	-1.809514000
6	3.391125000	-0.737133000	0.323483000
6	-4.333664000	-1.148987000	1.178009000
6	-3.332539000	-0.677573000	-1.462323000
6	-1.841083000	-0.505784000	2.398273000
6	-3.280004000	1.410375000	0.798220000
6	-2.077802000	-2.522436000	0.351989000
6	-1.162777000	2.904675000	-1.598994000
6	-0.639691000	4.113972000	-1.260938000
6	0.832976000	4.015453000	-1.237374000
6	1.212096000	2.741702000	-1.563269000
6	-0.097574000	1.190037000	-3.129122000
6	-2.568333000	2.658250000	-2.045872000
6	-1.367289000	5.407787000	-1.049048000
6	1.709127000	5.207343000	-0.982798000
6	2.608575000	2.263743000	-1.787547000
8	-3.792291000	-0.840623000	-2.503409000
8	-5.354997000	-1.498966000	1.587860000
8	-1.930758000	-3.661905000	0.361242000
8	-3.745072000	2.428738000	1.067158000
8	-1.466230000	-0.527618000	3.488302000
8	3.355785000	-4.237341000	-0.873927000
8	0.783611000	-2.700935000	2.202869000
8	-0.449224000	-2.987097000	-2.516173000
8	4.388859000	-0.405014000	0.791039000
8	3.223055000	-0.750719000	-3.387855000
1	-1.015021000	0.598207000	-3.236314000
1	0.755286000	0.525906000	-3.289895000
1	-0.092945000	1.949736000	-3.923559000
1	-2.917823000	1.653355000	-1.805427000
1	-2.638850000	2.764585000	-3.141056000
1	-3.269981000	3.374149000	-1.604424000
1	-1.068475000	5.886314000	-0.103583000
1	-2.453125000	5.269838000	-1.022714000
1	-1.140399000	6.129058000	-1.850986000
1	1.496892000	5.661033000	-0.001959000
1	1.524290000	5.993423000	-1.730145000
1	2.775804000	4.961781000	-1.018311000
1	2.877307000	1.436403000	-1.119511000
1	3.336468000	3.068841000	-1.639515000
1	2.740917000	1.892468000	-2.813728000
1	0.619979000	2.917411000	0.553738000
6	1.788711000	1.708970000	2.239349000
6	1.861347000	0.775051000	3.280570000
6	2.885368000	2.520707000	1.921594000
6	3.051427000	0.650111000	3.999620000
6	4.064059000	2.391646000	2.656261000
6	4.150968000	1.454978000	3.690192000
1	0.998300000	0.162068000	3.536999000
1	2.818797000	3.249143000	1.114903000
1	3.113621000	-0.079087000	4.807598000
1	4.920076000	3.021528000	2.412976000
1	5.077947000	1.352059000	4.255085000

Cp*P{W(CO)$_5$}$_2$·SeHPh

74	-1.952273000	0.925033000	-0.958416000
6	-0.850187000	-1.869775000	1.659566000
6	-3.276466000	1.395775000	-2.400678000
6	-3.559041000	0.669918000	0.344419000
6	-0.438769000	1.395360000	-2.299603000
6	-2.224932000	-0.972227000	-1.816277000
6	-2.091466000	2.958990000	-0.523306000
6	-1.999332000	-1.387655000	2.533126000
6	-3.141124000	-2.007780000	2.133306000
6	-2.856703000	-2.903161000	1.001206000
6	-1.526342000	-2.868208000	0.718635000
6	0.257436000	-2.504207000	2.517426000
6	-1.861381000	-0.599924000	3.810625000
6	-4.484026000	-1.926947000	2.793275000
6	-3.921756000	-3.731796000	0.349022000
6	-0.796107000	-3.728653000	-0.264098000
8	-4.031409000	1.622067000	-3.242865000
8	0.329954000	1.722640000	-3.084446000
8	-2.470079000	-1.917361000	-2.413406000
8	-2.270174000	4.085413000	-0.389304000
8	-4.520778000	0.674571000	0.970600000
1	0.741238000	-1.764411000	3.167380000
1	1.032587000	-2.970435000	1.904674000
1	-0.186722000	-3.281909000	3.154945000
1	-2.296519000	-1.159830000	4.651893000
1	-2.382956000	0.367894000	3.772350000
1	-0.818004000	-0.391128000	4.065120000
1	-5.285268000	-1.768105000	2.057747000
1	-4.536235000	-1.110980000	3.522197000
1	-4.719057000	-2.866545000	3.319358000
1	-4.705957000	-3.093559000	-0.087951000
1	-4.422680000	-4.382051000	1.083201000
1	-3.528325000	-4.367371000	-0.450588000
1	-0.207129000	-3.150935000	-0.988393000
1	-1.492347000	-4.350115000	-0.836899000
1	-0.091560000	-4.405360000	0.241687000
74	2.411988000	-1.005165000	-0.492702000
6	4.242350000	-1.286442000	-1.285287000
6	3.268146000	-0.834684000	1.385187000
6	1.566142000	-1.329863000	-2.362458000
6	2.760856000	0.996643000	-0.950501000
6	2.446205000	-3.051233000	-0.211509000
8	5.293780000	-1.437010000	-1.737580000
8	3.090865000	2.045020000	-1.282946000
8	3.776087000	-0.806847000	2.418116000
8	2.598733000	-4.187506000	-0.102653000
8	1.126264000	-1.555459000	-3.400016000
15	-0.064832000	-0.497997000	0.477840000
34	-0.311305000	1.440076000	1.788735000
6	1.257090000	2.562964000	1.613655000
6	1.199228000	3.741491000	0.858324000
6	2.393599000	2.269997000	2.380586000
6	2.290898000	4.612906000	0.855206000
6	3.481100000	3.145736000	2.366810000
6	3.433122000	4.315375000	1.602362000
1	0.312981000	3.987801000	0.278782000
1	2.429447000	1.370775000	2.991915000
1	2.246235000	5.525544000	0.259925000
1	4.365743000	2.911795000	2.960551000
1	4.285260000	4.996160000	1.592107000

Cp*P{W(CO)$_5$}$_2$·TeHPh

52	0.291815000	2.112856000	1.232046000
15	-0.166935000	0.246070000	-0.578623000
74	-2.615419000	-0.543022000	0.512741000
74	1.622738000	-1.788867000	-0.706210000
6	-0.106433000	1.563049000	-2.104401000
6	2.621130000	-3.538627000	-0.700851000
6	2.421285000	-1.505379000	-2.590633000
6	1.034281000	-2.281903000	1.226092000
6	0.076783000	-2.792066000	-1.671662000
6	3.342027000	-0.911177000	0.050142000
6	-4.352371000	-1.104449000	1.350232000
6	-3.468022000	-0.840858000	-1.367639000
6	-1.804454000	-0.409229000	2.399898000
6	-3.322195000	1.388081000	0.729852000
6	-2.167526000	-2.575582000	0.550775000
6	-1.154295000	2.661678000	-1.963708000
6	-0.532219000	3.870851000	-1.884123000
6	0.921295000	3.679237000	-2.016615000
6	1.196046000	2.346937000	-2.163178000
6	-0.349631000	0.707153000	-3.363642000
6	-2.614910000	2.451708000	-2.207407000
6	-1.168815000	5.226357000	-1.802484000
6	1.877974000	4.834952000	-2.064736000
6	2.538194000	1.752660000	-2.432493000
8	-3.971643000	-1.061641000	-2.376649000
8	-5.357761000	-1.409485000	1.830927000
8	-2.049470000	-3.712146000	0.665089000
8	-3.786297000	2.421439000	0.943452000
8	-1.377658000	-0.350590000	3.471216000
8	3.181591000	-4.547975000	-0.686809000
8	0.799383000	-2.615964000	2.300684000
8	-0.701934000	-3.378038000	-2.279285000
8	4.364390000	-0.515787000	0.401684000
8	2.926706000	-1.446926000	-3.624382000
1	-1.309813000	0.179668000	-3.313831000
1	0.439419000	-0.036163000	-3.509281000
1	-0.368805000	1.362333000	-4.246312000
1	-2.970032000	1.494250000	-1.824201000
1	-2.819657000	2.455448000	-3.291039000
1	-3.226036000	3.242814000	-1.758975000
1	-0.726452000	5.831526000	-0.996143000
1	-2.247090000	5.165749000	-1.621415000
1	-1.017978000	5.792547000	-2.736052000
1	1.776240000	5.478773000	-1.177297000
1	1.670438000	5.476748000	-2.935172000
1	2.922714000	4.514075000	-2.130081000
1	2.827640000	1.023347000	-1.665794000
1	3.314832000	2.524014000	-2.475142000
1	2.555472000	1.219384000	-3.393789000
1	1.100403000	3.044917000	0.080529000
6	2.124870000	1.634463000	2.240749000
6	2.093443000	0.702783000	3.285845000
6	3.306840000	2.314313000	1.920042000
6	3.263474000	0.446344000	4.006728000
6	4.466822000	2.052020000	2.652541000
6	4.447280000	1.118559000	3.692562000
1	1.175302000	0.176441000	3.546188000
1	3.336457000	3.036844000	1.104568000
1	3.243203000	-0.283290000	4.816861000
1	5.390587000	2.574040000	2.400259000
1	5.357457000	0.912359000	4.257017000

Cp*P{W(CO)$_5$}$_2$·SPh

74	-1.992750000	1.005900000	-0.807302000
6	-0.751392000	-1.954454000	1.588454000
6	-3.336923000	1.514408000	-2.212286000
6	-3.582615000	0.566188000	0.467793000
6	-0.506190000	1.658050000	-2.101454000
6	-2.173835000	-0.830207000	-1.808053000
6	-2.248005000	2.992674000	-0.219931000
6	-1.895187000	-1.566812000	2.513194000
6	-3.023616000	-2.201197000	2.098306000
6	-2.734852000	-3.011664000	0.904050000
6	-1.413430000	-2.911818000	0.597174000
6	0.394548000	-2.605744000	2.381972000
6	-1.752423000	-0.841643000	3.825755000
6	-4.353406000	-2.208027000	2.788966000
6	-3.786347000	-3.830462000	0.218145000
6	-0.674190000	-3.675414000	-0.456433000
8	-4.103666000	1.767030000	-3.036654000
8	0.243786000	2.087417000	-2.854549000
8	-2.375209000	-1.740713000	-2.471522000
8	-2.493920000	4.092226000	-0.000251000
8	-4.542301000	0.470030000	1.088945000
1	0.863730000	-1.895777000	3.074564000
1	1.174446000	-2.999313000	1.725498000
1	-0.009955000	-3.441203000	2.970889000
1	-2.130766000	-1.464066000	4.650482000
1	-2.318279000	0.100972000	3.850453000
1	-0.712345000	-0.591789000	4.055414000
1	-5.176070000	-2.030815000	2.081824000
1	-4.415051000	-1.441840000	3.569492000
1	-4.545306000	-3.186178000	3.259306000
1	-4.598490000	-3.191070000	-0.162481000
1	-4.252350000	-4.542918000	0.916784000
1	-3.388591000	-4.399978000	-0.627918000
1	-0.120736000	-3.027935000	-1.149579000
1	-1.359959000	-4.280113000	-1.059156000
1	0.064095000	-4.359755000	-0.012534000
74	2.443382000	-0.789125000	-0.528450000
6	4.263095000	-0.929461000	-1.381903000
6	3.357387000	-0.764317000	1.330883000
6	1.578754000	-0.972476000	-2.408731000
6	2.708466000	1.261331000	-0.781472000
6	2.545815000	-2.850481000	-0.431949000
8	5.307021000	-0.999546000	-1.869261000
8	2.988582000	2.353711000	-0.996986000
8	3.912533000	-0.817845000	2.337877000
8	2.733122000	-3.986514000	-0.422318000
8	1.135474000	-1.120098000	-3.458699000
15	-0.036209000	-0.479079000	0.501830000
16	-0.416212000	1.252478000	1.809262000
6	1.010226000	2.337385000	1.914279000
6	0.973404000	3.610777000	1.329738000
6	2.099283000	1.962583000	2.715199000
6	2.034985000	4.495006000	1.531189000
6	3.158284000	2.850690000	2.905600000
6	3.130290000	4.116279000	2.311224000
1	0.122007000	3.915721000	0.726590000
1	2.112350000	0.987341000	3.197040000
1	2.005592000	5.481729000	1.068096000
1	4.004821000	2.551594000	3.524631000
1	3.960502000	4.807839000	2.459678000

Cp*P{W(CO)$_5$}$_2$·SePh

74	-1.952273000	0.925033000	-0.958416000
6	-0.850187000	-1.869775000	1.659566000
6	-3.276466000	1.395775000	-2.400678000
6	-3.559041000	0.669918000	0.344419000
6	-0.438769000	1.395360000	-2.299603000
6	-2.224932000	-0.972227000	-1.816277000
6	-2.091466000	2.958990000	-0.523306000
6	-1.999332000	-1.387655000	2.533126000
6	-3.141124000	-2.007780000	2.133306000
6	-2.856703000	-2.903161000	1.001206000
6	-1.526342000	-2.868208000	0.718635000
6	0.257436000	-2.504207000	2.517426000
6	-1.861381000	-0.599924000	3.810625000
6	-4.484026000	-1.926947000	2.793275000
6	-3.921756000	-3.731796000	0.349022000
6	-0.796107000	-3.728653000	-0.264098000
8	-4.031409000	1.622067000	-3.242865000
8	0.329954000	1.722640000	-3.084446000
8	-2.470079000	-1.917361000	-2.413406000
8	-2.270174000	4.085413000	-0.389304000
8	-4.520778000	0.674571000	0.970600000
1	0.741238000	-1.764411000	3.167380000
1	1.032587000	-2.970435000	1.904674000
1	-0.186722000	-3.281909000	3.154945000
1	-2.296519000	-1.159830000	4.651893000
1	-2.382956000	0.367894000	3.772350000
1	-0.818004000	-0.391128000	4.065120000
1	-5.285268000	-1.768105000	2.057747000
1	-4.536235000	-1.110980000	3.522197000
1	-4.719057000	-2.866545000	3.319358000
1	-4.705957000	-3.093559000	-0.087951000
1	-4.422680000	-4.382051000	1.083201000
1	-3.528325000	-4.367371000	-0.450588000
1	-0.207129000	-3.150935000	-0.988393000
1	-1.492347000	-4.350115000	-0.836899000
1	-0.091560000	-4.405360000	0.241687000
74	2.411988000	-1.005165000	-0.492702000
6	4.242350000	-1.286442000	-1.285287000
6	3.268146000	-0.834684000	1.385187000
6	1.566142000	-1.329863000	-2.362458000
6	2.760856000	0.996643000	-0.950501000
6	2.446205000	-3.051233000	-0.211509000
8	5.293780000	-1.437010000	-1.737580000
8	3.090865000	2.045020000	-1.282946000
8	3.776087000	-0.806847000	2.418116000
8	2.598733000	-4.187506000	-0.102653000
8	1.126264000	-1.555459000	-3.400016000
15	-0.064832000	-0.497997000	0.477840000
34	-0.311305000	1.440076000	1.788735000
6	1.257090000	2.562964000	1.613655000
6	1.199228000	3.741491000	0.858324000
6	2.393599000	2.269997000	2.380586000
6	2.290898000	4.612906000	0.855206000
6	3.481100000	3.145736000	2.366810000
6	3.433122000	4.315375000	1.602362000
1	0.312981000	3.987801000	0.278782000
1	2.429447000	1.370775000	2.991915000
1	2.246235000	5.525544000	0.259925000
1	4.365743000	2.911795000	2.960551000
1	4.285260000	4.996160000	1.592107000

Cp*P{W(CO)$_5$}$_2$·TePh

74	-1.903961000	0.903184000	-1.080920000
6	-1.047411000	-1.785449000	1.695286000
6	-3.218073000	1.408052000	-2.526322000
6	-3.487758000	0.925232000	0.272568000
6	-0.385495000	1.093201000	-2.484952000
6	-2.378851000	-1.015009000	-1.796101000
6	-1.799519000	2.964933000	-0.822360000
6	-2.205166000	-1.189167000	2.484138000
6	-3.362166000	-1.776534000	2.079780000
6	-3.081360000	-2.760836000	1.024186000
6	-1.741378000	-2.809575000	0.793228000
6	-0.014313000	-2.423533000	2.638831000
6	-2.080198000	-0.307509000	3.698973000
6	-4.728088000	-1.576347000	2.662543000
6	-4.162851000	-3.582276000	0.390410000
6	-1.028513000	-3.773639000	-0.101966000
8	-3.971304000	1.653109000	-3.364271000
8	0.392193000	1.262357000	-3.309909000
8	-2.716228000	-1.967090000	-2.334659000
8	-1.846365000	4.113379000	-0.801474000
8	-4.418397000	1.082207000	0.926619000
1	0.480395000	-1.671841000	3.266867000
1	0.761059000	-2.961833000	2.088780000
1	-0.525321000	-3.140120000	3.297495000
1	-2.648482000	-0.732583000	4.539029000
1	-2.478811000	0.706251000	3.539164000
1	-1.044153000	-0.203154000	4.037710000
1	-5.472249000	-1.374109000	1.878614000
1	-4.758597000	-0.740351000	3.369224000
1	-5.065760000	-2.482248000	3.191334000
1	-4.902293000	-2.939462000	-0.112691000
1	-4.715896000	-4.160113000	1.147373000
1	-3.775807000	-4.285404000	-0.353550000
1	-0.399174000	-3.279755000	-0.853256000
1	-1.740284000	-4.406544000	-0.642157000
1	-0.367162000	-4.439865000	0.471141000
74	2.312918000	-1.313734000	-0.438203000
6	4.140436000	-1.772250000	-1.146789000
6	3.112643000	-0.966268000	1.438069000
6	1.469911000	-1.787038000	-2.277754000
6	2.774897000	0.595323000	-1.128574000
6	2.240984000	-3.316899000	0.059898000
8	5.192471000	-2.024914000	-1.550639000
8	3.164938000	1.572252000	-1.589675000
8	3.566956000	-0.829139000	2.487556000
8	2.335838000	-4.442156000	0.287116000
8	1.023387000	-2.089129000	-3.292869000
15	-0.138975000	-0.543552000	0.452351000
52	-0.087388000	1.643186000	1.812556000
6	1.682450000	2.724645000	1.256253000
6	1.605459000	3.785626000	0.343693000
6	2.881173000	2.466950000	1.937651000
6	2.735572000	4.569982000	0.097799000
6	4.005502000	3.256966000	1.683539000
6	3.935457000	4.305573000	0.762154000
1	0.677286000	4.011748000	-0.176317000
1	2.946127000	1.659904000	2.665363000
1	2.673622000	5.388764000	-0.619993000
1	4.937284000	3.049287000	2.211454000
1	4.816277000	4.917802000	0.563862000

3.5 References

[1] a) M. E. García, D. García-Vivó, A. Ramos, M. A. Ruiz, *Coord. Chem. Rev.* **2017**, *330*, 1; b) G. Huttner, K. Evertz, *Acc. Chem. Res.* **1986**, *19*, 406; c) U. Schmidt, *Angew. Chem.* **1975**, *87*, 535.

[2] M. P. Duffy, Y. Lin, L. Y. Ting, F. Mathey, *New J. Chem.* **2011**, *35*, 2001.

[3] X. Li, S. I. Weissman, T.-S. Lin, P. P. Gaspar, A. H. Cowley, A. I. Smirnov, *J. Am. Chem. Soc.* **1994**, *116*, 7899.

[4] M. T. Nguyen, A. van Keer, L. G. Vanquickenborne, *J. Org. Chem.* **1996**, *61*, 7077.

[5] L. Liu, D. A. Ruiz, D. Munz, G. Bertrand, *Chem* **2016**, *1*, 147.

[6] K. Lammertsma in *Topics in Current Chemistry*, *Vol. 229* (Eds.: J.-P. Majoral, T. Chivers), Springer, Berlin, **2003**, pp. 95–119.

[7] M. Scheer, E. Leiner, P. Kramkowski, M. Schiffer, G. Baum, *Chem. Eur. J.* **1998**, *4*, 1917.

[8] P. Jutzi, R. Kroos, *J. Organomet. Chem.* **1990**, *390*, 317.

[9] P. Jutzi, G. Reumann, *Dalton Trans.* **2000**, 2237.

[10] M. Scheer, D. Himmel, B. P. Johnson, C. Kuntz, M. Schiffer, *Angew. Chem. Int. Ed.* **2007**, *46*, 3971.

[11] M. Seidl, R. Weinzierl, A. Y. Timoshkin, M. Scheer, *Chem. Eur. J* **2016**, *22*, 5484.

[12] M. Scheer, C. Kuntz, M. Stubenhofer, M. Linseis, R. F. Winter, M. Sierka, *Angew. Chem. Int. Ed.* **2009**, *48*, 2600.

[13] M. Schiffer, E. Leiner, M. Scheer, *Eur. J. Inorg. Chem.* **2001**, *2001*, 1661.

[14] A. Schönberg, A. Stephenson, H. Kaltschmitt, E. Petersen, H. Schulten, *Ber. dtsch. Chem. Ges. A/B* **1933**, *66*, 237.

[15] a) W. Mörke, A. Jezierski, H. Singer, *Z. Chem.* **1979**, *19*, 147; b) U. Schmidt, A. Müller, K. Markau, *Tetrahedron Lett.* **1963**, *4*, 1091; c) K. S. W. Rundel, *Z. Naturforsch. B* **1963**, *18B*, 984.

[16] a) B. Alvarez, M. A. Alvarez, I. Amor, M. E. García, D. García-Vivó, J. Suárez, M. A. Ruiz, *Inorg. Chem.* **2012**, *51*, 7810; b) B. Alvarez, M. Angeles Alvarez, I. Amor, M. E. García, M. A. Ruiz, *Inorg. Chem.* **2011**, *50*, 10561; c) A. Ordyszewska, N. Szynkiewicz, Ł. Ponikiewski, M. Scheer, J. Pikies, R. Grubba, *Inorg. Chem.* **2019**, *58*, 7905.

[17] C. M. E. Graham, T. E. Pritchard, P. D. Boyle, J. Valjus, H. M. Tuononen, P. J. Ragogna, *Angew. Chem. Int. Ed.* **2017**, *56*, 6236.

[18] C. Emmerich, G. Huttner, *J. Organomet. Chem.* **1993**, *447*, 81.

[19] M. Schiffer, M. Scheer, *Chem. Eur. J.* **2001**, *7*, 1855.

[20] G. C. Pappalardo, R. Chakravorty, K. J. Irgolic, E. A. Meyers, *Acta Crystallogr. Sect. C* **1983**, *39*, 1618.

[21] D. J. Darensbourg, K. M. Sanchez, J. Reibenspies, *Inorg. Chem.* **1988**, *27*, 3636.

[22] L. R. Krauth-Siegel, W. Schulze, M. L. Ziegler, *Angew. Chem. Int. Ed. Engl.* **1980**, *19*, 397.

[23] P. Pyykkö, *J. Phys. Chem. A* **2015**, *119*, 2326.

[24] P. Pyykkö, M. Atsumi, *Chem. Eur. J.* **2009**, *15*, 186.

[25] S. K. Latypov, F. M. Polyancev, D. G. Yakhvarov, O. G. Sinyashin, *Physical chemistry chemical physics : PCCP* **2015**, *17*, 6976.

[26] a) A. A. Pasynskij, I. L. Eremenko, D. Vegini, *Zh. Neorg. Khim+* **1996**, *41*, 2006; b) M. B. Hursthouse, M. A. Mazid, E. Abel, *CCDC 676233: Experimental Crystal Structure Determination*, Cambridge Crystallographic Data Centre, **2009**.

[27] P. Pyykkö, M. Atsumi, *Chem. Eur. J* **2009**, *15*, 12770.

[28] M. Bochmann, A. P. Coleman, K. J. Webb, M. B. Hursthouse, M. Mazid, *Angew. Chem.* **1991**, *103*, 975.

[29] M. Scheer, C. Kuntz, M. Stubenhofer, M. Zabel, A. Y. Timoshkin, *Angew. Chem. Int. Ed. Engl.* **2010**, *49*, 188.

[30] *TopSpin 3.0*, TopSpin 3.0, Bruker BioSpin GmbH, **2010**.

[31] P. M. Dickson, M. A. D. McGowan, B. Yearwood, M. J. Heeg, J. P. Oliver, *J. Organomet. Chem.* **1999**, *588*, 42.

[32] W.-W. Du Mont, H.-U. Meyer, S. Kubiniok, S. Pohl, W. Saak, *Chem. Ber.* **1992**, *125*, 761.

[33] O. V. Dolomanov, L. J. Bourhis, R. J. Gildea, J. A. K. Howard, H. Puschmann, *Appl. Crystallogr.* **2009**, *42*, 339.

[34] *CrysAlis Pro 171.38.46*, CrysAlis Pro Version 171.38.46, Rigaku Oxford Diffraction.

[35] G. Sheldrick, *Acta Crystallogr. Sect. A* **2015**, *71*, 3.

[36] G. M. Sheldrick, *Acta Crystallogr. C* **2015**, *71*, 3.

[37] a) Lee, Yang, Parr, *Physical review. B, Condensed matter* **1988**, *37*, 785; b) A. D. Becke, *J. Chem. Phys.* **1993**, *98*, 5648.

[38] a) D. Andrae, U. Huermann, M. Dolg, H. Stoll, H. Preu, *Theoret. Chim. Acta* **1990**, *77*, 123; b) F. Weigend, R. Ahlrichs, *Physical chemistry chemical physics : PCCP* **2005**, *7*, 3297; c) D. Rappoport, F. Furche, *J. Chem. Phys.* **2010**, *133*, 134105.

[39] M. J. Frisch, G. W. Trucks, H. B. Schlegel, G. E. Scuseria, M. A. Robb, J. R. Cheeseman, G. Scalmani, V. Barone, G. A. Petersson, H. Nakatsuji et al., *Gaussian 16 Rev. B.01*, Wallingford, CT, **2016**.

[40] a) D. Feller, *J. Comput. Chem.* **1996**, *17*, 1571; b) K. L. Schuchardt, B. T. Didier, T. Elsethagen, L. Sun, V. Gurumoorthi, J. Chase, J. Li, T. L. Windus, *J. Chem. Inf. Model.* **2007**, *47*, 1045.

[41] G. R. Clark, G. J. Palenik, *Aust. J. Chem.* **1975**, *28*, 1187.

[42] K. Wolinski, J. F. Hinton, P. Pulay, *J. Am. Chem. Soc.* **1990**, *112*, 8251.

4 THE REACTIVITY OF BRIDGING AMINOPNICTINIDENE COMPLEXES OF THE TYPE $[R^1R^2NE\{W(CO)_5\}_2]$ (E = P, As)

Lena Rummel,* Michael Seidl,* Christian Eisenhut,* Gabor Balázs, Alexey Y. Timoshkin and Manfred Scheer

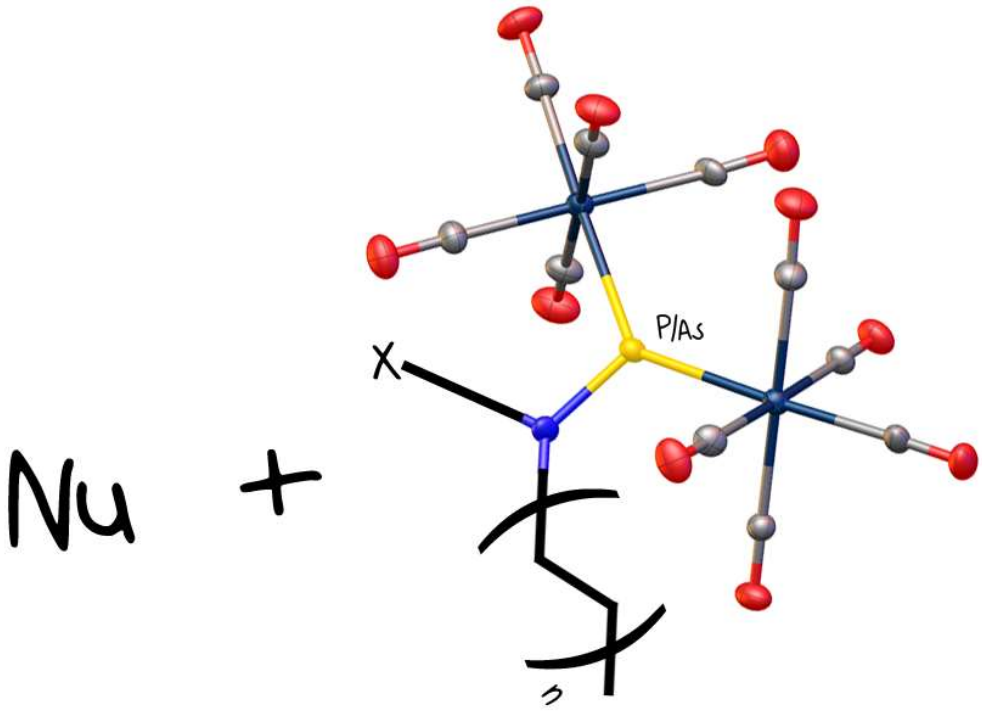

- ⇨ Synthesis and characterization of compounds **3**, **4**, **4Cl**, **5**, **5Cl** and **6** was carried out by Christian Eisenhut, except NMR characterization of **3**: Lena Rummel
- ⇨ Synthesis and characterization of compounds **2a**, **2b**, **7**, **8** was carried out by Michael Seidl
- ⇨ X-ray measurements were finalized by Michael Seidl
- ⇨ Frontier orbitals for **2a** were calculated by Gabor Balázs
- ⇨ DFT calculations regarding reaction mechanisms were done by Alexey Y. Timoshkin
- ⇨ Figures and manuscript were prepared by Lena Rummel

*: These authors contributed equally to this work.

4.1 Introduction

A commonality of aminopnictinidene complexes is the use of sterically demanding substituents such as tmp (tmp = tetramethylpiperidine), $(Me_3Si)_2N$ or $^iPr_2N$, which have two equal substituents at the N atom. We now found synthetic pathways to sterically less demanding aminopnictinidene complexes of the type $[R^1R^2NE\{W(CO)_5\}_2]$ (**2a**: E = P, $R^1 = {}^iPr$, R^2 = H; **2b**: E = As, $R^1 = {}^iPr$, R^2 = H; **3**: E = P, $R^1 = R^2 = {}^iPr$; **4**: E = P, $R^1 = {}^sBu$, R^2 = H; **5**: E = P, $R^1 = R^2$ = Et) with also different substituents using alkyl substituted amines. The reaction of **3** and **4** with $^tBuPH_2$ yields the triphosphine complex $[(CO)_5W(^tBuP(H)P(H)P(H)^tBu)W(CO)_5]$ (**6**), whereas the reaction of **2a** with carbodiimides results in the formation of heterocyclic compounds $[(^iPrNH)C(NR^3)_2P\{W(CO)_5\}_2]$ (**7**: $R^3 = {}^iPr$; **8**: R^3 = Cy).

Phosphinidenes are low valent main group compounds of the general formula R-P, where the phosphorus atom possesses 6 valence electrons. Thus, phosphinidenes can exist in two different spin states: as a singlet or triplet, with the latter representing the usual ground state. Theoretical calculations for H-P show an energy difference ΔE_{ST} between the two spin states of only 28 kcal·mol^{-1},[1] which can be influenced by variation of the substituent R. For example, when R = NH_2, ΔE_{ST} is reduced to -3.4 kcal·mol^{-1} and in phosphidophosphinidenes (R = PH_2), ΔE_{ST} is even reduced to -6.9 kcal·mol^{-1}, suggesting that singlet phosphinidenes should be feasible.[2] Just a few years ago, Bertrand and co-workers were able to synthesize a singlet phosphinophosphinidene stable at room temperature from a (phosphino)phosphaketene, using extremely bulky substituents to prevent the resulting singlet phosphinidene from dimerizing.[3] A corresponding parent aminophosphinidene complex is not known, because these compounds still have to be sterically stabilized in order to be used for synthetic purposes. Recently, Cummins et al. even generated singlet aminophosphinidenes of the type $[R_2NP]$ (R = Me, Et, ^iPr, Me_2Pip; Pip = piperidine) as intermediates in the thermal reaction of $R_2NPC_{14}H_{10}$ with 1,3-cyclohexadiene, where a transfer of the terminal aminophosphinidene unit from anthracene to 1,3-cyclohexene takes place.[4] The stabilisation is also possible by coordination to transition-metal complex fragments, which can occur in different coordination modes ranging from η^1 to μ_4.[2] In the field of terminal aminophosphinidenes, Carty and co-workers have done extensive research and were able to synthesize a variety of terminal aminophosphinidene complexes of different transition metals (M) of the type $[(^iPr_2N)_2PML_n]^+$.[5] In respect to the bridging μ_2 coordination mode, the first aminophosphinidene complex, $[(Me_3Si)_2NP\{Cr(CO)_5\}_2]$, was synthesized in 1983 by the Power group through the reaction of $(Me_3Si)_2NPCl_2$ and $Na_2[Cr(CO)_5]$. This group has also successfully synthesized the first aminoarsinidene complexes, $[(Me_3Si)_2NAs\{Cr(CO)_5\}_2\}]$ and $[(Me_3Si)_2NAs\{Fe(CO)_4\}_2\}$.[6] Huttner and co-workers reported the synthesis of the N-substituted arsinidene complexes $[XAs\{Mn(CO)_2Cp'\}_2]$ (X = NCS, N_3; Cp' = η^5-$C_5H_4CH_3$) afterwards, although it has to be noted that the use of isothiocyanates and azides as substituents leads to very special cases of aminoarsenidene-like complexes.[7] Aside from the abovementioned examples, no other aminoarsinidene complexes are known in the literature, but there are a few examples of aminophosphinidene-bridged complexes, which are usually synthesized via

salt elimination reactions.[6,8,9] It has to be noted that all of the known aminopnictinidene complexes possess symmetrically substituted amines R_2N at the pnictogen atom and no aminopnictinidene complexes with asymmetrically substituted amines R^1R^2N are known to date.

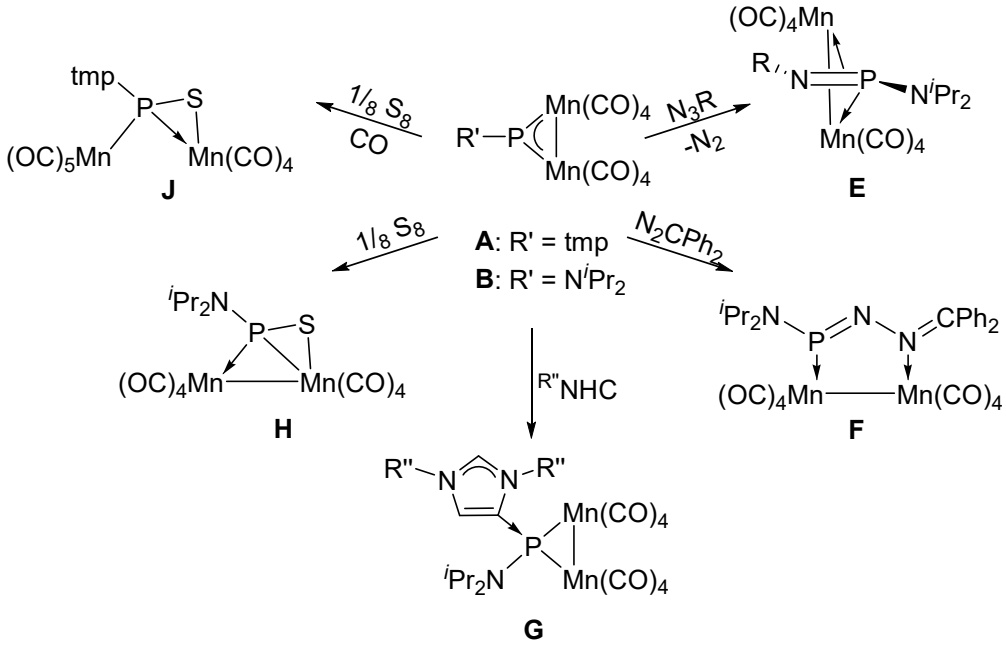

***Scheme 4.1**: Reaction of **A**,**B** with various nucleophiles.*

Besides the synthesis of bridging symmetrically substituted aminopnictinidene complexes, there have also been some initial investigations regarding their reaction behavior, namely of the compounds $[Mn_2(\mu\text{-PR'})(CO)_8]$ (**A**: R' = tmp, **B**: R' = N^iPr_2; tmp = tetramethylpiperidine) and $[Co_2(\mu\text{-PR'})(\mu\text{-}\kappa^1{:}\kappa^1\text{-dppm})(CO)_6]$ (**C**: R' = tmp, **D**: R' = N^iPr_2; dppm = $Ph_2PCH_2PPh_2$). Complexes **B**, **C** and **D** were reacted with diazoalkanes and organic azides but did not show a predictable reaction behavior (cf. Schemes 4.1 and 4.2).[10] On the other hand, the reaction of **B** and **D** with 1,3-bis(R'')imidazole-2-ylidene (R'' = ^{t}Bu, adamantyl) gave abnormal NHC-adducts of type **G** in which the carbene is bonded to the P atom of the aminophosphinidene via one of the 'backbone' carbon atoms.

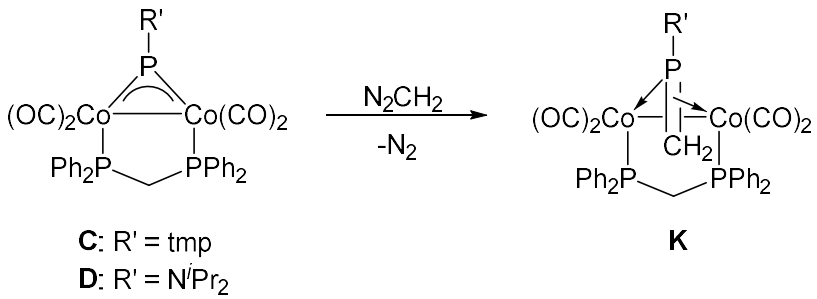

***Scheme 4.2**: Reaction of **C**, **D** with N_2CH_2.*

This unusual behavior is explained by unfavorable steric interactions of the carbene R-groups with either the amino-moiety of the phosphinidene group or the transition-metal moieties, which causes a rearrangement of the NHC.[11] **A** and **B** were also reacted with elemental sulfur, which resulted in either an octacarbonyl complex with the Mn-Mn bond being intact (**E**) and a μ-κ^1,κ^2-coordinated phosphinidene sulfide ligand in **H** or a derivative with one $Mn(CO)_5$ group and a similarly coordinated phosphinidene sulfide ligand (**J**).[9] .Taking all of these results into account, it can be stated that so far there are no aminopnictinidene complexes with asymmetrically substituted amine moieties. Additionally, there have been only initial investigations regarding the reaction behavior of symmetrically substituted bridging aminophosphinidene complexes Thus, the question arises, if asymmetrically substituted aminopnictinidene complexes can be synthesized, and if so, whether their reaction behavior differs from that of the known symmetrically substituted complexes. Herein, the synthesis of so far unknown asymmetrically substituted aminopnictinidene complexes of the type $[R^1R^2NE\{W(CO)_5\}_2]$ (E = P: $R^1 = R^2 = {}^i$Pr, Et; R^1 = H, $R^2 = {}^i$Pr, ^{s}Bu, ^{t}Bu; E = As: R^1 = H, $R^2 = {}^i$Pr) and the investigation of the reactivity of $[{}^i Pr_2NP\{W(CO)_5\}_2]$ (**3**) and $[{}^s BuHNP\{W(CO)_5\}_2]$ (**4**) towards ${}^t BuPH_2$ as well as the reactivity of $[{}^i PrHNP\{W(CO)_5\}_2]$ (**2a**) towards carbodiimides is reported.

4.2 Results and Discussion

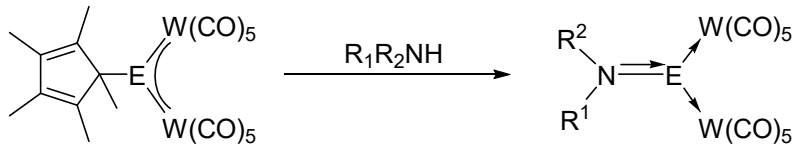

1a: E = P
1b: E = As

2b: E = As; R^1 = ^{i}Pr; R^2 = H
3: E = P; R^1 = R^2 = ^{i}Pr (68 %)
4: E = P; R^1 = ^{s}Bu; R^2 = H (72 %)
5: E = P; R^1 = R^2 = Et (63 %)

***Scheme 4.3**: Synthetic route **I**: Reaction of **1a,b** with amines.*

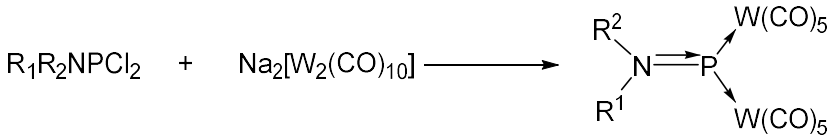

2a: R^1 = ^{i}Pr; R^2 = H (8%)
3: R^1 = R^2 = ^{i}Pr (22 %)
4: R^1 = ^{s}Bu; R^2 = H (41 %)
5: R^1 = R^2 = Et (29 %)

***Scheme 4.4**: Synthetic route **II**: Reaction of aminochlorophosphines with $Na_2[W_2(CO)_{10}]$.*

There are two possible synthetic routes to asymmetrically substituted aminopnictinidene complexes of the type $[R^1R^2NE\{W(CO)_5\}_2]$: The substitution of the Cp* substituent in $[Cp^*E\{W(CO)_5\}_2]$ (**1a**: E = P, **1b**: E = As; Cp* = C_5Me_5) with an amine (Route **I**: cf. Scheme 4.3) and the salt metathesis between $Na_2[W_2(CO)_{10}]$ and the corresponding aminochlorophosphine (Route **II**: cf. Scheme 4.4). The reactions of **1a**, **b** with primary and secondary amines are conducted at low temperatures. The amine is added to the pnictinidene complex in toluene and the reaction mixture is then warmed up to room temperature, where a color change from blue to red occurs. The aminopnictinidene complexes crystallize from the respective concentrated reaction solutions at -78 °C In these reactions, yields up to 72 % could be accomplished. In the case of the primary amines, the reaction products are the first RNH-substituted (R = alkyl) pnictinidene complexes that have been synthesized and characterized. However, as mentioned in the introduction, the synthetic routes to aminopnictinidene complexes largely rely on salt elimination reactions. Thus, we investigated a different approach and synthesized aminochlorophosphines $R^1R^2NPCl_2$ to make use of salt elimination reactions as an alternative route. The advantage of these aminochlorophosphine route over the route involving the pnictinidene complexes **1a**,**b** is, that they can be prepared on a larger scale, which should enable a route to synthesize aminopnictinidenes in larger quantities. However, the aminochlorophosphines $R^1R^2NPCl_2$ are known to dimerize after elimination of HCl, so they must be purified and handled very carefully. By this approach, the respective aminochlorophosphine is added to a suspension of $Na_2[W_2(CO)_{10}]$ in toluene at 0 °C. The

resulting red reaction mixture is warmed to room temperature and filtered. After storing the concentrated filtrates at -78 °C, the aminophosphinidene complexes **2a** (R^1 = ^{i}Pr, R^2 = H), **3**, **4** and **5** can be isolated as solids (cf. Scheme 4.4). This reaction pathway, in the case of **4** and **5**, yields 41 % and 29 % of the aminophosphinidene complex, respectively, which has to be separated from the respected chlorinated aminophosphine complex of the type [$R^1R^2NPCl_2\{W(CO)_5\}$] (**4Cl**: R^1 = sBu, R^2 = H; **5Cl**: R^1 = R^2 = Et) that is obtained as a byproduct in most cases. Nevertheless, these reactions can be carried out on a larger scale, so despite the smaller percentage of yield, the absolute yield is still larger in this reaction procedure.

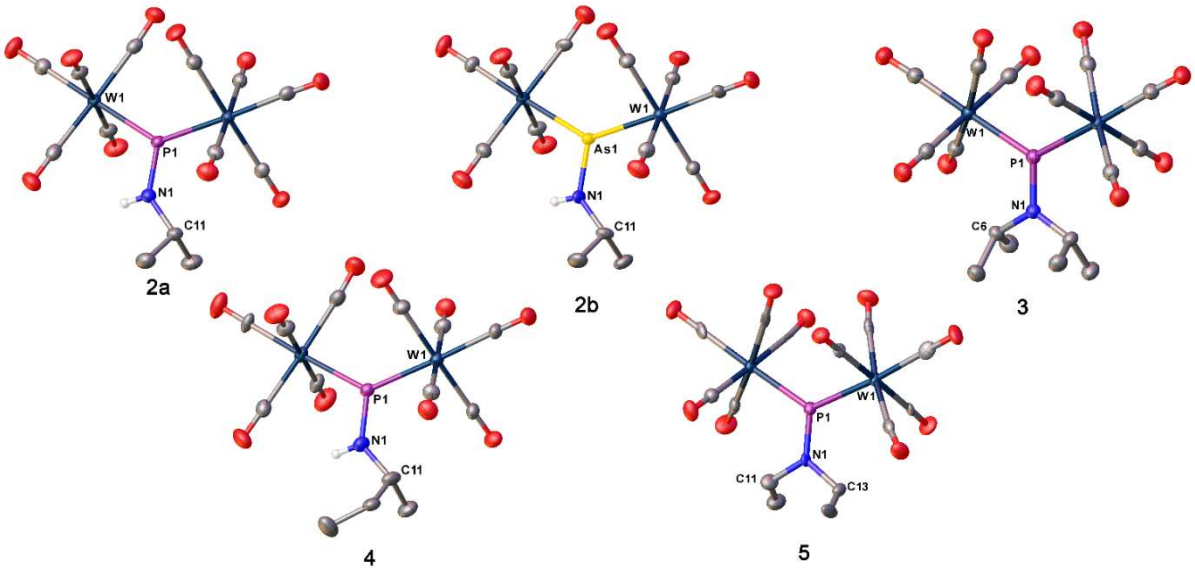

***Figure 4.1**: Molecular structures of **2a**, **2b**, **3**, **4** and **5**. Anisotropic displacement parameters are set to 50% probability level. H atoms bound to C atoms are omitted for clarity. Selected bond lengths [Å] and angles [°]: **2a**: N1-C11 1.481(5), N1-P1 1.636(3), W1-P1 2.4517(9), W2-P1 2.4187(9); C11-N1-P1 130.7(3), N1-P1-W1 109.77(13), N1-P1-W2 117.95(13), W2-P1-W1 132.28(4). **2b**: W1-As1 2.5080(8), W2-As1 2.5302(8), As1-N1 1.775(6), N1-C11 1.455(9); W1-As1-W2 134.38(3), N1-As1-W1 116.3(2), N1-As1-W2 109.3(2), C11-N1-As1 130.2(5). **3**: W1-P1 2.4996(4), P1-N1 1.658(3), N1-C6 1.495(3); W1[4]-P1-W1 123.74(3), N1-P1-W1 118.128(17), C6-N1-P1 120.68(13). **4**: W1-P1 2.4192(15), W2-P1 2.4466(15), P1-N1 1.641(6), N1-C11 1.469(8); W2-P1-W1 131.38(6), N1-P1-W1 117.7(2), N1-P1-W2 110.9(2), C11-N1-P1 130.2(5). **5**: W1-P1 2.476(2), W2-P1 2.470(2), P1-N1 1.636(7), N1-C11 1.464(11), N1-C13 1.498(10); W1-P1-W2 125.19(9) W1-P1-N1 117.6(2), W2-P1-N1 117.2(2), P1-N1-C11 124.7(6), P1-N1-C13 124.4(6), C11-N1-C13 110.9(7).*

The abovementioned compounds are readily soluble in organic solvents at room temperature and give deep red solutions. In the ^{31}P NMR spectra of the aminophosphinidene complexes, signals between 704.8 ppm and 763.0 ppm are detected. This is in agreement with the typical high downfield shifts characteristic for bridging phosphinidene complexes.[12] The $^1J_{PW}$ coupling constants lie between 189 Hz and 198 Hz. In the IR spectra, typical bands for the CO ligands between 2090 cm^{-1} and 1940 cm^{-1} could be observed. Molecular ion peaks were detected in the mass spectra of **2b**, **3**, **4** and **5**. The molecular structures of **2a**, **2b**, **3**, **4** and **5** are depicted in Figure 4.1. They all consist of a pnictogen atom in a nearly trigonal planar environment, which is bound to two $W(CO)_5$ moieties and an amine. The sum of

[4] 1-x, +y, 3/2-z

angles around the pentel atom is 360° for all abovementioned compounds. The N-E distances correspond to shortened N-E single bonds, while the E-W distances are within a slightly shortened single-bond range.[13] The shortened N-E distances show the interaction between the lone pair at the N atom and the empty p orbital at the E atom, resulting in a formal N=P double bond. This has been confirmed for **2a** through DFT calculations at the BP86/TZVP level (cf. Figure 4.2).

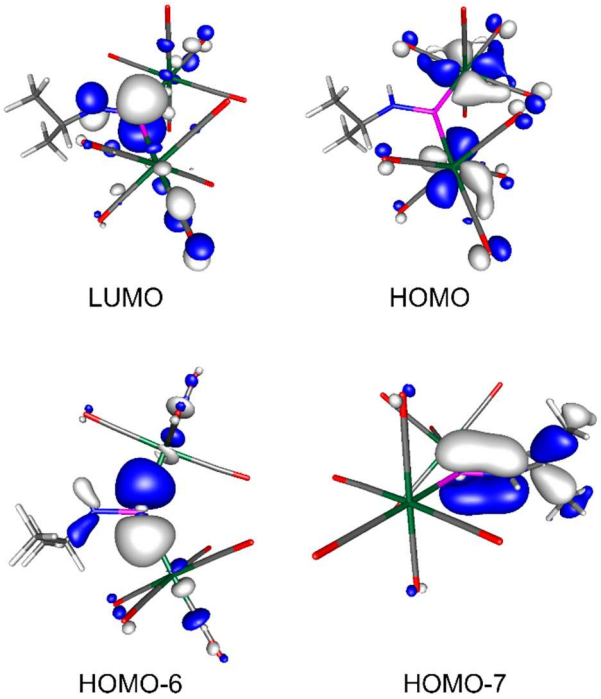

***Figure 4.2**: Selected molecular orbitals for **2a**, calculated at the BP86/def2-TZVP level of theory.*

The WBI for the N-P bond is 1.23, while the WBIs for the P-W bonds are 0.86 and 0.80, respectively. These values are in agreement with the proposed bonding model, where a donation from the lone pair of the N atom into the empty p orbital of the P atom takes place. The N atom is also trigonally planar configurated, which further undermines the donation of electron density from N to P. Both P-W bonds can be described as a dative interaction between P and the respective W atom. The frontier molecular orbitals involved in the bonding in the NPW_2 core are depicted in Figure 4.2. Looking at bond angles, W-E-W bond angles are larger than N-E-W bond angles because of the steric bulk of the $W(CO)_5$ fragments compared to the amines. Increasing the bulk of the amine, i.e. in the case of the secondary amine-substituted phosphinidene complexes, decreases the W-P-W bond angles as expected (**2a**: 132.28(4) °; **3**: 123.74(3) °). Due to this new synthetic route, we are now able to synthesize these bridging aminophosphinidene complexes in bigger scale and the investigation of their reaction behavior is now possible. Previously, we reported the reaction of **1a** with ^{t}BuPH$_2$ at 90 °C. In this reaction, after the formation of an adduct of the type [Cp*P{W(CO)$_5$}$_2$P^{t}Bu(H)$_2$], subsequent rearrangements and Cp*H elimination, as well as the addition of a second equivalent of ^{t}BuPH$_2$, the triphosphine [(CO)$_5$W(^{t}BuP(H)P(H)P(H)^{t}Bu)W(CO)$_5$] (**6**) was observed.[14] Using the aminophosphinidenes **3** and **4**

as starting materials, the analogous triphosphine complex could be obtained as a side product (cf. Scheme 4.5). However in this case, the reaction already proceeds at room temperature. The main product in this reaction is $^{t}BuPH_2\{W(CO)_5\}$, but **6** can be isolated from the reaction solution through layering and subsequent crystallization.

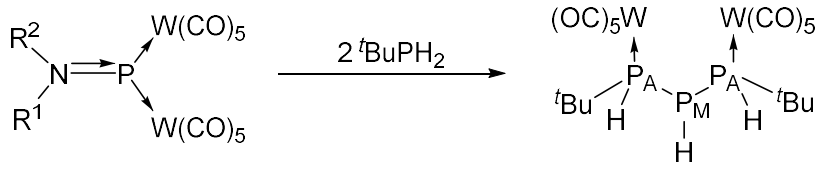

3: $R^1 = R^2 = {}^{i}Pr$
4: $R^1 = {}^{s}Bu$, $R^2 = H$

6

***Scheme 4.5**: Reaction of **3**, **4** with $^{t}BuPH_2$.*

The ^{31}P NMR spectrum of **6** shows an A_2M spin system with chemical shifts of -90.7 (P_M) and -13.4 ppm (P_A) and respective $^{1}J_{PP}$ coupling constants of 196 and 198 Hz and $^{1}J_{PW}$ coupling constants of 209 and 235 Hz. Additionally, $^{1}J_{PH}$ coupling constants of 224 Hz (P_M) and 322 Hz (P_A) can be found in the ^{31}P NMR spectrum as well as the ^{1}H NMR spectrum of **6**. All of these values are in agreement with the values found previously.[15] Both of the P_A atoms in **6** are chiral, thus there should be four diastereomers (**6a**: S,R; **6b**: R,S; **6c**: S,S; **6d**: R,R) formed, two of which (enantiomers **6c** and **6d**) are not distinguishable between each other by NMR spectroscopy. This results in three possible isomers, which should be deteceted in the ^{1}H NMR spectrum. However, there is only one set of signals in the ^{1}H NMR spectrum, suggesting the formation of only one isomer. The abovementioned splitting of the signals in the ^{31}P NMR spectrum, which can also be seen in the crude ^{31}P NMR spectrum, is typical for A_2M spin systems, which underlines the assumption that either only **6a** or **6b** are formed within the reaction. DFT computations at the B3LYP/6-31G* level of theory reveal that the first step of the proposed reaction pathway of **4** with $^{t}BuPH_2$ is the endergonic formation of a weakly bound adduct [$^{s}BuHNP\{W(CO)_5\}_2PH_2{}^{t}Bu$] (**I**) (cf. Figure 4.16). After the endergonic elimination of $^{s}BuNH_2$ from **I**, a diphosphene intermediate, [$^{t}BuHPP\{W(CO)_5\}_2$] (**II**) is formed, which can rearrange to the diphosphene complex [$^{t}Bu\{W(CO)_5\}PP\{W(CO)_5\}H$] (**III**) in an exergonic reaction (ΔG^0_{298} = 15.7 kJ mol^{-1}). Another equivalent of the phosphine reacts further with **III** and the resulting intermediate can be rearranged in a concerted hydrophosphination reaction to give only one diastereomer of **6**.[14] This is also in agreement with the calculated optimized geometries of **6** (cf. Figure 4.17). Interestingly, by the synthesis of $H_2NP(H)$-$P(H)$-$P(H)NH_2$ from white phosphorus and Na in liquid ammonia, the resulting 1,3-diaminotriphosphine was also received diastereomerically pure. The ^{31}P NMR spectrum of the reaction solution showed only signals for the erythro/erythro diastereomer.[16]

After testing the reactivity of the aminophosphinidene complexes **3** and **4** towards a primary phosphine, **2a** was reacted with N,N'-diisopropylcarbodiimide (DIC) and N,N'-cyclohexylcarbodiimide (DCC).

After thermolysis and workup of the reaction mixture, [(^{i}PrNH)C(NR^3)$_2$P{W(CO)$_5$}$_2$] (**7**: R^3 = ^{i}Pr; **8**: R^3 = Cy) were obtained in 55 % and 27 % yield, respectively (cf. Scheme 4.6). The ^{31}P NMR spectra show singlets at 306.5 ppm (**7**) and 309.1 ppm (**8**) as well as $^1J_{PW}$ couplings of 189 and 188 Hz. This is in accordance with the values that have been reported for compounds [Cp*C(NR^3)$_2$P{W(CO)$_5$}$_2$] with a Cp* substituent instead of an amine (R^3 = ^{i}Pr: δ = 298.8 ppm; R^3 = Cy: δ = 297.7 ppm).[17] The IR spectra of **7** and **8** show bands for the NH moieties as well as the CO vibrations. Their molecular structures are pictured in Figure 4.2.

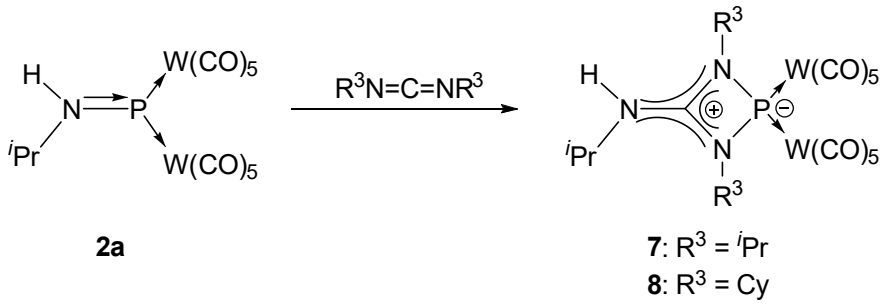

***Scheme 4.6**: Reaction of **2a** with carbodiimides.*

A planar four-membered ring consisting of the phosphorus atom and the respective guanidinate-ligand forms the central structural motif in both compounds. In both cases, a 1,3-migration of the amine from the phosphorus atom to the C atom of the carbodiimide has occurred. All C-N distances are in between single and double bonds[13], which is an indicator for the formation of a chelating guanidinate-ligand.

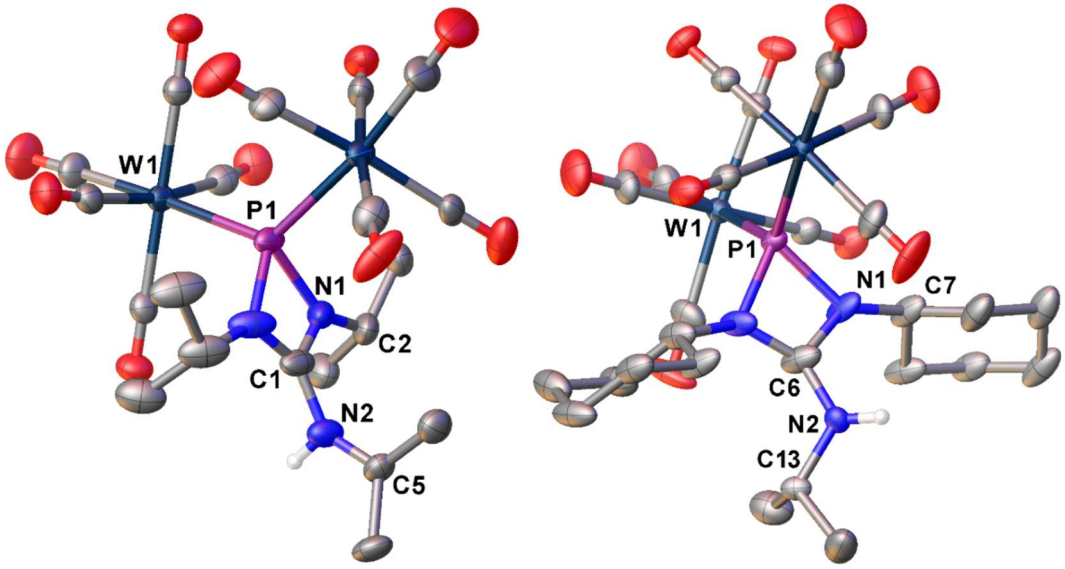

***Figure 4.2**: Molecular structures of **7** (left) and **8** (right). Anisotropic displacement parameters are set to 50% probability level. H atoms bound to C atoms are omitted for clarity. Selected bond lengths [Å] and angles [°]: **7**: P1-N1 1.808(4), N1-C2 1.468(7), N1-C1 1.328(6), N2-C1 1.379(9), N2-C5 1.209(19); W2-P1-W1 123.31(5), C2-N1-P1 139.4(3), C1-N1-P1 92.5(3), C1-N1-C2 127.8(4), C5-N2-C1 139.4(7). **8**: P1-N1 1.790(5), N1-C7 1.471(7), N1-C6 1.347(7), N2-C13 1.479(13), N2-C6 1.411(12); W1[5]-P1-W1 123.75(8), N1-P1-N1[8] 72.1(3), C7-N1-P1 130.0(4), C6-N1-P1 92.5(4), C6-N1-C7 133.0(5), C6-N2-C13 115.7(7).*

[5] 1-x, +y, ½-z

The proposed reaction pathway for this reaction is shown in Scheme 4.7. The first step is a nucleophilic attack of the lone pair at one N atom of the carbodiimide on the electrophilic P atom of the aminophosphinidene, resulting in a Lewis acid/base adduct **L**. Consecutively, the amine group is migrating towards the carbodiimide-C atom. Thus, another aminophosphinidene complex intermediate **M** is formed. The last step includes an intramolecular attack of the second N atom on the P atom, forming a new N-P bond. This reaction pathway is related to that one of the insertion of carbodiimides into an Al-Me- or Al-NMe_2-bond, as investigated by Barry et al.[18] or of reactions of carbodiimides with **1a,b** as shown by our group,[17,19] respectively.

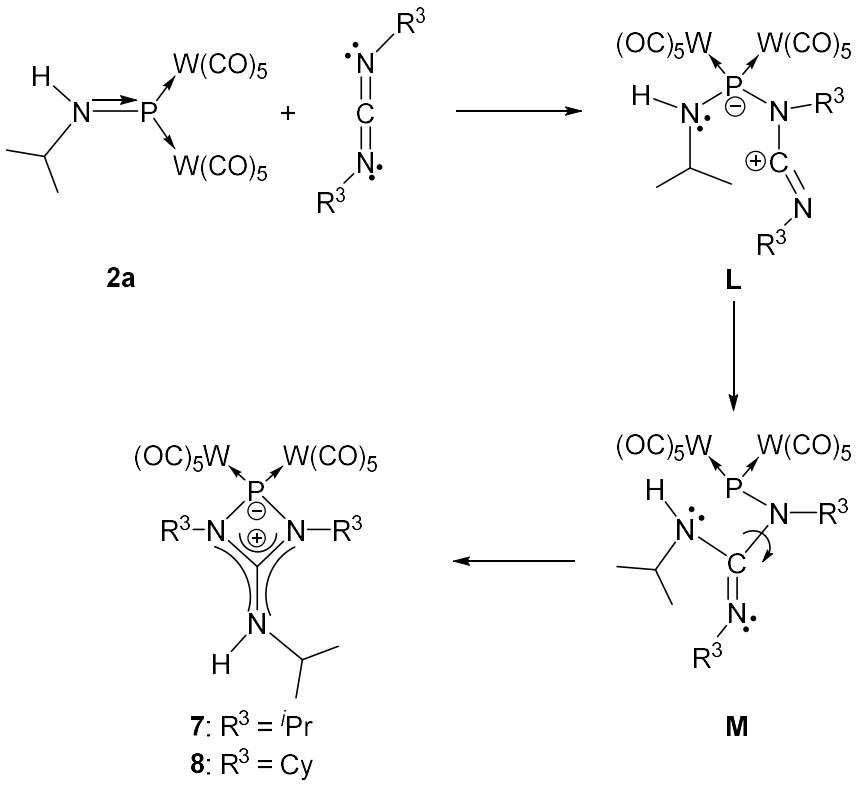

Scheme 4.7*: proposed reaction mechanism of the reaction of* ***2a*** *with carbodiimides.*

4.3 Conclusion

In summary, the synthesis, isolation and characterization of new aminophosphinidene complexes **2a**, **3**, **4** and **5** is reported. In comparison to reported aminophosphinidene complexes, the here reported complexes are substituted with sterically less demanding alkyl rests and **2a** and **4** represent first asymmetrically substituted aminophosphinidene complexes, coming from an primary amine. Additionally, the aminoarsinidene complex **2b**, belonging to a rare class of compounds, was synthesized and completely characterized. It represents the first aminoarsinidene complex possessing a primary amine-substituted As atom.

For their synthesis two different synthetic routes have been explored, which both allow the introduction of primary amines as substituents at the pnictogen atom in the resulting aminopnictinidene complexes for the first time. On the one hand, synthetic route I, the Cp*H elimination from **1a**,**b** with amines, shows higher yields but only smaller batch can be synthesized requiring to start from **1a,b**. It is also the first example of the use of substitution reactions to synthesize aminopnictinidene complexes. Synthetic route II, on the other hand, can be used to synthesize larger quantities, but the needed aminochlorophosphines as starting material in these reactions tend to decompose if not handled correctly.

Preliminary attempts to use the new aminopnictinidene complexes as starting materials for further reactions were carried out with **3** and **4**. They were reacted with $^{t}BuPH_2$ to give the already known triphosphine **6** in a stereoselective manner. The reaction of **2a** with carbodiimides resulted in the formation of complexes **7** and **8**, which represent new four-membered heterocycles with different substituents depending on the carbodiimide used. Both of these reactions showing the similarities between these aminophosphinidenes and phosphinidene **1a** in their reaction behavior towards phosphines.

4.4 Supporting Information

4.4.1 Working techniques

The following reactions were carried out under an atmosphere of dry Nitrogen or Argon using standard Schlenk techniques. Traces of water and oxygen were eliminated by leading the inert gas (N_2 or Ar) through a copper catalyst heated to 145 °C, subsequently washing it with concentrated sulphuric acid and drying it with orange gel and phosphorous pentoxide. Solvents were either collected from a solvent purification system (MBraun SPS 800) or dried, degassed and distilled according to standard techniques. Before use, the diatomaceous earth required for filtration was stored at 110 °C. The silica gel 60 (particle size 0.063-0.2 mm) was dried at 150 °C in vacuo for 3 d prior to use.

The **NMR spectra** were recorded on a BRUKER Avance 300 (^{1}H: 300.13 MHz, ^{13}C: 75.48 MHz, ^{31}P: 121.49 MHz) or Avance 400 (^{1}H: 400.13 MHz, ^{13}C: 100.61 MHz, ^{31}P: 161.98 MHz) spectrometer at room temperature unless stated otherwise. Chemical shifts δ refer to external standards of tetramethylsilane (^{1}H, ^{13}C NMR) and 85 % phosphoric acid (^{31}P NMR, ^{31}P{^{1}H} NMR), respectively, and are given in ppm. Coupling constants J are given in Hz without consideration of absolute signs. Analysis, simulations and graphic representations of the spectra were prepared with *TopSpin 3.0*.[20] **Infrared spectra** were recorded in solution (CH_2Cl_2) with a ThermoScientific Nicolet iS5 spectrometer using the iD5 Transmission element or as solids using an ATR element equipped with a Ge crystal. **Mass spectra** were recorded on a Jeol AccuTOF GCX (FD) spectrometer by the mass spectrometry department of the University of Regensburg or a ThermoQuest Finnigan MAT 95 spectrometer. **Elemental analysis** was conducted by the microanalytics laboratory of the University of Regensburg with the Elementar Vario MICRO cube**.**

The following substances were bought or synthesized according to standard techniques: [Cp*P{W(CO)$_5$}$_2$] (**1a**),[21] [Cp*As{W(CO)$_5$}$_2$] (**1b**),[12] ^{i}Pr$_2$NH, ^{i}Pr$_2$NPCl$_2$,[22] ^{i}PrNH$_2$, ^{i}PrHNPCl$_2$,[23] ^{s}BuNH$_2$, ^{s}BuHNPCl$_2$,[23] Et$_2$NH, Et$_2$NPCl$_2$,[22] Et$_3$N, ^{t}BuPH$_2$.[24]

4.4.2 Experimental Data with NMR Details

4.4.2.1 Synthesis of [^{i}PrHNP{W(CO)$_5$}$_2$] (2a)

A suspension of 4 g (5.7 mmol) $Na_2[W_2(CO)_{10}]$ in 150 mL toluene is cooled to 0 °C before 0.9 g (0.75 mL, 5.7 mmol) ^{i}PrHNPCl$_2$ in 20 mL toluene are added dropwise. After some time, a color change from yellow to red occurs. The suspension is warmed to room temperature and stirred for 3 h before the solid is filtered off and the remaining solution is concentrated in vacuo to approx. 30 mL. Storing the solution at -78 °C yields a mixture of [^{i}PrHNP{W(CO)$_5$}$_2$] (**2a**) and the side product [^{i}PrHNPCl$_2${W(CO)$_5$}]. Recrystallization in CH_2Cl_2 gives **2a** as red crystals with a metallic shine.

Analytical data for **2a**:

Yield:	0.315 g (8%).
^{1}H NMR (CD_2Cl_2, 400 MHz):	δ [ppm] = 1.49 (d, $^3J_{HH}$ = 6 Hz, 6H, CH_3), 4.52 (m, 1H, CH), 8.59 (br, 1H, NH).
^{31}P{^{1}H} NMR (CD_2Cl_2, 162 MHz):	δ [ppm] = 704.8 (s, $^1J_{PW}$ = 197 Hz).
^{31}P NMR (CD_2Cl_2, 162 MHz):	δ [ppm] = 704.8 (s, $^1J_{PW}$ = 197 Hz).

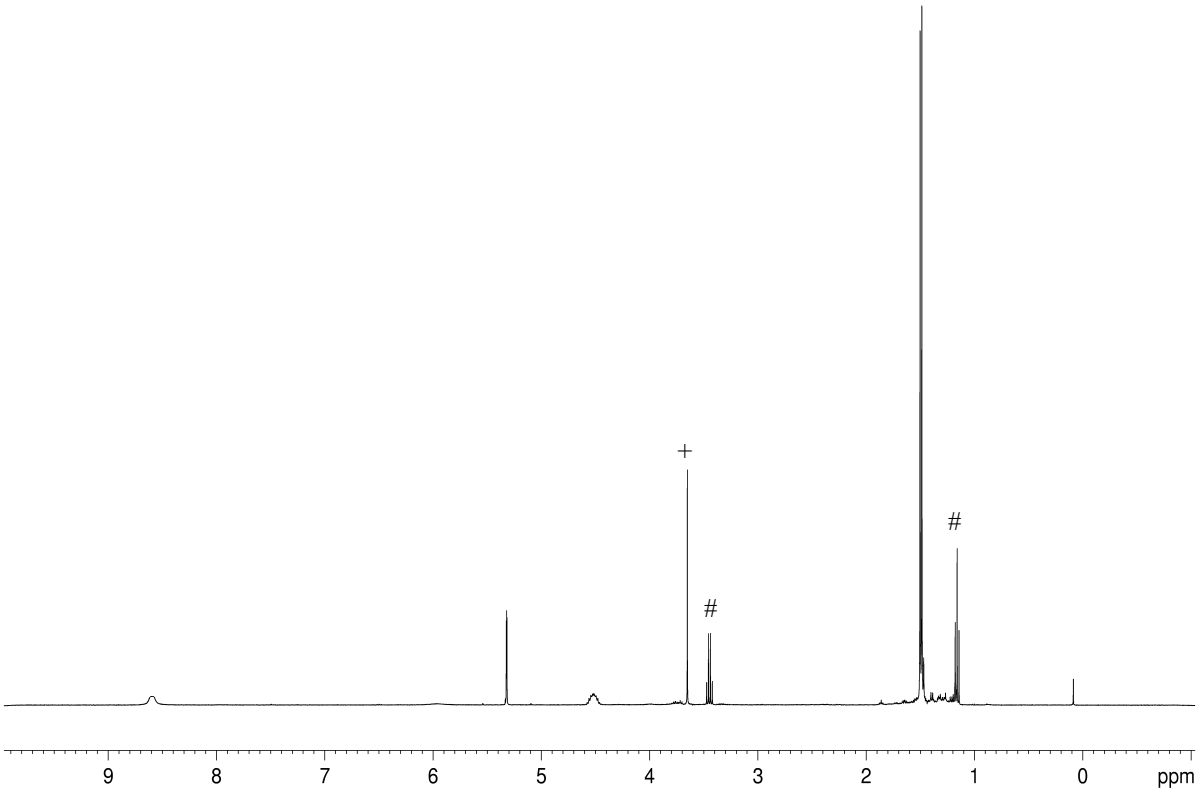

Figure 4.3: *^{1}H NMR spectrum of **2a** in CD_2Cl_2. # = Et_2O, + = 1,4-Dioxane.*

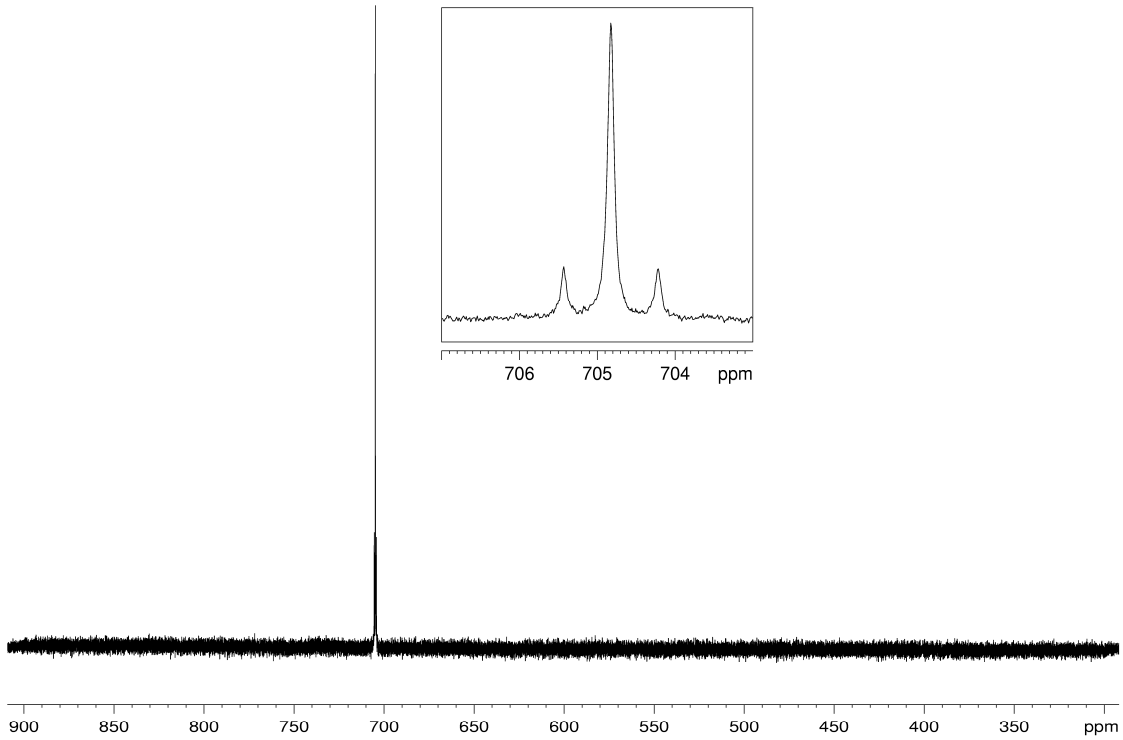

Figure 4.4: *$^{31}P\{^1H\}$ NMR spectrum of **2a** in CD_2Cl_2.*

4.4.2.2 Reaction of [Cp*As{W(CO)$_5$}$_2$] (1b) with ^{i}PrNH$_2$

A solution of 342 mg (0.4 mmol) **1b** in 20 mL CH_2Cl_2 is cooled to -78 °C before 0.17 mL (2 mmol) ^{i}PrNH$_2$ are added. The blue solution turns yellow and is warmed to room temperature, where another color change to blue occurs. The solution is stirred for 24 h in the dark and turns a reddish brown. After concentrating the solution to 3 mL and storing it at -27 °C, a few red crystals of [^{i}PrHNAs{W(CO)$_5$}$_2$] (**2b**) could be obtained.

Analytical data for **2b**:

Yield:	few crystals.
MS (FD):	m/z (%): 781.0 (20) [M$^+$].

4.4.2.3 Reaction of [Cp*P{W(CO)$_5$}$_2$] (1a) with ^{i}Pr$_2$NH

A blue solution of 163 mg (0.2 mmol) [Cp*P{W(CO)$_5$}$_2$] (**1a**) in 20 mL toluene is cooled to -78 °C before adding a solution of 0.03 mL (0.2 mmol) ^{i}Pr$_2$NH in 20 mL toluene dropwise. A quick color change to red occurs. The reaction mixture is concentrated in vacuo until crystallization starts and is then stored at -78 °C. [^{i}Pr$_2$NP{W(CO)$_5$}$_2$] (**3**) crystallizes as red crystals with a metallic shine.

Yield: 98 mg (68 %).

Alternate synthesis: **Reaction of Na$_2$W$_2$(CO)$_{10}$ with ^{i}Pr$_2$NPCl$_2$**

A suspension of 5.55 g (8 mmol) Na$_2$[W$_2$(CO)$_{10}$] in 230 mL toluene is cooled to 0 °C before 1.1 mL (1.2 g, 6 mmol) ^{i}Pr$_2$NPCl$_2$ in 40 mL toluene are added dropwise. A quick color change from yellow to red occurs. The suspension is warmed to room temperature and stirred for 16 h before the solid is filtered off and the remaining solution is dried in vacuo. The residue is redissolved in 80 mL Et$_2$O. Storing the solution at -78 °C yields [^{i}Pr$_2$NP{W(CO)$_5$}$_2$] (**3**) as a red powder that can be filtered off the solution and dried in vacuo.

Yield: 975 mg (22 %).

Analytical data for **3**:

^{1}H NMR (C$_6$D$_6$, 300 MHz):	δ [ppm] = 1.07 (d, $^3J_{HH}$ = 7 Hz, 6H, CH$_3$), 5.77 (m, 1H, CH).
^{31}P{^{1}H} NMR (C$_6$D$_6$, 162 MHz):	δ [ppm] = 761 (s).
^{31}P NMR (C$_6$D$_6$, 162 MHz):	δ [ppm] = 761 (br).
IR (CH$_2$Cl$_2$):	ν_{max}/cm^{-1} = 2080 (w, CO), 2039 (s, CO), 1995 (w, CO), 1968 (s, CO), 1955 (br, CO), 1940 (m, CO).
MS (EI, 70eV):	m/z (%): 778.8 (1) [M$^+$], 750.9 (1) [M$^+$ -CO], 694.9 (0.5) [M$^+$ - 3CO], 668.9 (0.5) [M$^+$ - 4CO], 638.9 (3.2) [M$^+$ - 5CO].

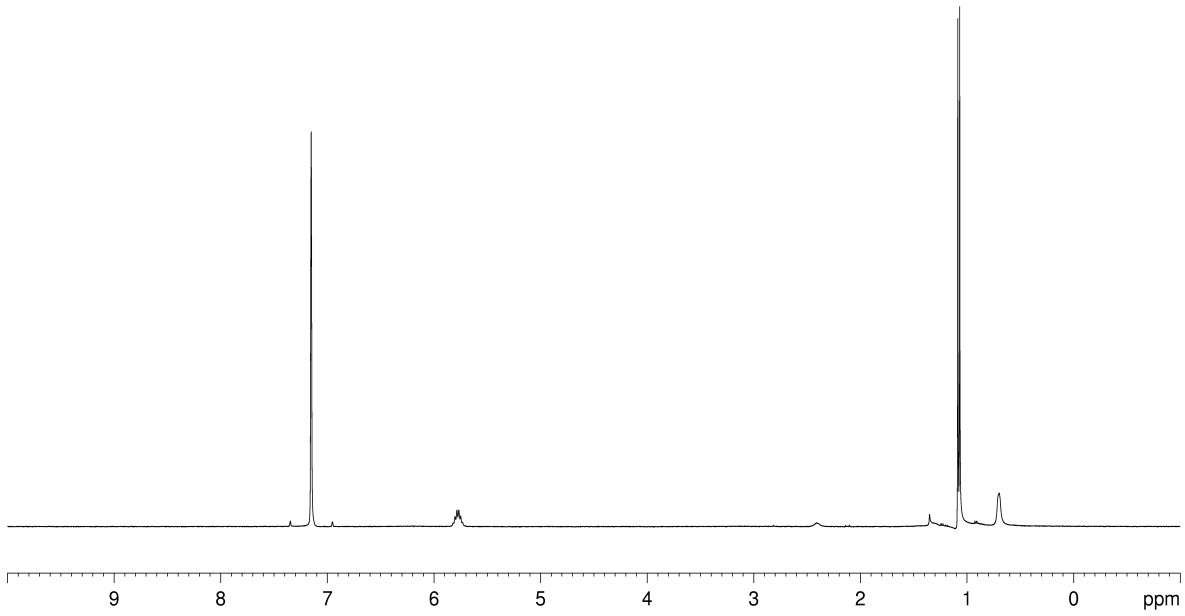

Figure 4.5: *^{1}H NMR spectrum of **3** in C_6D_6.*

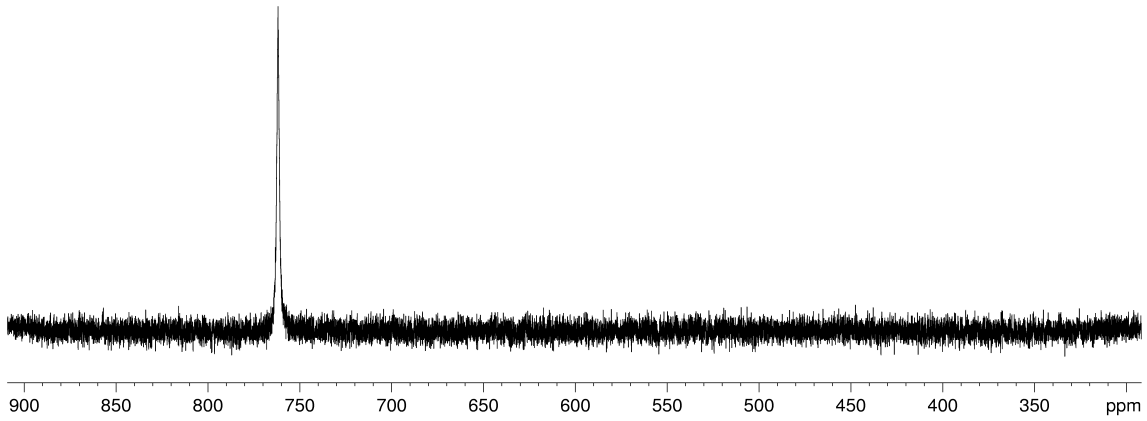

Figure 4.6: *$^{31}P\{^{1}H\}$ NMR spectrum of **3** in CD_2Cl_2.*

4.4.2.4 Reaction of 1a with $^{s}BuNH_2$

A blue solution of 163 mg (0.2 mmol) [Cp*P{W(CO)$_5$}$_2$] (**1a**) in 50 mL toluene is cooled to -78 °C before adding a solution of 0.03 mL (0.3 mmol) $^{s}BuNH_2$ in 20 mL toluene dropwise. A quick color change to red occurs. The reaction mixture is concentrated in vacuo until crystallization starts and is then stored at -78 °C. [^{s}BuHNP{W(CO)$_5$}$_2$] (**4**) can be isolated as red crystals.

Yield: 108 mg (72 %).

<u>Alternate synthesis</u>: Reaction of $Na_2W_2(CO)_{10}$ with $^{s}BuHNPCl_2$

A suspension of 2 g (2.88 mmol) $Na_2[W_2(CO)_{10}]$ in 100 mL toluene is cooled to 0 °C before 520 mg (3 mmol) $^{S}BuHNPCl_2$ in 20 mL toluene are added dropwise. A quick color change from yellow to red occurs. The suspension is warmed to room temperature and stirred for 6 h in the dark before the solid is filtered off and the remaining solution is concentrated in vacuo to approx. 25 mL. Storing the solution at -78 °C yields a mixture of [^{s}BuHNP{W(CO)$_5$}$_2$] (**4**) and [^{s}BuHNPCl$_2${W(CO)$_5$}] (**4Cl**), which can be separated by thin layer chromatography using toluene:hexane in a 1:2 ratio.

Yield: **4**: 894 mg (41 %), **4Cl**: 444 mg (31 %).

Analytical data for **4**:

^{1}H NMR ($CDCl_3$, 300 MHz):	δ [ppm] = 1.09 (t, $^3J_{HH}$ = 7 Hz, 3H, CH_3), 1.41 (d, $^3J_{HH}$ = 7 Hz, 3H, CH_3), 1.80 (m, 2H, CH_2), 3.41 (m, 1H, CH), 8.40 (m, 1H, NH).
^{31}P{^{1}H} NMR ($CDCl_3$, 162 MHz):	δ [ppm] = 706 (s, $^1J_{PW}$ = 195 Hz).
^{31}P NMR ($CDCl_3$, 162 MHz):	δ [ppm] = 706 (br).
IR (CH_2Cl_2):	ν_{max}/cm^{-1} = 2090 (w, CO), 2045 (s, CO), 2001 (w, CO), 1977 (s, CO), 1965 (br, CO), 1943 (m, CO).
MS (EI, 70eV):	m/z (%): 750.9 (4) [M$^+$], 698.0 (2) [M$^+$ - 2CO], 469 (0.4) [M$^+$ - 10CO].

Analytical data for **4Cl**:

^{1}H NMR ($CDCl_3$, 300 MHz):	δ [ppm] = 1.21 (t, $^3J_{HH}$ = 8.0 Hz, 3H, CH_3), 1.45 (d, $^3J_{HH}$ = 8.2 Hz, 3H, CH_3), 1.91 (m, 2H, CH_2), 3.78 (m, 1H, CH), 6.75 (br, 1H, NH).
^{31}P{^{1}H} NMR ($CDCl_3$, 162 MHz):	δ [ppm] = 105 (s, $^1J_{PW}$ = 374 Hz).
^{31}P NMR ($CDCl_3$, 162 MHz):	δ [ppm] = 105 (dd, J_{PH} = 14 Hz, 39 Hz).
IR (CH_2Cl_2):	ν_{max}/cm^{-1} = 3055 (w, NH), 2085 (w, CO), 1989 (br, CO).
MS (EI, 70eV):	m/z (%): 498.9 (22) [M$^+$], 464.0 (21) [M$^+$ - CH_3].

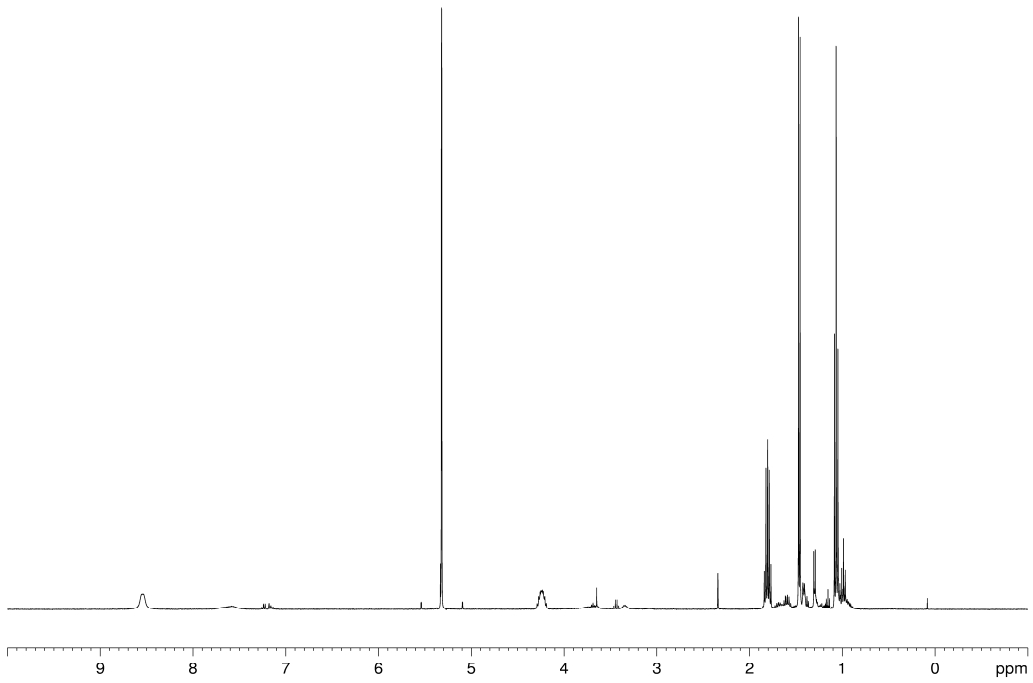

Figure 4.7: *^{1}H NMR spectrum of **4** and **4Cl** in $CDCl_3$.*

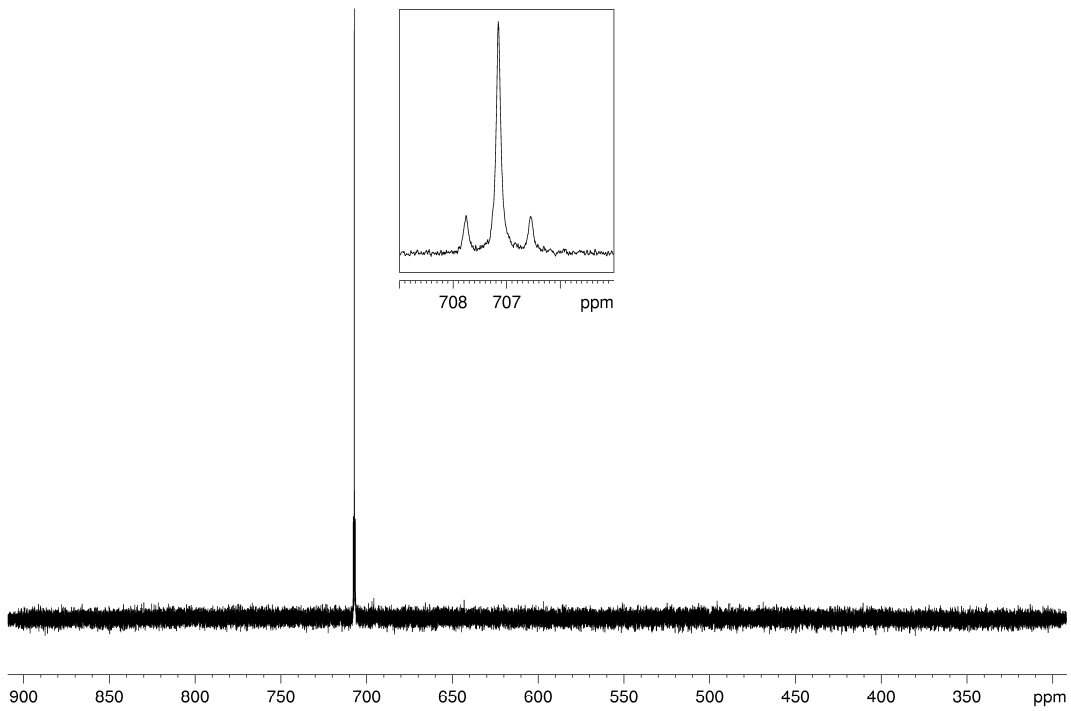

Figure 4.8: *$^{31}P\{^{1}H\}$ NMR spectrum of **4** in $CDCl_3$.*

4.4.2.5 Synthesis of $[Et_2NP\{W(CO)_5\}_2]$ (5)

A blue solution of 163 mg (0.2 mmol) $[Cp^*P\{W(CO)_5\}_2]$ (**1a**) in 20 mL toluene is cooled to -78 °C before adding a solution of 0.03 mL (0.2 mmol) Et_2NH in 20 mL toluene dropwise. A quick color change to red occurs. The reaction mixture is concentrated in vacuo until crystallization starts and is then stored at -78 °C. $[Et_2NP\{W(CO)_5\}_2]$ (**5**) can be isolated as red crystals with a metallic shine.

Yield: 94 mg (63 %).

Alternate synthesis: Reaction of $Na_2W_2(CO)_{10}$ with Et_2NPCl_2

A suspension of 2 g (2.88 mmol) $Na_2[W_2(CO)_{10}]$ in 100 mL toluene is cooled to 0 °C before 500 mg (2.88 mmol) Et_2NPCl_2 in 20 mL toluene are added dropwise. A quick color change from yellow to red occurs. The suspension is warmed to room temperature and stirred for 6 h in the dark before the solid is filtered off and the remaining solution is concentrated in vacuo to approx. 25 mL. Storing the solution at -78 °C yields a mixture of $[Et_2NP\{W(CO)_5\}_2]$ (**5**) and $[Et_2NPCl_2\{W(CO)_5\}]$ (**5Cl**), which can be separated by thin layer chromatography using toluene:hexane in a 1:2 ratio.

Yield: **5**: 314 mg (29 %), **5Cl**: 222 mg (31 %).

Analytical data for **5**:

^{1}H NMR ($CDCl_3$, 300 MHz):	δ [ppm] = 1.23 (t, $^3J_{HH}$ = 7.4 Hz, 3H, CH_3), 3.57 (m, 2H, CH_2).
$^{31}P\{^1H\}$ NMR ($CDCl_3$, 162 MHz):	δ [ppm] = 735 (s, $^1J_{PW}$ = 198 Hz).
^{31}P NMR ($CDCl_3$, 162 MHz):	δ [ppm] = 735 (s, $^1J_{PW}$ = 198 Hz).
IR (CH_2Cl_2):	ν_{max}/cm^{-1} = 2081 (w, CO), 2041 (s, CO), 2005 (w, CO), 1972 (s, CO), 1960 (br, CO), 1949 (m, CO).
MS (EI, 70eV):	m/z (%): 750.8 (0.3) [M^+], 697.4 (0.7) [M^+ - 2CO], 468.4 (0.7) [M^+ - 10CO], 92.1 (100) [$C_7H_8^+$].

4.4.2.6 Reaction of 3, 4 with ^{t}BuPH$_2$

0.05 mL (0.4 mmol) ^{t}BuPH$_2$ are added dropwise to a solution of 0.2 mmol [R^{1}R^{2}NP{W(CO)$_5$}$_2$] (**3**, **4**) in 20 mL toluene at 0 °C. The reaction mixture is stirred for 2 h at room temperature until a color change from red to yellow occurs. After concentrating the solution and layering it with n-hexane (1:1), [(CO)$_5$W(^{t}BuP(H)P(H)P(H)^{t}Bu)W(CO)$_5$] (**6**) can be obtained as yellow crystals.

Analytical data for **6**:

Yield:	using **3**: 27 mg (16 %), using **4**: 32 mg (18 %).
^{1}H NMR (CDCl$_3$, 300 MHz):	δ [ppm] = 1.39 (d, $^3J_{PH}$ = 16.7 Hz, 18H, CH$_3$), 3.72 (dm, $^1J_{PH}$ = 224 Hz, 1H, PH), 5.11 (dm, $^1J_{PH}$ = 322 Hz, 2H, PH).
^{31}P{^{1}H} NMR (CDCl$_3$, 162 MHz):	δ [ppm] = -90.7 (dd, $^1J_{PP}$ = 196 and 198 Hz, P$_M$), -13.4 (d, $^1J_{PP}$ = 196 Hz, $^1J_{PW}$ = 209 and 235 Hz, P$_A$).
^{31}P NMR (CDCl$_3$, 162 MHz):	δ [ppm] = -90.7 (ddd, $^1J_{PP}$ = 196 and 198 Hz, $^1J_{PH}$ = 224 Hz, P$_M$), -13.4 (dd, $^1J_{PP}$ = 197 Hz, $^1J_{PH}$ = 322 Hz, P$_A$).
IR (CH$_2$Cl$_2$):	ν_{max}/cm^{-1} = 2075 (m, CO), 2072 (m, CO), 1985 (s, CO), 1948 (vs, CO), 1927 (m, CO).
MS (EI, 70eV):	m/z (%): 857.8 (0.4) [M$^+$], 829.7 (1.2) [M$^+$ -CO].

4.4.2.7 Synthesis of [(^{i}PrNH)C(N^{i}Pr)$_2$P{W(CO)$_5$}$_2$] (7)

0.076 mL (0.48 mmol) N,N'-diisopropylcarbodiimide (DIC) are added dropwise to a solution of 295 mg (0.4 mmol) **2a** in 30 mL toluene. The reaction solution is heated to 105 °C for 1 h until a color change from red to brown occurs. The solid is filtered off and the clear solution is concentrated and stored at room temperature. [(^{i}PrNH)C(N^{i}Pr)$_2$P{W(CO)$_5$}$_2$] (**7**) crystallizes as colorless blocks from the solution. To increase the yield, the mother liquor is concentrated further and stored at -28 °C.

Analytical data for **7**:

Yield:	189 mg (55 %).
^{1}H NMR (CD$_2$Cl$_2$, 400 MHz):	δ [ppm] = 1.35 (d, $^3J_{HH}$ = 6.7 Hz, 6H, CH$_3$), 1.58 (d, $^3J_{HH}$ = 6.8 Hz, 12H, CH$_3$), 3.95 (m, 3H, CH), 4.26 (d, $^3J_{HH}$ = 9.8 Hz, 1H, NH); ^{31}P{^{1}H} NMR (162 MHz, CD$_2$Cl$_2$): δ [ppm] = 306.5 (s, $^1J_{PW}$ = 189 Hz).
^{31}P{^{1}H} NMR (CD$_2$Cl$_2$, 162 MHz):	δ [ppm] = 306.5 (s, $^1J_{PW}$ = 189 Hz).
^{31}P NMR (CD$_2$Cl$_2$, 162 MHz):	δ [ppm] = 306.5 (t, $^3J_{PH}$ = 11 Hz, $^1J_{PW}$ = 189 Hz).
^{13}C{^{1}H} NMR (CD$_2$Cl$_2$, 100 MHz):	δ [ppm] = 22.2 (s, CH$_3$), 23.9 (s, CH$_3$), 47.1 (s, CH), 47.6 (s, CH), 144.7 (d, $^2J_{PC}$ = 10 Hz, C), 199.7 (d, $^2J_{PC}$ = 3 Hz, $^1J_{WC}$ = 126 Hz, CO), 202.1 (s, CO), 202.2 (s, CO);

IR (KBr): ν_{max}/cm^{-1} = 3400 (v, NH), 2072 (w, CO), 2054 (s, CO), 1977 (s, CO), 1949 (sh, CO), 1922 (vs, CO), 1908 (vs, CO).

MS (EI, 70eV): m/z (%): 862.9 (18) [M^+ - H], 834.9 (34) [M^+ - H - CO], 807.0 (9) [M^+ - H - 2CO], 778.9 (18) [M^+ - H - 3CO], 723.0 (30) [M^+ - H - 5CO], 695.0 (100) [M^+ - H - 6CO], 667.1 (57) [M^+ - H - 7CO], 637.0 (32) [M^+ - H - 8CO], 609.0 (47) [M^+ - H – 9CO], 581.0 (40) [M^+ - H – 10CO].

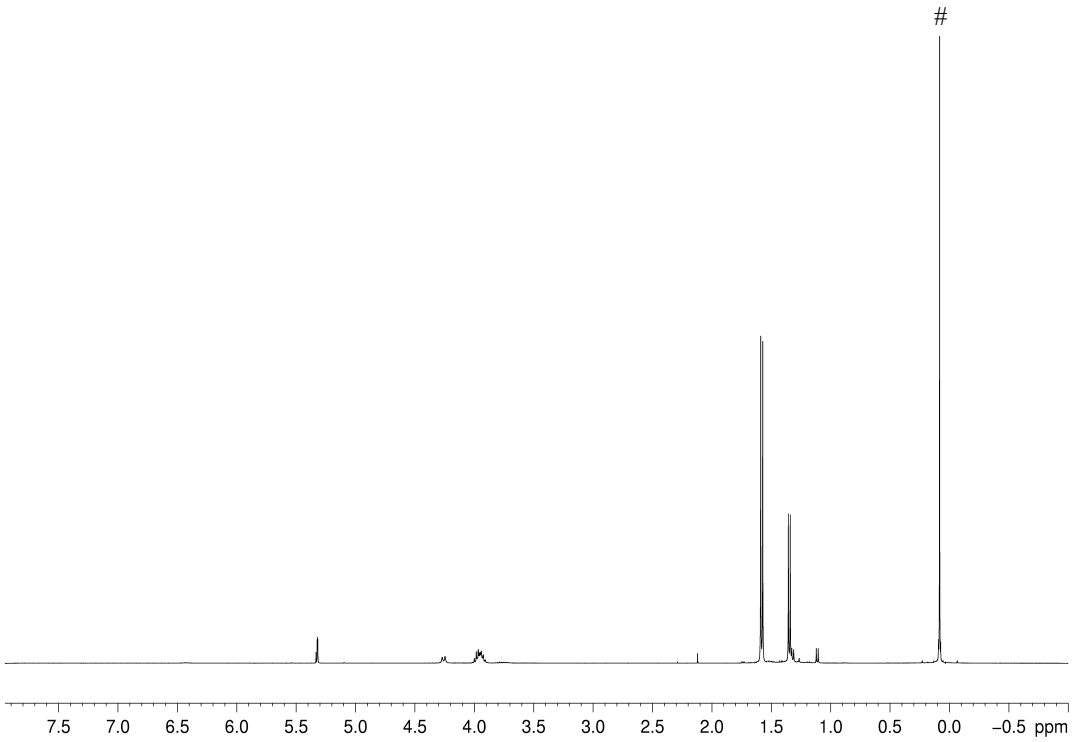

Figure 4.9: *^{1}H NMR spectrum of **7** in CD_2Cl_2. # = grease.*

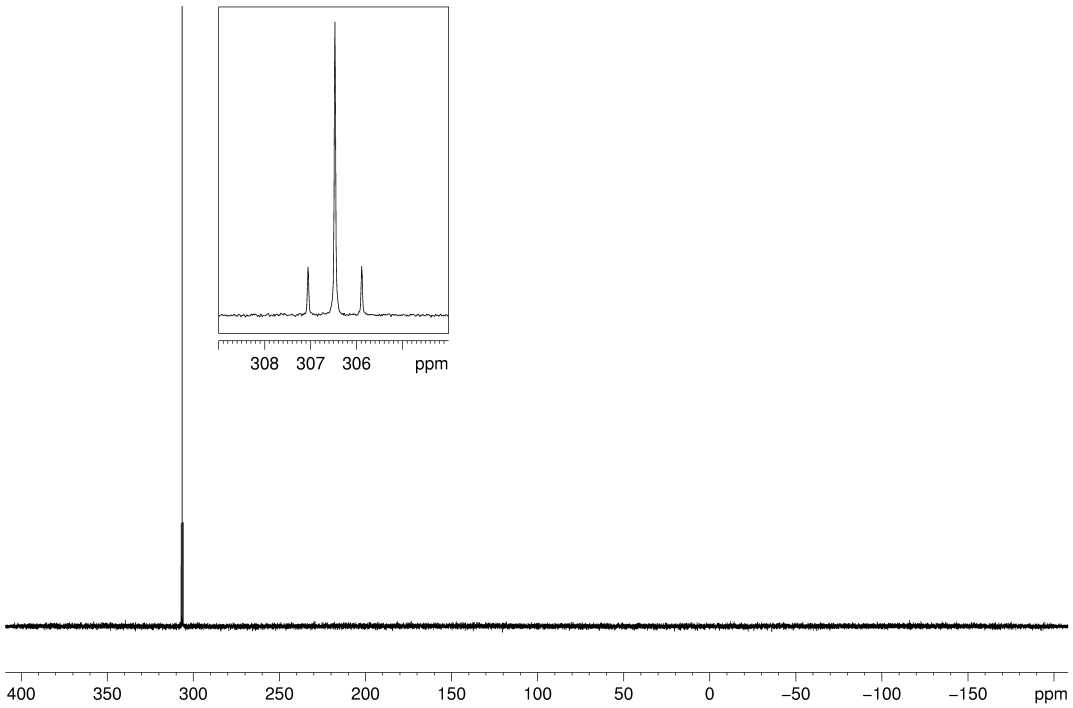

Figure 4.10: *$^{31}P\{^{1}H\}$ NMR spectrum of **7** in CD_2Cl_2.*

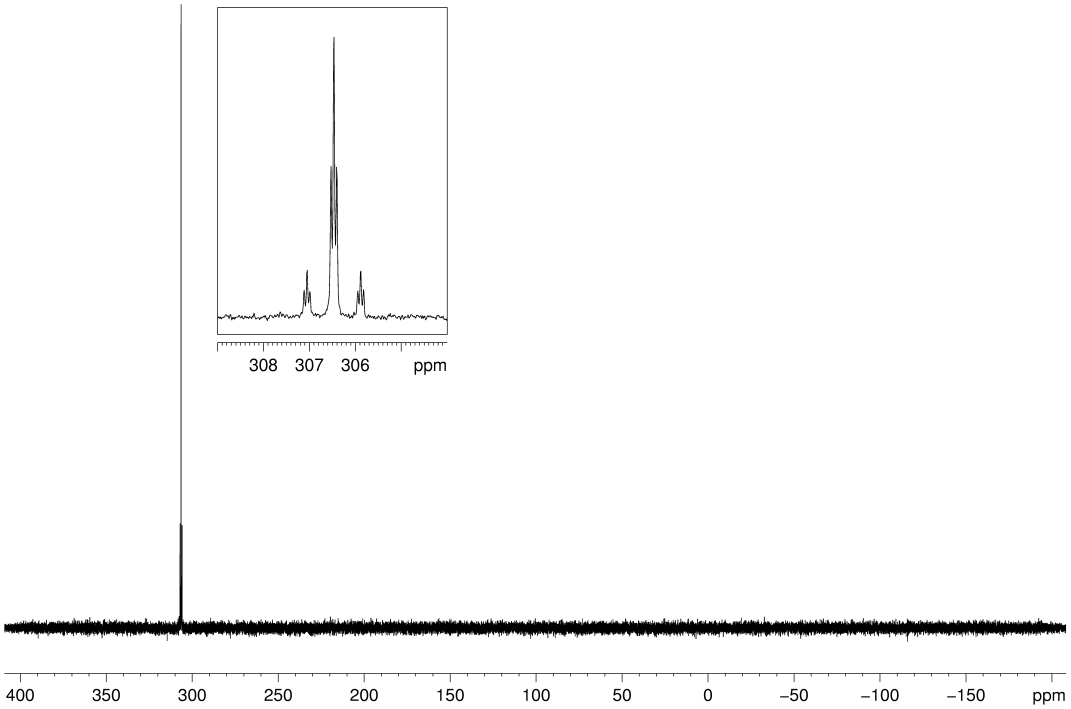

Figure 4.11: *^{31}P NMR spectrum of **7** in CD_2Cl_2.*

4.4.2.8 Synthesis of [(^{i}PrNH)C(NCy)$_2$P{W(CO)$_5$}$_2$] (8)

45 mg (0.22 mmol) N,N'-cyclohexylcarbodiimide (DCC) are added to a solution of 147.4 mg (0.2 mmol) **2a** in 20 mL toluene. The reaction solution is heated to 110 °C for 1 h until a color change from red to brownish yellow occurs. Afterwards, the reaction mixture is stirred at room temperature overnight. The solution is filtered, concentrated and stored at -28 °C. [(^{i}PrNH)C(NCy)$_2$P{W(CO)$_5$}$_2$] (**8**) crystallizes as colorless plates from the solution.

Analytical data for **8**:

Yield:	50 mg (27 %).
^{1}H NMR (C_6D_6, 400 MHz):	δ [ppm] = 0.68 (d, $^3J_{HH}$ = 6.2 Hz, 6H, CH_3), 0.91-2.23 (m, 20H, CH_2), 3.35 (m, 2H, CH), 3.41 (m, 1H, CH), 3.56 (d, $^3J_{HH}$ = 9.8 Hz, 1H, NH).
^{31}P{^{1}H} NMR (C_6D_6, 162 MHz):	δ [ppm] = 309.1 (s, $^1J_{PW}$ = 188 Hz).
^{31}P NMR (C_6D_6, 162 MHz):	δ [ppm] = 309.1 (t, $^3J_{PH}$ = 11 Hz, $^1J_{PW}$ = 188 Hz).
^{13}C{^{1}H} NMR (C_6D_6, 100 MHz):	δ [ppm] = 23.2 (s, CH_3), 24.9 (s, CH_3), 25.8 (s, CH_2), 32.3 (s, CH_2), 46.6 (s, CH), 199.8 (s, CO), 202.6 (s, CO).
IR (KBr):	ν_{max}/cm^{-1} = 3400 (w, NH), 2072 (w, CO), 2055 (s, CO), 1975 (sh, CO), 1957 (sh, CO), 1936, (vs, CO), 1911 (vs, CO).
MS (EI, 70eV):	m/z (%): 942.9 (9) [M$^+$], 914.9 (24) [M$^+$ -CO], 886.9 (6) [M$^+$ - 2CO], 859.9 (33) [M$^+$ - 3CO] 803.1 (20) [M$^+$ - 5CO], 775.1 (45) [M$^+$ - 6CO], 747.0 (100) [M$^+$ - 7 CO].

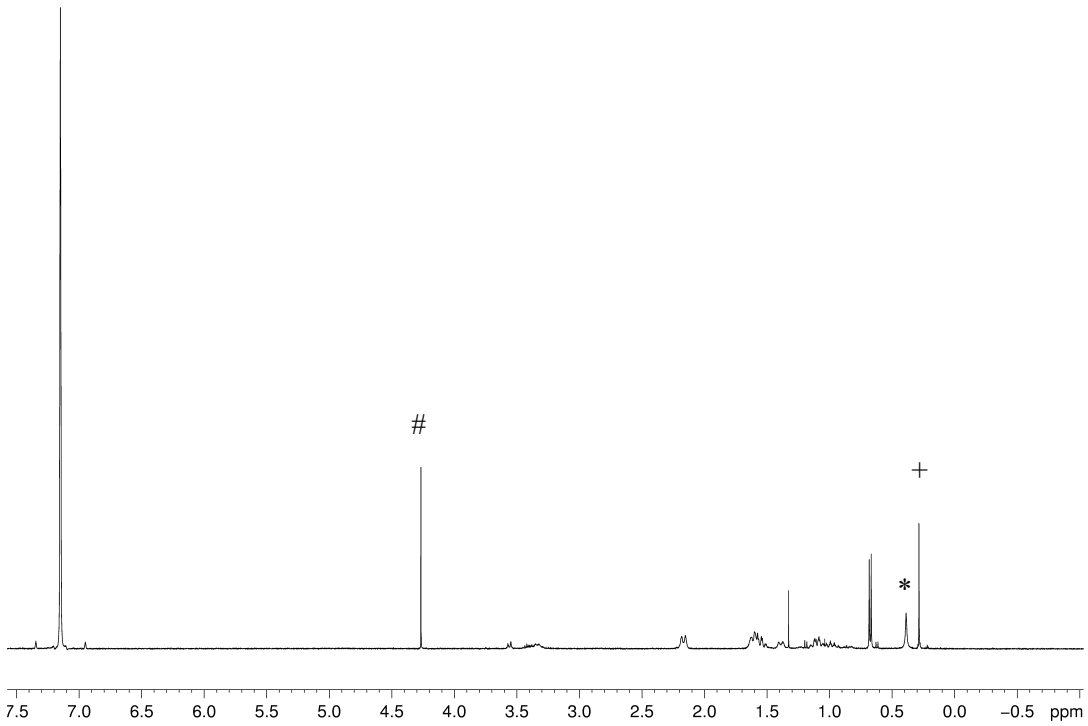

Figure 4.12: *^{1}H NMR spectrum of **8** in C_6D_6. # = CH_2Cl_2; + = grease; * = water*

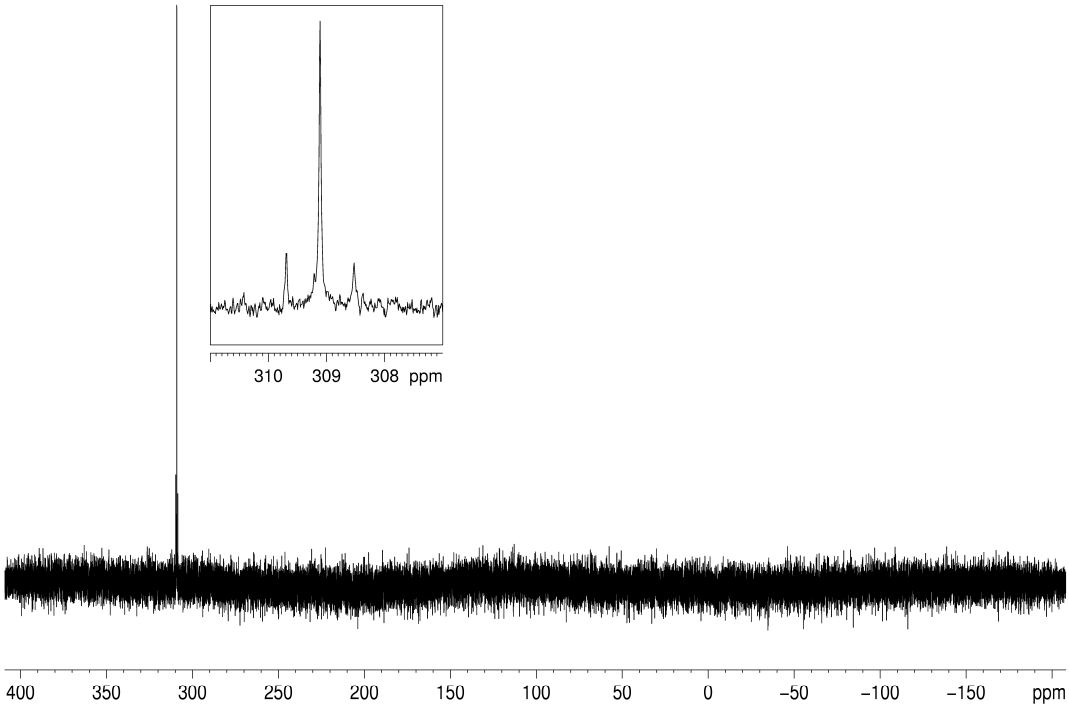

Figure 4.13: *$^{31}P\{^{1}H\}$ NMR spectrum of **8** in C_6D_6.*

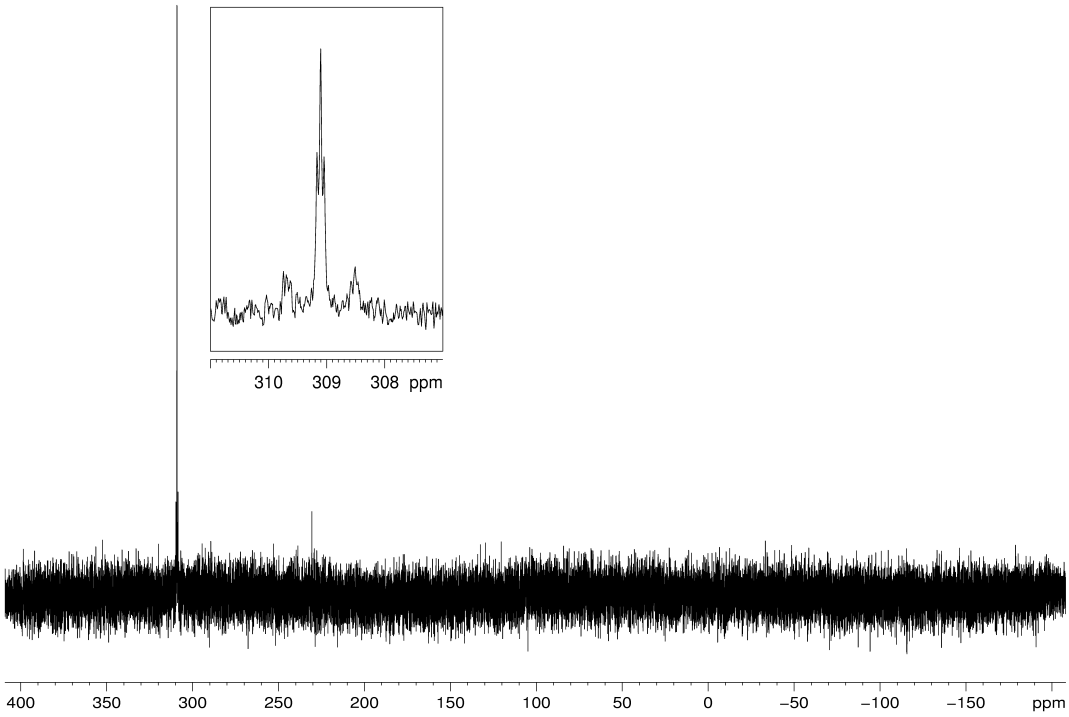

Figure 4.14: *^{31}P NMR spectrum of **8** in CD_2Cl_2.*

4.4.3 Crystallographic Data

Single crystal X-ray structure analyses were either carried out on a Gemini Ultra Diffractometer (Rigaku Oxford Diffraction, formerly Agilent Technologies), a GV50 diffractometer (Rigaku Oxford Diffraction) or on a XtaLAB Synergy R, DW system. The Gemini Ultra diffractometer was equipped with either a molybdenum X-ray radiation source (Mo-K_α = 0.71072 Å) or a copper X-ray radiation source (Cu-K_α = 1.5406 Å) and an AtlasS2 CCD detector as well as an Oxford Systems CryoJet cooling system. The GV50 diffractometer was equipped with a copper X-ray radiation source and a TitanS2 detector as well as an Oxford Cryosystems CryoStream 700 cooling system. The XtaLAB Synergy R was equipped with a rotating anode using copper radiation, a HyPix-Arc 150 detector as well as an Oxford Cryosystems CryoStream 700 cooling system. Figures of the molecular structures were prepared with the program *Olex2*.[25]

Due to their air and water sensitivity, the crystals were coated with mineral oil (Sigma Aldrich, CAS 8042-47-5). Suitable single crystals were picked under the microscope from the oil and transferred onto a MiTeGen MicroLoop attached to a goniometer head. The goniometer head was then placed onto the goniometer with the loop sitting in a current of cold nitrogen. After collection of the crystal structure data, integration and data reduction were carried out with the program *CrysAlisPro*.[26] Structure elucidation was carried out with the program *SHELXT*[27] using direct methods. Refinement occurred with the least squares method with the program *SHELXL*.[28] Both were used within *Olex2*[25] as the platform.

4.4.3.1 Crystal Structure Data for 2a

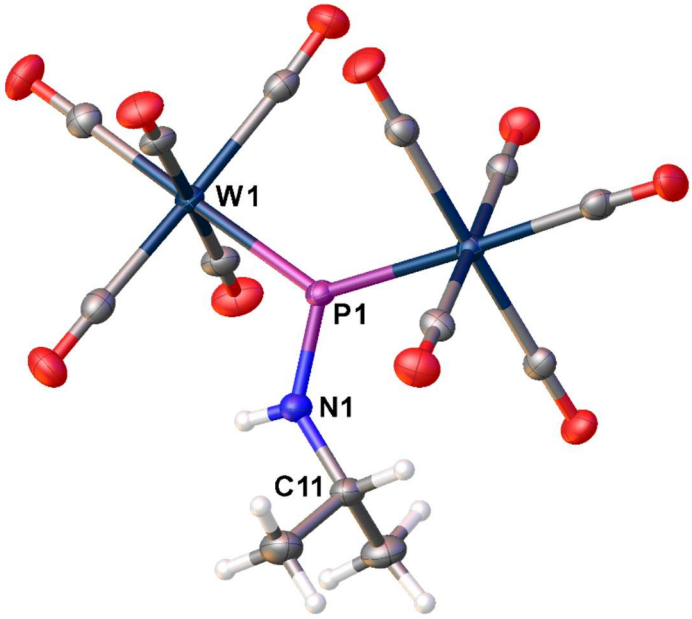

Molecular structure of **2a**. Anisotropic displacement parameters are set to 50% probability level. Selected bond lengths [Å] and angles [°]: N1-C11 1.481(5), N1-P1 1.636(3), W1-P1 2.4517(9), W2-P1 2.4187(9); C11-N1-P1 130.7(3), N1-P1-W1 109.77(13), N1-P1-W2 117.95(13), W2-P1-W1 132.28(4).

Compound	**2a**
Formula	$C_{13}H_8NO_{10}PW_2$
$D_{calc.}$/ g cm^{-3}	2.545
μ/mm^{-1}	23.063
Formula Weight	736.87
Colour	red
Shape	needle
Size/mm^3	0.09×0.03×0.03
T/K	123.00(10)
Crystal System	triclinic
Space Group	P-1
a/Å	6.5873(5)
b/Å	10.1008(6)
c/Å	14.8828(7)
α/°	77.191(5)
β/°	85.617(5)
γ/°	86.043(6)
V/Å^3	961.41(11)
Z	2
Z'	1
Wavelength/Å	1.54178
Radiation type	Cu K_α
Θ_{min}/°	3.051
Θ_{max}/°	73.130
Measured Refl's.	18265
Indep't Refl's	3747
Refl's I≥2 s(I)	3434
R_{int}	0.0376
Parameters	250
Restraints	0
Largest Peak	1.316
Deepest Hole	-1.386
GooF	1.067
wR_2 (all data)	0.0593
wR_2	0.0574
R_1 (all data)	0.0262
R_1	0.0227

4.4.3.2 Crystal Structure Data for 2b

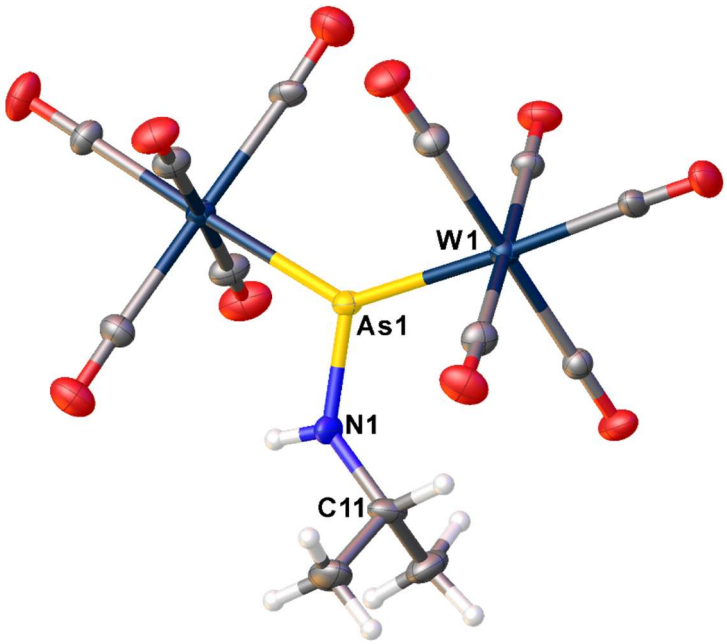

Molecular structure of **2b**. Anisotropic displacement parameters are set to 50% probability level. Selected bond lengths [Å] and angles [°]: W1-As1 2.5080(8), W2-As1 2.5302(8), As1-N1 1.775(6), N1-C11 1.455(9); W1-As1-W2 134.38(3), N1-As1-W1 116.3(2), N1-As1-W2 109.3(2), C11-N1-As1 130.2(5).

Compound	**2b**
Formula	$C_{13}H_8AsNO_{10}W_2$
$D_{calc.}$/ g cm^{-3}	2.649
μ/mm^{-1}	23.757
Formula Weight	780.82
Colour	red
Shape	needle
Size/mm^3	0.38×0.05×0.03
T/K	123.00(10)
Crystal System	triclinic
Space Group	P-1
a/Å	6.5765(4)
b/Å	10.2068(7)
c/Å	14.9934(10)
α/°	77.287(6)
β/°	86.534(6)
γ/°	86.601(6)
V/Å^3	978.87(11)
Z	2
Z'	1
Wavelength/Å	1.54178
Radiation type	Cu K_α
Θ_{min}/°	4.446
Θ_{max}/°	73.839
Measured Refl's.	6689
Indep't Refl's	3767
Refl's I≥2 s(I)	3401
R_{int}	0.0440
Parameters	250
Restraints	0
Largest Peak	1.402
Deepest Hole	-1.510
GooF	1.045
wR_2 (all data)	0.0941
wR_2	0.0902
R_1 (all data)	0.0404
R_1	0.0360

4.4.3.3 Crystal Structure Data for 3

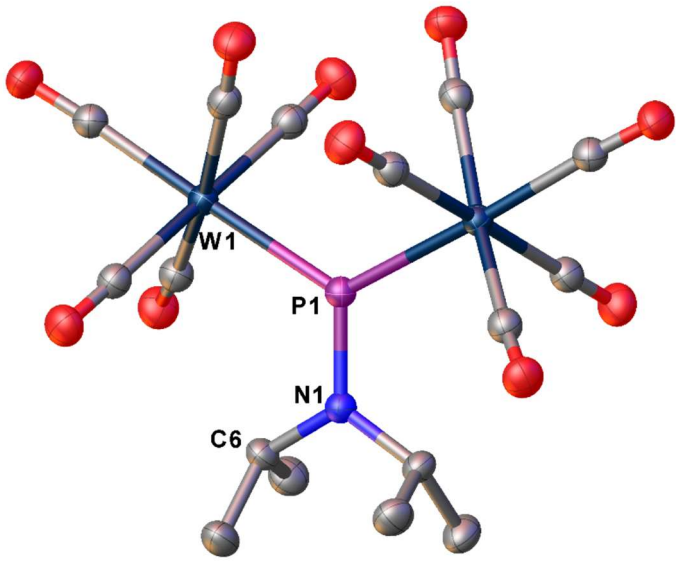

Molecular structure of **3**. Anisotropic displacement parameters are set to 50% probability level. H atoms are omitted for clarity. Selected bond lengths [Å] and angles [°]: W1-P1 2.4996(4), P1-N1 1.658(3), N1-C6 1.495(3); W1[6]-P1-W1 123.74(3), N1-P1-W1 118.128(17), C6-N1-P1 120.68(13).

Compound	**3**
Formula	$C_{16}H_{14}NO_{10}PW_2$
$D_{calc.}$/ g cm^{-3}	2.434
μ/mm^{-1}	10.942
Formula Weight	778.95
Colour	clear intense red
Shape	needle
Size/mm^3	
T/K	293(2)
Crystal System	monoclinic
Space Group	$C2/c$
a/Å	16.9811(5)
b/Å	10.6959(2)
c/Å	12.5009(4)
α/°	90
β/°	110.580(3)
γ/°	90
V/Å^3	2125.62(11)
Z	4
Z'	0.5
Wavelength/Å	0.71073
Radiation type	Mo K_α
Θ_{min}/°	3.482
Θ_{max}/°	34.960
Measured Refl's.	16900
Indep't Refl's	4380
Refl's I≥2 s(I)	3769
R_{int}	0.0158
Parameters	139
Restraints	0
Largest Peak	2.952
Deepest Hole	-0.533
GooF	1.081
wR_2 (all data)	0.0899
wR_2	0.0858
R_1 (all data)	0.0375
R_1	0.0328

[6] 1-x, +y, 3/2-z

4.4.3.4 Crystal Structure Data for 4

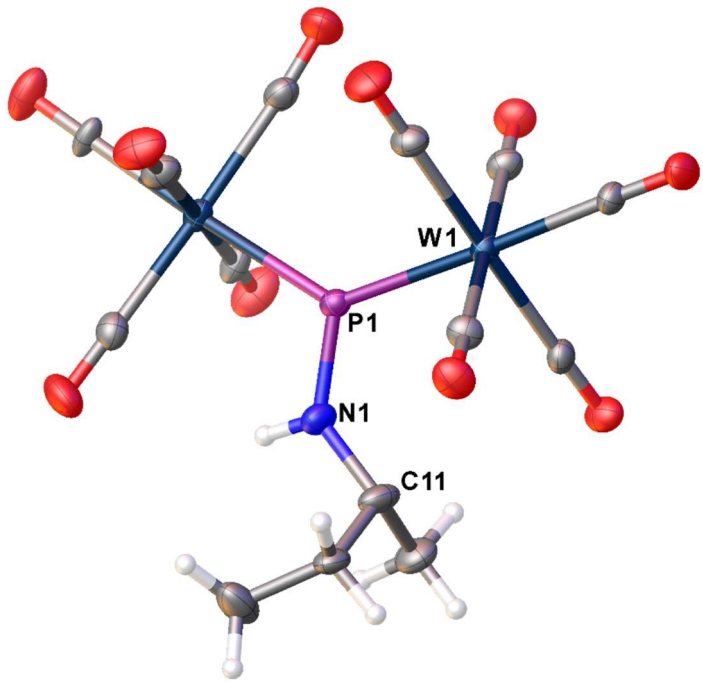

Molecular structure of **4**. Anisotropic displacement parameters are set to 50% probability level. Selected bond lengths [Å] and angles [°]: W1-P1 2.4192(15), W2-P1 2.4466(15), P1-N1 1.641(6), N1-C11 1.469(8); W2-P1-W1 131.38(6), N1-P1-W1 117.7(2), N1-P1-W2 110.9(2), C11-N1-P1 130.2(5).

Compound	**4**
Formula	$C_{14}H_{10}NO_{10}PW_2$
$D_{calc.}$/ g cm^{-3}	2.496
μ/mm^{-1}	22.208
Formula Weight	750.893
Colour	dark red
Shape	plate
Size/mm^3	0.18×0.12×0.07
T/K	123(1)
Crystal System	triclinic
Space Group	P-1
a/Å	6.7471(5)
b/Å	10.0844(7)
c/Å	15.0424(12)
α/°	78.436(6)
β/°	87.160(6)
γ/°	85.487(6)
V/Å^3	999.01(13)
Z	2
Z'	1
Wavelength/Å	1.54184
Radiation type	Cu K$_\alpha$
Θ_{min}/°	3.00
Θ_{max}/°	75.44
Measured Refl's.	6224
Indep't Refl's	3928
Refl's I≥2 s(I)	3710
R_{int}	0.0278
Parameters	285
Restraints	12
Largest Peak	1.8215
Deepest Hole	-1.4132
GooF	1.0563
wR_2 (all data)	0.1055
wR_2	0.1036
R_1 (all data)	0.0400
R_1	0.0380

4.4.3.5 Crystal Structure Data for 5

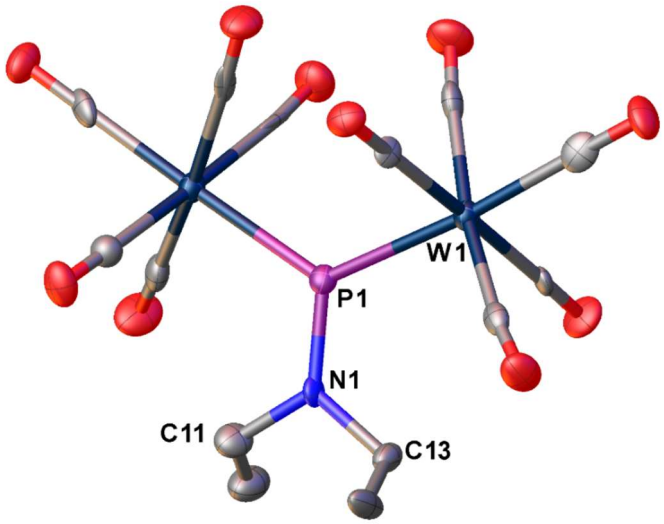

Molecular structure of **5**. Anisotropic displacement parameters are set to 50% probability level. H atoms are omitted for clarity. Selected bond lengths [Å] and angles [°]: W1-P1 2.476(2), W2-P1 2.470(2), P1-N1 1.636(7), N1-C11 1.464(11), N1-C13 1.498(10); W1-P1-W2 125.19(9) W1-P1-N1 117.6(2), W2-P1-N1 117.2(2), P1-N1-C11 124.7(6), P1-N1-C13 124.4(6), C11-N1-C13 110.9(7).

Compound	**5**
Formula	$C_{14}H_{10}NO_{10}PW_2$
$D_{calc.}$/ g cm^{-3}	2.515
μ/mm^{-1}	22.384
Formula Weight	750.88
Colour	red
Shape	needle
Size/mm^3	0.10×0.02×0.02
T/K	123
Crystal System	triclinic
Space Group	P-1
a/Å	6.9085(12)
b/Å	10.2806(17)
c/Å	14.904(3)
α/°	81.793(14)
β/°	85.419(14)
γ/°	71.236(16)
V/Å^3	991.4(3)
Z	2
Z'	1
Wavelength/Å	1.5418
Radiation type	Cu K$_\alpha$
Θ_{min}/°	3.00
Θ_{max}/°	51.42
Measured Refl's.	6232
Indep't Refl's	2122
Refl's I≥2 s(I)	1520
R_{int}	0.0365
Parameters	250
Restraints	0
Largest Peak	1.295
Deepest Hole	-0.593
GooF	0.910
wR_2 (all data)	0.0450
wR_2	0.0438
R_1 (all data)	0.0410
R_1	0.0254

4.4.3.6 Crystal Structure Data for 7

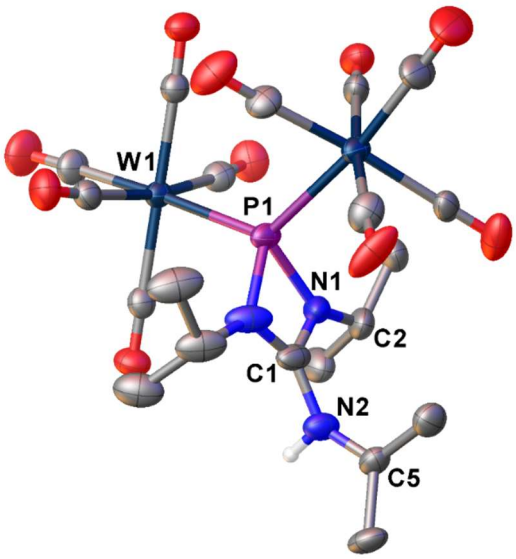

Molecular structure of **7**. Anisotropic displacement parameters are set to 50% probability level. H atoms bound to C atoms are omitted for clarity. Selected bond lengths [Å] and angles [°]: W1-P1 2.5341(13), P1-N1 1.808(4), N1-C2 1.468(7), N1-C1 1.328(6), N2-C1 1.379(9), N2-C5 1.209(19); N1-P1-W1 113.77(14), N1[7]-P1-W2 115.62(13), N1-P1-W2 107.28(12), W2-P1-W1 123.31(5), C2-N1-P1 139.4(3), C1-N1-P1 92.5(3), C1-N1-C2 127.8(4), C5-N2-C1 139.4(7).

Compound	**7**
Formula	$C_{20}H_{22}N_3O_{10}PW_2$
$D_{calc.}$/ g cm^{-3}	2.162
μ/mm^{-1}	16.874
Formula Weight	863.07
Colour	light yellow
Shape	block
Size/mm^3	0.21×0.19×0.10
T/K	122.95(10)
Crystal System	monoclinic
Space Group	$C2/m$
a/Å	15.3670(3)
b/Å	11.9111(2)
c/Å	14.6380(3)
α/°	90
β/°	98.269(2)
γ/°	90
V/Å^3	2651.45(9)
Z	4
Z'	0.5
Wavelength/Å	1.54184
Radiation type	Cu K_α
Θ_{min}/°	4.716
Θ_{max}/°	66.484
Measured Refl's.	5103
Indep't Refl's	2424
Refl's I≥2 s(I)	2233
R_{int}	0.0258
Parameters	245
Restraints	24
Largest Peak	0.489
Deepest Hole	-0.788
GooF	1.053
wR_2 (all data)	0.0610
wR_2	0.0591
R_1 (all data)	0.0275
R_1	0.0246

[7] +x, 1-y, +z

4.4.3.7 Crystal Structure Data for 8

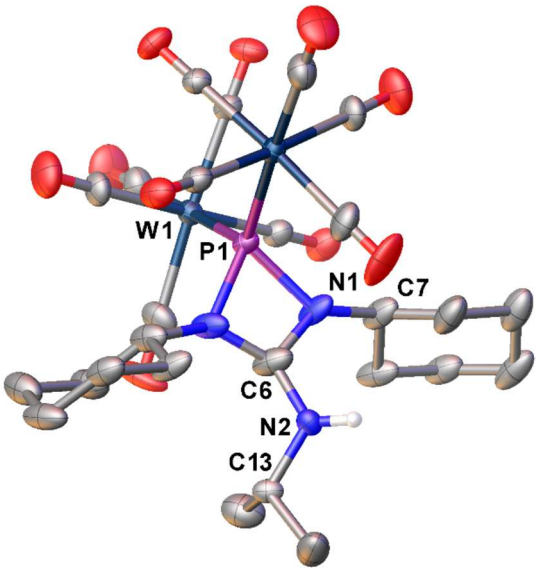

Molecular structure of **8**. Anisotropic displacement parameters are set to 50% probability level. H atoms bound to C atoms are omitted for clarity. Selected bond lengths [Å] and angles [°]: W1-P1 2.5127(9), P1-N1 1.790(5), N1-C7 1.471(7), N1-C6 1.347(7), N2-C13 1.479(13), N2-C6 1.411(12); W1[8]-P1-W1 123.75(8), N1-P1-W1 113.44(17), N1[8]-P1-W1 111.37(19), N1-P1-N1[8] 72.1(3), C7-N1-P1 130.0(4), C6-N1-P1 92.5(4), C6-N1-C7 133.0(5), C6-N2-C13 115.7(7).

Compound	**8**
Formula	$C_{26}H_{30}N_3O_{10}PW_2$
$D_{calc.}$/ g cm^{-3}	1.994
μ/mm^{-1}	14.311
Formula Weight	943.20
Colour	yellow
Shape	rod
Size/mm^3	0.23×0.09×0.04
T/K	123(1)
Crystal System	monoclinic
Space Group	$C2/c$
a/Å	13.2496(3)
b/Å	16.8461(4)
c/Å	14.0915(3)
α/°	90
β/°	92.801(2)
γ/°	90
V/Å^3	3141.52(12)
Z	4
Z'	0.5
Wavelength/Å	1.54178
Radiation type	Cu K_α
Θ_{min}/°	4.248
Θ_{max}/°	70.577
Measured Refl's.	5634
Indep't Refl's	2933
Refl's I≥2 s(I)	2709
R_{int}	0.0239
Parameters	212
Restraints	6
Largest Peak	1.580
Deepest Hole	-1.771
GooF	1.089
wR_2 (all data)	0.1068
wR_2	0.1039
R_1 (all data)	0.0400
R_1	0.0374

[8] 1-x, +y, ½-z

4.4.4 Computational Details

4.4.4.1 Molecular orbitals

All calculations have been performed with the TURBOMOLE program package[29] using the RI-[30,31]BP86[32] functional together with the def2-TZVP basis set for all atoms.[31,33,34] To speed up the calculations, the Coulomb part was evaluated by using the Multipole Accelerated Resolution of Identity method (MARI-*J*)[30,35] along with optimized auxiliary basis sets on all atoms.[33]

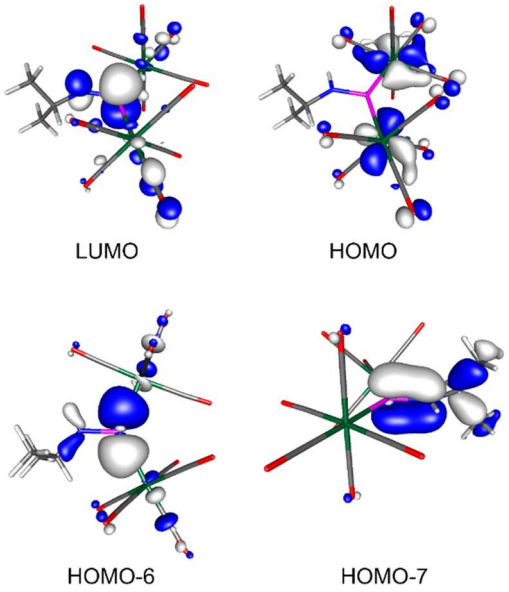

Figure 4.14: *Selected Molecular Orbitals in [(^{i}PrN(H)P{W(CO)$_5$}$_2$], calculated at the BP86/def2-TZVP level of theory.*

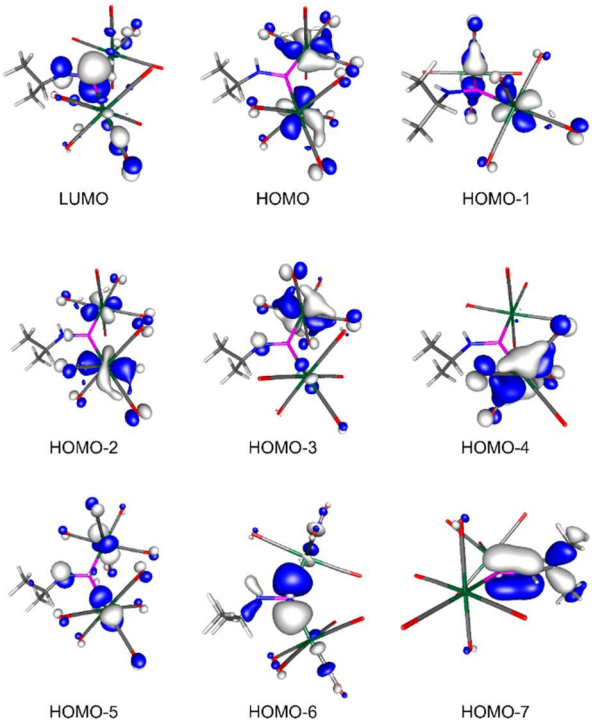

Figure 4.15: *Frontier Molecular Orbitals in [(^{i}PrN(H)P{W(CO)$_5$}$_2$], calculated at the BP86/def2-TZVP level of theory.*

Table 4.1: *Orbital energies and occupations in [(^{i}PrN(H)P{W(CO)$_5$}$_2$], calculated at the BP86/def2-TZVP level of theory.*

Nr.	Orbital	Occupation	Energy	
125.	125 a		-0.018350 H =	-0.499 eV
124.	124 a		-0.025847 H =	-0.703 eV
123.	123 a		-0.049349 H =	-1.343 eV
122.	122 a		-0.051593 H =	-1.404 eV
121.	121 a		-0.056518 H =	-1.538 eV
120.	120 a		-0.060473 H =	-1.646 eV
119.	119 a		-0.064135 H =	-1.745 eV
118.	118 a		-0.069583 H =	-1.893 eV
117.	117 a		-0.086235 H =	-2.347 eV
116.	116 a		-0.086928 H =	-2.365 eV
115.	115 a		-0.094816 H =	-2.580 eV
114.	114 a		-0.097179 H =	-2.644 eV
113.	113 a		-0.098698 H =	-2.686 eV
112.	112 a		-0.100628 H =	-2.738 eV
111.	111 a		-0.101275 H =	-2.756 eV
110.	110 a		-0.115246 H =	-3.136 eV
109.	109 a		-0.146938 H =	-3.998 eV
108.	108 a	2.000	-0.223676 H =	-6.087 eV
107.	107 a	2.000	-0.228965 H =	-6.230 eV
106.	106 a	2.000	-0.232437 H =	-6.325 eV
105.	105 a	2.000	-0.234919 H =	-6.392 eV
104.	104 a	2.000	-0.238596 H =	-6.493 eV
103.	103 a	2.000	-0.240976 H =	-6.557 eV
102.	102 a	2.000	-0.272683 H =	-7.420 eV
101.	101 a	2.000	-0.306646 H =	-8.344 eV
100.	100 a	2.000	-0.334953 H =	-9.115 eV
99.	99 a	2.000	-0.347606 H =	-9.459 eV
98.	98 a	2.000	-0.360531 H =	-9.811 eV
97.	97 a	2.000	-0.371696 H =	-10.114 eV
96.	96 a	2.000	-0.374842 H =	-10.200 eV
95.	95 a	2.000	-0.377294 H =	-10.267 eV
94.	94 a	2.000	-0.377437 H =	-10.271 eV
93.	93 a	2.000	-0.377533 H =	-10.273 eV

Table 4.2: *Cartesian coordinates of the optimized geometry of [(^{i}PrN(H)P{W(CO)$_5$}$_2$] at the BP86/def2-TZVP level of theory. E = −1783.913142545 au.*

Atom	x	y	z
W	1.984453200	1.445976900	0.125898500
W	-2.612879400	1.177856400	0.088036100
P	-0.250417200	0.310799300	0.027142200
N	-0.249352800	-1.367954900	-0.112850200
H	-1.175364300	-1.800035200	-0.154125300
C	3.740443400	2.507368800	0.203476900
C	1.239277300	2.868302100	-1.193691600
C	1.293212700	2.550355900	1.746073500
C	2.738694300	0.368470300	-1.475378100
C	2.794522100	0.073546300	1.449439200
O	4.734122600	3.100265400	0.245860300
O	0.857965800	3.669587800	-1.934152200
O	0.943903200	3.166027000	2.659480100
O	3.183536400	-0.216037300	-2.370765400
O	3.273897100	-0.669061400	2.198027000
C	-3.421321700	-0.693370500	-0.216197600
C	-2.669954000	0.851778000	2.141734700
C	-1.920378100	3.111872900	0.385948500
C	-4.517149900	1.941981900	0.153880400
C	-2.563070900	1.465468700	-1.972537700
C	0.854162800	-2.342671400	-0.190270000
O	-3.905521100	-1.735261700	-0.388794200
O	-2.711352700	0.658806800	3.280805900
O	-1.598107800	4.210365300	0.549459100
O	-5.594481900	2.365206000	0.192619900
O	-2.548056600	1.614578300	-3.118580300
H	1.780998700	-1.755402800	-0.142850000
C	0.797254300	-3.295887500	1.010520800
C	0.799302300	-3.091380900	-1.528197600
H	0.854035300	-2.744814900	1.958293600
H	1.637747800	-4.002914700	0.970983300
H	-0.135108700	-3.881633300	1.003581600
H	-0.133679400	-3.669218400	-1.617645100
H	1.638927500	-3.797015600	-1.599753600
H	0.859739600	-2.395953600	-2.375472900

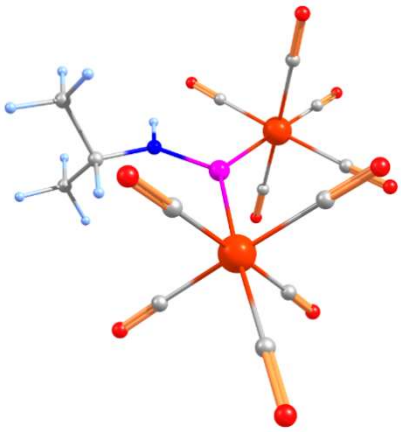

Table 4.3: *Wiberg Bond Indices*

Number of electrons: 216.00000

p	3	-	w	1	0.85847		
p	3	-	w	2	0.80440		
n	4	-	w	1	0.02600		
n	4	-	w	2	0.04781		
n	4	-	p	3	1.22664		
h	5	-	n	4	0.87118		
c	6	-	w	1	0.78902		
c	6	-	p	3	0.07330		
c	7	-	w	1	0.87422		
c	7	-	p	3	0.03904		
c	8	-	w	1	0.87202		
c	8	-	p	3	0.04113		
c	9	-	w	1	0.88323		
c	9	-	p	3	0.03446		
c	9	-	c	8	0.07439		
c	10	-	w	1	0.88316		
c	10	-	p	3	0.03145		
c	10	-	c	7	0.07531		
o	11	-	w	1	0.11090		
o	11	-	p	3	0.02176		
o	11	-	c	6	2.22114		
o	12	-	w	1	0.08628		
o	12	-	c	7	2.25011		
o	12	-	c	10	0.02917		
o	13	-	w	1	0.08593		
o	13	-	c	8	2.25151		
o	13	-	c	9	0.02902		
o	14	-	w	1	0.09354		
o	14	-	c	8	0.02811		
o	14	-	c	9	2.22411		
o	15	-	w	1	0.09424		
o	15	-	c	7	0.02834		
o	15	-	c	10	2.22214		
c	16	-	w	2	0.91068		
c	16	-	p	3	0.02581		
c	17	-	w	2	0.87673		
c	17	-	p	3	0.04388		
c	17	-	c	16	0.02088		
c	18	-	w	2	0.89675		
c	18	-	p	3	0.02624		
c	18	-	c	16	0.07049		
c	19	-	w	2	0.78514		
c	19	-	p	3	0.08403		
c	20	-	w	2	0.87345		
c	20	-	p	3	0.04347		
c	20	-	c	16	0.02284		
c	20	-	c	17	0.07442		
c	21	-	n	4	0.81542		
o	22	-	w	2	0.10496		
o	22	-	c	16	2.18991		
o	22	-	c	18	0.02959		
o	23	-	w	2	0.08888		
o	23	-	c	17	2.24844		
o	23	-	c	20	0.02777		
o	24	-	w	2	0.08583		
o	24	-	c	16	0.03200		
o	24	-	c	18	2.24421		
o	25	-	w	2	0.11011		
o	25	-	c	19	2.22067		
o	26	-	w	2	0.08784		
o	26	-	c	17	0.02765		
o	26	-	c	20	2.24938		
h	27	-	c	21	0.95962		
c	28	-	c	21	0.95420		
c	29	-	c	21	0.95415		
h	30	-	c	28	0.95938		
h	31	-	c	28	0.96235		
h	32	-	c	28	0.96158		
h	33	-	c	29	0.96208		
h	34	-	c	29	0.96245		
h	35	-	c	29	0.95959		

4.4.4.2 Reaction enthalpies

The geometries of the compounds have been fully optimized with gradient-corrected density functional theory (DFT) in form of Becke's three-parameter hybrid method B3LYP[36] with 6-31G* all electron basis set (effective core potentials LANL2DZ basis set on W[37]). Gaussian 03 program package[38] was used throughout. All structures correspond to minima on their respective potential energy surfaces as verified by computation of second derivatives.

Table 4.4: *Total energies E^o_0, sum of electronic and thermal enthalpies H^o_{298} (Hartree) and standard entropies S^o_{298} (cal mol^{-1}K^{-1}) for studied compounds. B3LYP/6-31G* (LANL2DZ on W) level of theory.*

Compound	E^o_0	H^o_{298}	S^o_{298}
$NH_2{}^sBu$	-213.7966311	-213.638725	78.93
$PH_2{}^tBu$	-500.3916798	-500.243082	81.48
$\{W(CO)_5\}_2PNH^sBu$	-1823.768397	-1823.506218	228.844
$\{W(CO)_5\}_2PNH^sBu\cdot PH_2{}^tBu$ **(I)**	-2324.163455	-2323.750339	276.823
cis-$\{W(CO)_5\}_2P{=}PH^tBu$ **(II)**	-2110.340155	-2110.084676	228.671
trans-$\{W(CO)_5\}HP{=}P^tBu\{W(CO)_5\}$ **(III)**	-2110.343569	-2110.087918	234.422
$\{W(CO)_5\}PH^tBu\text{-}PH\text{-}PH^tBu\{W(CO)_5\}$	-2610.775407	-2610.367777	266.685
$W(CO)_5\}PH^tBu\text{-}PH\text{-}PH^tBu\{W(CO)_5\}$ conformer 2	-2610.771042	-2610.363418	269.476
$W(CO)_5\}PH^tBu\text{-}PH\text{-}PH^tBu\{W(CO)_5\}$ conformer 3	-2610.768689	-2610.361263	264.731

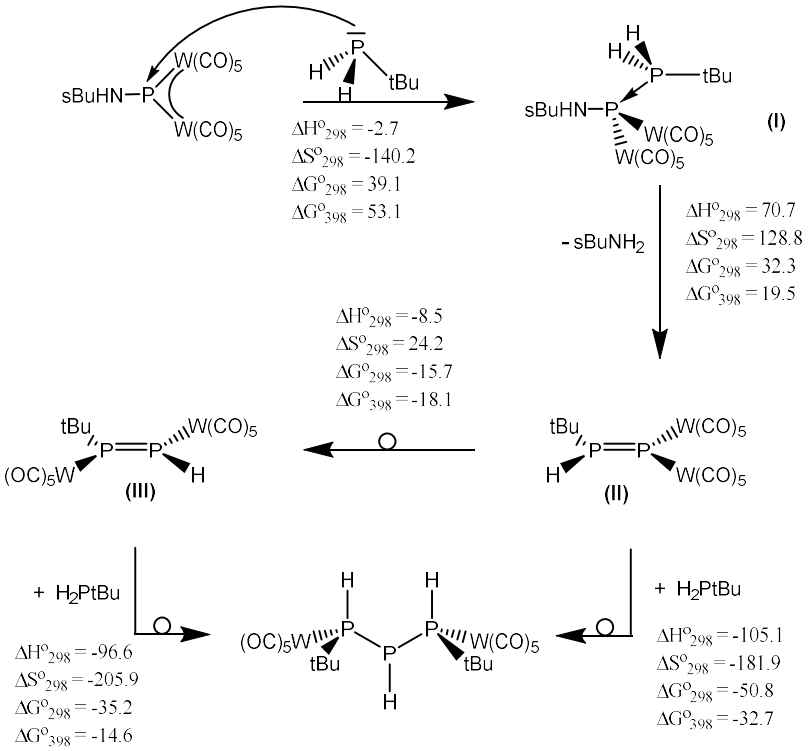

Figure 4.16: *Thermodynamic characteristics for the gas phase reactions for P compounds. B3LYP/6-31G* (LANL2DZ on W) level of theory. Standard enthalpies and Gibbs energies are in kJ mol^{-1}, standard entropies in J mol^{-1} K^{-1}.*

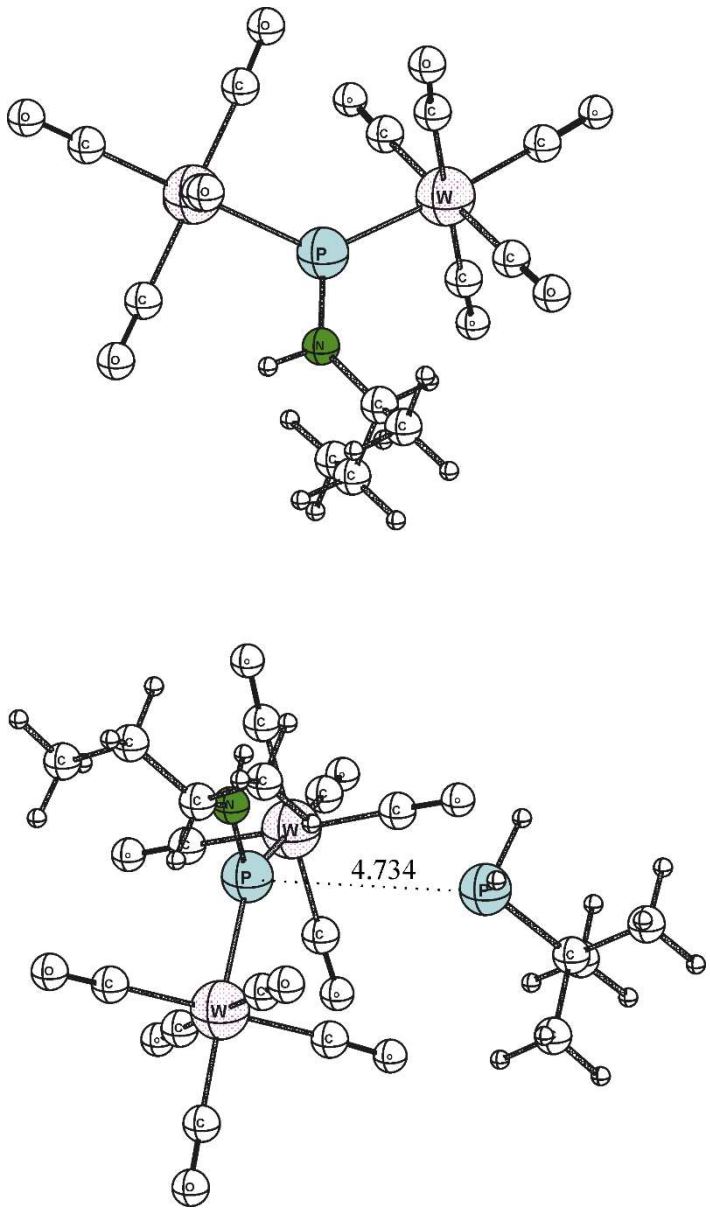

Figure 4.17: *Optimized geometries of* $\{W(CO)_5\}_2PNH^sBu$ *(top) and its weakly bound complex with* $PH_2{}^tBu$ *(bottom).*

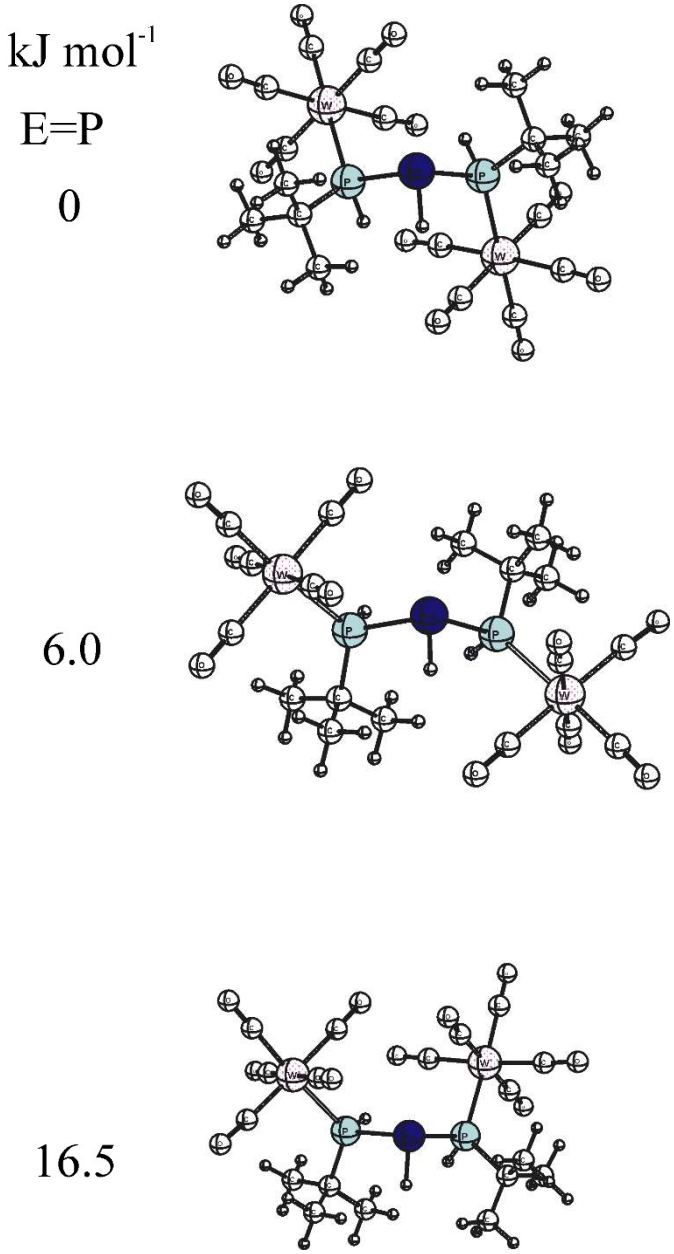

Figure 4.18: *Optimized geometries and relative energies of the considered conformers of {W(CO)5}PH^{t}Bu-PH-PH^{t}Bu{W(CO)5}.*

Table 4.5: *Optimized xyz coordinates (in Angstroms) for studied compounds. B3LYP/6-31G* (LANL2DZ ECP on W) level of theory.*

$NH_2{}^{s}Bu$

1	0.185778000	1.968345000	-0.175990000
7	-0.646822000	1.436925000	0.073504000
6	-0.492733000	0.030718000	-0.333212000
1	-0.720033000	1.487850000	1.090827000
6	0.730394000	-0.695050000	0.270999000
1	-0.369856000	0.042673000	-1.426593000
6	-1.790917000	-0.714429000	-0.008278000
1	-1.757348000	-1.747618000	-0.372176000
1	-2.646808000	-0.206835000	-0.463052000
1	-1.957007000	-0.750102000	1.077237000
1	0.719893000	-1.742708000	-0.061714000
1	0.617670000	-0.720186000	1.365861000
6	2.079672000	-0.067164000	-0.093527000
1	2.910973000	-0.629319000	0.346221000
1	2.157159000	0.964911000	0.269685000
1	2.228836000	-0.049945000	-1.180730000

$PH_2{}^{t}Bu$

H	0.604441532	-0.4225522916	-0.1343160818
P	0.1669958896	0.0397833343	1.1425819575
C	-0.8504597449	-1.4956653578	1.6206351238
H	-0.9043283751	0.8025382919	0.5893634488
C	0.146937858	-2.6134572045	1.9820248295
C	-1.7754696302	-1.9645253186	0.4858356426
C	-1.6861368598	-1.125037688	2.8612567423
H	-1.0529025463	-0.7870388254	3.6895505396
H	-2.254386478	-1.9981951788	3.2087699281
H	-2.4070609005	-0.3290286153	2.6391227079
H	0.8209306018	-2.3085533611	2.7907688986
H	0.7605521317	-2.9010661934	1.1197812222
H	-0.3938447966	-3.5089173129	2.3163635219
H	-1.2064437345	-2.2336380341	-0.411333794
H	-2.4956179769	-1.1868546794	0.2070169606
H	-2.3457043889	-2.8513050687	0.7981734494

$\{W(CO)_5\}_2PNH^sBu$

74	2.36992	-0.21365	0.01061
6	1.70702	-2.15608	0.24857
6	3.06695	1.6987	-0.24003
6	2.17577	-0.40231	-2.04428
6	4.28734	-0.92753	-0.11569
6	2.58233	-0.00957	2.05959
8	2.70355	0.11316	3.19951
8	5.3701	-1.32116	-0.18553
8	2.07555	-0.49878	-3.188
8	3.44913	2.78366	-0.37106
8	1.36804	-3.25123	0.37162
74	-2.15017	-0.62003	-0.01946
6	-3.83995	-1.76915	-0.19142
6	-2.87732	0.63225	-1.48867
6	-1.49005	-1.88291	1.48457
6	-3.09669	0.52848	1.40448
6	-1.24426	-1.80617	-1.44977
8	-4.79211	-2.41343	-0.29067
8	-3.30745	1.33029	-2.30147
8	-1.14368	-2.58097	2.33286
8	-0.75144	-2.47432	-2.24932
8	-3.65026	1.1561	2.20062
7	-0.02718	2.25119	0.39104
15	0.0113	0.60091	0.15056
6	-1.13657	3.21363	0.52385
6	-0.91549	4.40837	-0.42552
6	-1.26549	3.66873	1.98468
6	-0.86608	4.05121	-1.91345
1	0.01096	4.92413	-0.13137
1	-1.72821	5.12292	-0.24303
1	-2.10829	4.35984	2.09386
1	-0.35705	4.18878	2.31262
1	-1.43309	2.81731	2.64994
1	-2.04654	2.68643	0.22558
1	0.8839	2.69577	0.47861
1	-0.03799	3.36989	-2.1376
1	-0.72625	4.9525	-2.51962
1	-1.79418	3.5696	-2.24011

$\{W(CO)_5\}_2PNH^sBu \cdot PH_2{}^tBu$

74	-2.31556	1.06	-0.24363
6	-1.47908	1.04068	-2.13254
6	-3.17326	1.09698	1.61767
6	-3.45677	-0.6006	-0.72735
6	-3.8071	2.26859	-0.95678
6	-1.20499	2.73591	0.24792
8	-0.60377	3.68066	0.52373
8	-4.65073	2.95164	-1.35045
8	-4.10045	-1.52008	-0.98856
8	-3.64182	1.11649	2.6765
8	-1.04042	1.04752	-3.19905
74	1.15953	-1.83465	-0.68443
6	2.46895	-2.89854	-1.84678
6	0.67064	-3.57804	0.30204
6	1.72937	-0.11914	-1.69032
6	2.66383	-1.48788	0.68235
6	-0.3233	-2.19099	-2.0789
8	3.2072	-3.50038	-2.49918
8	0.4229	-4.56621	0.84614
8	2.07479	0.8235	-2.25726
8	-1.14373	-2.39648	-2.86257
8	3.52346	-1.30955	1.43193
7	-0.5155	-0.56292	2.22968
6	0.2745	-1.35763	3.18836
6	-0.66748	-2.10363	4.15561
6	1.25529	-0.45097	3.94523
6	-1.6322	-3.08987	3.49147
1	-1.23243	-1.35945	4.73695
1	-0.03522	-2.63368	4.87926
1	0.71508	0.29586	4.54034
1	1.91979	0.07454	3.25442
1	1.86875	-1.04681	4.63014
1	0.83513	-2.08966	2.60141
1	-1.18853	0.04301	2.69339
1	-2.3046	-2.58434	2.78975
1	-2.25272	-3.58554	4.24561
1	-1.09312	-3.86713	2.93926
15	-0.5009	-0.46447	0.56645
15	2.92752	2.70066	1.36481
6	3.9236	3.76419	0.14347
1	3.94737	2.54678	2.34973
1	2.2869	3.76377	2.06496
6	4.95779	2.8432	-0.53238
6	4.63842	4.93129	0.84433
6	2.93951	4.30519	-0.91211
1	5.20612	5.52353	0.11266
1	5.34412	4.57495	1.60349
1	3.92569	5.60363	1.3353
1	3.47969	4.91053	-1.65199
1	2.17022	4.94258	-0.46025
1	2.43737	3.49314	-1.44892
1	5.53473	3.40835	-1.27637
1	4.476	2.00729	-1.05151
1	5.66892	2.43117	0.19381

cis-{W(CO)$_5$}$_2$P=PH^{t}Bu **(II)**

W	-2.1359841899	-0.7322254434	0.0052852367
C	-1.1963165583	-2.1148657875	1.2154226148
C	-3.0815920944	0.6009782162	-1.2515927759
C	-2.77611375	0.3197919662	1.6702645881
C	-3.8572124891	-1.8501164998	0.0796208527
C	-1.5760582007	-1.8358392067	-1.6636086251
O	-1.2847944866	-2.4477307845	-2.5933547304
O	-4.8257745196	-2.4760245006	0.1209236842
O	-3.1481076386	0.8961251274	2.5971068714
O	-3.63410913	1.3117320811	-1.9727602145
O	-0.685996326	-2.9074568436	1.8791347574
P	0.0148322009	0.4973419201	-0.1747390669
W	2.3626248141	-0.3033828074	0.0039304316
P	-0.1068346267	2.5164925323	-1.0209888799
C	4.2859813127	-1.0020928368	0.1911443322
C	2.9762947664	1.5424217839	0.677668062
C	1.760612386	-2.173487713	-0.6421103153
C	2.7758746501	0.2932388799	-1.9390926912
C	2.0033614292	-0.8927023809	1.9594150911
O	5.3666983879	-1.393551032	0.2923111684
O	3.3240580224	2.5756701617	1.0582454833
O	1.440624165	-3.2263524224	-0.9839733972
O	1.8199266276	-1.2088160678	3.0512110146
O	3.0181080444	0.6333534621	-3.0122925264
C	-0.9098243269	3.8163047303	0.145769814
C	-2.4425192076	3.7683498431	0.0531565356
C	-0.4087570781	5.1672599339	-0.4099682144
C	-0.4469601377	3.6485711402	1.6031704505
H	-0.7049546672	5.3168789163	-1.4541754609
H	0.6807421069	5.2606560409	-0.3422843138
H	-0.8481917263	5.9811304338	0.1812840645
H	-0.8069037384	2.7098968934	2.0369020224
H	-0.8470704314	4.470049882	2.2132844512
H	0.6447217342	3.6705824336	1.6874756999
H	-2.8524237291	2.8454810223	0.471128533
H	-2.7935107409	3.8628973975	-0.9792133714
H	-2.8631490678	4.6011087834	0.6314578884
H	1.2336810739	2.926346109	-0.8198749709

trans-{W(CO)$_5$}HP=P^{t}Bu{W(CO)$_5$} **(III)**

W	-1.473060677	2.3762892897	7.4760141552
C	-1.0165258264	0.6446294429	6.437401296
C	-1.9058342367	4.1264086987	8.4875649677
C	-3.3818501478	2.3430196201	6.6996633139
C	-0.8299135639	3.4570680015	5.8823371919
C	0.4463100888	2.4006130441	8.2489476985
O	1.5186452555	2.4152188204	8.6703950482
O	-0.4617578014	4.0699713365	4.9746360768
O	-4.4514083541	2.3237434977	6.2652952052
O	-2.1427655152	5.1090582865	9.0421718149
O	-0.7551258813	-0.3103974693	5.8483526905
P	-2.1153246582	0.9081130965	9.4120892963
W	-3.330103128	-1.6647055902	12.24766334
P	-3.5686282269	0.3556336491	10.7592118997
C	-3.1283936587	-3.3191145522	13.4122607424
C	-5.3016318056	-2.1682233905	11.9193448461
C	-1.3503891294	-1.1766144032	12.5876019355
C	-3.8770558923	-0.5764948204	13.9168634505
C	-2.7619306184	-2.7643605662	10.5928548044
O	-3.0144396779	-4.2601054489	14.0730100189
O	-6.4057714293	-2.457898629	11.7440187433
O	-0.2451299299	-0.9049407618	12.7709448172
O	-2.4373983226	-3.369718181	9.6671915665
O	-4.1755289136	0.0131673644	14.8622895843
H	-1.1856080955	-0.0868298351	9.7932578348
C	-5.1239657383	1.4471235983	10.5912994289
C	-4.7777206382	2.895673648	10.2092123099
C	-5.8408890379	1.4455111147	11.9563567709
C	-6.0391518227	0.8117141166	9.5202150985
H	-5.2210291002	1.8796426976	12.7475685245
H	-6.1423489093	0.4415757551	12.2665274775
H	-6.7508669638	2.0526049364	11.8734734973
H	-5.5768730729	0.8243259068	8.5284614013
H	-6.9726487353	1.3868189744	9.4623035568
H	-6.3032376617	-0.2219876557	9.7664456371
H	-4.336694248	2.9648871945	9.2130142973
H	-4.0906743157	3.3575777265	10.9256567153
H	-5.7004706474	3.4894166555	10.198669307

{W(CO)$_5$}PH^{t}Bu-PH-PH^{t}Bu{W(CO)$_5$}

74	-3.48964	0.29526	-0.33859
6	-4.792	-0.91983	0.69752
6	-2.27344	1.56647	-1.40281
6	-3.40118	1.55321	1.2846
6	-5.09177	1.30459	-1.05717
6	-3.56129	-0.97881	-1.96256
8	-3.60428	-1.6888	-2.87144
8	-6.00551	1.88018	-1.47245
8	-3.34444	2.2673	2.19301
8	-1.61907	2.30381	-2.0094
8	-5.55435	-1.57805	1.26451
74	3.46142	-0.31581	-0.34759
6	5.03264	-1.40376	-1.02196
6	4.79387	0.84824	0.70765
6	2.22122	-1.54522	-1.43258
6	3.62062	0.94246	-1.97433
6	3.3061	-1.54888	1.2958
8	5.92745	-2.02485	-1.41195
8	5.57147	1.47621	1.28851
8	1.55419	-2.25946	-2.05313
8	3.24265	-2.24697	2.21422
8	3.71232	1.64767	-2.884
15	0.06667	-0.0051	1.8568
15	-1.40286	-1.00905	0.4476
1	-0.51518	-1.27712	-0.61974
1	-0.79944	1.0798	2.14627
15	1.42346	1.07158	0.39943
1	0.54148	1.3657	-0.66708
6	1.60063	2.8428	1.10261
6	2.19391	2.78056	2.52143
6	0.2445	3.57278	1.1121
6	2.5574	3.59928	0.15756
1	-0.4854	3.11454	1.78523
1	-0.19587	3.62281	0.11078
1	0.39878	4.60236	1.45902
1	3.16278	2.27254	2.53997
1	1.52651	2.27135	3.22624
1	2.34801	3.80041	2.89508
1	3.56132	3.16876	0.1534
1	2.64225	4.63898	0.49797
1	2.18563	3.61975	-0.87321
6	-1.51915	-2.77619	1.15902
6	-2.17269	-2.72222	2.55157
6	-0.1211	-3.41297	1.25235
6	-2.38786	-3.60132	0.18851
1	-2.4438	-4.63502	0.55225
1	-1.96111	-3.63003	-0.82063
1	-3.40976	-3.21944	0.11946
1	-0.21928	-4.43794	1.63237
1	0.53865	-2.87435	1.93888
1	0.36553	-3.4687	0.27269
1	-2.2657	-3.74087	2.94791
1	-3.17639	-2.28783	2.52132
1	-1.56631	-2.14941	3.26299

{W(CO)$_5$}PH^{t}Bu-PH-PH^{t}Bu{W(CO)$_5$} conformer 2

W	-3.7142567984	-0.6247042954	0.1653551554
C	-4.9723511552	0.0716951818	-1.3085843032
C	-2.5069037336	-1.3726962546	1.6541271847
C	-2.8233752682	-1.8694220361	-1.2240858047
C	-5.0819761005	-2.0588543786	0.5912132612
C	-4.6056121374	0.6419444264	1.5215563027
O	-5.0981209385	1.3616662265	2.2793504186
O	-5.8622420542	-2.8750087437	0.8420901487
O	-2.3494171973	-2.5761684638	-2.0034728609
O	-1.8312474306	-1.7948982718	2.4924746742
O	-5.7031721256	0.4386656995	-2.1258031283
W	3.8185602215	-0.4405710096	-0.2778205515
C	5.3898838938	-1.5599505599	-0.895610354
C	4.0605622965	-1.1563050958	1.6345014007
C	3.547123566	0.2527980699	-2.2029555344
C	5.1208995276	1.1072243883	0.1043266864
C	2.5778598581	-2.0463435416	-0.6678669187
O	6.2941591118	-2.1882456947	-1.2505358056
O	4.2034241476	-1.5703344389	2.705049353
O	3.3929297705	0.642112656	-3.2786952223
O	1.9267681488	-2.9741464222	-0.8863130649
O	5.8613492082	1.9689794218	0.3157694314
P	0.0826975965	0.3380769715	-0.6491785418
P	-1.9558468056	1.2097812091	-0.213091296
H	-1.7752435616	2.0244622903	0.9292305326
H	-0.0668857283	-0.7704771066	0.2156754582
P	1.8988541361	1.1390201519	0.4046141335
H	1.9917598498	2.3865137246	-0.2579985867
C	1.6506225579	1.7622456445	2.1935831398
C	1.0156459833	0.6515838049	3.0465617283
C	0.7831854256	3.0327875421	2.2108892294
C	3.0487873441	2.1168197165	2.7420132203
H	-0.2245451352	2.853605787	1.8297042775
H	1.2344640617	3.8393608567	1.621774494
H	0.6851524224	3.3909654374	3.2434665683
H	1.6255353156	-0.2574583168	3.0544038918
H	0.0117494559	0.3848476697	2.7012562053
H	0.9272322633	0.9962733016	4.0842635284
H	3.6964513334	1.2410154949	2.8194204453
H	2.9358331472	2.5381168314	3.7491760755
H	3.5570487617	2.8672531916	2.1258737255
C	-2.1422954132	2.5819830151	-1.5179459885
C	-2.2660243029	1.9505900495	-2.9163437294
C	-0.9330394019	3.5344433233	-1.4782847208
C	-3.4224947518	3.3679718895	-1.1682573261
H	-3.5538747254	4.1812179548	-1.8930827184
H	-3.3652239361	3.8204173237	-0.171161302
H	-4.3171684536	2.7407989893	-1.210242717
H	-1.0898804926	4.3510713353	-2.1942825843
H	-0.0033512493	3.0297874156	-1.7639331318
H	-0.795473829	3.9842581073	-0.4886657841
H	-2.3920429665	2.7458364646	-3.6615801391
H	-3.1322970069	1.2876638772	-2.9901457136
H	-1.3717009992	1.3796000902	-3.1882140426

{W(CO)$_5$}PH^{t}Bu-PH-PH^{t}Bu{W(CO)$_5$} conformer 3

W	2.9843004473	-0.8981387073	0.229224674
C	1.480148933	-1.2893793298	1.5786908563
C	4.5520569355	-0.6484015026	-1.0807630987
C	1.8523567641	-1.6117254394	-1.3477272228
C	3.6863363889	-2.7656704031	0.5926079974
C	4.1336284885	-0.1373866074	1.7560647939
O	4.7799817144	0.3019892689	2.6078612155
O	4.0875326524	-3.828953049	0.8069797748
O	1.2504205744	-2.0152792455	-2.2447759277
O	5.4484168478	-0.5511483729	-1.8051213642
O	0.665074204	-1.5439800869	2.3588459217
W	-3.2718691563	-0.5665839993	-0.2237816776
C	-4.6174280632	-1.9916790076	-0.7374336282
C	-4.7976607013	0.8083393493	-0.2273643797
C	-1.8047710136	-2.019766936	-0.2186877686
C	-3.6228839744	-0.9535314604	1.7685970726
C	-2.9276512189	-0.1731737724	-2.2225874632
O	-5.3845855572	-2.8080904362	-1.0265443091
O	-5.6808911822	1.5565000852	-0.2302282607
O	-1.0136908993	-2.860210693	-0.206831021
O	-2.7614765592	0.0400389991	-3.3445404705
O	-3.826986202	-1.1698901192	2.8849504464
P	0.0472632376	1.5256738064	-1.1485265892
P	2.06642077	1.4753970722	-0.1191862514
C	3.0949425839	2.8305246701	-0.9970545787
H	-0.1447433032	2.9360931106	-1.1566660249
P	-1.4841887324	1.1331418548	0.4924953535
H	-0.6297896249	0.6227575726	1.4970279211
C	-1.9386989085	2.7878513775	1.3393557968
C	-2.6752569032	3.7090864879	0.3508989786
C	-0.6919500238	3.4958965069	1.8944185884
C	-2.875154684	2.4219964527	2.5105946132
H	-0.0018468208	3.802212505	1.1025133308
H	-0.147321793	2.8649644831	2.6059269521
H	-0.9996893698	4.4048462541	2.4268703665
H	-3.5833570186	3.2478104897	-0.0461666467
H	-2.0409027287	4.0028306512	-0.492900156
H	-2.9724288048	4.6290363155	0.8696544073
H	-3.8056120211	1.9647647466	2.1646166431
H	-3.1362261273	3.3373149841	3.0567404136
H	-2.3990187073	1.736879417	3.2213134174
H	1.8190391714	2.1656007567	1.0925842024
C	4.48015755	2.8461846153	-0.3171597633
C	2.4523257708	4.2194026454	-0.8275095907
C	3.2360756259	2.4877316309	-2.4911043404
H	3.1099955255	4.9755874283	-1.2743068336
H	2.3203900321	4.480594795	0.2286497888
H	1.4832681641	4.3004322421	-1.3285559736
H	3.6943142936	1.5069979849	-2.6462624369
H	3.8778946827	3.2338358481	-2.9760219463
H	2.2698458513	2.4980869881	-3.0085961908
H	5.0198758301	1.9064997172	-0.4523109064
H	4.407749453	3.0491695579	0.7577471569
H	5.0864126131	3.6443669728	-0.7641661342

4.5 References

[1] M. T. Nguyen, A. van Keer, L. G. Vanquickenborne, *J. Org. Chem.* **1996**, *61*, 7077.

[2] K. Lammertsma in *Topics in Current Chemistry*, *Vol. 229* (Eds.: J.-P. Majoral, T. Chivers), Springer, Berlin, **2003**, pp. 95–119.

[3] L. Liu, D. A. Ruiz, D. Munz, G. Bertrand, *Chem* **2016**, *1*, 147.

[4] a) W. J. Transue, A. Velian, M. Nava, C. García-Iriepa, M. Temprado, C. C. Cummins, *J. Am. Chem. Soc.* **2017**, 10822; b) T. W. Graham, R. P.-Y. Cariou, J. Sánchez-Nieves, A. E. Allen, K. A. Udachin, R. Regragui, A. J. Carty, *Organometallics* **2005**, *24*, 2023.

[5] a) B. T. Sterenberg, A. J. Carty, *J. Organomet. Chem.* **2001**, *617-618*, 696; b) B. T. Sterenberg, K. A. Udachin, A. J. Carty, *Organometallics* **2001**, *20*, 2657; c) B. T. Sterenberg, K. A. Udachin, A. J. Carty, *Organometallics* **2003**, *22*, 3927; d) J. Sánchez-Nieves, B. T. Sterenberg, K. A. Udachin, A. J. Carty, *J. Am. Chem. Soc.* **2003**, *125*, 2404.

[6] K. M. Flynn, B. D. Murray, M. M. Olmstead, P. P. Power, *J. Am. Chem. Soc.* **1983**, *105*, 7460.

[7] A. Strube, G. Huttner, L. Zsolnai, W. Imhof, *J. Organomet. Chem.* **1990**, *399*, 281.

[8] a) J. Borm, G. Huttner, L. Zsolnai, K. Evertz, H. Berke, *J. Organomet. Chem.* **1987**, *327*, 223; b) A. M. Arif, A. H. Cowley, N. C. Norman, A. G. Orpen, M. Pakulski, *Organometallics* **1988**, *7*, 309; c) J. Sánchez-Nieves, B. T. Sterenberg, K. A. Udachin, A. J. Carty, *J. Clust. Sci.* **2004**, *15*, 151; d) J. Sánchez-Nieves, B. T. Sterenberg, K. A. Udachin, A. J. Carty, *Inorg. Chim. Acta* **2003**, *350*, 486; e) T. W. Graham, K. A. Udachin, A. J. Carty, *Chem. Comm.* **2005**, 4441; f) M. Seidl, R. Weinzierl, A. Y. Timoshkin, M. Scheer, *Chem. Eur. J* **2016**, *22*, 5484.

[9] T. W. Graham, K. A. Udachin, A. J. Carty, *Inorg. Chim. Acta* **2007**, *360*, 1376.

[10] T. W. Graham, K. A. Udachin, A. J. Carty, *Chem. Comm.* **2005**, 4441.

[11] T. W. Graham, K. A. Udachin, A. J. Carty, *Chem. Comm.* **2006**, 2699.

[12] G. Huttner, *J. Organomet. Chem.* **1986**, *308*, C11-C13.

[13] P. Pyykkö, *J. Phys. Chem. A* **2015**, *119*, 2326.

[14] M. Scheer, C. Kuntz, M. Stubenhofer, M. Zabel, A. Y. Timoshkin, *Angew. Chem. Int. Ed. Engl.* **2010**, *49*, 188.

[15] C. Kuntz, *PhD thesis*, University of Regensburg, Regensburg, **2008**.

[16] D. D. M. Baudler, *Z. Naturforsch.* **1987**, 330.

[17] M. Seidl, C. Kuntz, M. Bodensteiner, A. Y. Timoshkin, M. Scheer, *Angew. Chem. Int. Ed.* **2015**, *54*, 2771.

[18] C. N. Rowley, G. A. DiLabio, S. T. Barry, *Inorg. Chem.* **2005**, *44*, 1983.

[19] M. Seidl, *PhD thesis*, University of Regensburg, Regensburg, **2014**.

[20] *TopSpin 3.0*, TopSpin 3.0, Bruker BioSpin GmbH, **2010**.

[21] P. Jutzi, R. Kroos, *J. Organomet. Chem.* **1990**, *390*, 317.

[22] R. B. King, N. D. Sadanani, *Syn. React. Inorg. Met.* **1985**, *15*, 149.

[23] R. Jefferson, J. F. Nixon, T. M. Painter, R. Keat, L. Stobbs, *J. Chem. Soc., Dalton Trans.* **1973**, *4*, 151.

[24] D. V. Shenai-Khatkhate, A. Amamchyan, M. B. Power, R. L. Dicarlo, J. E. Felton, US 2005/0033073 A1.

[25] O. V. Dolomanov, L. J. Bourhis, R. J. Gildea, J. A. K. Howard, H. Puschmann, *Appl. Crystallogr.* **2009**, *42*, 339.

[26] *CrysAlis Pro 171.38.46*, CrysAlis Pro Version 171.38.46, Rigaku Oxford Diffraction.

[27] G. M. Sheldrick, *Acta Crystallogr. A* **2015**, *71*, 3.

[28] G. M. Sheldrick, *Acta Crystallogr. C* **2015**, *71*, 3.

[29] a) F. Furche, R. Ahlrichs, C. Hättig, W. Klopper, M. Sierka, F. Weigend, *WIREs Comput. Mol. Sc.i* **2014**, *4*, 91; b) R. Ahlrichs, M. Bär, M. Häser, H. Horn, C. Kölmel, *Chem. Phys. Lett.* **1989**, *162*, 165; c) O. Treutler, R. Ahlrichs, *J. Chem. Phys.* **1995**, *102*, 346; d) University of Karlsruhe and Forschungszentrum Karlsruhe GmbH, *TURBOMOLE V6.4*.

[30] K. Eichkorn, O. Treutler, H. Öhm, M. Häser, R. Ahlrichs, *Chem. Phys. Lett.* **1995**, *242*, 652.

[31] K. Eichkorn, F. Weigend, O. Treutler, R. Ahlrichs, *Theor. Chim. Acta* **1997**, *97*, 119.

[32] a) A. D. Becke, *Phys. Rev. A* **1988**, *38*, 3098; b) J. P. Perdew, *Phys. Rev. B* **1986**, *33*, 8822; c) J. P. Perdew, *Phys. Rev. B* **1986**, *34*, 7406.

[33] F. Weigend, *Phys. Chem. Chem. Phys.* **2006**, *8*, 1057.

[34] a) F. Weigend, R. Ahlrichs, *Phys. Chem. Chem. Phys.* **2005**, *7*, 3297; b) A. Schäfer, C. Huber, R. Ahlrichs, *J. Chem. Phys.* **1994**, *100*, 5829.

[35] M. Sierka, A. Hogekamp, R. Ahlrichs, *J. Chem. Phys.* **2003**, *118*, 9136.

[36] a) A. D. Becke, *J. Chem. Phys.* **1993**, 98, 5648; b) Lee, Yang, Parr, *Phys. Rev. B* **1988**, 37, 785.

[37] P. J. Hay, W. R. Wadt, *J. Chem. Phys.* **1985**, 82, 299-310.

[38] M. J. Frisch, G. W. Trucks, H. B. Schlegel, G. E. Scuseria, M. A. Robb, J. R. Cheeseman, J. A. Montgomery, Jr., T. Vreven, K. N. Kudin, J. C. Burant, J. M. Millam, S. S. Iyengar, J. Tomasi, V. Barone, B. Mennucci, M. Cossi, G. Scalmani, N. Rega, G. A. Petersson, H. Nakatsuji, M. Hada, M. Ehara, K. Toyota, R. Fukuda, J. Hasegawa, M. Ishida, T. Nakajima, Y. Honda, O. Kitao, H. Nakai, M. Klene, X. Li, J. E. Knox, H. P. Hratchian, J. B. Cross, V. Bakken, C. Adamo, J. Jaramillo, R. Gomperts, R. E. Stratmann, O. Yazyev, A. J. Austin, R. Cammi, C. Pomelli, J. W. Ochterski, P. Y. Ayala, K. Morokuma, G. A. Voth, P. Salvador, J. J. Dannenberg, V. G. Zakrzewski, S. Dapprich, A. D. Daniels, M. C. Strain, O. Farkas, D. K. Malick, A. D. Rabuck, K. Raghavachari, J. B. Foresman, J. V. Ortiz, Q. Cui, A. G. Baboul, S. Clifford, J. Cioslowski, B. B. Stefanov, G. Liu, A. Liashenko, P. Piskorz, I. Komaromi, R. L. Martin, D. J. Fox, T. Keith, M. A. Al-Laham, C. Y. Peng, A. Nanayakkara, M. Challacombe, P. M. W. Gill, B. Johnson, W. Chen, M. W. Wong, C. Gonzalez, and J. A. Pople, Gaussian 03, Revision D.01, Gaussian, Inc., Wallingford CT, 2004.

5 REACTIVITY OF THE BRIDGING STIBINIDENE COMPLEX [ClSb{Cr(CO)$_5$}$_2$(thf)]

Lena Rummel, Michael Seidl, Alexey Y. Timoshkin and Manfred Scheer

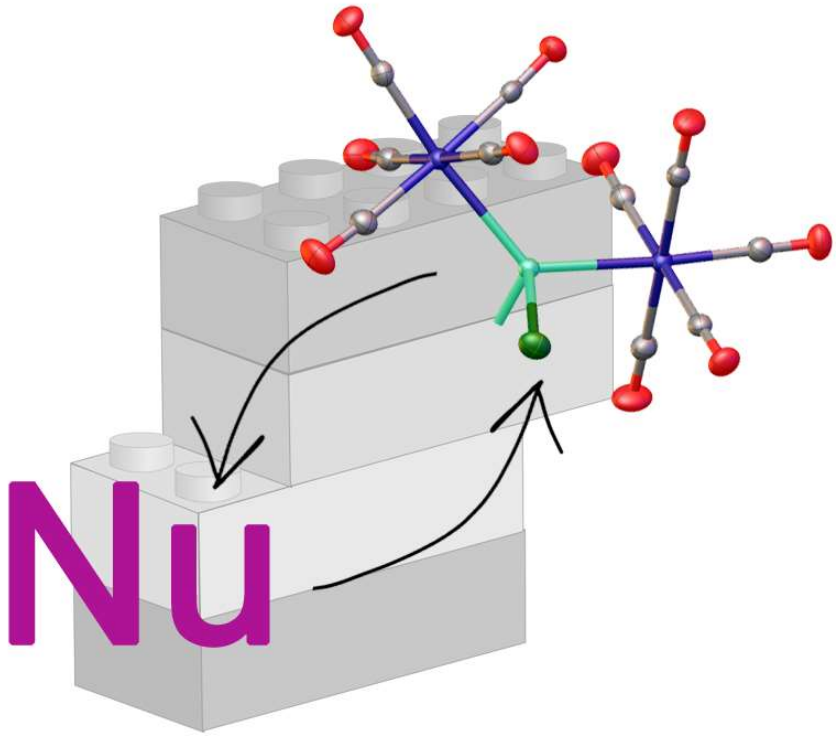

- ⇨ Synthesis and characterization of compounds **2**, **3**, **6**, **7**, **8a** and **8b** was carried out by Lena Rummel
- ⇨ Synthesis of compounds **4** and **5** was carried out by Michael Seidl, characterization of compounds **4** and **5** were done by Lena Rummel
- ⇨ X-ray measurements, structure solution and refinement were done by Lena Rummel, except **4** and **5**: Michael Seidl
- ⇨ X-ray measurements were finalized by Michael Seidl
- ⇨ DFT calculations were performed by Alexey Y. Timoshkin
- ⇨ Figures and manuscript were prepared by Lena Rummel except DFT calculation part: Alexey Y. Timoshkin

5.1 Introduction

Stibinidene complexes are rare and highly sensitive low-valent main group compounds, which have not been studied extensively for their reaction behavior so far. In the reaction with $GaCl_3$ the stibinidene complex $[ClSb\{Cr(CO)_5\}_2(thf)]$ (**1**) shows a dimerization to $[ClSb\{Cr(CO)_5\}_2]_2$ (**2**) and yields the anionic double-chlorinated compound $[Cl_2Sb\{Cr(CO)_5\}_2]^-$ (**3**) in the reaction with different ionic nucleophiles. When using neutral nucleophiles (such as amines, isocyanides and phosphines) as reaction partners, tetrahedral complexes of the type $[ClSb\{Cr(CO)_5\}_2Nu]$ (**4**: Nu = NH_2Mes; **5**: Nu = CN(dmp); **6**: Nu = PPh_3; **7**: Nu = PPh_2H) are formed, which can be used in subsequent reactions. All of these products are among the first of their type to be synthesized and isolated.

Since the first synthesis of a stable carbene in 1988 in the group of Bertrand[1] and the subsequent synthesis of the first N-heterocyclic carbene (NHC) by *Arduengo et. al.* a few years later,[2] low valent main group compounds have been the target of a major research interest. Although in the field of low valent pnictogen compounds, the first stable nitrene (R-N) was synthesized only in 2012.[3] Its heavier homologues, the phosphinidenes (R-P), are considered to be very reactive and are often stabilized, e.g. by transition metal fragments in order to be able to use them for synthetic purposes. Their coordination modes range from η^1 to μ_4.[4] Phosphinidene complexes also exhibit various interesting properties, such as a small HOMO-LUMO gap and unusually high downfield shifts in the ^{31}P NMR, and reaction behaviors.[5,6] Going further down the periodic table, arsinidene complexes are already more uncommon and their reaction behavior as well as applications are not as well-studied as its lighter homologues. Stibinidene and bismuthinidene complexes, on the other hand, are scarce and their properties only scarcely studied. Just recently though, the group of Cornella successfully activated N_2O under very mild conditions by using a bismuthinidene complex as a catalyst,[7] emphasizing the potential of pnictinidene complexes in the catalytic activation of small molecules. The first trigonal planar stibinidene complex, $PhSb[Mn(CO)_2Cp]_2$, has been synthesized by Huttner *et al.* in 1978 from a diiodostibane. Back then, the authors already proposed the presence of Sb-Mn π bonding in this complex due to its unusual bond lengths and angles as well as the trigonal planar environment of the Sb atom.[8] A few years later, in 1984, they reported the first synthesis of the chlorosubstituted stibinidene complex $[ClSb\{Cr(CO)_5\}_2]$, which has a 3 center 4 π electron bond across both Sb-Cr bonds analogously to related phosphinidene and arsinidene complexes with similar spectroscopical data. In thf solution, the chlorostibinidene complex forms the adduct $[ClSb\{Cr(CO)_5\}_2(thf)]$ (**1**), which can be crystallized and isolated.[9,10] The trigonal planar stibinidene complexes $[ClSb\{M(CO)_5\}_2]$ (**A**; M = Cr, Mo, W; cf. Scheme 5.1) are typically synthesized via a salt elimination reaction between $Na_2[M_2(CO)_{10}]$ and $SbCl_3$. Since the stibinidene complex **A** is quite unstable and not easy to isolate (in the case of M = Mo, W), it can be trapped using Lewis bases **B** to form stable adducts with the general formula $[ClSb\{M(CO)_5\}_2B]$ (**B**).[10]

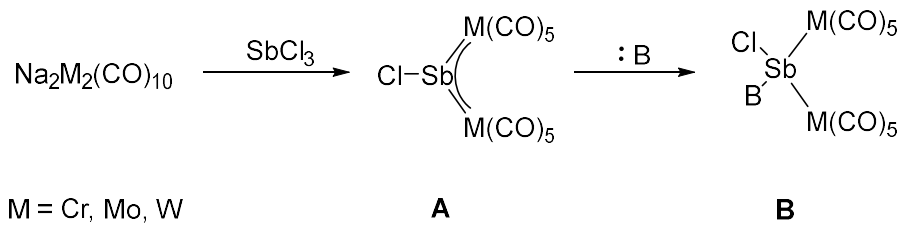

***Scheme 5.1**: Synthesis of chlorostibinidene complexes **A** and subsequent addition of a base.*

Huttner and co-workers could also observe the occurrence of distibene complexes of the type $[RSb{=}SbR][W(CO)_5]_3$ as side products during the synthesis of stibinidene complexes, especially when using non-donor solvents and Lewis-acidic complex fragments in the reaction. The group also proposed a valence tautomerism for trigonal planar stibinidene complexes (cf. Scheme 5.2). In the type **A** complex, the empty *p* orbital of the Sb atom is saturated by backbonding of the filled metal *d* orbitals, making these compounds stable under inert gas at standard conditions and thus revealing a Lewis acidic behavior. Adding a base to stibinidene complexes typically results in the formation of adducts, even in cases where **A** is not isolable (M = Mo, W). Most importantly, the geometry at the Sb atom changes from trigonally planar in the starting material to tetrahedral in its adducts. The Huttner group further undermines their claim with the synthesis and characterization of a type **C** adduct, $[(^t Bu)Sb\{W(CO)_5\}_3]$, in the reaction of $Na_2[W_2(CO)_{10}]$ with $^t BuSbCl_2$.

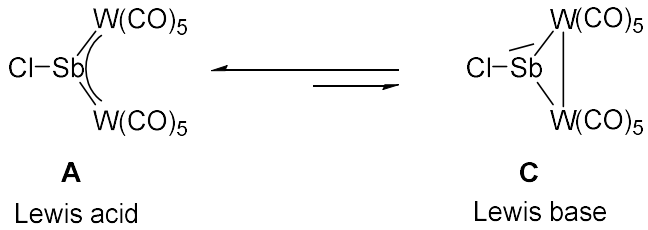

***Scheme 5.2**: Valence tautomerism in trigonal planar stibinidene complexes.*

These adducts are characterized by the formation of a W-W bond, resulting in the gain of two electrons as a lone pair at the Sb atom. Thus, the resulting type **C** stibinidene complexes are Lewis bases in contrast to type **A** complexes.[11] To date, the overall research for stibinidene complexes has been focused on their synthesis and their properties, as it has recently been published for $[Sb\{Cr(CO)_5\}_3]^-$.[12]

In this work, $[ClSb\{Cr(CO)_5\}_2(thf)]$ (**1**)was used as a starting material in the reactions with various nucleophiles. Diverse products have been isolated and characterized.

5.2 Results and Discussion

Compound [ClSb{Cr(CO)$_5$}$_2$(thf)] (**1**) offers a variety of interesting properties, including thermochromism as well as solvatochromism, as was already mentioned for these types of compounds.[9] In n-pentane, the compound is orange at low temperatures (-90 °C to -30 °C) and barely soluble, while at room temperature, **1** dissolves to give a turquoise solution. This phenomenon has previously been described as the result of the reversible formation of adducts of stibinidene complexes in solution. While the trigonal planar complexes of the type [ClSb{M(CO)$_5$}$_2$] are known to give intensively green colored solutions, their adducts on the other hand are known to form less intensively colored products, mostly between a yellow and orange color.[9] We also found that in ether or dme, at room temperature **1** exhibits a red color and in toluene, **1** forms an orange suspension at -90 °C and a green solution at room temperature, respectively. All these color changes are reversible upon cooling down or warming the respective solutions.

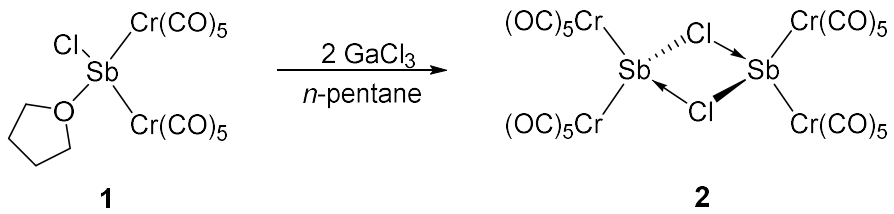

***Scheme 5.3**: Reaction of **1** with 2 eq. GaCl$_3$.*

As reported for [ClSb{Mn(CO)$_2$Cp*}$_2$], its reaction with GaCl$_3$ leads to the formation of the linear heterocumulene cation [Cp*(CO)$_2$Mn=Sb=Mn(CO)$_2$Cp*]$^+$ (Cp* = C$_5$Me$_5$).[13] We wanted to see if that would be true for **1**, too. Thus, we conducted the reaction accordingly, with 2 equivalents of GaCl$_3$ in *n*-pentane (cf. Scheme 5.3). The formation of a heterocumulene was not observed, but instead the dimer [ClSb{Cr(CO)$_5$}$_2$]$_2$ (**2**) could be crystallized from the reaction solution. Apparently, GaCl$_3$ is not strong enough to abstract Cl$^-$ from **1**. Instead, in a non-polar solvent like pentane, the starting material is partly dissociated into thf and [ClSb{Cr(CO)$_5$}$_2$], which one of the lone pairs of a Cl atom of **1** can add itself to, resulting in the dimer **2**. Notably, this is the first time that crystals of this type of stibinidene could be obtained without thf as an additional Lewis base. The molecular structure of **2** is shown in Figure 1. The two Sb{Cr(CO)$_5$} fragments are connected through two bridging Cl atoms, forming a Sb$_2$Cl$_2$ four membered ring. The Sb-Cl distances are 2.5093(9) Å and 2.8997(10) Å, respectively, and are both significantly longer than the sum of the single-bond covalent radii of 2.39 Å for Sb and Cl according to *Pyykkö and Atsumi*, revealing the dative nature of the Sb-Cl bonds ($\chi_{Cl\text{-}Sb}$= 1.11).[14] The Sb-Cr distances in **2** are also worth mentioning, since they are shorter compared to **1**, indicating a partial double bond character because of the backbonding from a Cr d orbital into the p orbital at the Sb atom. The Sb atoms possess a distorted tetrahedral geometry, with a Cr1-Sb1-Cr2 angle of 137.28(2) ° and a Cl1-Sb1-Cl1^9 angle of 76.39(3) °. This can be explained with the steric bulk of the Cr(CO)$_5$ groups, which are arranged

in the biggest possible distance. A similar Bi compound, $[(Cp(CO)_2Mn)_2BiCl]_2$, is known, obtained in the reaction of $Cp(CO)_2Mn(thf)$ with $BiCl_3$, with $Cp(CO)_2Mn$ as a metal fragment. The authors point out its asymmetric Bi-Cl distances, which are explained by the halogen's tendency to form adducts.[15]

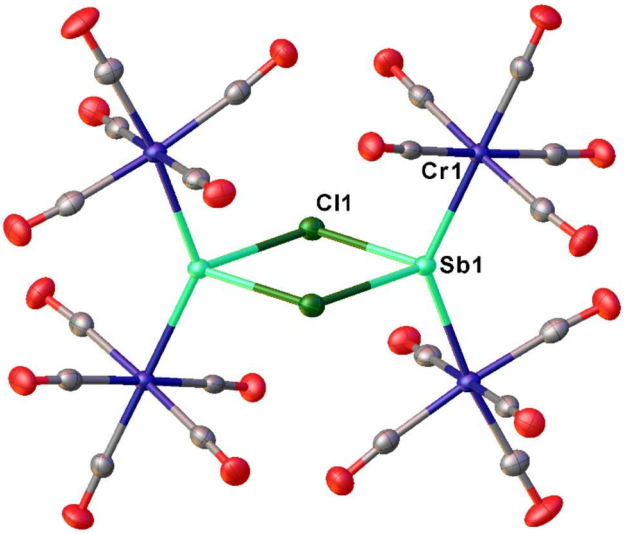

***Figure 5.1**: Molecular structure of **2**. Anisotropic displacement parameters are set to 50% probability level. Selected bond lengths [Å] and angles [°]: Sb1-Cr1 2.5126(6), Sb1-Cr2 2.5167(6), Sb1-Cl1 2.5091(9), Sb1-Cl19 2.8999(9); Cr1-Sb1-Cr2 137.28(2), Cr1-Sb1-Cl1[9] 104.78(2), Cr2-Sb1-Cl1[9] 105.62(2), Cl1-Sb1-Cr1 107.20(3), Cl1-Sb1-Cr2 108.60(3), Cl1-Sb1-Cl1[9] 76.39(3), Sb1-Cl-Sb1[9] 103.61(3).*

Optimized at the B3LYP/def2-TZVP level of theory (see SI for details), the gas phase structure of **2** is different from the one observed in the solid state. Optimized Sb-Cl distances are almost equal (2.692-2.696 Å) while in the experimental structure they are markedly different: 2.5093(9) and 2.8997(10) Å. This leads to very different Wiberg bond index (WBI) values for the optimized (0.401 and 0.397) and experimental (0.536 and 0.251) Sb-Cl bonds. The bonding in **2** can be described using the donor-acceptor bonding model, similar to the one used for the description of a CAAC stabilized Sb^+ atom,[16] with the difference that in **2** the stabilization results from the interaction of two Lewis acids $Cr(CO)_5$ and a Lewis base. The interaction of the LUMO of a $ClSb\{Cr(CO)_5\}_2$ monomer (cf. Figure 5.2a) with lone pairs of the Cl atom of the second molecule results in **2** (respective MOs are given in Figure 5.2b,c). The LUMO of $ClSb\{Cr(CO)_5\}_2$ can also interact with Lewis bases, forming **1** and **4-7** (vide infra).

DFT computationals show that reaction (1) is exothermic by 18 kJ·mol^{-1}, validating the experimental observations.

$$\mathbf{1} + \tfrac{1}{2}\, Ga_2Cl_6 = \tfrac{1}{2} \cdot \mathbf{2} + GaCl_3{\bullet}THF \qquad (1)$$

[9] 1-x, 1-y, 1-z

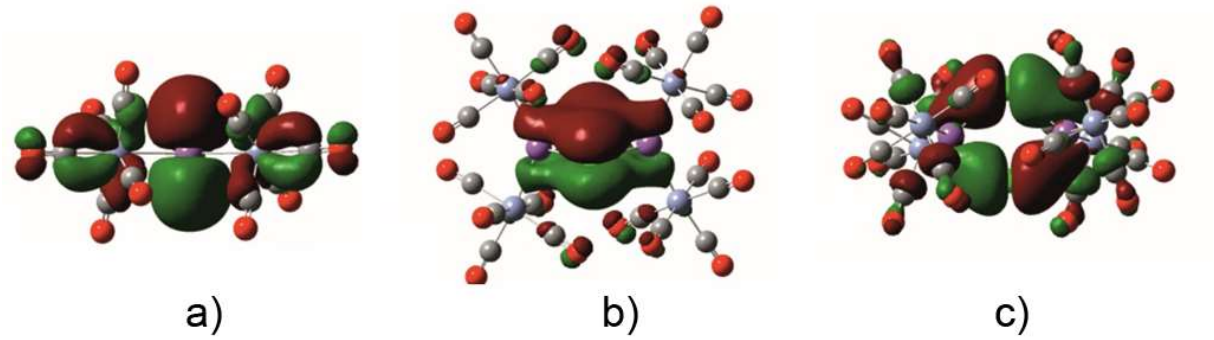

***Figure 5.2**: a) LUMO of ClSb{Cr(CO)$_5$}$_2$ (side view); b) HOMO-16 (perspective view) and c) HOMO-19 (top view) of **2** (both compounds at gas phase optimized geometries).*

However, dissociation of **2** into two ClSb{Cr(CO)$_5$}$_2$ monomers in the gas phase is predicted to be endothermic by only 2 kJ mol^{-1} and the entropy factor favors dissociation both in the gas phase and in solution. Since **2** is experimentally observed in the solid state, additional stabilization due to intermolecular interactions is expected, for example there are Sb…OC contacts of 3.448 Å and 3.872 Å, respectively. Next, **1** was reacted with different ionic nucleophiles to test its reactivity. Huttner investigated the adduct formation of pnictinidene complexes mostly on the basis of [ClE{M(CO)$_5$}$_2$] (E = As, Sb) with only a few examples for the stibinidene and only a few products with non-ionic nucleophiles could be isolated: [ClSb{M(CO)$_5$}$_2$B] (B = PPh$_3$, SC(NHNCH$_3$)$_2$).[6,10,17] The reactivity of the trigonal planar pnictinidene complexes [Cp*E{W(CO)$_5$}$_2$] (E = P,As) towards ionic nucleophiles has been investigated in our group and shows that adducts of the type [Cp*E{W(CO)$_5$}$_2$Nu]$^-$ (Nu = CN, ^{n}Bu, N$_3$, NH$_2$, OH, F, Cl, Br, I) are generated as was initially proposed by Huttner.[18] Surprisingly, in the case of the reactions of **1** with Nu$^-$ (Nu = NH$_2$, AsH$_2$, PH$_2$, CN) no formation of adducts of the type [ClSb{Cr(CO)$_5$}$_2$Nu]$^-$ could be observed. Instead, in all cases, the anionic chloride adduct [Cl$_2$Sb{Cr(CO)$_5$}$_2$]$^-$ (**3**) was the only product that could be isolated. Initial thoughts that the chlorination of **1** happens because of the use of CH$_2$Cl$_2$ as solvent could not be confirmed since even after exclusion of CH$_2$Cl$_2$ and using Et$_2$O or thf instead, the only product that could be isolated in all these reactions was the anionic complex [Cl$_2$Sb{Cr(CO)$_5$}$_2$]$^-$ (**3**). Using NH$_2^-$ as a nucleophile, **3** could be isolated in 30 % yield. An explanation for the formation of **3** might be the additional formation of neutral stibinidene complexes of the type [NuSb{Cr(CO)$_5$}$_2$] alongside, as was described in the similar reaction of [ClSb{Cp'Mn(CO)$_2$}$_2$] with 2,2'-bipyridine.[19] However, we could never isolate such complexes. In the crude ^{31}P{^{1}H} NMR spectrum of the reaction of **1** with LiPH$_2$·dme, a signal at -172 ppm could be found, which could be hinting at the formation of the stibinidene complex [(PH$_2$)Sb{Cr(CO)$_5$}$_2$]. A similar chemical shift of -244.3 ppm has been reported for tBu$_2$SbPH$_2$,[20] but unfortunately due to its instability in solution, no NMR data with better resolution could be recorded for [(PH$_2$)Sb{Cr(CO)$_5$}$_2$].

However, due to the crystallization of the more stable **3**, no such compound could be isolated. The ^{1}H and $^{13}C\{^{1}H\}$ NMR spectra of **3** with different counteranions show the typical chemical shifts for the crown ether used in the respective reaction (cf. chapter 5.4). In the IR spectrum typical CO-resonances could be detected.

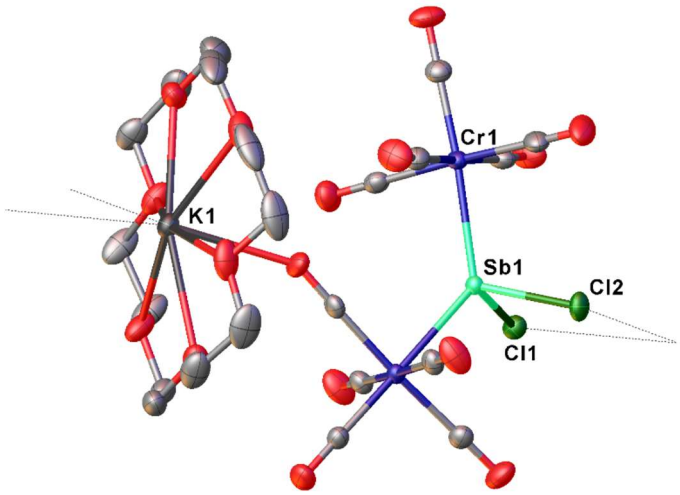

***Figure 5.3**: Molecular structure of [Na@(18-crown-6)·dioxane]$^{+}$[$Cl_2Sb\{Cr(CO)_5\}_2$]$^{-}$. Anisotropic displacement parameters are set to 50% probability level. H atoms are omitted for clarity. Selected bond lengths [Å] and angles [°]: Sb1-Cr2 2.5683(3), Sb1-Cr1 2.5807(3), Sb1-Cl1 2.4218(5), Sb1-Cl2 2.4129(5); Cr2-Sb1-Cr1 129.830(11), Cl1-Sb1-Cr2 104.959(15), Cl1-Sb1-Cr1 108.716(15), Cl2-Sb1-Cr2 106.161(16), Cl2-Sb1-Cr1 109.598(16), Cl2-Sb1-Cl1 90.434(18).*

The molecular structure of [Na@(18-crown-6)·dioxane]$^{+}$[$Cl_2Sb\{Cr(CO)_5\}_2$]$^{-}$ is shown in Figure 5.3. The Cr2-Sb1-Cr1 angle is 129.830(11) ° and the Cl2-Sb1-Cl1 angle is 90.434(18) °, revealing a distorted tetrahedral geometry at the Sb atom. One of the CO-groups as well as both Cl atoms also act as a bridge between the anionic [$Cl_2Sb\{Cr(CO)_5\}_2$]$^{-}$ moiety and its counterion, K(18-c-6). Thus, a one-dimensional polymeric structure of the type [K(18-c-6)]$_n$[$Cl_2Sb\{Cr(CO)_5\}_2$]$_n$ (K = counter-ion) is formed (cf. chapter 5.4). Comparing **3** to the previously reported [Na(thf)][$Cl_2Sb\{W(CO)_5\}_2$], it can be said that the Cl1-Sb-Cl2 angle of the latter is slightly larger (94.1(4) °) than that of **3**, which can be explained by the coordination of both Cl atoms to the K atom in contrast to only one in [Na(thf)][$Cl_2Sb\{W(CO)_5\}_2$].[21]

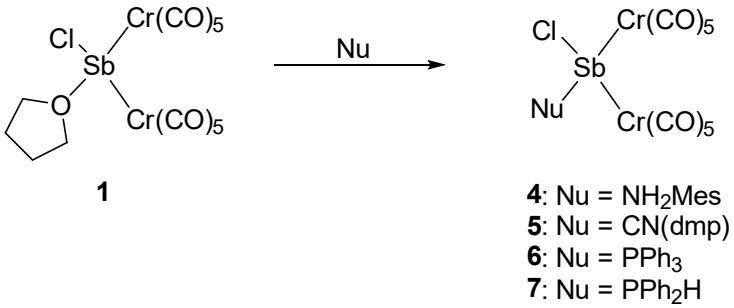

***Scheme 5.5**: Reaction of **1** with different Nucleophiles.*

Since the reactions of **1** with ionic nucleophiles did not lead to the expected products, non-ionic nucleophiles were used instead and adducts of the type [ClSb{Cr(CO)$_5$}$_2$Nu] (**4**: Nu = NH_2Mes, **5**: Nu = CN(dmp), **6**: Nu = PPh_3, **7**: Nu = PPh_2H; Mes = 2,4,6- triisopropylphenyl, dmp = 2,6-dimethylphenyl) could be obtained and isolated (cf. Scheme 5.5). The reactions were conducted in toluene, except for the reaction of **1** with dmp(NC), where CH_2Cl_2 was used. With the exception of **4**, which crystallizes at room temperature, single crystals of the products were crystallized at low temperatures. [ClSb{Cr(CO)$_5$}$_2$$NH_2Mes$] (**4**) was isolated in 53 % crystalline yield. Its ^{1}H NMR spectrum shows signals at chemical shifts of 1.86 and 1.95 ppm for the methyl groups of the mesityl substituent and a signal at 6.43 ppm for its CH groups, respectively. The chemical shift of the NH_2 protons can be detected at 4.64 ppm. In its IR spectrum, **4** shows typical CO bands for metal carbonyl complexes between 1904 cm^{-1} and 2073 cm^{-1} as well as bands for the N-H stretching vibrations at 3260 cm^{-1} and 3316 cm^{-1}. In the reaction of **1** with (dmp)NC, [ClSb{Cr(CO)$_5$}$_2$CN(dmp)] (**5**) was obtained in 10 % yield. Signals at chemical shifts of 7.14 and 7.45 ppm were detected by ^{1}H NMR spectroscopy as well as a signal at δ = 2.43 ppm. The IR spectrum shows CO bands between 1904 cm^{-1} and 2076 cm^{-1}. Compound **6** could be obtained in 60 % yield and shows a singlet at δ = -24.1 ppm in the ^{31}P{^{1}H} NMR spectrum, which is in good agreement with the chemical shift of -24.7 ppm that Huttner and co-workers published for the same compound in 1985, considering they recorded the spectrum in a different solvent and at 0°C. However, they described this product obtained by the reaction of $Na_2Cr_3(CO)_{10}$, $SbCl_3$ and PPh_3 and its structure in the solid state could not be determined.[10] Typical CO bands can be observed for **6** between 1915 cm^{-1} and 2065 cm^{-1} for the Cr(CO)$_5$ moieties in its IR spectrum.

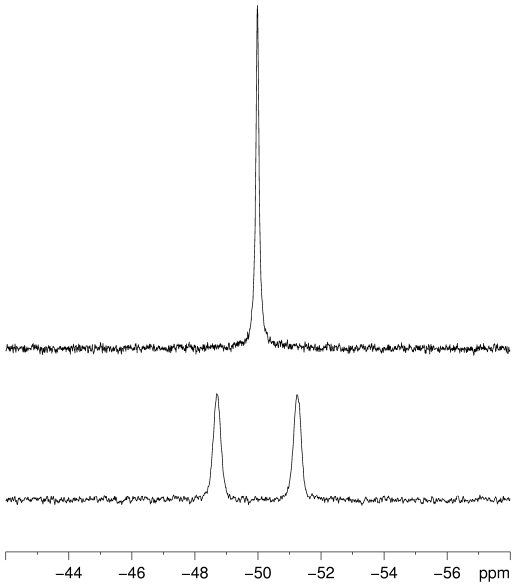

***Figure 5.4**: Excerpt of the ^{31}P{^{1}H} (top) and ^{31}P NMR (bottom) spectra of **7** in C_6D_6.*

Compound **7** was isolated in 40 % yield. Its $^{31}P\{^{1}H\}$ NMR spectrum shows a singlet at -50 ppm, which splits into a doublet in the ^{31}P NMR spectrum with a P,H coupling constant of 411 Hz (cf. Figure 5.4). In the IR spectrum, multiple CO bands could be detected between 1890 cm^{-1} and 2067 cm^{-1}. To see if an HCl elimination can be induced in this compound in order to generate a phosphinostibinidene complex, an attempt was made to deprotonate **7** with DBU (DBU = 1,8-Diazabicyclo[5.4.0]undec-7-ene). The color change of the reaction solution indicates that a reaction took place, but unfortunately no phosphinostibinidene complex could be isolated. In the ^{31}P NMR spectrum of the reaction solution, a variety of new signals could be detected, which cannot be identified. Due to the extreme instability of this solution towards moisture and air, the products cannot be separated. Nevertheless, this can be seen as a starting point towards further investigations of phosphine-substituted stibinidene complexes.

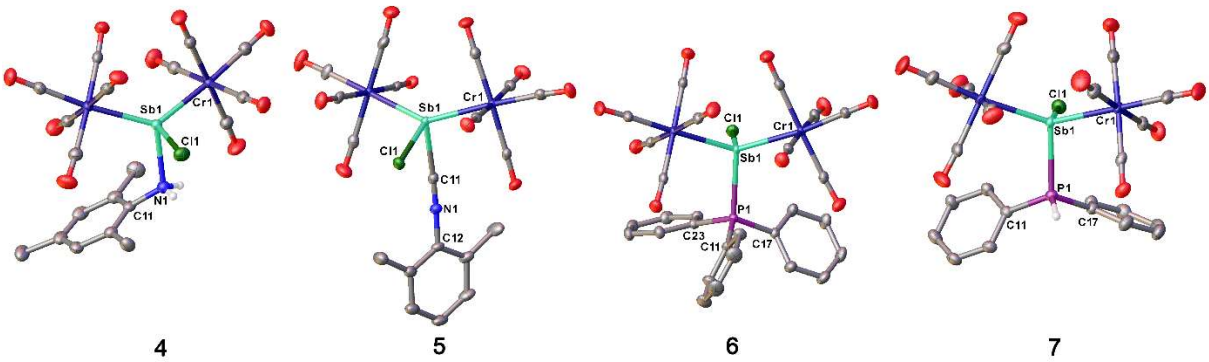

***Figure 5.5**: Molecular structures of compounds **4-7**. Anisotropic displacement parameters are set to 50% probability level. H atoms at C atoms are omitted for clarity. Selected bond lengths [Å] and angles [°]: **4**: Sb1-N1 2.3745(16), Sb1-Cl1 2.4018(5); Cr2-Sb1-Cr1 128.217(10), N1-Sb1-Cl1 82.52(5). **5**: Sb1-C11 2.286(3), Sb1-Cl1 2.4439(8); Cr1-Sb1-Cr2 141.578(17), C11-Sb1-Cl1 79.68(8). **6**: Sb1-P1 2.6143(3), Sb1-Cl1 2.4071(3); Cr2-Sb1-Cr1 127.447(7), Cl1-Sb1-P1 88.546(11). **7**: Sb1-P1 2.6091(4), Sb1-Cl1 2.4143(5); Cr1-Sb1-Cr2 131.787(10), Cl1-Sb1-P1 85.571(15).*

The molecular structures of complexes **4-7** are shown in Figure 5.5. All of them consist of a $[ClSb\{Cr(CO)_5\}_2]$ unit which forms an adduct with the respective nucleophile via the Sb atom, resulting in a tetrahedrally configurated Sb atom. The tetrahedral geometries are distorted, with the Cr-Sb-Cr angles between 127.447(7)° (**6**) and 141.578(17)° (**5**) and the Cl-Sb-Nu angles between 79.68(8) ° (**5**) and 88.546(11) ° (**6**). This is most likely due to the steric bulk of the $Cr(CO)_5$ groups. All of the Sb-E (E = C, N, P) bonds are slightly elongated single bonds, agreeing with the proposed coordinative nature of the bonds, while the Sb-Cl distances are all well within the range of single bonds.[14] Compound **6** has been reported before, with no X-ray crystal structure. However, a similar compound, $[MeSb\{W(CO)_5\}_2PPh_3]$, has been characterized by X-ray crystallography. Comparing both of these compounds, it can be said that their Sb-P distances are similar to each other.[10]

After reacting **1** with these various C, N and P nucleophiles, the intention was to use a Sb-based nucleophile, too, in order to generate novel Sb-Sb bonds. For this, $(Me_3Si)_2CHSbH_2$ was used as a nucleophile, since it is stable enough to be used for synthesis and the formation of a Sb=Sb double bond compound through HCl or H_2- elimination was aimed for. In the reaction of **1** with $(Me_3Si)_2CHSbH_2$,

only a few crystals of the isomers *d,l*-[$(Me_3Si)_2CHSb(H)\{Cr(CO)_5\}]_2$ (**8a**) and *meso*-[$(Me_3Si)_2CHSb(H)\{Cr(CO)_5\}]_2$ (**8b**) suitable for X-ray crystallography could be obtained, respectively. **8a** crystallizes as yellow blocks from a mixture of diethyl ether and *n*-pentane, while **8b** crystallizes from a concentrated hexane solution as greenish yellow blocks. Due to their low stability in solution and its low quantity due to the low yield of the reaction, the recording of additional NMR spectra of the crystalline compounds with more scans was not possible. The molecular structures of **8a** and **8b** are shown in Figure 5.6. They can both be described as distibanes with 3 different moieties (H, $CH(SiMe_3)_2$ and $Cr(CO)_5$) attached in different ways. **8a** is the *R,R/S,S*-enantiomer of *d,l*-[$(Me_3Si)_2CHSb(H)\{Cr(CO)_5\}]_2$ and **8b** its *meso*-isomer. The X-ray crystallographic data also reveal disorders in both structures (cf. chapter 5.4).

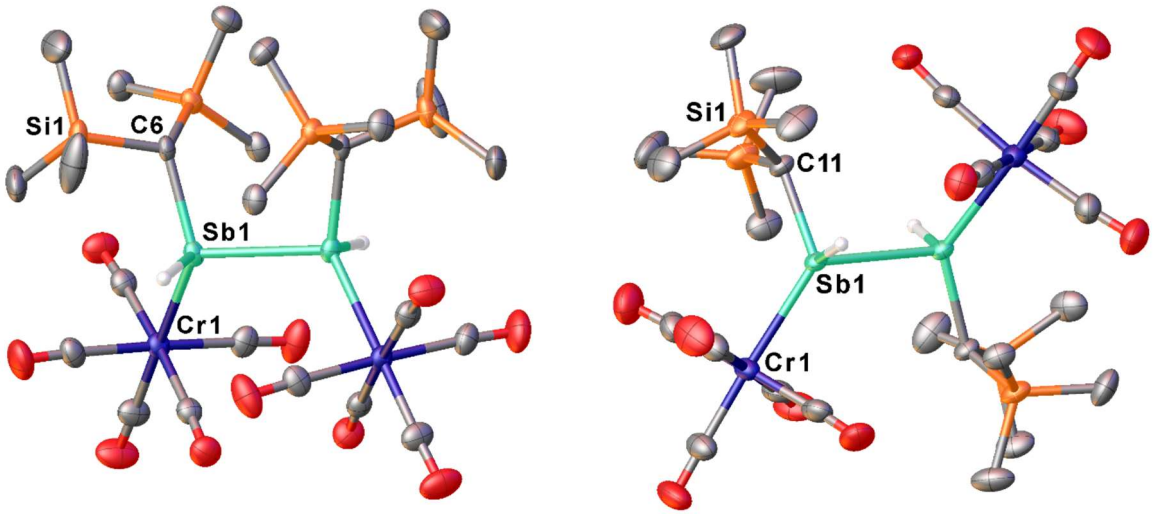

Figure 5.6*: Molecular structures of* ***8a*** *(left) and* ***8b*** *(right). Anisotropic displacement parameters are set to 50 % probability level. H atoms bound to C atoms and disordered parts omitted for clarity. Selected bond lengths [Å] and angles [°]:* ***8a****: Sb1-Sb1*[10] *2.8533(3), Sb1-Cr1 2.6342(4), Sb1-C6 2.161(2); Cr1-Sb1-Sb1*[10] *117.732(9) C6-Sb1-Sb1*[10] *102.29(5).* ***8b****: Sb1-Sb2 2.8395(3), Sb1-Cr1 2.6325(6), Sb1-C11 2.151(3), Sb2-Cr2 2.6471(6), Sb2-C18 2.164(3); Cr1-Sb1-Sb2 124.229(15), C11-Sb1-Sb2 97.77(9), Cr2-Sb2-Sb1 115.460(16), C18-Sb2-Sb1 102.38(9).*

The formation mechanism of **8a** and **8b** is not clear, however there has to be a formal migration of $Cr(CO)_5$ fragments during the reaction. Similar compounds have already been synthesized by *Breunig et al.* in 2003 via the reaction of R(H)Sb-Sb(H)R (R = $(Me_3Si)_2CH$) with 2 equivalents of $W(CO)_5$thf. *d,l*- and *meso*-[$(Me_3Si)_2CHSb(H)\{W(CO)_5\}]_2$ show Sb-Sb single bond lengths of 2.8417(13) and 2.8325(1) Å, which are similar to the Sb-Sb bond lengths of **8a** and **8b**. Additionally, the tetrahedral environment of the Sb atoms is significantly distorted from the ideal geometry because of the steric repulsion between the bulky $Cr(CO)_5$ moieties and $CH(SiMe_3)_2$ groups. The same applies for [$(Me_3Si)_2CHSb(H)\{W(CO)_5\}]_2$.[22]

[10] 1-x, +y, 3/2-z

With the exception of **2**, all of the abovementioned compounds are fairly stable as solids, even under air. In solution, however, the compounds readily decompose, which can easily be seen in the color change of the solutions from yellow to green.

5.3 Conclusion

In conclusion, the synthesis, isolation and characterization of various antimony-containing compounds via the reaction of the stibinidene complex **1** with various nucleophiles was reported. Compounds **2**, **4**, **5** and **7** are the first of their kind to be isolated and characterized, while **6** has already been reported, but now its X-ray structure could be obtained. The X-ray structures of compounds **3** and **8a**,**b** reveal similarities to other reported complexes and were characterized by NMR spectroscopy. The synthesis of these compounds paves the way to a deeper understanding of the reaction behavior of stibinidene complexes.

5.4 Supporting Information

5.4.1 Working techniques

The following reactions were carried out under an atmosphere of dry nitrogen or argon using standard Schlenk techniques. Traces of O_2 and water were eliminated by leading the inert gas (N_2 or Ar) through a copper catalyst heated to 145 °C, subsequently washing it with concentrated sulphuric acid and drying it with orange gel and phosphorous pentoxide. Solvents were either collected from a solvent purification system (MBraun SPS 800) or dried, degassed and distilled according to standard techniques. Before use, the diatomaceous earth required for filtration was stored at 110 °C. The silica gel 60 (particle size 0.063-0.2 mm) was dried at 150 °C in vacuo for 3 d prior to use.

The **NMR spectra** were recorded on a BRUKER Avance 300 (^{1}H: 300.13 MHz, ^{13}C: 75.48 MHz, ^{31}P: 121.49 MHz) or Avance 400 (^{1}H: 400.13 MHz, ^{13}C: 100.61 MHz, ^{31}P: 161.98 MHz) spectrometer at room temperature unless stated otherwise. Chemical shifts δ refer to external standards of tetramethylsilane (^{1}H, ^{13}C NMR) and 85 % phosphoric acid (^{31}P NMR, ^{31}P{^{1}H} NMR), respectively, and are given in ppm. Coupling constants J are given in Hz without consideration of absolute signs. Analysis and graphic representations of the spectra were prepared with *TopSpin 3.0*[23]. **Infrared spectra** were recorded in solution (CH_2Cl_2) or respectively as solids with a ThermoScientific Nicolet iS5 spectrometer using the iD5 Transmission element or an ATR element equipped with a diamond or Ge crystal. **Mass spectra** were recorded on a Jeol AccuTOF GCX (FD) spectrometer by the mass spectrometry department of the University of Regensburg or a ThermoQuest Finnigan MAT 95 spectrometer. **Elemental analysis** was conducted by the microanalytics laboratory of the University of Regensburg with the Elementar Vario MICRO cube**.**

The following substances were bought or synthesized according to standard techniques: $SbCl_3$, $Na_2[Cr_2(CO)_{10}]$[24], $GaCl_3$, NaCp'''[11], $NaNH_2$, $KAsH_2$[25], PPh_3, $LiPH_2$, KCN, Tl[TEF][12][26], PPh_2H, DBU[13], $MesNH_2$, 2,6-Dimethylphenylisonitrile, $(Me_3Si)_2CHSbH_2$[27]

[11] Cp''' = 1,2,4-tri-*tert*-butylcyclopentadienyl
[12] $[TEF]^- = [AlO_4C_{16}F_{36}]^-$
[13] DBU = 1,8-Diazabicyclo[5.4.0]undec-7-ene

5.4.2 Experimental Data with NMR details

5.4.2.1 Synthesis of 1

A clear colorless solution of 912 mg (4 mmol) $SbCl_3$ in 20 mL thf is added dropwise to a yellow suspension of 2.15 g (5 mmol) $Na_2[Cr_2(CO)_{10}]$ in 150 mL thf. The solution slowly turns orange and then brownish red before it is filtered over diatomaceous earth. Silica gel is then added to the deep red filtrate solution and the solvent removed in vacuo. The brownish residue is then transferred into a Soxhlet apparatus and extracted with 700 mL pentane at 44 °C for 4 h until the solution is a dark turquoise. The solvent is largely removed in vacuo and the remaining solution stored at -80 °C. After 3 days, an orange powder of $[ClSb\{Cr(CO)_5\}_2(thf)]$ (**1**) has formed which is filtered off quickly from the clear solution (which turns turquoise again upon warming to room temperature) and dried in vacuo.

Analytical data for **1**:

Yield:	817 mg (1.3 mmol, 33 %).
^{1}H NMR (CD_2Cl_2, 400 MHz):	δ [ppm] = 2.07 (s, 2H, CH_2), 4.13 (s, 2H, CH_2).
$^{13}C\{^1H\}$ NMR (CD_2Cl_2, 100 MHz):	δ [ppm] = 25.3 (s, CH_2), 78.5 (s, CH_2), 213.7 (s, CO), 220.4 (s, CO).
IR (ATR, Diamond):	ν_{max}/cm^{-1} = 1917 (m, CO), 2042 (w, CO).

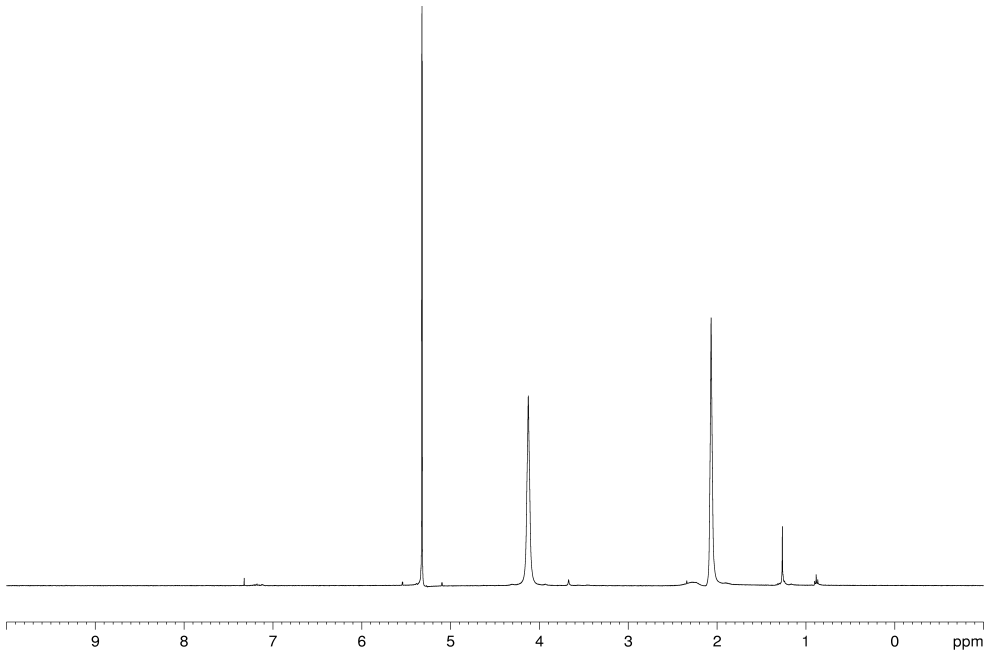

***Figure 5.7**: ^{1}H NMR spectrum of **1** in CD_2Cl_2.*

5.4.2.2 Reaction of 1 with $GaCl_3$

62 mg (0.1 mmol) **1** and 35 mg (0.2 mmol) $GaCl_3$ are dissolved in 10 mL pentane. The solution immediately turns turquoise and then brown. After 1h of stirring at room temperature, the solution turns green while a black residue has formed which is filtered off. $[ClSb\{Cr(CO)_5\}_2]_2$ (**2**) crystallizes as dark blocks from the concentrated pentane solution at -28 °C.

Analytical data for **2**:

Yield:	35 mg (0.03 mmol, 30 %).
$^{13}C\{^1H\}$ NMR (C_6D_6, 100 MHz):	δ [ppm] = 211.2 (s, CO), 211.4 (s, CO).
MS (FD):	m/z (%): 889.4 $[M^+\text{-}Cr(CO)_5]$ (54), 804.9 $[M^+\text{-}Cr(CO)_5\text{ -3CO}]$ (54), 746.2 $[M^+\text{-12CO}]$ (51), 711.0 $[M^+\text{-}ClCr(CO)_{10}]$ (57), 576.6 $[M^+\text{-}SbCr_2(CO)_{10}]$ (55), 550.1 $[M^+\text{ -19 CO}]$ (100), 522.2 $[M^+\text{ -20 CO}]$ (51), 473.8 $[M^+\text{ -}Cr_2(CO)_{18}]$ (64).
IR (ATR, Ge):	ν_{max}/cm^{-1} = 1930 (s, CO), 1944 (s, CO), 1991 (m, CO), 2042 (m, CO).

5.4.2.3 Reaction of 1 with various nucleophiles

General procedure: A solution of 0.1 mmol of the nucleophile (and 0.1 mmol of a suitable crown ether) in the respective solvent was added dropwise to 62 mg (0.1 mmol) **1** in the same solvent at -80 °C. The solution was warmed to room temperature and stirred until a color change occurred. The reaction solution was then filtered, and either concentrated and layered with another solvent or recrystallized from another solvent. $[Cl_2Sb\{Cr(CO)_5\}_2]^-$ (**3**) crystallizes as yellow blocks.

Specifics:

Nucleophile	solvent	color change	crystallization method	counterion
$NaNH_2$	Et_2O	yellow	Layering: Et_2O/ pentane 1:2	$[Na@(18\text{-crown-}6)\cdot dioxane]^+$
$KAsH_2$	thf	brown	Layering: Et_2O/ pentane 1:2	$[K@18\text{-crown-}6]^+$
$LiPH_2$	thf	red	Layering: thf/ pentane 1:2	$[Li@(12\text{-crown-}4)_2]^+$
KCN	thf	orange	Layering: Et_2O/ pentane 1:2	$[K@18\text{-crown-}6]^+$

Analytical data for $[Na@(18\text{-crown-6})\cdot dioxane]^+[Cl_2Sb\{Cr(CO)_5\}_2]^-$ (Nu = $NaNH_2$):

Yield:	30 mg (0.03 mmol, 30 %).
^{1}H NMR (CD_2Cl_2, 400 MHz):	δ [ppm] = 3.68 (s, CH_2).
$^{13}C\{^1H\}$ NMR (CD_2Cl_2, 100 MHz):	δ [ppm] = 69.2 (s, CH_2), 216.7 (s, CO), 217.5 (s, CO).
IR (ATR, Diamond):	ν_{max}/cm^{-1} = 1872 (s, CO), 2032 (m, CO).

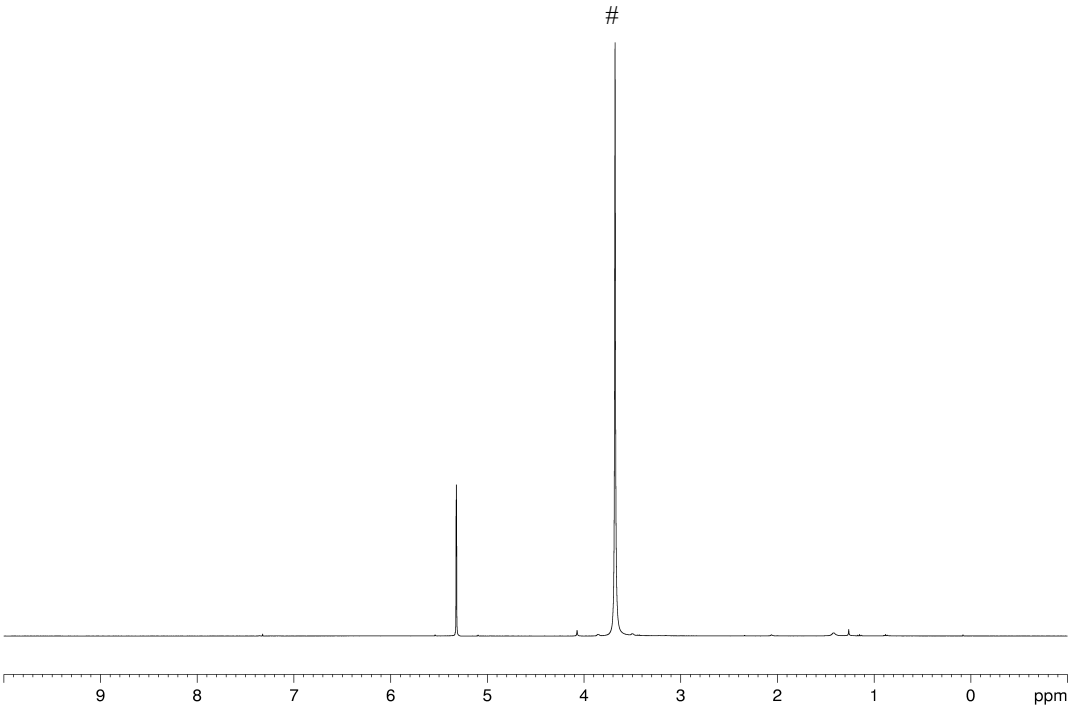

Figure 5.8: *^{1}H NMR spectrum of $[Na@(18\text{-crown-6})\cdot dioxane]^+[Cl_2Sb\{Cr(CO)_5\}_2]^-$ in CD_2Cl_2. # = 18-crown-6.*

5.4.2.4 Synthesis of 4

A solution of 246 mg (0.4 mmol) **1** in 20 mL toluene is added dropwise to a solution of 0.11 mL (108 mg, 0.8 mmol) of $MesNH_2$ in 30 mL toluene at -20 °C. To the resulting orange suspension a few mL CH_2Cl_2 are added and the reaction mixture is warmed to room temperature and stirred for 16 h. The solvent is then removed in vacuo and hexane is added to the residue. The resulting orange suspension is then filtered, the solvent of the filtrate once more removed in vacuo and the residue is dissolved in warm hexane (50-60 °C), concentrated and stored at room temperature. $[ClSb\{Cr(CO)_5\}_2NH_2Mes]$ (**4**) crystallizes as orange rods and yellowish orange blocks.

Analytical data for **4**:

Yield:	140 mg (0.21 mmol, 53 %).
^{1}H NMR (C_6D_6, 400 MHz):	δ [ppm] = 1.86 (s, 6H, CH_3), 1.95 (s, 3H, CH_3), 4.64 (s, 2H, NH_2), 6.43 (s, 2H, CH).
IR (ATR, Diamond):	ν_{max}/cm^{-1} = 1904 (s, CO), 2009 (s, CO), 2043 (s, CO), 2073 (m, CO), 3260 (w, NH), 3316 (w, NH).
elemental analysis:	calcd (%) for **4**: C 33.73, H 1.94, N 2.07; found: C 33.77, H 1.77, N 2.14.

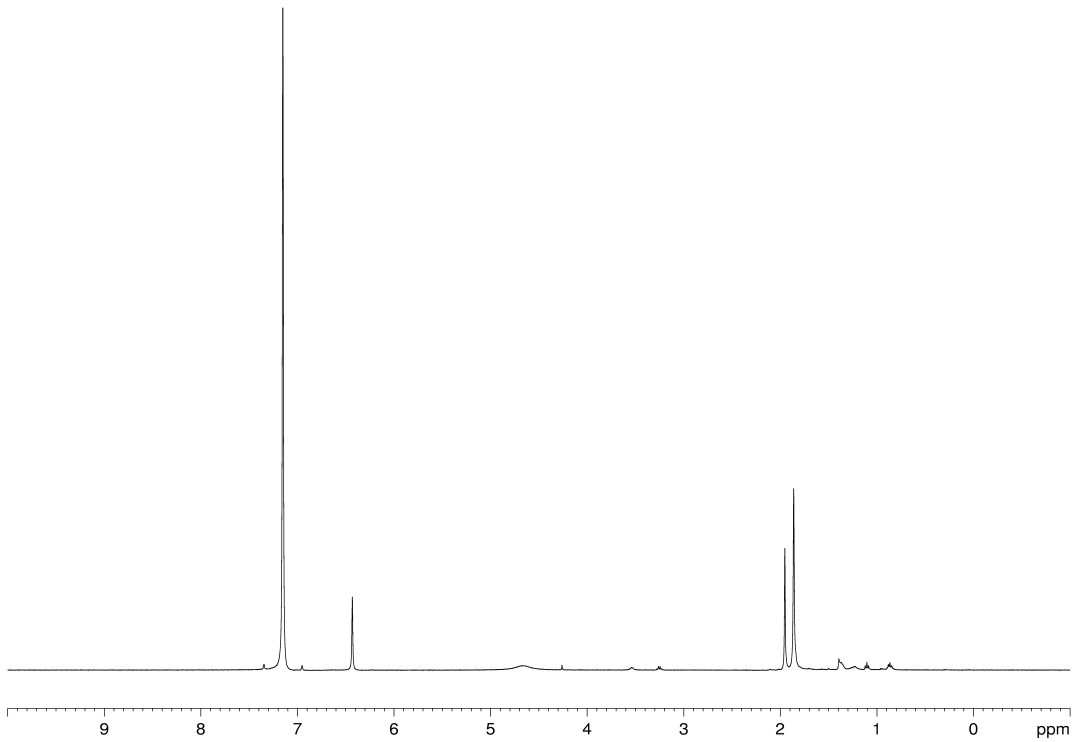

Figure 5.9. *^{1}H NMR spectrum of **4** in C_6D_6.*

5.4.2.5 Synthesis of 5

A solution of 13 mg (0.1 mmol) (dmp)NC in 10 mL CH_2Cl_2 is added dropwise to a solution of 62 mg (0.1 mmol) **1** in 10 mL CH_2Cl_2 at -78 °C. The resulting yellow solution is stirred and warmed to room temperature. After removing the solvent in vacuo, hexane is added to the residue and the resulting suspension is filtered. The solvent is once again removed from the filtrate, the residue is dissolved in Et_2O. [ClSb{Cr(CO)$_5$}$_2$CN(dmp)] (**5**) is obtained as greenish yellow plates from the concentrated Et_2O solution at 4 °C.

Analytical data for **5**:

Yield:	9 mg (0.01 mmol, 10 %).
^{1}H NMR (CD_2Cl_2, 400 MHz):	δ [ppm] = 2.43 (s, 6H), 7.14 (m, 2H), 7.45 (m, 1H).
^{13}C{^{1}H} NMR (CD_2Cl_2, 100 MHz):	δ [ppm] = 18.2 (s), 127.9 (s), 128.4 (s), 137.5 (s), 214.6 (s, CO), 214.8 (s, CO), 217.2 (s, CO), 221.0 (s, CO).
MS (FD):	m/z (%): 626.8 [M^+-CO -CH_3] (8), 541.7 [M^+ -3CO -C_3H_9] (37), 426.1 [M^+ -5CO -$C_6H_3(CH_3)_2$] (100), 372.9 [M^+ -Cr(CO)$_5$ -$C_6H_3(CH_3)_2$] (9), 323.0 [M^+ -Cr(CO)$_5$ -CO -Cl -$C_5H_3(CH_3)_2$] (54).
IR (ATR, Diamond):	ν_{max}/cm^{-1} = 1904 (s, CO), 1987 (s, CO), 2047 (m, CO), 2076 (m, CO).

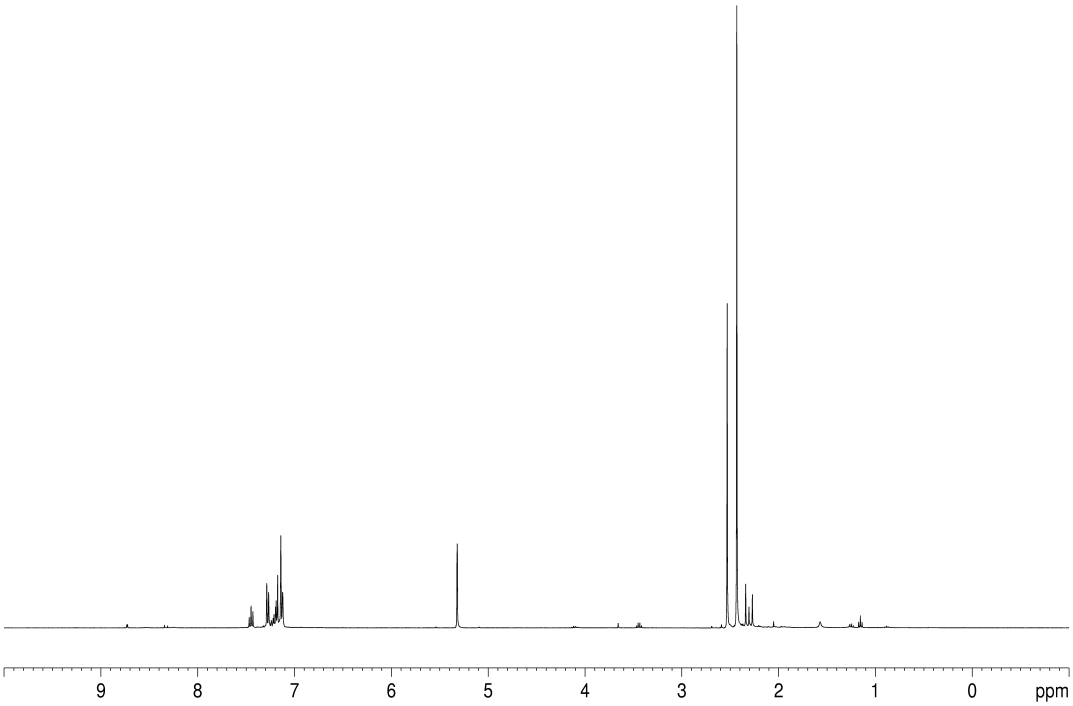

***Figure 5.10**: ^{1}H NMR spectrum of **5** in CD_2Cl_2.*

5.4.2.6 Synthesis of 6

A solution of 26 mg (0.1 mmol) PPh_3 in 10 mL toluene is added dropwise to a dark green solution of 62 mg (0.1 mmol) **1** in 15 mL toluene. The reaction mixture turns brown and then a bright orange. After filtration of the solution it is stored at -28 °C, where $[ClSb\{Cr(CO)_5\}_2PPh_3]$ (**6**) crystallizes as yellow plates.

Analytical data for **6**:

Yield:	20 mg (0.06 mmol, 60 %).
^{1}H NMR (C_6D_6, 400 MHz):	δ [ppm] = 6.99 (m, 12H, arom.), 7.50 (m, 6H, arom.).
^{31}P{^{1}H} NMR (C_6D_6, 162 MHz):	δ [ppm] = -24.1 (s).
^{31}P NMR (C_6D_6, 162 MHz):	δ [ppm] = -24.8 (br).
^{13}C{^{1}H} NMR (C_6D_6, 100 MHz):	δ [ppm] = 129.9 (d, arom. C), 133.6 (d, arom. C), 134.1 (d, arom. C), 216.1 (s, CO).
MS (FD):	m/z (%): 803.7 [M+] (100), 759.9 [M+ -C3H6] (4), 485.9 [M+ -PPh3 -2CO] (13), 454.0 [M+ -PPh3 -3CO] (7).
IR (ATR, Ge):	ν_{max}/cm^{-1} = 1915 (s, CO), 1957 (s, CO), 1998 (m, CO), 2043 (s, CO), 2065 (m, CO).
elemental analysis:	calcd (%) for **6** · 0.17 C_7H_8: C 42.77, H 2.01; found: C 42.81, H 1.91.

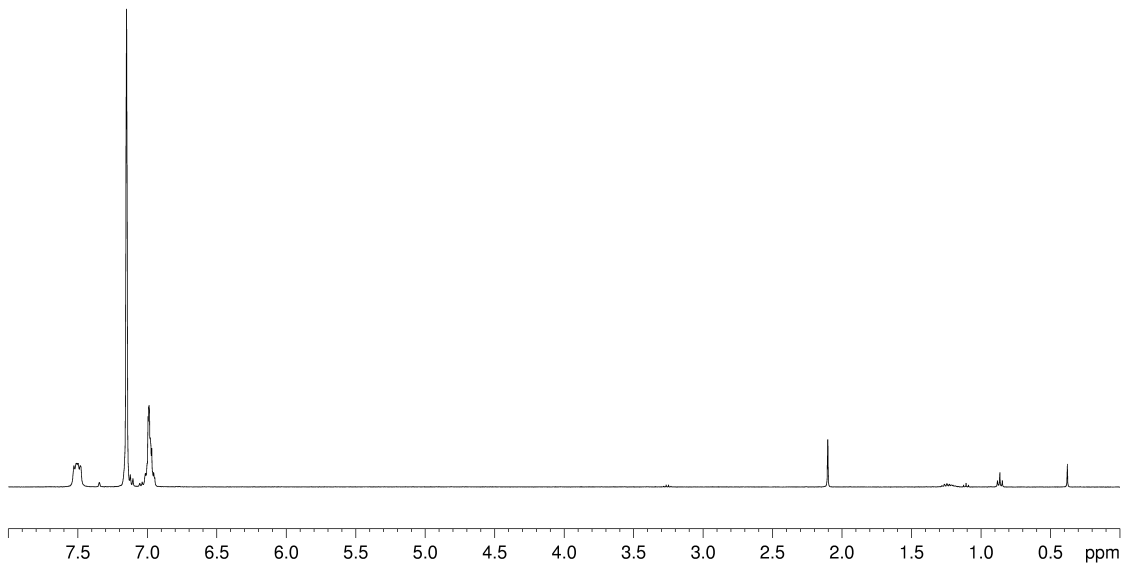

Figure 5.11: *^{1}H NMR spectrum of **6** in C_6D_6.*

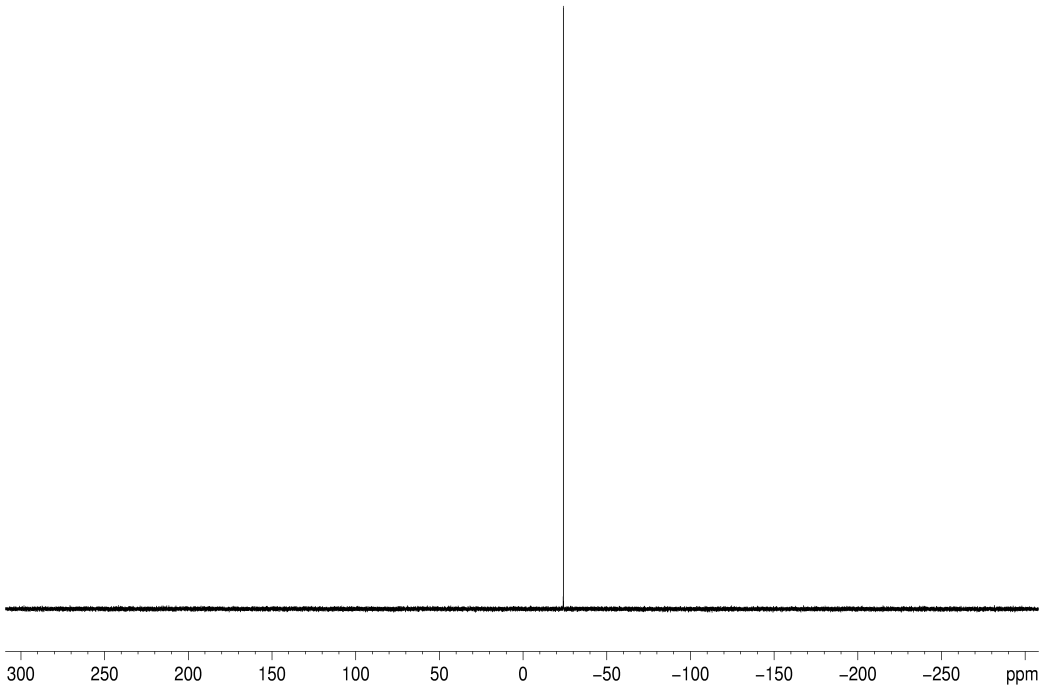

Figure 5.12: *$^{31}P\{^1H\}$ NMR spectrum of **6** in C_6D_6.*

5.4.2.7 Synthesis of 7

A solution of 0.08 mL (0.4 mmol) Ph_2PH in 3 mL toluene is added dropwise to a dark green solution of 246 mg (0.4 mmol) **1** in 20 mL toluene. The reaction mixture turns red, brown and then orange. After filtration of the solution it is stored at -28 °C, where $[ClSb\{Cr(CO)_5\}_2PPh_2H]$ (**7**) crystallizes as yellow blocks.

Analytical data for **7**:

Yield:	119 mg (0.16 mmol, 40 %).
^1H NMR (C_6D_6, 400 MHz):	δ [ppm] = 6.11 (s, 1H, PH), 6.93 (m, 8H, arom. CH), 7.33 (s, 4H, arom. CH).
$^{31}P\{^1H\}$ NMR (C_6D_6, 162 MHz):	δ [ppm] = -50.0 (s).
^{31}P NMR (C_6D_6, 162 MHz):	δ [ppm] = -50.0 (d, $^1J_{PH}$ = 411 Hz).
$^{13}C\{^1H\}$ NMR (C_6D_6, 100 MHz):	δ [ppm] = 130.0 (d, arom. C), 133.8 (d, arom. C), 215.9 (s, CO), 221.6 (s, CO).
MS (FD):	m/z (%): 727.8 $[M^+]$ (100), 562.1 $[M^+ -4CO -C_4H_4]$ (40), 478.9 $[M^+ -6CO -Ph -H]$ (38), 291.0 $[M^+ -Cr(CO)_5 -2CO -PPh_2H]$ (38).
IR (ATR, Ge):	ν_{max}/cm^{-1} = 1890 (m, CO), 1923 (s, CO), 1953 (s, CO), 1999 (m, CO), 2043 (m, CO), 2067 (m, CO).
elemental analysis:	calcd (%) for **7**: C 36.32, H 1.52; found: C 37.08, H 1.51.

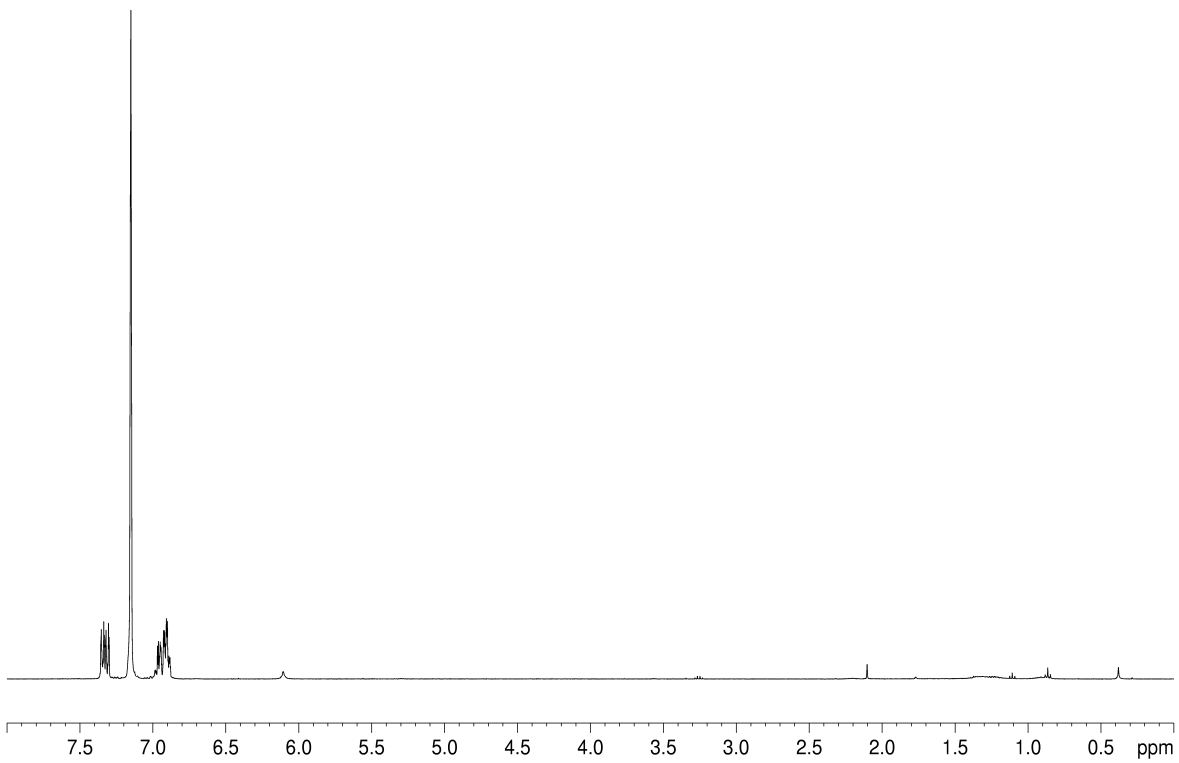

Figure 5.13: *^{1}H NMR spectrum of **7** in C_6D_6.*

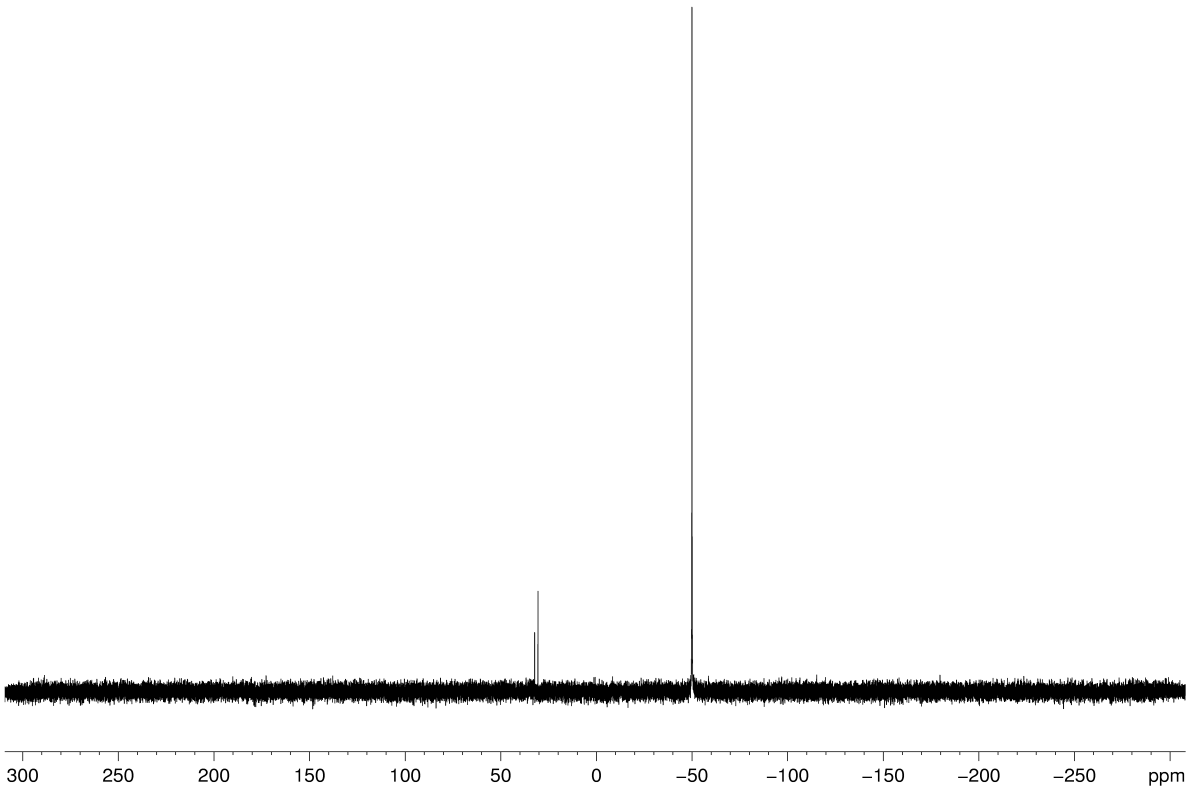

Figure 5.14: *$^{31}P\{^{1}H\}$ NMR spectrum of **7** in C_6D_6.*

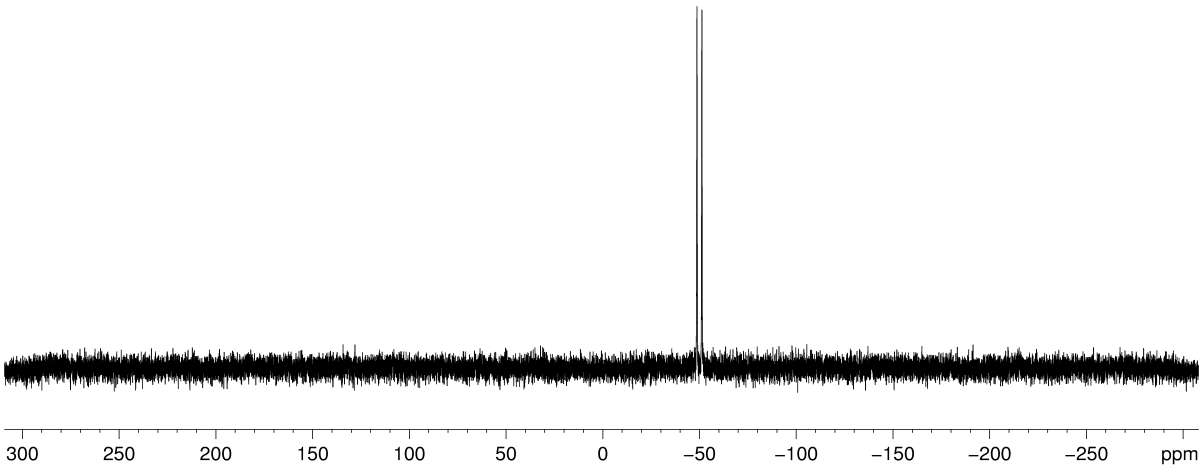

Figure 5.15: *^{31}P NMR spectrum of 7 in C_6D_6.*

5.4.2.8 Reaction of 7 with DBU

A colorless solution of 0.5 mL (0.05 mmol, 0.1 mmol·mL^{-1} in Et_2O) DBU in 2 mL EtO_2 is added dropwise to a dark yellow solution of 36 mg (0.05 mmol) **7** in 15 mL Et_2O. The solution turns red for a short time before it slowly turns a bright yellow. After 15 min of stirring, a brown residue forms, which is filtered off. The remaining solution is analyzed via NMR spectroscopy.

5.4.2.9 Synthesis of 8

A solution of 0.02 mL (0.1 mmol) of $(Me_3Si)_2CHSbH_2$ in 3 mL toluene is added dropwise to a dark green solution of 62 mg (0.1 mmol) **1** in 20 mL toluene. Upon stirring, the reaction mixture turns red. The solvent is removed and the residue dissolved in a few mL of a 1:3 mixture of Et_2O and pentane. *d,l*-$[(Me_3Si)_2CHSb(X)\{Cr(CO)_5\}]_2$ (**8a**, X = H, Cl) crystallizes as yellow blocks at -28 °C. From the decanted solution, the solvent is removed in vacuo and the residue extracted with hexane. From the concentrated green hexane solution, *meso*-$[(Me_3Si)_2CHSb(X)\{Cr(CO)_5\}]_2$ (**8b**) crystallizes as greenish yellow blocks.

Yield (**8a**+**8b**): few crystals

5.4.3 Crystallographic Data

Single crystal X-ray structure analyses were either carried out on a Gemini Ultra Diffractometer (Rigaku Oxford Diffraction, formerly Agilent Technologies) or a GV50 diffractometer (Rigaku Oxford Diffraction). The Gemini Ultra diffractometer was equipped with a molybdenum X-ray radiation source (Mo-K_α = 0.71073 Å) and an AtlasS2 CCD detector as well as an Oxford Systems CryoJet cooling system. The GV50 diffractometers were equipped with a copper X-ray radiation source (Cu-K_α = 1.54184Å and Cu-K_β = 1.3922 Å) and TitanS2 detectors as well as Oxford Cryosystems CryoStream 700 cooling systems. Figures of the molecular structures were prepared with the program *Olex2*[28].

Due to their air and water sensitivity, the crystals were coated with mineral oil (Sigma Aldrich, CAS 8042-47-5). Suitable single crystals were picked under the microscope from the oil and transferred onto a MiTeGen MicroLoop attached to a goniometer head. The goniometer head was then placed onto the goniometer with the loop sitting in a current of cold nitrogen. After collection of the crystal structure data, integration and data reduction were carried out with the program *CrysAlis Pro*[29]. Structure elucidation was carried out with the program *SHELXT*[30] using direct methods. Refinement occurred with the least squares method with the program *SHELXL*[31]. Both were used within *Olex2*[28] as the platform.

5.4.3.1 Crystal Structure Data for 2

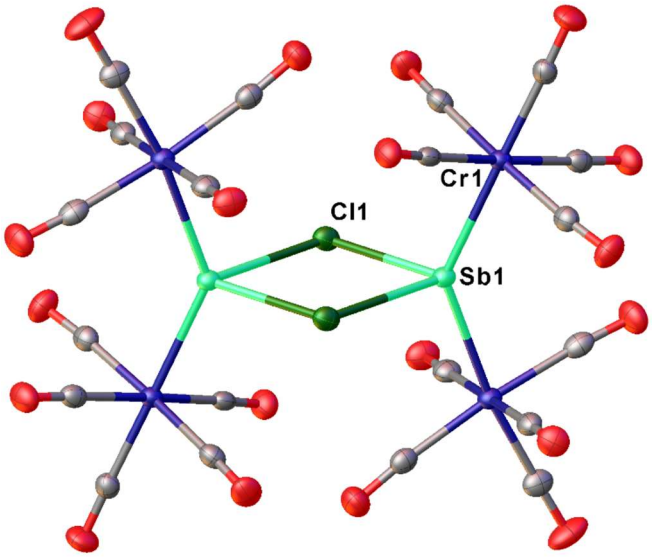

Molecular structure of **2**. Anisotropic displacement parameters are set to 50% probability level. Selected bond lengths [Å] and angles [°]: Sb1-Cr1 2.5126(6), Sb1-Cr2 2.5167(6), Sb1-Cl1 2.5091(9), Sb1-Cl1[14] 2.8999(9); Cr1-Sb1-Cr2 137.28(2), Cr1-Sb1-Cl1[9] 104.78(2), Cr2-Sb1-Cl1[9] 105.62(2), Cl1-Sb1-Cr1 107.20(3), Cl1-Sb1-Cr2 108.60(3), Cl1-Sb1-Cl1[9] 76.39(3), Sb1-Cl-Sb1[9] 103.61(3).

Compound	**2**
Formula	$C_{20}Cl_2Cr_4O_{20}Sb_2$
$D_{calc.}$/ g cm^{-3}	2.326
μ/mm^{-1}	20.636
Formula Weight	1082.60
Colour	metallic dark violet
Shape	cube
Size/mm^3	0.21×0.07×0.07
T/K	123.00(10)
Crystal System	triclinic
Space Group	P-1
a/Å	6.5841(4)
b/Å	9.9152(6)
c/Å	12.3608(8)
α/°	102.142(5)
β/°	100.531(5)
γ/°	92.377(5)
V/Å^3	772.92(9)
Z	1
Z'	0.5
Wavelength/Å	1.39222
Radiation type	Cu K_β
Θ_{min}/°	3.368
Θ_{max}/°	60.175
Measured Refl's.	8562
Indep't Refl's	3024
Refl's I≥2 s(I)	2851
R_{int}	0.0415
Parameters	217
Restraints	0
Largest Peak	0.898
Deepest Hole	-1.187
GooF	1.111
wR_2 (all data)	0.0812
wR_2	0.0793
R_1 (all data)	0.0322
R_1	0.0299

[14] 1-x, 1-y, 1-z

5.4.3.2 Crystal Structure Data for 3

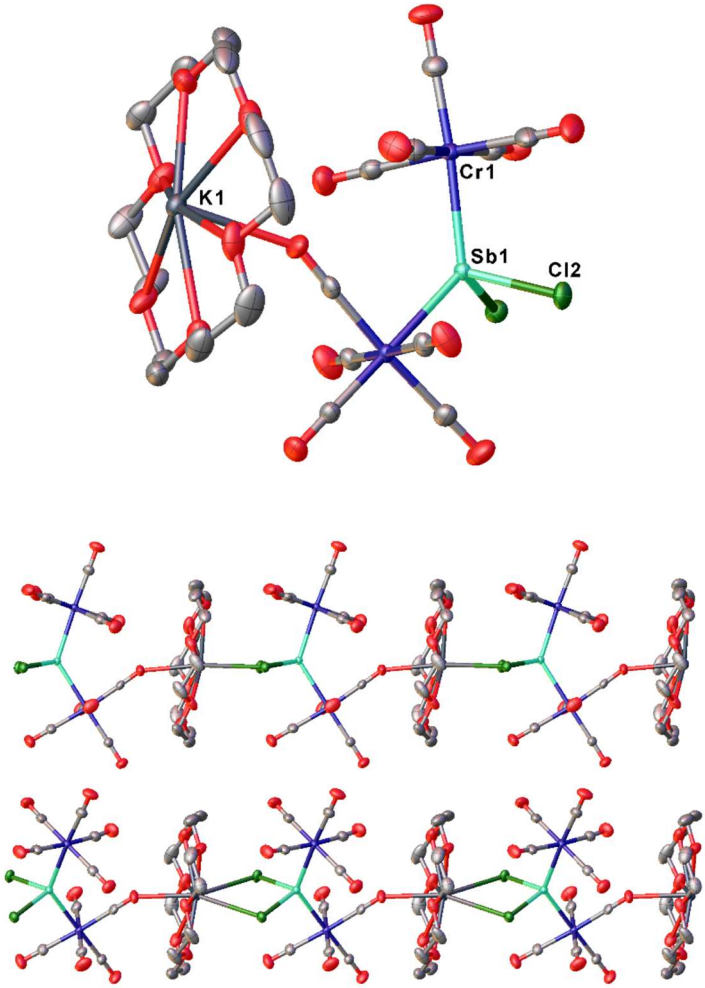

Molecular structure of **3** (top) and its 1D polymer (middle and bottom). Anisotropic displacement parameters are set to 50% probability level. H atoms are omitted for clarity. Selected bond lengths [Å] and angles [°]: Sb1-Cr2 2.5683(3), Sb1-Cr1 2.5807(3), Sb1-Cl1 2.4218(5), Sb1-Cl2 2.4129(5); Cr2-Sb1-Cr1 129.830(11), Cl1-Sb1-Cr2 104.959(15), Cl1-Sb1-Cr1 108.716(15), Cl2-Sb1-Cr2 106.161(16), Cl2-Sb1-Cr1 109.598(16), Cl2-Sb1-Cl1 90.434(18).

Compound	**3**
Formula	$C_{22}H_{24}Cl_2Cr_2KO_{16}Sb$
$D_{calc.}$/ g cm^{-3}	1.694
μ/mm^{-1}	1.736
Formula Weight	880.16
Colour	clear yellow
Shape	block
Size/mm^3	0.58×0.41×0.25
T/K	123(1)
Crystal System	triclinic
Space Group	P-1
a/Å	9.8591(3)
b/Å	11.1669(4)
c/Å	16.2464(6)
α/°	91.081(3)
β/°	101.013(3)
γ/°	100.182(3)
V/Å^3	1725.50(11)
Z	2
Z'	1
Wavelength/Å	0.71073
Radiation type	Mo K_α
Θ_{min}/°	3.387
Θ_{max}/°	29.233
Measured Refl's.	11797
Indep't Refl's	7824
Refl's I≥2 s(I)	7155
R_{int}	0.0157
Parameters	397
Restraints	0
Largest Peak	0.592
Deepest Hole	-0.417
GooF	1.032
wR_2 (all data)	0.0576
wR_2	0.0561
R_1 (all data)	0.0285
R_1	0.0248

5.4.3.3 Crystal Structure Data for 4

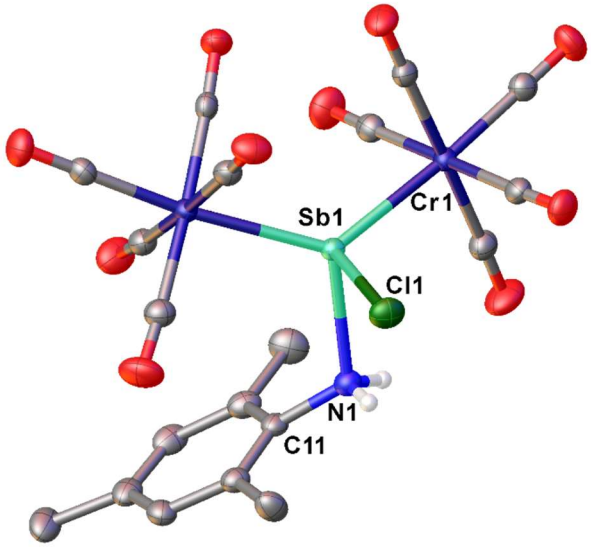

Molecular structure of **4**. Anisotropic displacement parameters are set to 50% probability level. H atoms bound to C atoms are omitted for clarity. Selected bond lengths [Å] and angles [°]: Sb1-Cr1 2.5632(3), Sb1-Cr2 2.5516(3), Sb1-Cl1 2.4018(5), Sb1-N1 2.3745(16), N1-C11 1.450(2), Cr2-Sb1-Cr1 128.217(10), Cl1-Sb1-Cr1 108.097(15), Cl1-Sb1-Cr2 106.513(15), N1-Sb1-Cr1 107.77(5) N1-Sb1-Cr2 113.93(4), N1-Sb1-Cl1 82.52(5), C11-N1-Sb1 117.44(12).

Compound	**4**
Formula	$C_{19}H_{13}ClCr_2NO_{10}Sb$
$D_{calc.}$/ g cm^{-3}	1.839
μ/mm^{-1}	2.132
Formula Weight	676.50
Colour	clear orange
Shape	block
Size/mm^3	0.18×0.13×0.12
T/K	123(1)
Crystal System	monoclinic
Space Group	$C2/c$
a/Å	17.6350(6)
b/Å	13.0947(4)
c/Å	21.9605(7)
α/°	90
β/°	105.452(4)
γ/°	90
V/Å^3	4887.9(3)
Z	8
Z'	1
Wavelength/Å	0.71073
Radiation type	Mo K_α
Θ_{min}/°	3.451
Θ_{max}/°	32.648
Measured Refl's.	16663
Indep't Refl's	7982
Refl's I≥2 s(I)	6956
R_{int}	0.0247
Parameters	318
Restraints	0
Largest Peak	0.535
Deepest Hole	-0.446
GooF	1.056
wR_2 (all data)	0.0602
wR_2	0.0573
R_1 (all data)	0.0365
R_1	0.0286

5.4.3.4 Crystal Structure Data for 5

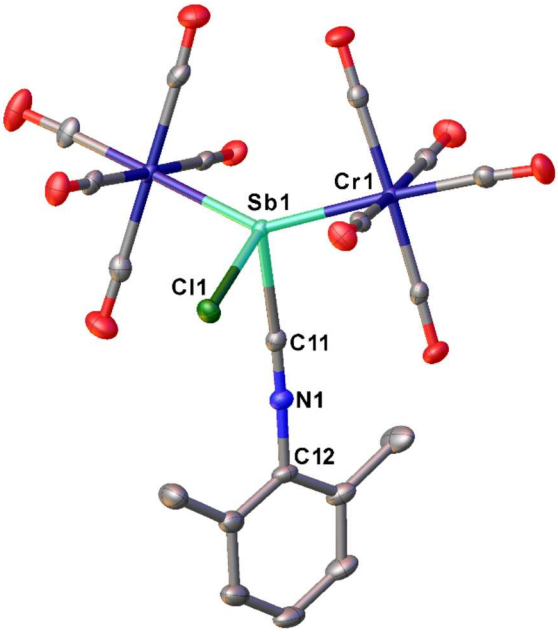

Molecular structure of **5**. Anisotropic displacement parameters are set to 50% probability level. H atoms are omitted for clarity. Selected bond lengths [Å] and angles [°]: Sb1-Cr1 2.5696(5), Sb1-Cr2 2.5706(5), Sb1-Cl1 2.4439(8), Sb1-C11 2.286(3), N1.C11 1.145(4), N1-C12 1.411(4); Cr1-Sb1-Cr2 141.578(17), Cl1-Sb1-Cr1 105.73(2), Cl1-Sb1-Cr2 105.25(2), C11-Sb1-Cl1 79.68(8), C11-N1-C12 177.0(3), N1.C11-Sb1 172.1(3).

Compound	**5**
Formula	$C_{19}H_9ClCr_2NO_{10}Sb$
$D_{calc.}$/ g cm^{-3}	1.916
μ/mm^{-1}	18.231
Formula Weight	672.47
Colour	yellow
Shape	block
Size/mm^3	0.10×0.04×0.02
T/K	123.00(15)
Crystal System	monoclinic
Space Group	$P2_1/c$
a/Å	9.9087(2)
b/Å	6.53990(10)
c/Å	36.0011(8)
α/°	90
β/°	91.953(2)
γ/°	90
V/Å^3	2331.58(8)
Z	4
Z'	1
Wavelength/Å	1.54184
Radiation type	Cu K_α
Θ_{min}/°	2.456
Θ_{max}/°	74.220
Measured Refl's.	11191
Indep't Refl's	4496
Refl's I≥2 s(I)	4229
R_{int}	0.0256
Parameters	309
Restraints	0
Largest Peak	0.594
Deepest Hole	-0.631
GooF	1.129
wR_2 (all data)	0.0580
wR_2	0.0570
R_1 (all data)	0.0302
R_1	0.0270

5.4.3.5 Crystal Structure Data for 6 · 0.5 toluene

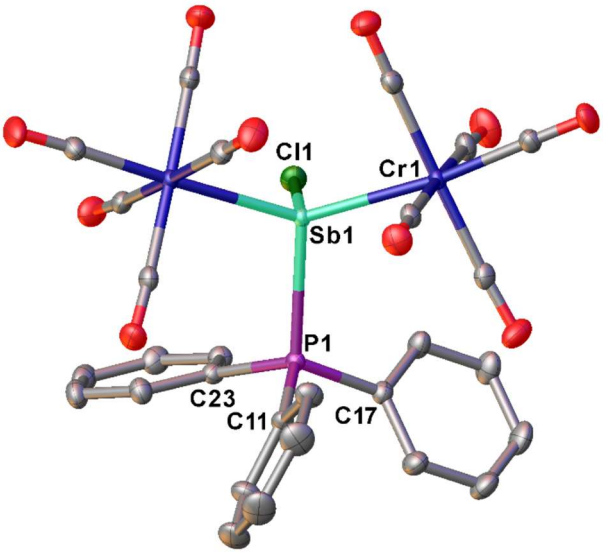

Molecular structure of **6**. Anisotropic displacement parameters are set to 50% probability level. H atoms and half a toluene solvent molecule were omitted for clarity. Selected bond lengths [Å] and angles [°]: Sb1-Cr1 2.6057(2), Sb1-Cr2 2.5834(2), Sb1-Cl1 2.4073(3), Sb1-P1 2.6144(3), P1-C11 1.8026(13), P1-C17 1.8101(13), P1-C23 1.8046(13); Cr2-Sb1-Cr1 127.450(7), Cr2-Sb1-P1 108.787(9), Cr1-Sb1-P1 112.470(9), Cl1-Sb1-Cr2 104.123(10), Cl1-Sb1-Cr1 107.976(10), Cl1-Sb1-P1 88.542(11), C23-P1-C17 110.73(6), C11-P1-C23 108.24(6), C11-P1-C17 107.56(6).

Compound	**6** · 0.5 toluene
Formula	$C_{31.5}H_{19}ClCr_2O_{10}PSb$
$D_{calc.}$/ g cm^{-3}	1.706
μ/mm^{-1}	1.640
Formula Weight	849.64
Colour	clear yellow
Shape	plate
Size/mm^3	0.31×0.19×0.06
T/K	123(1)
Crystal System	triclinic
Space Group	P-1
a/Å	10.1350(2)
b/Å	11.0514(2)
c/Å	15.5897(4)
α/°	85.665(2)
β/°	75.354(2)
γ/°	78.419(2)
V/Å^3	1654.44(6)
Z	2
Z'	1
Wavelength/Å	0.71073
Radiation type	Mo K_α
Θ_{min}/°	3.333
Θ_{max}/°	35.208
Measured Refl's.	52031
Indep't Refl's	13798
Refl's I≥2 s(I)	12064
R_{int}	0.0321
Parameters	452
Restraints	57
Largest Peak	0.624
Deepest Hole	-0.606
GooF	1.038
wR_2 (all data)	0.0548
wR_2	0.0521
R_1 (all data)	0.0338
R_1	0.0256

5.4.3.6 Crystal Structure Data for 7

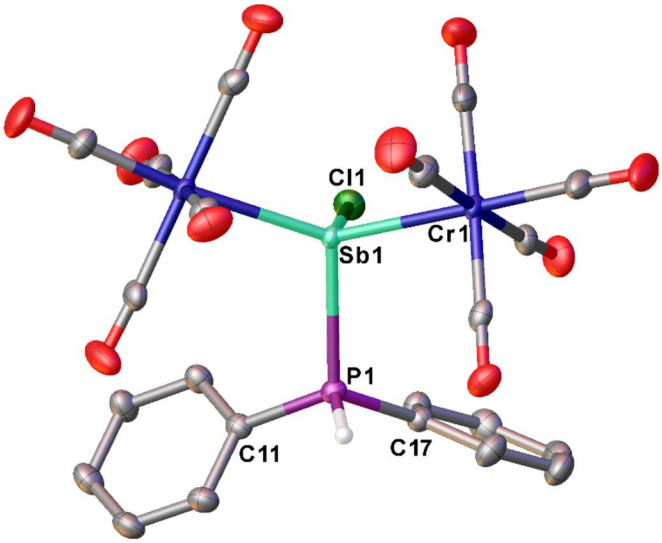

Molecular structure of **7**. Anisotropic displacement parameters are set to 50% probability level. H atoms bound to C atoms are omitted for clarity. Selected bond lengths [Å] and angles [°]: Sb1-Cr1 2.5878(3), Sb1-Cr2 2.5979(3), Sb1-Cl1 2.4143(5), Sb1-P1 2.6091(4), P1-C17 1.8003(16), P1-C11 1.7919(19); Cr2-Sb1-P1 111.912(13), Cr1-Sb1-Cr2 131.787(10), Cr1-Sb1-P1 106.323(13), Cl1-Sb1-Cr2 106.937(14), Cl1-Sb1-Cr1 104.179(15), Cl1-Sb1-P1 85.570(15), C11-P1-C17 111.07(8).

Compound	**7**
Formula	$C_{22}H_{11}ClCr_2O_{10}PSb$
$D_{calc.}$/ g cm^{-3}	1.845
μ/mm^{-1}	2.055
Formula Weight	727.48
Colour	clear yellow
Shape	block
Size/mm^3	0.18×0.13×0.10
T/K	123(1)
Crystal System	triclinic
Space Group	P-1
a/Å	10.2609(4)
b/Å	11.1217(4)
c/Å	12.6994(5)
α/°	107.711(4)
β/°	101.556(3)
γ/°	99.931(3)
V/Å^3	1309.58(9)
Z	2
Z'	1
Wavelength/Å	0.71073
Radiation type	Mo K_α
Θ_{min}/°	3.361
Θ_{max}/°	34.841
Measured Refl's.	20630
Indep't Refl's	10600
Refl's I≥2 s(I)	9117
R_{int}	0.0247
Parameters	338
Restraints	0
Largest Peak	0.582
Deepest Hole	-0.637
GooF	1.071
wR_2 (all data)	0.0622
wR_2	0.0589
R_1 (all data)	0.0403
R_1	0.0306

5.4.3.7 Crystal Structure Data for 8a

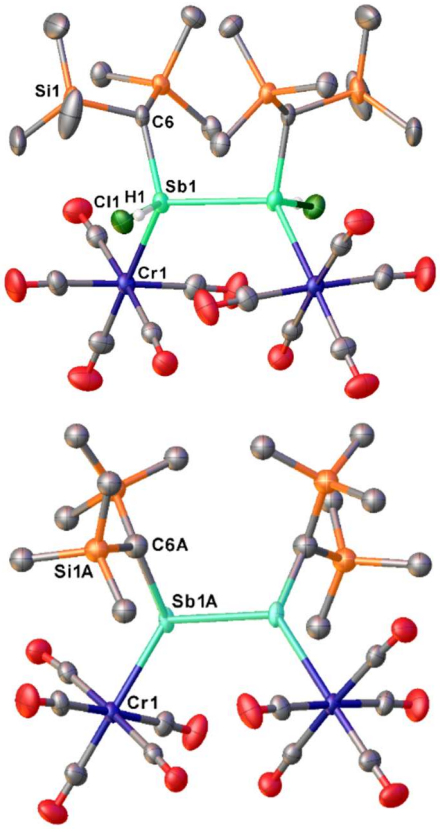

Molecular structure of **8a**. top: *d,l*-[$(Me_3Si)_2CHSb(X)\{Cr(CO)_5\}]_2$ (97 %; X = H, Cl), bottom: *cis*-[$(Me_3Si)_2CHSbCr(CO)_5\}]_2$ (3 %). Anisotropic displacement parameters are set to 50% probability level. H atoms at C atoms are omitted for clarity. Selected bond lengths [Å] and angles [°] of the main component: Sb1-Sb1[15] 2.8533(3), Sb1-Cr1 2.6342(4), Sb1-C6 2.161(2); Cr1-Sb1-Sb1[10] 117.732(9) C6-Sb1-Sb1[10] 102.29(5).

For **8a**, several disorders have been found in the crystal structure: one main component, where the Sb atom is additionally substituted with an atom X (H or Cl) and a minor component, where there is no additional substitution on the Sb atom and the Sb-Sb distance is widened. The main compound consists of 3 possible isomers: 1) both X = H; 2) both X = Cl; 3) X_1 = H; X_2 = Cl. The actual composition in the crystal could not be determined via single crystal X-Ray diffractometry.

Compound	**8a**
Formula	$C_{24}H_{39.64}Cl_{0.36}Cr_2O_{10}Sb_2Si_4$
$D_{calc.}$/ g cm^{-3}	1.618
μ/mm^{-1}	2.080
Formula Weight	960.82
Colour	clear dark yellow
Shape	block
Size/mm^3	0.33×0.19×0.09
T/K	123(1)
Crystal System	monoclinic
Space Group	$C2/c$
a/Å	17.5101(5)
b/Å	10.8904(3)
c/Å	21.0548(6)
α/°	90
β/°	100.810(3)
γ/°	90
V/Å^3	3943.7(2)
Z	4
Z'	0.5
Wavelength/Å	0.71073
Radiation type	Mo K_α
Θ_{min}/°	3.353
Θ_{max}/°	32.434
Measured Refl's.	22505
Indep't Refl's	6439
Refl's I≥2 s(I)	5818
R_{int}	0.0205
Parameters	245
Restraints	46
Largest Peak	0.900
Deepest Hole	-0.672
GooF	1.199
wR_2 (all data)	0.0661
wR_2	0.0645
R_1 (all data)	0.0348
R_1	0.0295

[15] 1-x, +y, 3/2-z

5.4.3.8 Crystal Structure Data for 8b

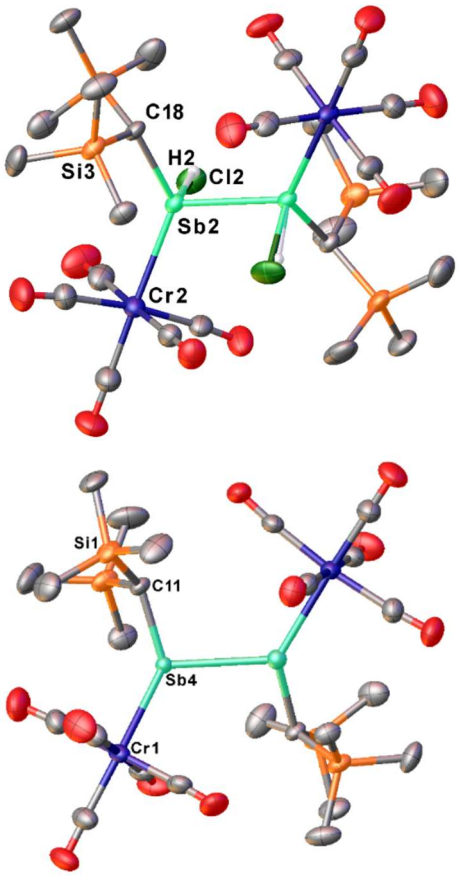

Molecular structure of **8b**. left: *meso*-[$(Me_3Si)_2CHSb(X)\{Cr(CO)_5\}]_2$ (98 %; X = H, Cl), right: *trans*-[$(Me_3Si)_2CHSbCr(CO)_5\}]_2$ (2 %). Anisotropic displacement parameters are set to 50% probability level. H atoms at C atoms are omitted for clarity. Selected bond lengths [Å] and angles [°] of the main component: Sb1-Sb2 2.8395(3), Sb1-Cr1 2.6325(6), Sb1-C11 2.151(3), Sb2-Cr2 2.6471(6), Sb2-C18 2.164(3); Cr1-Sb1-Sb2 124.229(15), C11-Sb1-Sb2 97.77(9), Cr2-Sb2-Sb1 115.460(16), C18-Sb2-Sb1 102.38(9).

Compound	**8b**
Formula	$C_{24}H_{39.86}Cl_{0.14}Cr_2O_{10}Sb_2Si_4$
$D_{calc.}$/ g cm^{-3}	1.618
μ/mm^{-1}	2.081
Formula Weight	953.24
Colour	clear dark yellow
Shape	block
Size/mm^3	0.43×0.20×0.14
T/K	123(1)
Crystal System	triclinic
Space Group	P-1
a/Å	8.9881(3)
b/Å	13.9592(6)
c/Å	15.8153(5)
α/°	85.489(3)
β/°	86.513(3)
γ/°	82.139(3)
V/Å^3	1957.04(12)
Z	2
Z'	1
Wavelength/Å	0.71073
Radiation type	Mo K_α
Θ_{min}/°	3.490
Θ_{max}/°	30.507
Measured Refl's.	23904
Indep't Refl's	11879
Refl's I≥2 s(I)	9988
R_{int}	0.0308
Parameters	425
Restraints	7
Largest Peak	2.184
Deepest Hole	-1.404
GooF	1.051
wR_2 (all data)	0.1085
wR_2	0.1010
R_1 (all data)	0.0527
R_1	0.0424

Similarly to **8a**, there are also several disorders in the crystal structure of **8b**. Two compounds have been found: one main component, where the Sb atoms are substituted with an additional atom X (H or Cl) and a minor component, where there is no additional substitution on the Sb atoms. The main compound also consists of 3 possible isomers: 1) both X = H; 2) both X = Cl; 3) X_1 = H; X_2 = Cl. The actual composition in the crystal could not be determined via single crystal X-Ray diffractometry.

5.4.4 Computational Details

The geometries of the compounds have been fully optimized with gradient-corrected density functional theory (DFT) in form of Becke's three-parameter hybrid method B3LYP[32] with def2-TZVP all electron basis set (ECP on Sb).[33] Gaussian 16 program package[34] was used throughout. All structures correspond to minima on their respective potential energy surfaces as verified by computation of second derivatives. Basis sets were obtained from the EMSL basis set exchange database.[35] Standard entropies of the reactions in solution were estimated by taking the entropy of the solvation of one gaseous mole in the inert solvent (90 J mol^{-1} K^{-1}) into account.[36]

The Computational results show that reaction (1) is exothermic by 18 kJ mol^{-1}.

1 + ½ Ga_2Cl_6 = ½ **2** + $GaCl_3 \cdot THF$ (1)

However, dissociation of **2** into two $SbCl\{Cr(CO)_5\}_2$ monomers in the gas phase is predicted to be endothermic only by 2 kJ mol^{-1}, with entropy favoring dissociation both in the gas phase and in solution. Optimized gas phase structure of **2** is markedly different from the experiment: the Sb-Cl distances are almost equal (2.692-2.696 Å) while in experiment they are markedly different: 2.5093(9) and 2.8997(10) Å. The analysis of bonding situation reveals that in case of optimized structure, there are several MOs responsible for the interaction in the Sb_2Cl_2 cycle: for σ-bonding Sb-Cl there are HOMO-19, smaller contribution is also provided by HOMO-27, and for π-bonding there are HOMO-15 and HOMO-16, which involve p-orbitals of bridging Cl atoms (cf. Table 5.4). Note that both HOMO-16 and HOMO-15 are delocalized other all four atoms in the Sb_2Cl_2 symmetric ring. In contrast, for **2** in the experimental geometry HOMO-19 is more localized at Cl atoms, and π-bonding HOMO-15 is localized between Sb and Cl atoms at shorter interatomic distance. This leads to very different Sb-Cl Wiberg bond index (WBI) values for the experimental (0.536 and 0.251) and optimized (0.401 and 0.397) structures, while the sum of WBIs for two Sb-Cl bonds are close: 0.787 at experimental and 0.798 at optimized geometry. Since **2** is stable in the solid state, it is expected that **2** is additionally stabilized via intermolecular interactions in the solid state. There are Sb…OC contacts of 3.448 and 3.872 Å. The single point energy difference between optimized structure and structure in experimental solid state geometry is 41 kJ mol^{-1}. Taking into account that this energy difference also includes rearrangement of $Cr(CO)_5$ groups, one can assume that the energy difference for the structures with the different position of bridging Cl atoms is not large, and in this case packing effects should play a role. In order to estimate the stabilization, a fragment of the solid state structure of **2**, containing three molecules of **2**, was computed. In order to understand the trends in bonding situation, the monomeric SbCl, its dimers and their complexes with one and two $Cr(CO)_5$ moieties were also considered. For the isolated gas phase SbCl the triplet state is a ground state, which is by 100 kJ mol^{-1} lower in energy

compared to the singlet state. Dimerization of the "naked" triplet SbCl with formation of singlet *trans*-Cl-Sb=Sb-Cl is exothermic by 191 kJ mol^{-1} (per mole of dimer). The trapezoid *cis*-isomer is by 14 kJ mol^{-1} less stable, and the structures with bridging Cl atoms are found to be high order stationary points, lying more than 260 kJ mol^{-1} higher in energy. The Wiberg bond index (WBI) for the Sb-Sb bond in *trans*-Cl-Sb=Sb-Cl is 1.885, indicating high double bond character. Complex formation of *trans*-Cl-Sb=Sb-Cl with two $Cr(CO)_5$ is exothermic by 126 kJ mol^{-1} and results in antimony-antimony bonded dimer *trans*-Cl{$Cr(CO)_5$}SbSb{$Cr(CO)_5$}Cl. The Sb=Sb double bond becomes weaker upon complex formation (WBI 1.218), the Sb-Cr WBI is 0.823.

Note also, that the exothermic (-117 kJ mol^{-1}) complexation of SbCl even with one $Cr(CO)_5$ molecule also strongly favors the singlet state, which for SbCl·$Cr(CO)_5$ complex is by 57 kJ mol^{-1} lower in energy compared to the triplet. Its Complex with two $Cr(CO)_5$ molecules, SbCl{$Cr(CO)_5$}$_2$, has a singlet ground state, which is by 93 kJ mol^{-1} lower in energy compared to the triplet state. The Interaction of triplet SbCl with two $Cr(CO)_5$ is exothermic by 234 kJ mol^{-1}, which is twice larger as the exothermicity of the interaction with one $Cr(CO)_5$. Thus, the exothermicity of the subsequent reaction of SbCl with the first (117) and the second (117) molecule of $Cr(CO)_5$ is the same, indicating similar type of chemical bonding and independence of interaction on the presence of the first $Cr(CO)_5$. This can be explained by the model, in which SbCl in the singlet ground state has two lone pairs and a vacant orbital. The two lone pairs coordinate to $Cr(CO)_5$, while the vacant orbital on Sb (LUMO of SbCl{$Cr(CO)_5$}$_2$, cf. Table 5.3) allows to interaction with Lewis bases, such as THF, amines, phosphines, and also dimerization with neighboring monomeric SbCl{$Cr(CO)_5$}$_2$ via accepting a lone pair from Cl atom. Taking into account, that Sb^+ is valence-isoelectronic to "tetrilones" (neutral group 14 element compounds in the excited singlet electronic state), its bonding can be satisfactorily described using donor-acceptor interactions in its singlet electronic state. Very recently, a donor-stabilized Sb^+ was reported by Roesky.[37] In the present report, the SbCl is stabilized by two Lewis acids and acts as a Lewis acid towards itself and N,P-containing Lewis bases.

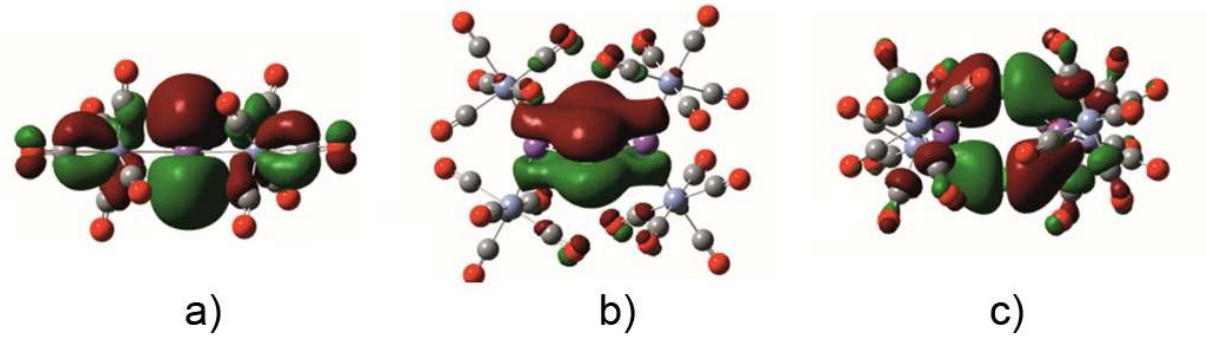

Figure 5.15*: a) LUMO of SbCl{$Cr(CO)_5$}$_2$ (side view); b) HOMO-16 (perspective view) and c) HOMO-16 (top view) of 2 (both compounds at gas phase optimized geometries).*

Table 5.1: *MOs of SbCl (triplet ground state).*

αMO	Energy, eV	Shape	βMO	Energy, eV	Shape
UMO	-0.0732	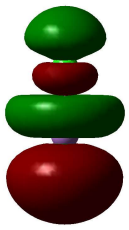	UMO	-0.0578	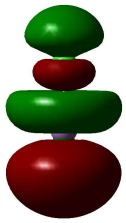
SOMO	-0.2236	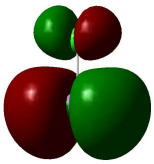	UMO	-0.1251	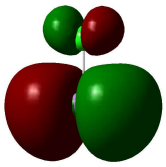
SOMO	-0.2236	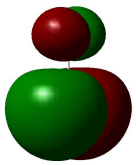	UMO	-0.1251	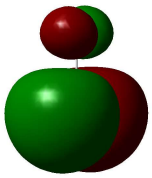
SOMO	-0.3402	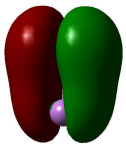	SOMO	-0.2275	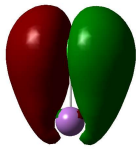
SOMO	-0.3402	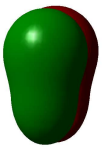	SOMO	-0.2275	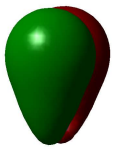

SOMO -0.3597

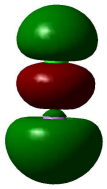

SOMO -0.3471

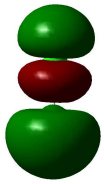

SOMO -0.5594

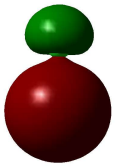

SOMO -0.5136

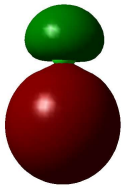

SOMO -0.8133

SOMO -0.8063

Table 5.2: *MOs of SbCl (singlet state).*

MO	Energy, eV	Shape	MO	Energy, eV	Shape
LUMO+2	+0.1086	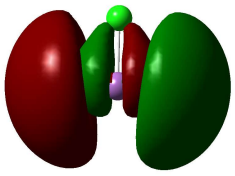	LUMO +1	-0.0672	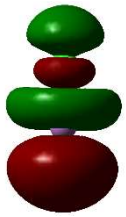
LUMO	-0.1651	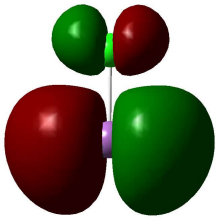 front view	LUMO	-0.1651	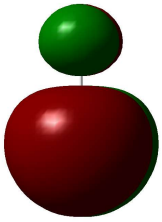 side view
HOMO	-0.1891	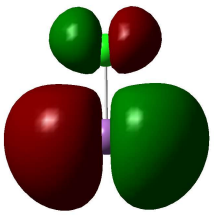 front view	HOMO	-0.1891	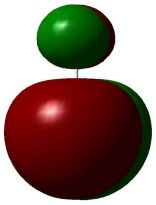 side view
			HOMO-1	-0.3376	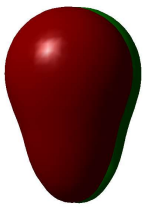
HOMO-2	-0.3344	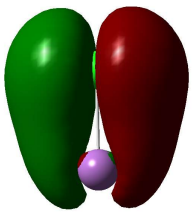	HOMO-3	-0.3596	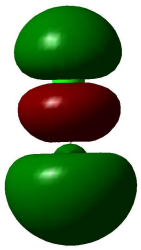

Table 5.3: *MOs of $SbCl\{Cr(CO)_5\}_2$ (singlet state).*

MO	Energy, eV	Shape	MO	Energy, eV	Shape
LUMO+9	-0.0447	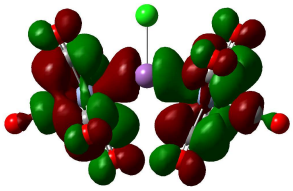	LUMO+8	-0.0456	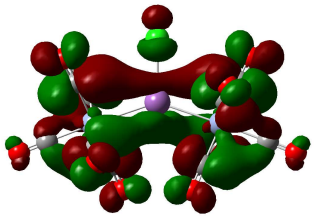
LUMO+7	-0.0513	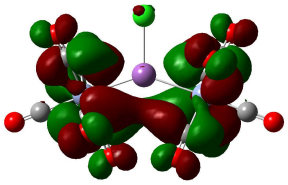	LUMO+6	-0.0534	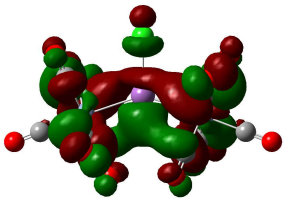
LUMO+5	-0.0549	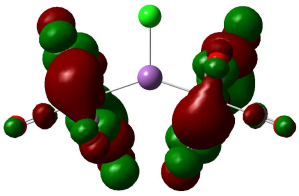	LUMO+4	-0.0579	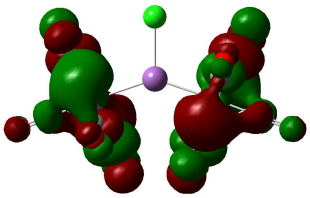
LUMO+3	-0.0596	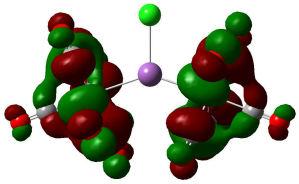	LUMO+2	-0.0692	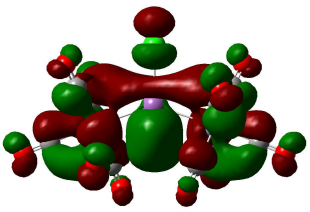
LUMO+1	-0.1039	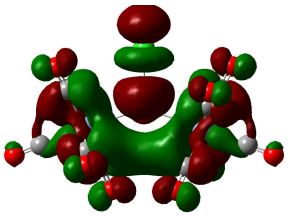	LUMO	-0.1543	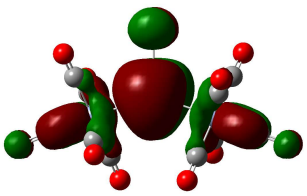
HOMO	-0.2565	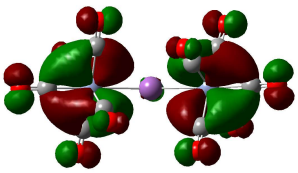	LUMO	-0.1543	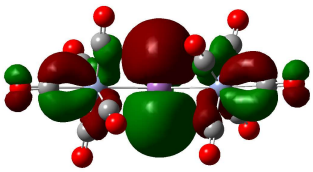
		side view			side view

HOMO -0.2565

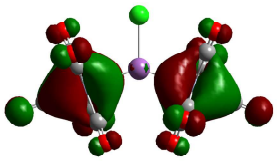

HOMO-1 -0.2610

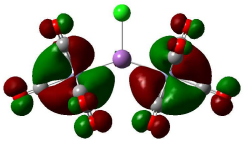

HOMO-2 -0.2653

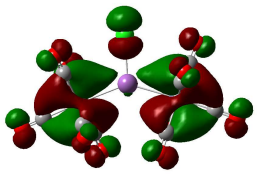

HOMO-3 -0.2673

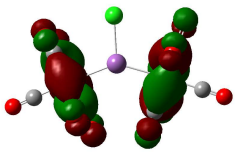

HOMO-4 -0.2681

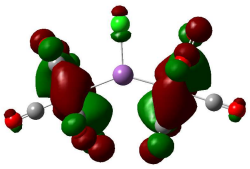

HOMO-5 -0.2797

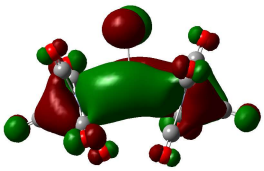

HOMO-6 -0.2847

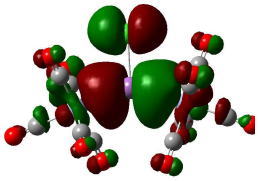

HOMO-7 -0.3488

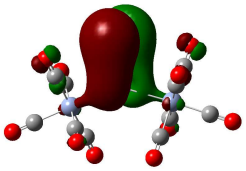

HOMO-8 -0.3505

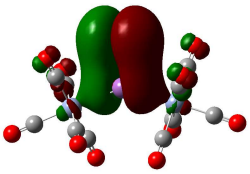

HOMO-9 -0.3774

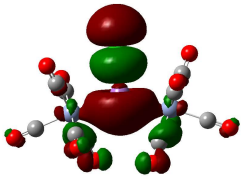

Table 5.4: *Selected MOs of **2** at the experimental geometry (left) and optimized geometry (right).*

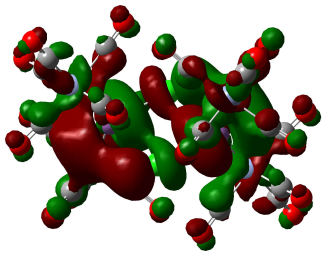

LUMO+2 -0.1205 eV

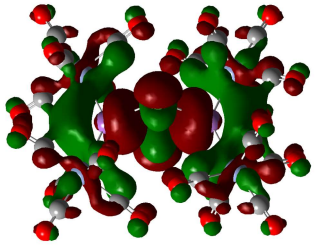

LUMO+2 -0.1294 eV

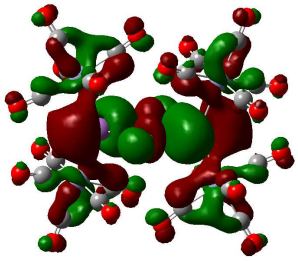

LUMO+1 -0.1274 eV

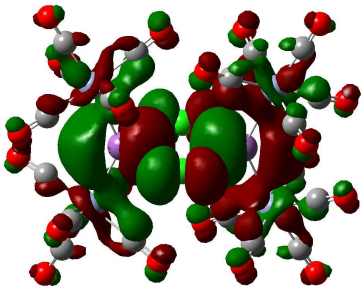

LUMO +1 -0.1398 eV

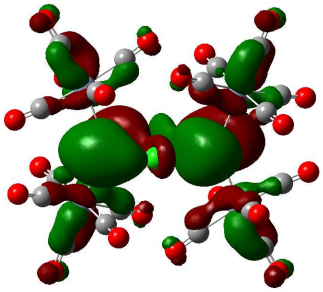

LUMO -0.1546 eV

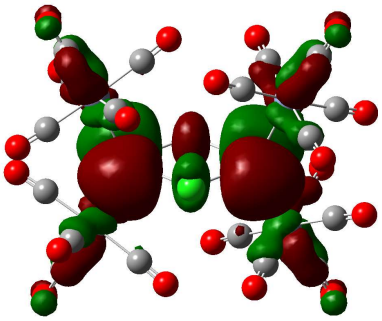

LUMO -0.1509 eV

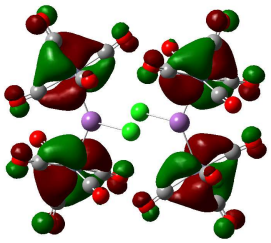

HOMO -0.2587 eV

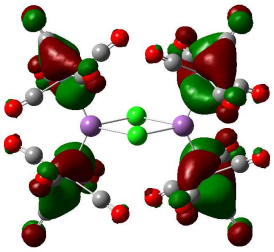

HOMO -0.2591 eV

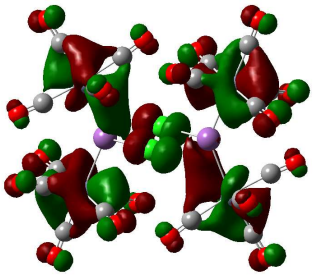

HOMO-6 -0.2684 eV

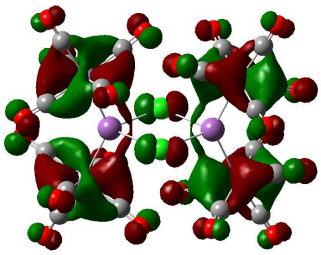

HOMO-6 -0.2678 eV

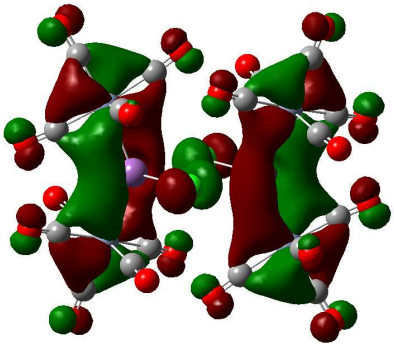

HOMO-10 -0.2744 eV

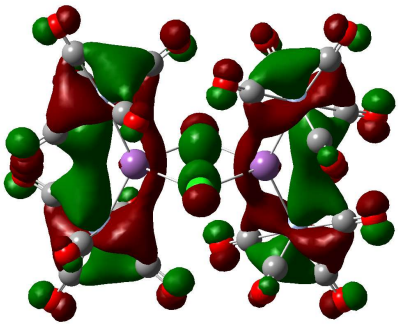

HOMO-10 -0.2710 eV

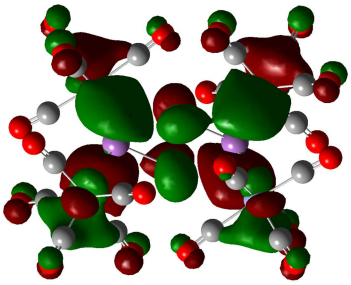

HOMO-11 -0.2849 eV

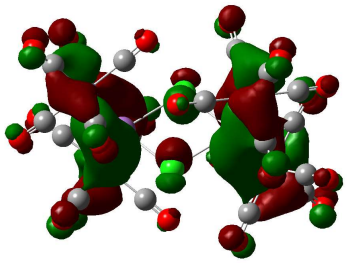

HOMO-11 -0.2800 eV

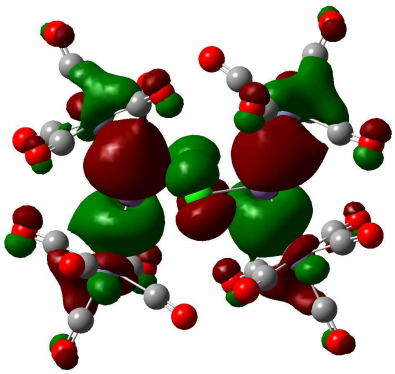

HOMO-12 -0.2870 eV

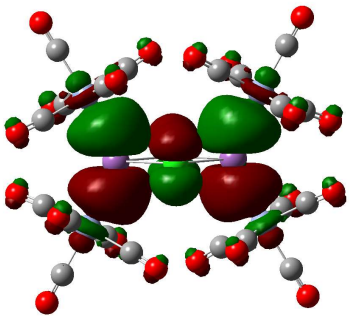

HOMO-12 -0.2848 eV

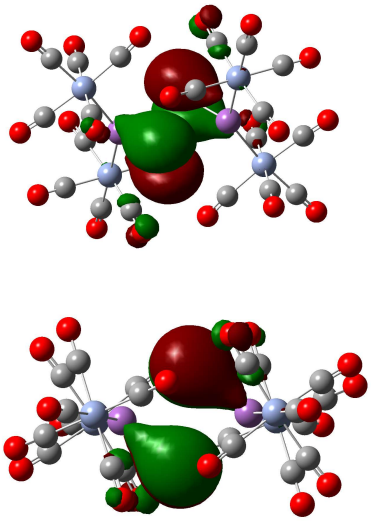

HOMO-15 -0.3522 eV

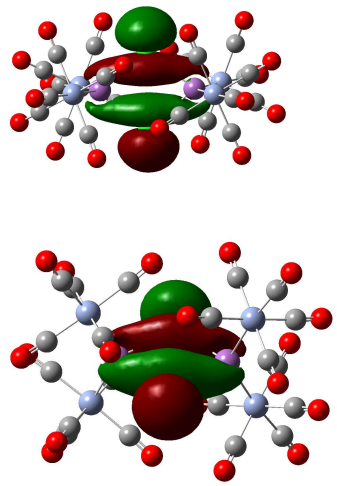

HOMO-15 -0.3593 eV

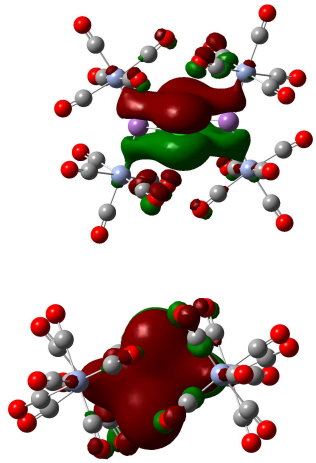

HOMO-16 -0.3705 eV

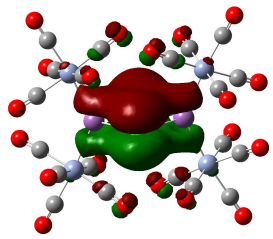

HOMO-16 -0.3750 eV

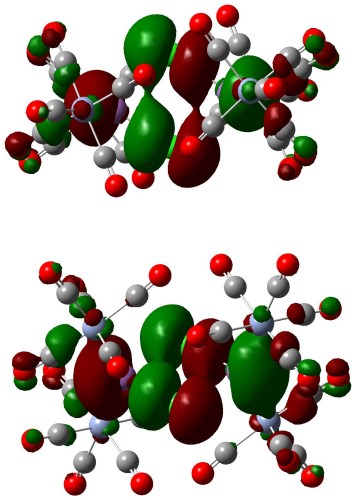

HOMO-17 -0.3796 eV

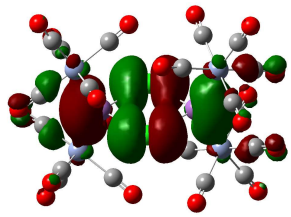

HOMO-17 -0.3766 eV

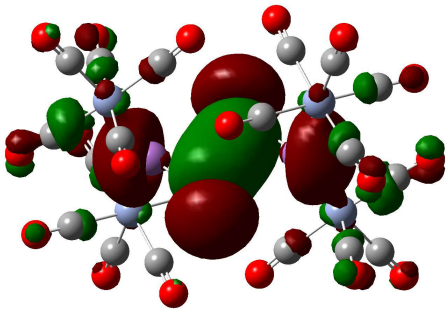

HOMO-18 -0.3979 eV

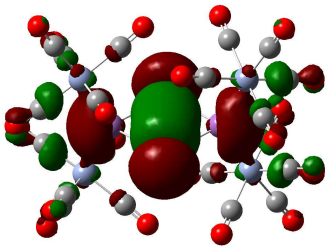

HOMO-18 -0.3997 eV

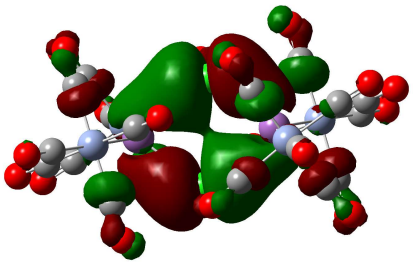

HOMO-19 -0.4032 eV

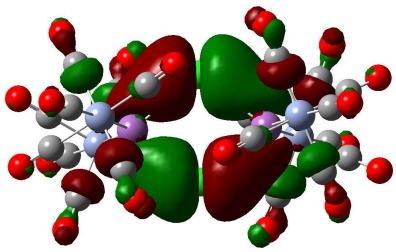

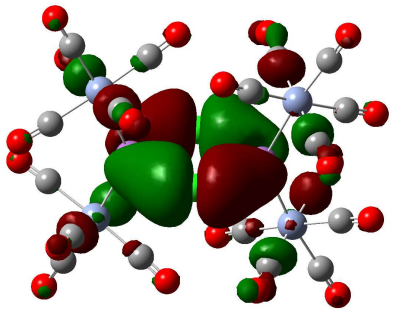

HOMO-19 -0.4087 eV

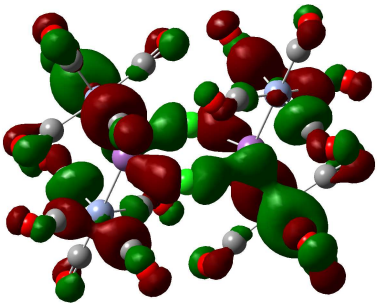

HOMO-27 -0.4410 eV

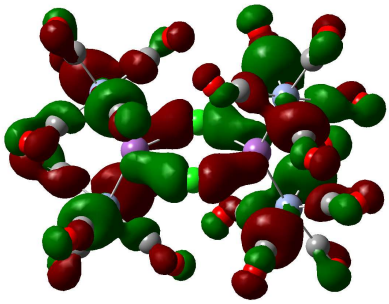

HOMO-27 -0.4413 eV

Table 5.5: *Optimized bond lengths (Å) and corresponding WBI for selected compounds. B3LYP/def2-TZVP (ECP on Sb) level of theory.*

Compound	R (Sb-Cl)	WBI (Sb-Cl)	R (Sb-Cr)	WBI (Sb-Cr)	R (Sb-Sb)	WBI (Sb-Sb)	Cl-Sb-Cr	Cr-Sb-Cr	Cl-Sb-Sb
SbCl (triplet)	2.367	0.806							
$SbClCr(CO)_5$ (triplet)	2.370	0.572	2.747	0.696			109.9		
SbCl (singlet)	2.357	0.981							
$SbClCr(CO)_5$ (singlet)	2.388	0.847	2.530	1.209			106.7		
$SbCl\{Cr(CO)_5\}_2$ (singlet)	2.391	0.802	2.558	0.963			108.6	142.8	
$[SbCl\{Cr(CO)_5\}_2]_2$ (opt.)	2.693	0.400	2.576	0.890			107.5	132.5	
	2.696	0.397		0.892			108.9		
	2.692	0.401							
	2.696	0.397							
$[SbCl\{Cr(CO)_5\}_2]_2$ (exp.)	2.509	0.536	2.513	0.910			107.2	137.3	
	2.900	0.251	2.517	0.898			108.6		
cis_ClSbSbCl (singlet) C_{2v}	2.371	0.840			2.686	1.854			103.4
trans_ClSbSbCl (singlet) C_{2h}	2.397	0.790			2.664	1.885			94.6
Dimer trans $Cl\{Cr(CO)_5\}SbSb\{Cr(CO)_5\}Cl$	2.389	0.775	2.615	0.823	2.744	1.218	112.7		94.7

5.5 References

[1] A. Igau, H. Grutzmacher, A. Baceiredo, G. Bertrand, *J. Am. Chem. Soc.* **1988**, *110*, 6463.

[2] A. J. Arduengo, R. L. Harlow, M. Kline, *J. Am. Chem. Soc.* **1991**, *113*, 361.

[3] F. Dielmann, O. Back, M. Henry-Ellinger, P. Jerabek, G. Frenking, G. Bertrand, *Science* **2012**, *337*, 1526.

[4] K. Lammertsma in *Topics in Current Chemistry*, *Vol. 229* (Eds.: J.-P. Majoral, T. Chivers), Springer, Berlin, **2003**, pp. 95–119.

[5] M. E. García, D. García-Vivó, A. Ramos, M. A. Ruiz, *Coord. Chem. Rev.* **2017**, *330*, 1.

[6] G. Huttner, K. Evertz, *Acc. Chem. Res.* **1986**, *19*, 406.

[7] Y. Pang, M. Leutzsch, N. Nöthling, J. Cornella, *J. Am. Chem. Soc.* **2020**, *142*, 19473.

[8] a) J. von Seyerl, G. Huttner, *Angew. Chem. Int. Ed. Engl.* **1978**, *17*, 843; b) J. von Seyerl, G. Huttner, *Angew. Chem.* **1978**, *90*, 911.

[9] U. Weber, L. Zsolnai, G. Huttner, *J. Organomet. Chem.* **1984**, *260*, 281.

[10] B. Sigwarth, U. Weber, L. Zsolnai, G. Huttner, *Chem. Ber.* **1985**, *118*, 3114.

[11] U. Weber, G. Huttner, O. Scheidsteger, L. Zsolnai, *J. Organomet. Chem.* **1985**, *289*, 357.

[12] M. Shieh, Y.-H. Li, C.-H. Lin, T.-Y. Sun, *Inorg. Chem.* **2020**, *59*, 16073.

[13] A. Strube, G. Huttner, L. Zsolnai, *J. Organomet. Chem.* **1990**, *399*, 267.

[14] P. Pyykkö, M. Atsumi, *Chem. Eur. J.* **2009**, *15*, 186.

[15] J. von Seyerl, G. Huttner, *J. Organomet. Chem.* **1980**, *195*, 207.

[16] M. M. Siddiqui, S. K. Sarkar, M. Nazish, M. Morganti, C. Köhler, J. Cai, L. Zhao, R. Herbst-Irmer, D. Stalke, G. Frenking et al., *J. Am. Chem. Soc.* **2021**, *143*, 1301.

[17] a) J. von Seyerl, B. Sigwarth, H.-G. Schmid, G. Mohr, A. Frank, M. Marsili, G. Huttner, *Chem. Ber.* **1981**, *114*, 1392; b) J. von Seyerl, B. Sigwarth, G. Huttner, *Chem. Ber.* **1981**, *114*, 1407.

[18] M. Stubenhofer, *Dissertation*, Regensburg, Universität, Regensburg, **2012**.

[19] A. Strube, G. Huttner, L. Zsolani, *J. Organomet. Chem.* **1990**, *399*, 255.

[20] C. von Hänisch, K. Volz, W. Stolz, E. Sterzer, A. Beyer, D. Keiper, B. Ringler, WO 2016/046394 A1, **2015**.

[21] M. Schiffer, B. P. Johnson, M. Scheer, *Z. anorg. allg. Chem.* **2000**, *626*, 2498.

[22] G. Balázs, H. J. Breunig, E. Lork, S. Mason, *Organometallics* **2003**, *22*, 576.

[23] *TopSpin 3.0*, TopSpin 3.0, Bruker BioSpin GmbH, **2010**.

[24] E. Lindner, H. Behrens, S. Birkle, *J. Organomet. Chem.* **1968**, *15*, 165.

[25] W. C. Johnson, A. Pechukas, *J. Am. Chem. Soc.* **1937**, *59*, 2068.

[26] M. Gonsior, I. Krossing, N. Mitzel, *Z. anorg. allg. Chem.* **2002**, *628*, 1821.

[27] G. Balázs, H. J. Breunig, E. Lork, W. Offermann, *Organometallics* **2001**, *20*, 2666.

[28] O. V. Dolomanov, L. J. Bourhis, R. J. Gildea, J. A. K. Howard, H. Puschmann, *Appl. Crystallogr.* **2009**, *42*, 339.

[29] *CrysAlis Pro 171.38.46*, CrysAlis Pro Version 171.38.46, Rigaku Oxford Diffraction.

[30] G. M. Sheldrick, *Acta Cryst. A* **2015**, *71*, 3.

[31] G. M. Sheldrick, *Acta Cryst. C* **2015**, *71*, 3.

[32] a) A. D. Becke, J. Chem. Phys. 1993, 98, 5648; b) Lee, Yang, Parr, Phys. Rev. B, Condensed matter 1988, 37, 785.

[33] a) D. Rappoport, F. Furche, J. Chem. Phys. 2010, 133, 134105; b) F. Weigend, R. Ahlrichs, Physical chemistry chemical physics : PCCP 2005, 7, 3297; c) D. Andrae, U. Huermann, M. Dolg, H. Stoll, H. Preu, Theoret. Chim. Acta 1990, 77, 123.

[34] M. J. Frisch, G. W. Trucks, H. B. Schlegel, G. E. Scuseria, M. A. Robb, J. R. Cheeseman, G. Scalmani, V. Barone, G. A. Petersson, H. Nakatsuji et al., Gaussian 16 Rev. B.01, Wallingford, CT, 2016.

[35] a) K. L. Schuchardt, B. T. Didier, T. Elsethagen, L. Sun, V. Gurumoorthi, J. Chase, J. Li, T. L. Windus, J. Chem. Inform. Model. 2007, 47, 1045; b) D. Feller, J. Comput. Chem. 1996, 17, 1571.

[36] A. S. Lisovenko, A. Y. Timoshkin, Inorg. Chem. 2010, 49, 10357.

[37] M. M. Siddiqui, S. K. Sarkar, M. Nazish, M. Morganti, C. Köhler, J. Cai, L. Zhao, R. Herbst-Irmer, D. Stalke, G. Frenking, H. W. Roesky, J. Am. Chem. Soc. 2021, 143, 3, 1301–1306. https://doi.org/10.1021/jacs.0c12084

6 THESIS TREASURY: THE REACTION OF BRIDGING PNICTINIDENE COMPLEXES WITH NUCLEOPHILES

- ⇨ Synthesis and characterizations were carried out by Lena Rummel
- ⇨ X-ray measurements, structure solution and refinement were done by Lena Rummel
- ⇨ X-ray measurements were finalized by Michael Seidl
- ⇨ Figures and manuscript were prepared by Lena Rummel

Preface

In this chapter, preliminary results are presented, which are not fully investigated as of the time of the publication of this thesis. Therefore, the compounds shown in the following pages do not qualify for publication. This chapter's introduction will only brush the body of literature since an in-depth compilation of the state of literature is given at the beginning of this work.

6.1 Introduction

Pnictinidene complexes are versatile compounds which are able to react as nucleophiles or electrophiles, depending on the substituents at the pnictogen atom. Usually, terminal electrophilic phosphinidene complexes are generated from $M(CO)_5$ (M = Cr, Mo, W) complexed 7-phosphanorbornadienes as intermediates, which are subsequently trapped with olefins and alkynes to yield phosphiranes and phosphirenes, respectively.[1] As of now, there are various other examples of electrophilic pnictinidene complexes with one notable group being terminal aminophosphinidene complexes of different transition metals (M) of the type $[(^iPr_2N)_2PM]^+$ investigated in the group of Carty.[2] In our group, we focus on bridging pnictinidene complexes with the general formula $[XE\{M(CO)_5\}_2]$ (**1a**: X = Cp*, E = P, M = W; **1b**: X = Cp*, E = As, M = W; **1c**: X = Cl, E = Sb, M = Cr), which are typically synthesized via salt elimination reactions.[3] According to DFT calculations for **1a**, the HOMO is mainly localized at the diene system of the Cp* substituent, thus being the preferred position for electrophilic attacks. Nucleophilic attacks, on the other hand, can occur at the LUMO, representing the empty p Orbital at the pnictogen atom.[4] As mentioned in chapter 1 of this thesis, a variety of classes of nucleophiles have already been used in the reactions with **1a** and **1b**, for example phosphines[5,6] and isonitriles[7], highlighting the synthetic possibilities arising from using **1a** and **1b** as starting materials. In the light of these results, the question arises whether exchanging the Cp* substituent in **1a** and **1b** for amines, resulting in the corresponding aminopnictinidene complexes, leads to different reaction behavior, especially since the electronic structure of aminopnictinidene complexes is different from the Cp* substituted pnictinidene complexes (cf. chapter 4). The reactivity of the stibinidene complex **1c** is far less investigated than that of the corresponding phosphinidene and arsinidene complexes, however, the research available on this topic revolves mostly about exchanging substituent X or the formation of adducts of the type $[ClSb\{Cr(CO)_5\}_2B]$ with Lewis Bases B.[8] In the following chapter, the reaction behavior of aminophosphinidene complexes as well as stibinidene complex **1c** is investigated and preliminary results are presented.

6.2 Results and Discussion

*6.2.1 Reaction of the aminophosphinidene complex **1d** with $NaPPh_2$*

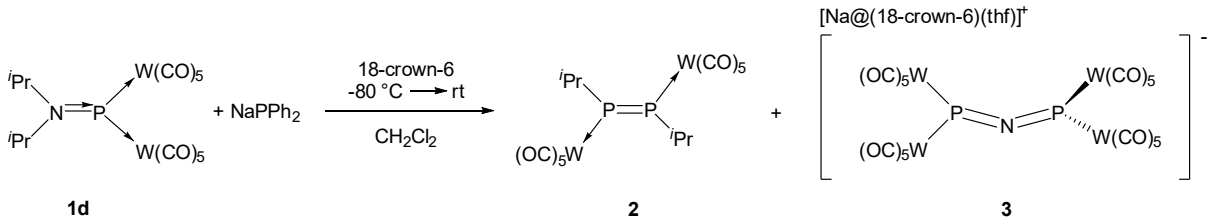

***Scheme 6.1**: Reaction of **1d** with $NaPPh_2$.*

The reaction of the secondary aminophosphinidene complex [^{i}Pr$_2$NP{W(CO)$_5$}$_2$] (**1d**) with $NaPPh_2$ was investigated (cf. Scheme 6.1). The reaction was conducted at -80 °C and after warming the reaction mixture to room temperature, concentration and subsequent layering with n-hexane, a few crystals of the diphosphene derivative [^{i}Pr$_2$NP{W(CO)$_5$}]$_2$ (**2**) were obtained. A possible reaction pathway could be the abstraction of a W(CO)$_5$ moiety from **1d** through $NaPPh_2$ and the formation of [^{i}Pr$_2$NP{W(CO)$_5$}] as an intermediate, which, in turn, can dimerize to give **2**. Unfortunately, upon storing the reaction solution with the crystals at room temperature, **2** could not be isolated, but instead a few crystals of [Na@(18-crown-6)(thf)][{(CO)$_5$W}$_2$P=N=P{W(CO)$_5$}$_2$}] (**3**) were found. Both crystallize as red blocks from the reaction solution. A temperature dependency of the formation of these compounds has to be investigated still. A ^{31}P NMR spectroscopic investigation of the crude reaction mixture showed that there are various P-containing compounds present, so unfortunately it could not be determined which of these signals belong to **2**. In the ^{1}H NMR spectrum of the crude reaction mixture, signals of the *iso*-propyl H atoms were identified, but it is unclear whether they belong to **2** or unreacted starting material. Since after warming the reaction mixture to room temperature, **2** was not present anymore, only a single crystal X-ray structure measurement could be conducted. The molecular structure of the diphosphene derivative **2** is shown in Figure 6.1.

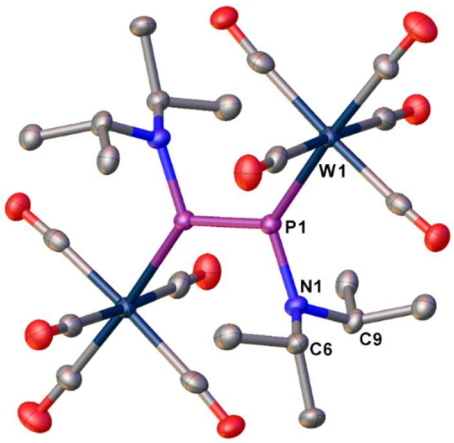

***Figure 6.1**: structure of **2**. Anisotropic displacement parameters are set to 50% probability level. H atoms are omitted for clarity. Selected bond lengths [Å] and angles [°]: W1-P1 2.4825(14), P1-P1^{17} 2.044(3), P1-N1 1.697(5), N1-C6 1.503(7), N1-C9 1.500(6); P1^{17}-P1-W1 131.51(10), N1-P1-W1 124.46(17), N1-P1-P1^{17} 104.01(18), C9-N1-C6 115.8(4).*

It consists of a *trans*-substituted RP=PR diphosphene[9] with N^iPr_2 substituents which are coordinated via the phosphorus lone pairs to two $W(CO)_5$ units. A similar compound – $[Cy_2NP\{W(CO)_5\}]_2$ – was obtained by Sinyashin *et al.* as a dimerization product of the highly reactive electrophilic phosphinidene complex $[Cy_2NPW(CO)_5]$ at room temperature,[10] strengthening the assumption that **2** might also be a dimerization product. As for $\mathbf{3}^-$, the single crystal X-ray structure analysis was not conclusive of whether an N or an O atom was present bridging the two P atoms, but EI mass spectral analysis revealed the molecule ion peak of the N bridging compound. Its molecular structure (cf. Figure 6.2) consist of a P=N=P chain where each P atom is coordinated to two $W(CO)_5$ moieties. The P=N bond distances lie within the double bond range,[11] revealing $\mathbf{3}^-$ to be an azide-analogous compound i.e. 1,3-diphosphaazide. Both P atoms have a trigonal planar geometry and the $P\{W(CO)_5\}_2$ moieties are twisted in a 93.1 ° angle to each other. The P units are connected through the N atom, forming a P-N-P angle of 150.0(0) °.

A similar, albeit electronically different, organosubstituted compound, $HN[P(^iPr)_2]_2$, has been reported as a versatile ligand in CO_2 insertion reactions or in the formation of the first neutral *catena-4* bismuth derivative. The P-N distances of $\mathbf{3}^-$ are similar to the P-N bond lengths of the deprotonated $N[P(^iPr)_2]_2^-$ as a ligand (1.623(6)–1.643(7) Å).[12]

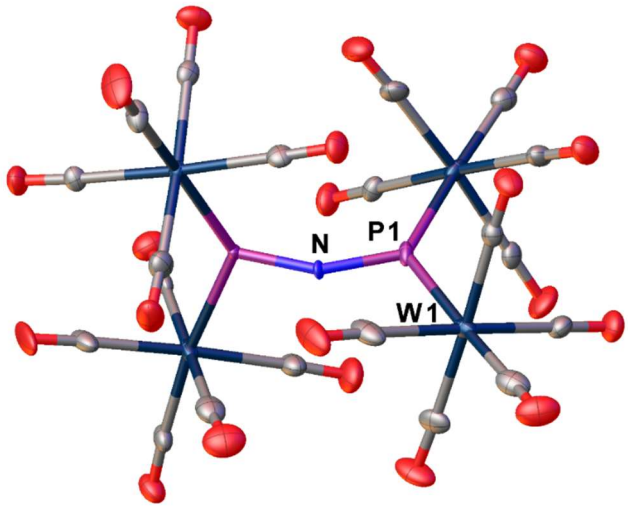

***Figure 6.2**: Molecular structure of **3**. Anisotropic displacement parameters are set to 50% probability level. Cation is omitted for clarity. Selected bond lengths [Å] and angles [°]: W2-P1 2.410(2), W1-P1 2.463(2), P1-N1A 1.648(19), P2B-N1A 1.605(12); W2-P1-W1 131.24(8), N1A-P1-W2 126.7(5), N1A-P1-W1 120.0(6), P2B-N1A-P1 150.0(10), P2a-N1B-P1 169.9(11).*

Clearly, further investigations need to be made to determine whether **2** is present in the starting material or formed during the reaction. Another future point of research is the investigation of the reaction pathway and reaction conditions for the formation of **3** and **2**. Additionally, it needs to be investigated if the proposed reaction of PPh_2^- with **1d** takes place and an adduct of the type $[^iPr_2N(PPh_2)P\{W(CO)_5\}_2]^-$ is formed.

6.2.2 Reactions of the stibinidene complex **1c** with Nucleophiles

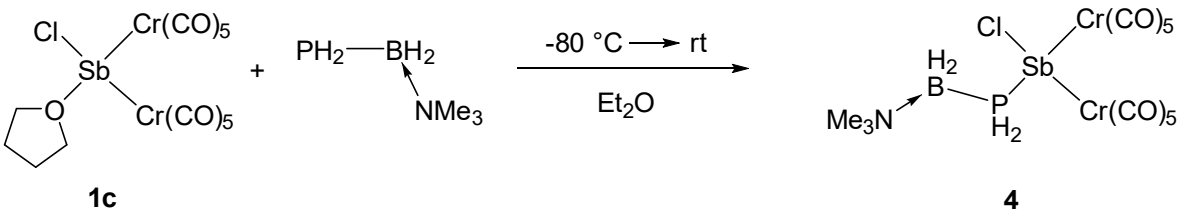

***Scheme 6.2**: Reaction of **1c** with $H_2PBH_2{\cdot}NMe_3$.*

The reaction of **1c** with $H_2PBH_2{\cdot}NMe_3$ in Et_2O at low temperatures results in the formation of $[ClSb\{Cr(CO)_5\}_2PH_2BH_2{\cdot}NMe_3]$ (**4**, cf. Scheme 6.2), which crystallizes as yellow blocks from the reaction solution in 10 % yield. Due to their high sensitivity towards moisture and air, it was not possible to conduct long-time NMR experiments or elemental analysis so far. In the ^{1}H NMR spectrum of **4**, signals at 2.65 ppm, 2.71 ppm and 3.00 ppm were detected which could not be assigned doubtlessly. The $^{31}P\{^1H\}$ NMR spectrum of the yellow blocks shows two singlets at -180.0 ppm and -182.0 ppm, respectively. Compound **4** cannot be doubtlessly assigned to one of these signals, although it can be assumed that the other signal is caused by a very similar compound. The signals are more upfield shifted compared to the phosphanylborane-substituted derivative $[Cp^*P\{W(CO)_5\}_2PH_2BH_2{\cdot}NMe_3]$ (PH_2: $\delta(^{31}P)$ = -56.7 ppm[5]), which can be explained with the coordination to the Sb in **4**. Additionally, the ^{31}P NMR chemical shift of the free phosphanylborane $PH_2BH_2{\cdot}NMe_3$ is found at -215.5 ppm (C_6D_6),[13] further underlining the assumption that in **4** the P nucleus of the PH_2 group is more shielded than in the phosphinidene analog. The mass spectrum of the dissolved crystals in CH_2Cl_2 does not show a molecule ion peak of **4** but only fragments, underlining its unstable nature. The molecular structure of **4** is shown in Figure 6.3.

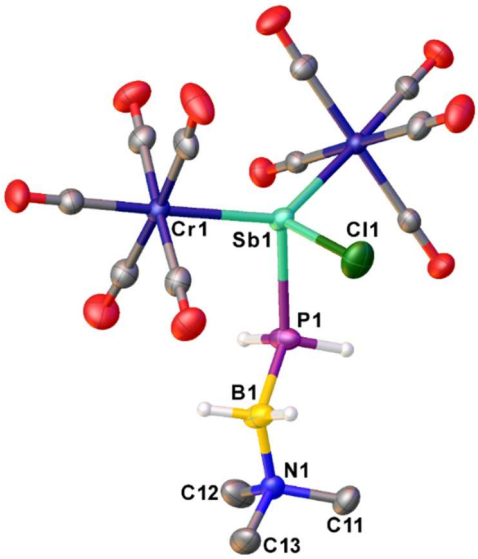

***Figure 6.3**: Molecular structure of **4**. Anisotropic displacement parameters are set to 50% probability level. H atoms omitted for clarity. Selected bond lengths [Å] and angles [°]: Sb1-Cr1 2.6185(5), Sb1-Cr2 2.6148(6), Sb1-P1 2.5616(16), Sb1-Cl1 2.3910(10), P1-B1 1.977(4), N1-B1 1.591(5); Cr2-Sb1-Cr1 134.813(17), P1-Sb1-Cr2 105.81(4). P1-Sb1-Cr1 103.46(4), Cl1-Sb1-Cr2 105.17(3), Cl1-Sb1-Cr1 109.84(3), Cl1-Sb1-P1 87.39(5), B1-P1-Sb1 117.91(15), C12-N1-C11 108.5(3), C11-N1-C13 107.7(3), C12-N1-C13 108.7(3), N1-B1-P1 112.1(3).*

It consists of a $[ClSb\{Cr(CO)_5\}_2]$ unit attached to a $PH_2BH_2{\cdot}NMe_3$ molecule via the Sb atom, resulting in a tetrahedral geometry at the Sb, which is distorted because of the steric bulk of the $Cr(CO)_5$ moieties. The Sb-P distance (2.5616(16) Å) lies in the typical single bond range.[11]

In search for ways to change the reactivity of **1c**, attempts were made to replace the Cl substituent. Previous attempts synthesizing $[Cp^xSb\{Cr(CO)_5\}_2]$ (Cp^x = Cp, Cp*; Cp* = C_5Me_5) were successful, but the high sensitivity of these complexes towards light, temperature and air, especially in solution, made it difficult to use them for synthetic purposes.[14] Choosing Cp'''Na (Cp''' = 2,4,6-tri-tert-butyl-cyclopentadienyl) as the reaction partner for **1c**, we hoped that the increased steric bulk of the substituent would result in a stibinidene complex that was easier to handle than the previously synthesized Cp^x substituted ones and at the same time would show a different reactivity in comparison to **1c**. Unfortunately, in the reaction, only a few crystals of the 1D polymer $[\{Na(18\text{-}c\text{-}6)\}\{ClCr(CO)_5\}]_n$ (**5**) could be obtained after workup of the crude reaction solution. The polymer consists of a $[ClCr(CO)_5]^-$ unit that is connected to a $[Na(18\text{-crown-}6)]^+$ moiety via one CO group on one side and through a Cl^- ion on the other side. An excerpt of its molecular structure is shown in Figure 6.4.

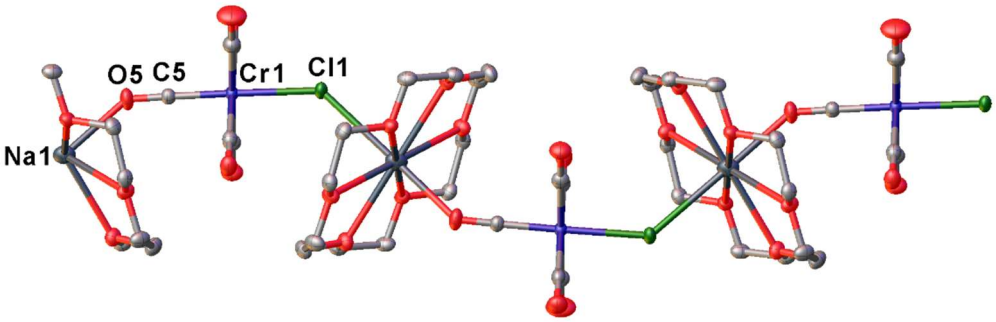

Figure 6.4: *Excerpt of the molecular structure of **5**. Anisotropic displacement parameters are set to 50 % probability level. H atoms omitted for clarity. Selected bond lengths [Å] and angles [°]: Cr1-Cl1 2.5135(10), Na1-O5 2.398(3); C6-Cr-Cl1 178.87(9), C5-O5-Na1 140.0(2).*

6.3 Conclusion

The reaction of **1d** with $NaPPh_2$ resulted in the formation of the diphosphene complex **2** and the azide-analogous complex **3**. Only a few crystals suitable for X-ray analysis of both compounds could be obtained in the reaction. The reaction pathway remains unclear and is a subject of future investigations.

A novel phosphanylborane-substituted stibinidene complex, **4**, was generated in the reaction of **1c** with $PH_2BH_2{\cdot}NMe_3$. Its full chemical analysis could not yet be conducted due to its high air and moisture sensitivity. Nonetheless, it is a representative of nucleophile-substituted stibinidene complexes. The attempt to exchange the Cl substituent in **1c** with Cp''' via the reaction of **1c** with Cp'''Na was unsuccessful but instead resulted in the formation of a few crystals of the 1D polymer **5**. For both compounds, a full analysis has to be conducted in the future.

6.4 Experimental

6.4.1 Working techniques

The following reactions were carried out under an atmosphere of dry Nitrogen or Argon using standard Schlenk techniques. Traces of O_2 and water were eliminated by leading the inert gas (N_2 or Ar) through a copper catalyst heated to 145 °C, subsequently washing it with concentrated sulphuric acid and drying it with orange gel and phosphorous pentoxide. Solvents were either collected from a solvent purification system (MBraun SPS 800) or dried, degassed and distilled according to standard techniques. Before use, the diatomaceous earth required for filtration was stored at 110 °C. The **NMR spectra** were recorded on a BRUKER Avance 300 (^{1}H: 300.13 MHz, ^{13}C: 75.48 MHz, ^{31}P: 121.49 MHz) or Avance 400 (^{1}H: 400.13 MHz, ^{13}C: 100.61 MHz, ^{31}P: 161.98 MHz) spectrometer at room temperature unless stated otherwise. Chemical shifts δ refer to external standards of tetramethylsilane (^{1}H, ^{13}C NMR) and 85 % phosphoric acid (^{31}P NMR, ^{31}P{^{1}H} NMR), respectively, and are given in ppm. Coupling constants J are given in Hz without consideration of absolute signs. Analyses and graphic representations of the spectra were prepared with *TopSpin 3.0.* **Infrared spectra** were recorded in solution (CH_2Cl_2) with a ThermoScientific Nicolet iS5 spectrometer using the iD5 Transmission element or as solids using an ATR element equipped with a Diamond or Ge crystal. **Mass spectra** were recorded on a Jeol AccuTOF GCX (FD) spectrometer by the mass spectrometry department of the University of Regensburg or a ThermoQuest Finnigan MAT 95 spectrometer. The synthesis of the **starting materials** has been described in previous chapters. Amines were purchased and distilled before further use. $H_2PBH_2{\cdot}NMe_3$ and $NaPPh_2$ have been kindly donated by Matthias Ackermann and Felix Lehnfeld, University of Regensburg. Cp'''Na[16] has been kindly provided by Julian Müller, University of Regensburg.

[16] Cp‘‘‘ = 2,4,6-tri-tert-butyl-cyclopentadienyl

6.4.2 Experimental Data

6.4.2.1 Reaction of [^{i}Pr$_2$NP{W(CO)$_5$}$_2$] with NaPPh$_2$

A solution of 0.2 mL (0.2 mmol, c = 1 mol·L^{-1} in thf) NaPPh$_2$ and 53 mg (0.2 mmol) 18-crown-6 in 5 mL CH_2Cl_2 are added to a solution of 156 mg (0.2 mmol) [^{i}Pr$_2$NP{W(CO)$_5$}$_2$] in 10 mL CH_2Cl_2 at -80 °C. The red solution is stirred and warmed to room temperature for 16 h. After concentrating the solution to ca. 3 mL, the same volume n-hexane is added. Storing the solution at -28 °C, [(^{i}Pr)$_2$NP{W(CO)$_5$}]$_2$ (**2**) crystallizes as a few red blocks from the solution. Upon storing the solution at room temperature, a few red blocks of [Na@(18-crown-6)(thf)]$^+$[{(CO)$_5$W}$_2$P=N=P{W(CO)$_5$}$_2$]$^-$ (**3**) suitable for X-ray analysis could be obtained.

Analytical data for **2**:

Yield:	few crystals
^{1}H NMR (CD_2Cl_2, 400 MHz):	δ [ppm] = 1.43 (d, $^3J_{HH}$ = 6.5 Hz, 12H, CH_3), 3.34 (m, $^2J_{HH}$ = 13.2 Hz, 2H, CH).

Analytical data for **3**:

Yield:	few crystals
MS (EI, 70eV):	Anions: *m/z* (%) = 1371.7 (100) [M$^-$], 966.9 (60) [M$^-$ -W(CO)$_5$ -3CO], 680.8 (20) [M$^-$ -NP{W(CO)$_5$}$_2$].

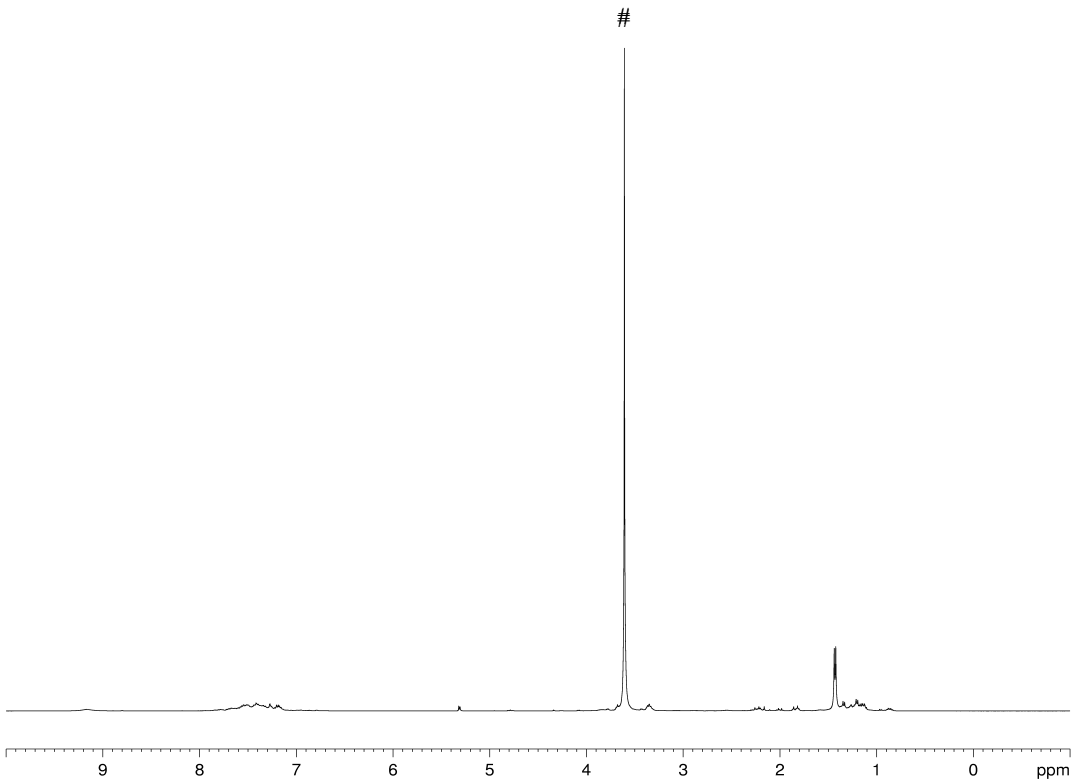

***Figure 6.5**. Crude ^{1}H NMR spectrum of the reaction of [^{i}Pr$_2$NP{W(CO)$_5$}$_2$] and NaPPh$_2$ in CD_2Cl_2. # = 18-c-6.*

6.4.2.2 Reaction of 1c with $H_2PBH_2{\cdot}NMe_3$

A solution of 0.4 mL (0.2 mmol) $H_2PBH_2{\cdot}NMe_3$ in 5 mL Et_2O is added dropwise to a red solution of 123 mg (0.2 mmol) **1c** in 15 mL Et_2O at -80 °C. The reaction mixture gets brighter and upon warming to room temperature turns orange and then red. $[ClSb\{Cr(CO)_5\}_2PH_2BH_2{\cdot}NMe_3]$ (**4**) crystallizes as yellow blocks from the reaction solution.

Analytical data for **4**:

Yield:	10 mg (10 %).
MS (FD):	*m/z* (%) = 520.9 $[M^+ -2H -NMe_3 -CO]$ (100), 420.0 $[M^+ -PH_2BH_2NMe_3 -3CO]$ (62), 326.0 $[M^+-4H -NMe_3 -Cr(CO)_6 -Cl]$ (67).

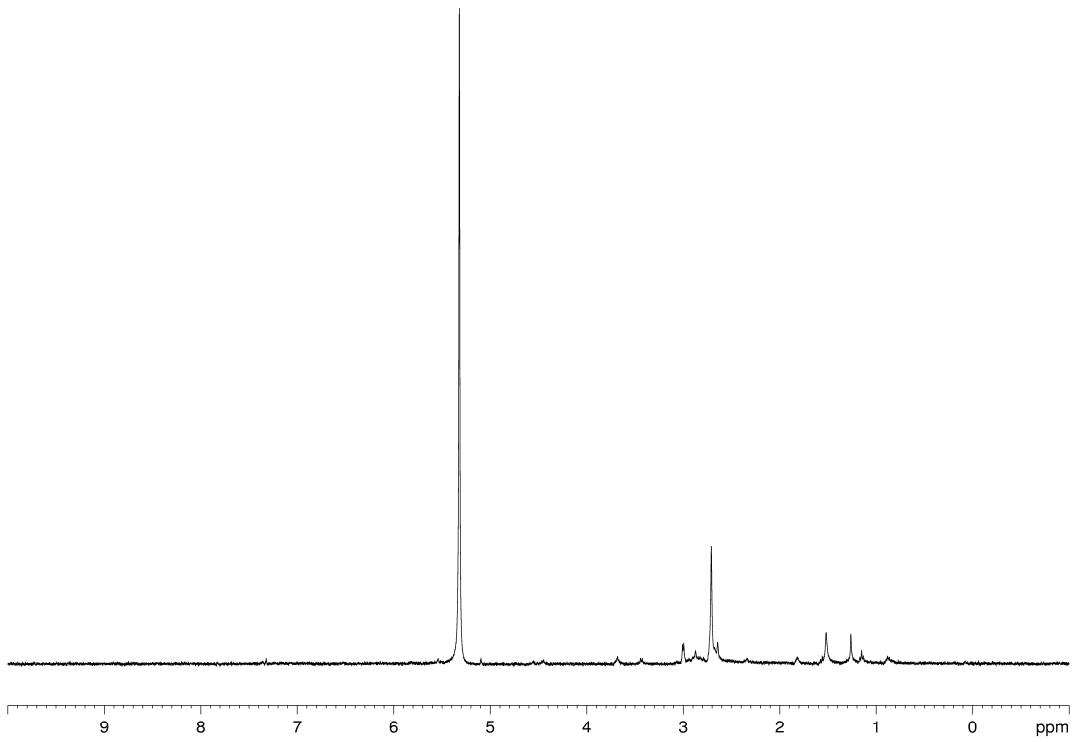

Figure 6.6. *^1H NMR spectrum of crystalline **4** in CD_2Cl_2.*

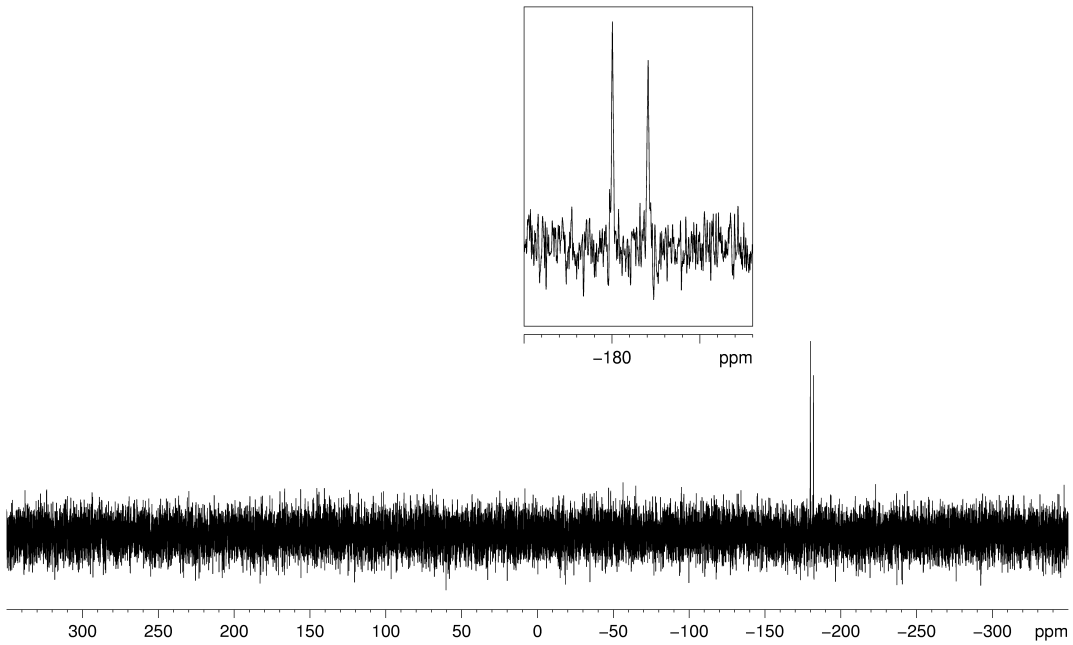

Figure 6.7. $^{31}P\{^{1}H\}$ NMR spectrum of crystalline **4** in CD_2Cl_2.

6.4.2.3 Reaction of 1c and NaCp'''

A Schlenk flask with 51 mg (0.2 mmol) Cp'''Na, 123 mg (0.2 mmol) **1c** and 53 mg (0.2 mmol) 18-crown-6 is cooled to -90 °C. 20 mL thf are added and the resulting brownish-orange suspension is then stirred and warmed to room temperature, where the suspension turns into a clear brownish-orange solution, which is dried in vacuo. The brown residue is extracted with Et_2O and filtered, leaving a yellow filtrate, which is concentrated and layered with *n*-pentane in a 1:2 ratio. The 1D polymer $[\{Na(18\text{-}c\text{-}6)\}\{ClCr(CO)_5\}]_n$ (**5**) crystallizes as yellow blocks from the layered solution at room temperature.

Yield: few crystals.

6.4.3 Crystallographic Data

Single crystal X-ray structure analyses were either carried out on a Gemini Ultra Diffractometer (Rigaku Oxford Diffraction, formerly Agilent Technologies) or on a XtaLAB Synergy R, DW system. The Gemini Ultra diffractometer was equipped with either a molybdenum X-ray radiation source (Mo-K_α = 0.71072 Å) or a copper X-ray radiation source (Cu-K_α = 1.5406 Å) and an AtlasS2 CCD detector as well as an Oxford Systems CryoJet cooling system. The XtaLAB Synergy R was equipped with a rotating anode using copper radiation, a HyPix-Arc 150 detector as well as an Oxford Cryosystems CryoStream 700 cooling system.

Due to their air and water sensitivity, the crystals were coated with mineral oil (Sigma Aldrich, CAS 8042-47-5). Suitable single crystals were picked under the microscope from the oil and transferred onto a MiTeGen MicroLoop attached to a goniometer head. The goniometer head was then placed onto the goniometer with the loop sitting in a current of cold nitrogen.

After collection of the crystal structure data, integration and data reduction were carried out with the program *CrysAlisPro.*[15] Structure elucidation was carried out with the program *SHELXT*[16] using direct methods. Refinement occurred with the least squares method with the program *SHELXL.*[17] Both were used within *Olex2*[18] as the platform. Figures of the molecular structures were prepared with the program *Olex2.*[18]

6.4.3.1 Crystal Structure Data for 2

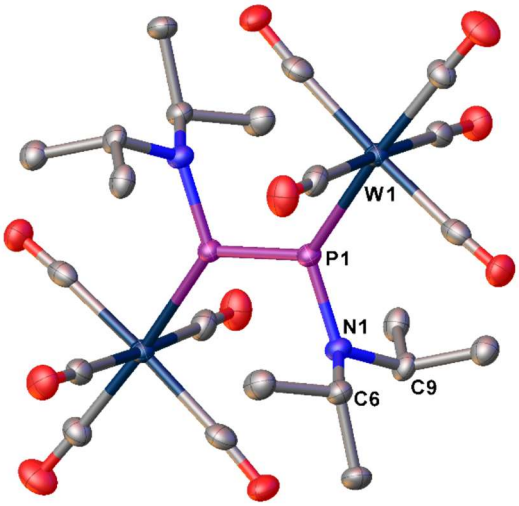

Molecular structure of **2**. Anisotropic displacement parameters are set to 50% probability level. H atoms are omitted for clarity. Selected bond lengths [Å] and angles [°]: W1-P1 2.4825(14), P1-P1[17] 2.044(3), P1-N1 1.697(5), N1-C6 1.503(7), N1-C9 1.500(6); P1[17]-P1-W1 131.51(10), N1-P1-W1 124.46(17), N1-P1-P1[17] 104.01(18), C9-N1-C6 115.8(4).

Compound	**2**
Formula	$C_{22}H_{28}N_2O_{10}P_2W_2$
$D_{calc.}$/ g cm^{-3}	2.091
μ/mm^{-1}	16.016
Formula Weight	910.10
Colour	clear red
Shape	block
Size/mm^3	0.43×0.15×0.13
T/K	123.01(10)
Crystal System	triclinic
Space Group	P-1
a/Å	8.79840(10)
b/Å	9.55180(10)
c/Å	10.48540(10)
α/°	99.3890(10)
β/°	105.6820(10)
γ/°	115.8000(10)
V/Å^3	722.644(15)
Z	1
Z'	0.5
Wavelength/Å	1.54184
Radiation type	Cu K$_\alpha$
Θ_{min}/°	4.630
Θ_{max}/°	75.571
Measured Refl's.	10728
Indep't Refl's	2886
Refl's I≥2 s(I)	2870
R_{int}	0.0353
Parameters	176
Restraints	0
Largest Peak	3.036
Deepest Hole	-3.320
GooF	1.081
wR_2 (all data)	0.1164
wR_2	0.1162
R_1 (all data)	0.0439
R_1	0.0438

[17] 1-x, 1-y, -z

6.4.3.2 Crystal Structure Data for 3

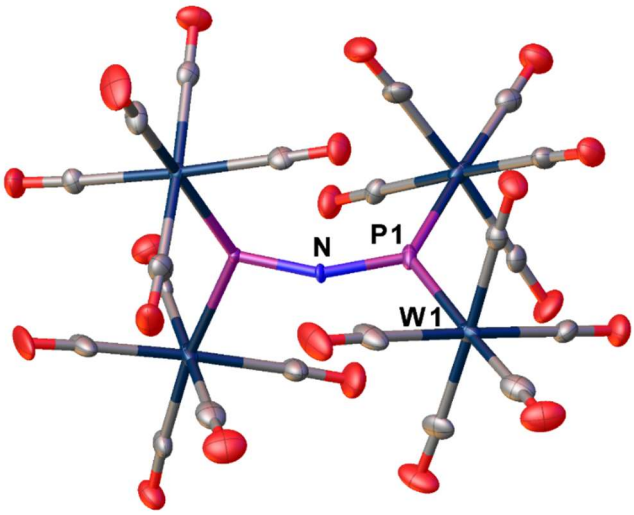

Molecular structure of **3**. Anisotropic displacement parameters are set to 50% probability level. Cation is omitted for clarity. Selected bond lengths [Å] and angles [°]: W2-P1 2.410(2), W1-P1 2.463(2), P1-N1A 1.648(19), P2B-N1A 1.605(12); W2-P1-W1 131.24(8), N1A-P1-W2 126.7(5), N1A-P1-W1 120.0(6), P2B-N1A-P1 150.0(10), P2a-N1B-P1 1699(11).

Compound	**3**
Formula	$C_{36}H_{32}NNaO_{27}P_2W_4$
$D_{calc.}$/ g cm^{-3}	2.347
μ/mm^{-1}	9.525
Formula Weight	1730.95
Colour	clear red
Shape	block-shaped
Size/mm^3	0.52×0.20×0.18
T/K	123.01(10)
Crystal System	triclinic
Space Group	P-1
a/Å	11.8731(8)
b/Å	15.2423(9)
c/Å	16.2536(9)
α/°	111.522(6)
β/°	108.380(7)
γ/°	100.204(5)
V/Å^3	2449.8(3)
Z	2
Z'	1
Wavelength/Å	0.71073
Radiation type	Mo K□
Θ_{min}/°	3.489
Θ_{max}/°	32.924
Measured Refl's.	63493
Indep't Refl's	16770
Refl's I≥2 s(I)	15697
R_{int}	0.0627
Parameters	676
Restraints	50
Largest Peak	2.669
Deepest Hole	-2.736
GooF	1.342
wR_2 (all data)	0.1252
wR_2	0.1234
R_1 (all data)	0.0651
R_1	0.0606

6.4.3.3 Crystal Structure Data for 4

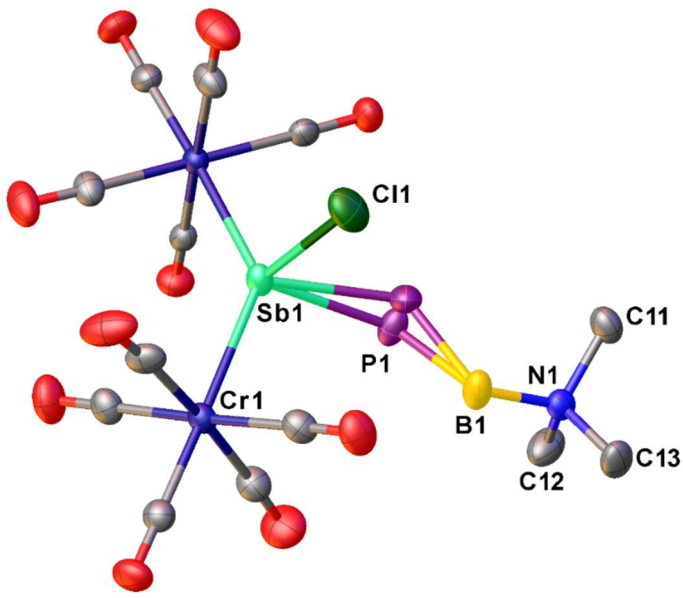

Molecular structure of **4**. Anisotropic displacement parameters are set to 50% probability level. H atoms omitted for clarity. Selected bond lengths [Å] and angles [°]: Sb1-Cr1 2.6185(5), Sb1-Cr2 2.6148(6), Sb1-P1 2.5616(16), Sb1-Cl1 2.3910(10), P1-B1 1.977(4), N1-B1 1.591(5); Cr2-Sb1-Cr1 134.813(17), P1-Sb1-Cr2 105.81(4). P1-Sb1-Cr1 103.46(4), Cl1-Sb1-Cr2 105.17(3), Cl1-Sb1-Cr1 109.84(3), Cl1-Sb1-P1 87.39(5), B1-P1-Sb1 117.91(15), C12-N1-C11 108.5(3), C11-N1-C13 107.7(3), C12-N1-C13 108.7(3), N1-B1-P1 112.1(3).

The P atom in **4** is disordered over two positions. The occupation is as follows: P1 (90 %), P1A (10 %).

Compound	**4**
Formula	$C_{13}H_{13}BClCr_2NO_{10}PSb$
$D_{calc.}$/ g cm^{-3}	1.847
μ/mm^{-1}	2.303
Formula Weight	646.22
Colour	clear yellow
Shape	block
Size/mm^3	0.25×0.19×0.10
T/K	123(1)
Crystal System	monoclinic
Space Group	$P2_1/c$
a/Å	6.7732(4)
b/Å	16.8656(6)
c/Å	20.4161(8)
α/°	90
β/°	94.983(4)
γ/°	90
V/Å^3	2323.40(18)
Z	4
Z'	1
Wavelength/Å	0.71073
Radiation type	Mo K_α
Θ_{min}/°	3.479
Θ_{max}/°	30.506
Measured Refl's.	23457
Indep't Refl's	7079
Refl's I≥2 s(I)	5709
R_{int}	0.0353
Parameters	293
Restraints	6
Largest Peak	1.991
Deepest Hole	-1.050
GooF	1.071
wR_2 (all data)	0.0981
wR_2	0.0912
R_1 (all data)	0.0591
R_1	0.0424

6.4.3.4 Crystal Structure Data for 5

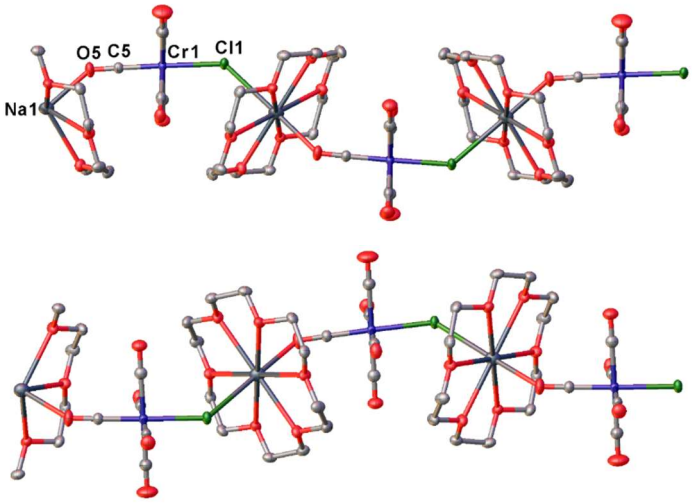

Top: Excerpt of the molecular structure of **5**. Bottom: View along crystallographic plane. Anisotropic displacement parameters are set to 50% probability level. H atoms are omitted for clarity. Selected bond lengths [Å] and angles [°]: Cr1-Cl1 2.5135(10), Na1-O5 2.398(3); C6-Cr-Cl1 178.87(9), C5-O5-Na1 140.0(2).

Compound	**5**
Formula	$C_{17}H_{24}ClCrNaO_{11}$
$D_{calc.}$/ g cm^{-3}	1.513
μ/mm^{-1}	0.698
Formula Weight	514.80
Colour	clear yellow
Shape	block
Size/mm^3	0.40×0.33×0.12
T/K	123(1)
Crystal System	orthorhombic
Space Group	*Pnma*
a/Å	16.3465(5)
b/Å	18.6983(6)
c/Å	7.3932(2)
α/°	90
β/°	90
γ/°	90
V/Å^3	2259.74(12)
Z	4
Z'	0.5
Wavelength/Å	0.71073
Radiation type	Mo K_α
Θ_{min}/°	3.311
Θ_{max}/°	32.356
Measured Refl's.	12862
Indep't Refl's	3829
Refl's I≥2 s(I)	3153
R_{int}	0.0243
Parameters	169
Restraints	0
Largest Peak	0.403
Deepest Hole	-0.349
GooF	1.054
wR_2 (all data)	0.0801
wR_2	0.0752
R_1 (all data)	0.0455
R_1	0.0336

6.4 References

[1] a) A. Marinetti, F. Mathey, J. Fischer, A. Mitschler, *J. Am. Chem. Soc.* **1982**, *104*, 4484; b) A. Marinetti, F. Mathey, J. Fischer, A. Mitschler, *J. Chem. Soc., Chem. Commun.* **1982**, 667.

[2] a) B. T. Sterenberg, K. A. Udachin, A. J. Carty, *Organometallics* **2001**, *20*, 2657; b) B. T. Sterenberg, A. J. Carty, *J. Organomet. Chem.* **2001**, *617-618*, 696; c) B. T. Sterenberg, K. A. Udachin, A. J. Carty, *Organometallics* **2003**, *22*, 3927; d) J. Sánchez-Nieves, B. T. Sterenberg, K. A. Udachin, A. J. Carty, *J. Am. Chem. Soc.* **2003**, *125*, 2404.

[3] K. E. G. Huttner, *Acc. Chem. Res.* **1986**, *19*, 406.

[4] D. Himmel, *Dissertation*, Regensburg, Universität, **2004**.

[5] M. Scheer, C. Kuntz, M. Stubenhofer, M. Zabel, A. Y. Timoshkin, *Angew. Chem. Int. Ed. Engl.* **2010**, *49*, 188.

[6] a) M. Stubenhofer, G. Lassandro, G. Balázs, A. Y. Timoshkin, M. Scheer, *Chem. Comm.* **2012**, *48*, 7262; b) M. Stubenhofer, C. Kuntz, M. Bodensteiner, A. Y. Timoshkin, M. Scheer, *Organometallics* **2013**, *32*, 3521.

[7] M. Seidl, M. Schiffer, M. Bodensteiner, A. Y. Timoshkin, M. Scheer, *Chem. Eur. J.* **2013**, *19*, 13783.

[8] B. Sigwarth, U. Weber, L. Zsolnai, G. Huttner, *Chem. Ber.* **1985**, *118*, 3114.

[9] P. Pyykkö, M. Atsumi, *Chem. Eur. J* **2009**, *15*, 12770.

[10] T. V. Gryaznova, Y. G. Budnikova, O. G. Sinyashin, *Russ. J. Electrochem.* **2007**, *43*, 1151.

[11] P. Pyykkö, *J. Phys. Chem. A* **2015**, *119*, 2326.

[12] a) R. D. Riley, D. A. Dickie, M. A. Land, R. A. Kemp, C. L. B. Macdonald, U. Werner-Zwanziger, K. N. Robertson, J. A. C. Clyburne, *Chem. Eur. J* **2020**, *26*, 7711; b) D. A. Dickie, U. Chadha, R. A. Kemp, *Inorg. Chem.* **2017**, *56*, 7292; c) D. A. Dickie, R. A. Kemp, *Organometallics* **2014**, *33*, 6511; d) D. A. Dickie, E. N. Coker, R. A. Kemp, *Inorg. Chem.* **2011**, *50*, 11288.

[13] K.-C. Schwan, A. Y. Timoskin, M. Zabel, M. Scheer, *Chemistry* **2006**, *12*, 4900.

[14] M. Schiffer, B. P. Johnson, M. Scheer, *Z. anorg. allg. Chem.* **2000**, *626*, 2498.

[15] *CrysAlis Pro 171.38.46*, CrysAlis Pro Version 171.38.46, Rigaku Oxford Diffraction.

[16] G. M. Sheldrick, *Acta Crystallogr. A* **2015**, *71*, 3.

[17] G. M. Sheldrick, *Acta Crystallogr. C* **2015**, *71*, 3.

[18] O. V. Dolomanov, L. J. Bourhis, R. J. Gildea, J. A. K. Howard, H. Puschmann, *Appl. Crystallogr.* **2009**, *42*, 339.

7 SUMMARY

Low valent main group compounds in general and pnictinidene complexes in particular have been an area of focus in organometallic chemistry since the second half of the last century. This becomes apparent when looking at the state of literature as presented in the introductory chapter. A variety of different pnictinidene complexes have been synthesized, characterized and their reaction behaviors have been diligently studied over the years. However, from this diverse research, a few questions remain unanswered. This work aims to answer some of these questions and make room for future research in this field. In this chapter, the findings of this thesis are recapitulated in the same order as discussed in the main part.

7.1 The Reactivity of the Bridging Pentelidene Complexes [Cp*E{W(CO)$_5$}$_2$] (E = P, As) towards Dichalcogenides and Chalcogenols

The pnictinidene complexes [Cp*E{W(CO)$_5$}$_2$] (**1a**: E = P; **1b**: E = As) are the starting material of the synthesis of numerous compounds. In these reactions, **1a** and **1b** typically react as electrophiles and the cleavage of the Cp* substituent is often one of the important steps within the reaction pathway. Cleaving off this substituent homolytically, e.g. by irradiation, leaves an ·E{W(CO)$_5$}$_2$ radical (**E**) which, in turn, can react with other radicals such as RCh· (Ch = chalcogen atom) radicals generated from dichalcogenides R_2Ch_2. In the reactions of **1a** and **1b** with various dichalcogenides R_2Ch_2 (Ch = S, Se, Te; R = Ph, Mes, Tipp), the chalcogenopnictinidene complexes **2a**, **2b**, **3a-II** and **3b** were isolated and fully characterized. Moreover, the generation of tellurophosphinidene complexes **4a-I** and **4a-II** was observed via ^{31}P NMR spectroscopy. Additionally, reactions of **1a** and chalcogenols PhChH were carried out. Compounds **2a** and **3a-I** were obtained in these reactions and characterized as well (cf. Figure 7.1). Notably, these are the first examples of 'true' chalcogenopnictinidene complexes ever reported. Single crystal X-ray diffraction experiments show that these compounds possess shortened E-W bond lengths and a double bond character of the E-Ch bond. Lastly, DFT calculations were carried out to determine the preferred reaction pathways for the abovementioned reactions. One possible pathway for the reaction of **1a** with R_2Ch_2 is the formation of the radical intermediate **E** and RCh·, respectively, and the recombination of these radicals into the respective chalcogenophosphinidene complexes. The reaction of **1a** with PhChH likely proceeds via nucleophilic addition of the chalcogenol onto the phosphinidene complex and a subsequent Cp*H elimination as observed in various other reactions of **1a** with nucleophiles.

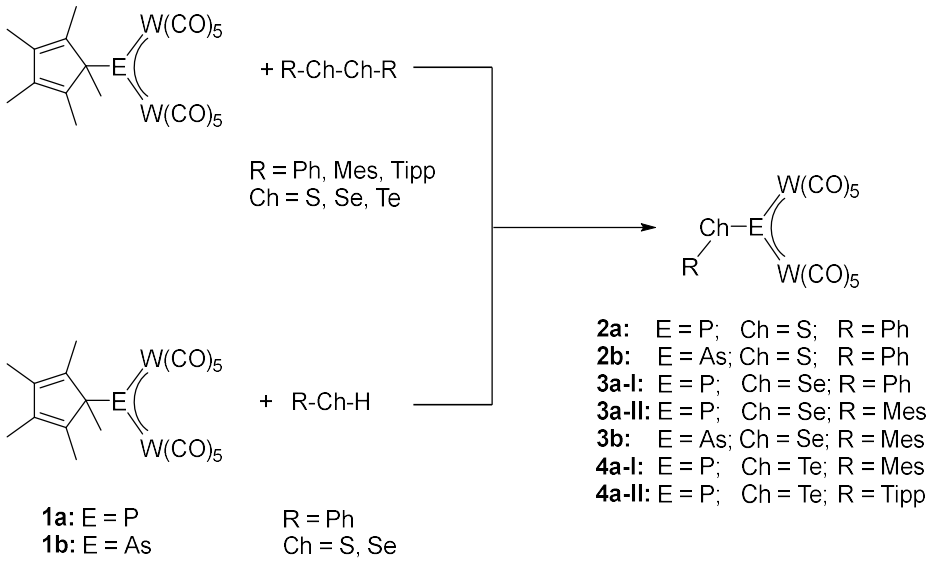

***Figure 7.1**: Reaction of **1a,b** with dichalcogenides and chalcogenols.*

7.2 The Reactivity of Bridging Aminopnictinidene Complexes of the type $[R^1R^2NE\{W(CO)_5\}_2]$ (E = P, As)

Aminopnictinidene complexes have been a subject of interest in organometallic chemistry for a long time. Their similarities as well as their slightly increased stability compared to pnictinidene complexes make them a popular research topic in organometallic chemistry. While there are numerous aminophosphinidene complexes of different types known, aminoarsinidene complexes are rare compounds. However, since this class of compounds is still difficult to isolate, sterically demanding substituents are used to increase their stability. Thus, their reaction behavior remains widely uninvestigated. As discussed in chapter 4, the aminophosphinidene complexes **2a**, **3**, **4** and **5** were synthesized in two different ways: By reaction of **1a** with the corresponding amines via Cp*H elimination and via salt elimination from the respective aminochlorophosphine and $Na_2[W_2(CO)_{10}]$ (cf. Figure 7.2). The aminoarsinidene complex **2b** was additionally synthesized via the first route, starting from **1b**. Although both synthetic routes showed promising results, higher yields were accomplished in the reaction of **1a**, **b** with amines. Notably, these compounds are substituted with alkyl groups, which are much less sterically demanding than the substituents that are typically used such as tmp (tetramethylpiperidine) or $(Me_3Si)_2N$. The reaction of **3** and **4** with $^tBuPH_2$ resulted in the formation of complex **6**, while using carbodiimides as reaction partners for **2a**, the heterocycles **7** and **8** were obtained. Both reactions show the similarity in the reaction behavior of the aminophosphinidene complexes and phosphinidene complex **1a**. Notably, because of the higher thermal stability of **2a**, less side products were obtained in the reaction with carbodiimides as opposed to using **1a** as a starting material.

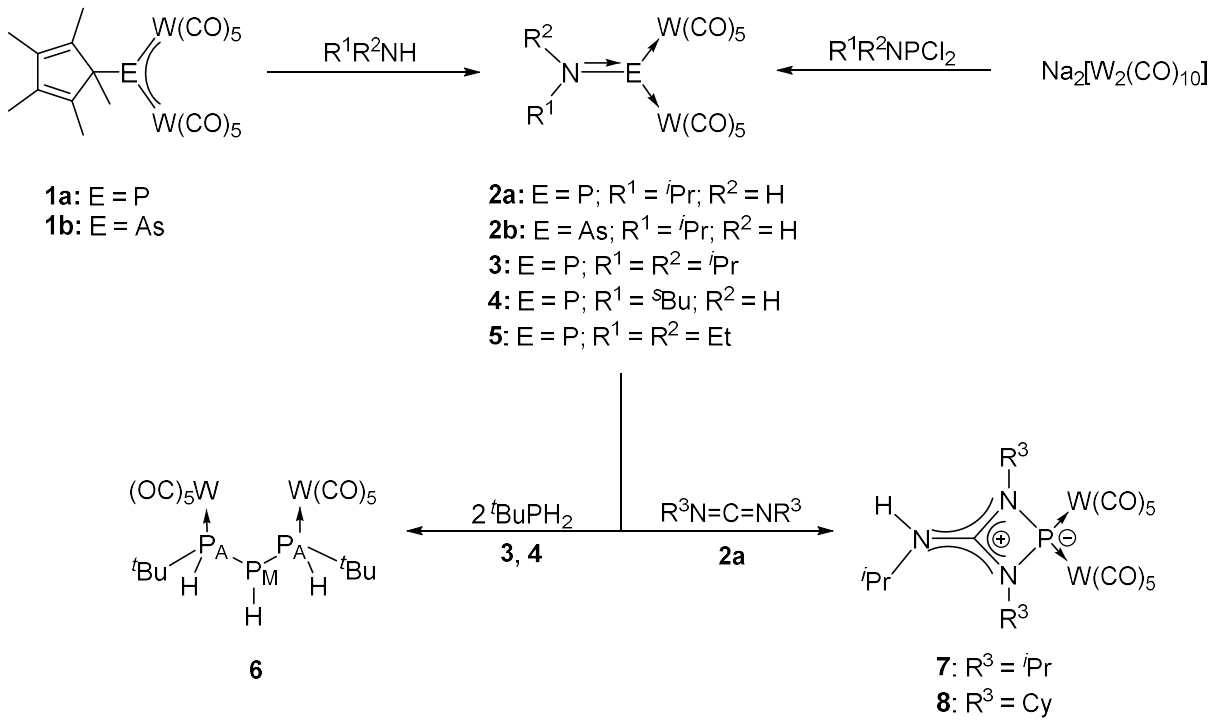

Figure 7.2: Synthesis of aminopnictinidene complexes and subsequent reactions.

7.3 Reactivity of the Bridging Stibinidene Complex [ClSb{Cr(CO)$_5$}$_2$(thf)]

Trigonal planar stibinidene complexes have been known since the late 1970s. Most of the research about these types of compounds, however, revolves around their synthesis and properties as presented in chapter 5. In this work, the reactivity of [ClSb{Cr(CO)$_5$}$_2$(thf)] (**1c**) as a representative of this class of compounds was explored.

The reaction of **1c** with two equivalents of $GaCl_3$ in *n*-pentane leads to the formation of the dimer [ClSb{Cr(CO)$_5$}$_2$]$_2$ (**2**, cf. Figure 7.3), which was isolated in 30 % crystalline yield from the solution. DFT calculations confirm the dative nature of the Cl-Sb bonds and undermine the hypothesis that **2** is consisting of two units of the stibinidene complex [ClSb{Cr(CO)$_5$}$_2$]. Using various ionic nucleophiles Nu^- (Nu = NH_2, AsH_2, PH_2, CN) as reaction partners for **1c**, the anionic chloride adduct [Cl_2Sb{Cr(CO)$_5$}$_2$]$^-$ (**3**) was obtained in all cases instead of the formation of [Cl(Nu)Sb{Cr(CO)$_5$}$_2$]$^-$. X-ray experiments reveal the molecular structure of one of these adducts, [Na@(18-crown-6)·dioxane][Cl_2Sb{Cr(CO)$_5$}$_2$], to be a one-dimensional polymer of the type [K(18-c-6)]$_n$[Cl_2Sb{Cr(CO)$_5$}$_2$]$_n$ (K = counter-ion). The reaction of **1c** with neutral nucleophiles results in the formation of adducts of the type [ClSb{Cr(CO)$_5$}$_2$Nu] (**4**: Nu = NH_2Mes, **5**: Nu = CN(dmp), **6**: Nu = PPh_3, **7**: Nu = PPh_2H; Mes = 2,4,6-triisopropylphenyl, dmp = 2,6-dimethylphenyl). These compounds have been isolated and characterized and are, with the exception of **6**, the first of their kind, while **6** was known but has not been characterized by X-ray crystallography so far. Lastly, reactions of **1c** with (Me_3Si)$_2$CHSbH_2 led to the isolation of low amounts of *d,l*-[(Me_3Si)$_2$CHSb(H){Cr(CO)$_5$}]$_2$ (**8a**) and *meso*-[(Me_3Si)$_2$CHSb(H){Cr(CO)$_5$}]$_2$ (**8b**). X-ray experiments reveal both isomers as distibanes with three different moieties (H, CH($SiMe_3$)$_2$ and Cr(CO)$_5$) bound in different positions. Unfortunately, the formation pathway for **8a** and **8b** is unknown. While in solution, all the abovementioned compounds readily decompose and are highly sensitive to air, they are stable as solids and can be stored over weeks under air, with exception of **2**.

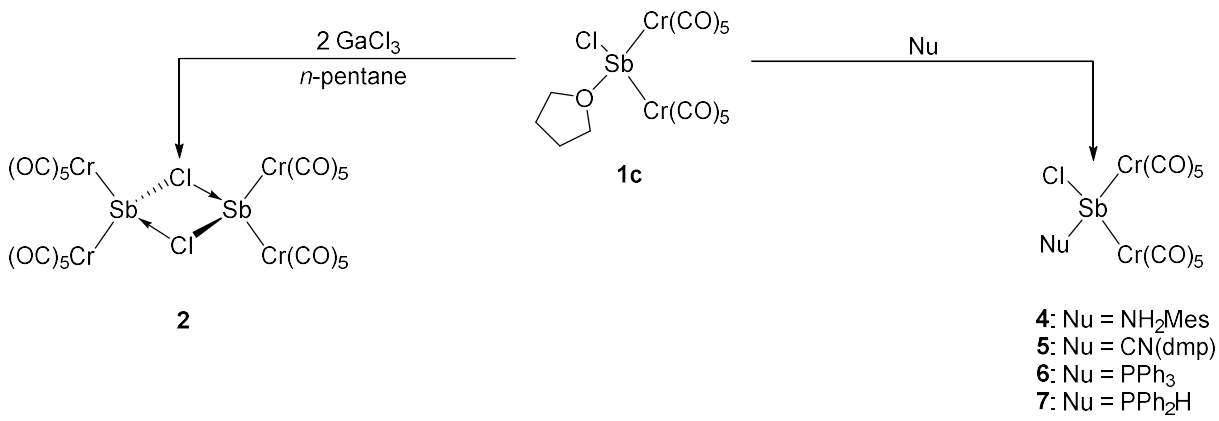

***Figure 7.3**: Reactions of **1c** with $GaCl_3$ (left) and various neutral nucleophiles (right).*

8 APPENDIX

8.1. List of abbreviations

Ar*	2,6-bis(diphenylmethyl)-4-methylphenyl
Cp	Cyclopentadienyl (C_5H_5)
Cp*	Pentamethyl-cyclopentadienyl ($C_5(CH_3)_5$)
Cp'''	1,2,4-tri-*tert*-butyl-cyclopentadienyl
Cy	Cyclohexyl ($-C_6H_{11}$)
Dipp	2,6-diisopropylphenyl
Et	Ethyl ($-CH_2CH_3$)
^{i}Pr	*iso*-propyl
Me	Methyl ($-CH_3$)
Mes*	2,4,6-tri-*tert*-butylphenyl
^{n}Bu	*neo*-butyl
NHC	N-heterocyclic carbene
Ph	Phenyl (C_6H_5)
^{t}Bu	*tert*-butyl
thf	Tetrahyrofuran (C_4H_8O)
tmp	tetramethylpiperidine

8.2. Acknowledgements

There are lots of people without whom the making of this thesis would have never been possible. I will be indefinitely grateful to my supervisor Prof. Scheer for having me in his working group and for nourishing not only my academical skills but also my personal development. Also, thank you to Gabor Balázs for writing fancy reactions on paper, being excited about NMR spectra and knowing when and how to motivate me. You are seriously the best. Another huge THANK YOU goes out to Laboropa Michael Seidl for answering all of my questions, proofreading, being critical, teaching me how to repair X-ray diffractometers, sharing some of his mad lab skills and still being the most calm and kind person. Another important person I want to mention is Michael Bodensteiner, not (only) as head of the X-ray department but also as the single person who helped me overcome lots of insecurities and recognized my talents before I did. Of course, this work would be nonexistent if it were not for all of the people who helped with analytics: Thanks to Sabine Stempfhuber and Birgit Hischa from the X-ray department, who are a great team and have been a pleasure to work and coordinate meausrements with. Fritz Kastner, Anette Schramm and Georgine Stühler for measuring lots of special NMRs, Josef Kiermaier and Wolfgang Söllner for measuring mass spectra at the speed of light and Helmut Schüller and Barbara Baumann for the elemental analyses. The glass blowing department (Markus Lindner, Carl-Heinz Hierl, Helena Ackermann) has to be mentioned, too: Thank you for the amazing work you do! I have also greatly enjoyed my time as coordinator of the Christmas experimental lecture in the JCF and want to thank everybody who helped making fire crackers and nitrocellulose and especially the people who were brave enough to be silly in front of an audience with me. These kinds of activities are the reason I got into chemistry in the first place, so I hope you guys are still paying it forward. Thank you to the current and former staff: Mina and Barbara, who are and have been doing their best to organize all of the chaos, Petra and Martina (for starting material and ratschen during the lab course), Schotti (for speeding up lab courses) and Matthias H. (for being a force of calmness). Among the members of the working group, there are some who I have formed special bonds with over the years. Vroni: Thank you for listening to all of my crazy stories, calming me down, getting snacks during long afternoons and being a great friend even though we are so different. I also want to mention my lab mates Lukas, Sophie and Lisa (for making me a lab-mom and brightening my days) and my former lab mates Rudi and Reini (for all the talks about pop culture). The 13/15-people Matthias A. aka Boi and Felix L. had to listen to me rant a lot, so thank you a lot for that (and even more for ranting with me). Also, thanks for letting me borrow your glassware and bringing mine back (mostly). All of the other former and current people of the working group I want to mention: Nase (bonsai), Robert, Felix R., Olli, Jens, Jana (all the talks), Christoph, Luis, Stephan (movie recommendations and pop culture awkwardness. Also: Memes), Martin P., Thach, Rebecca (JCF-silliness), Helena, Kevin (no hard feelings), Sabrina, Anna and Nicolò (you are two of the most amazing people, please don't ever change), Claudia, Lara, Mehdi, Julian, Maria, Moritz, Pavel and Martin W (hurz). Thank you to my friends Beate, Meike, Miri and Simone (you deserve everything!), Alex and Lukas (for studying with me for endless hours) and Domi (for enjoying the good things).

I want to genuinely thank my family for their endless love and support. Thanks to Mama and Papa for not pushing me ever and letting me be whatever I want to be. For supporting me without question and putting things into perspective. My sisters Julia and Eva for being the most selfless siblings of all time and letting me learn from their experiences. For giving advice and rooting for me and teaching me how to read - because Sailor Moon. Their partners Uli and Martin for making the family complete and my nephew Kilian for shining like the sun in a cloudy year.

Finally, I want to thank Ludwig. I cannot express how important you are to me. Without you I would have not made it through my undergrad studies and I certainly would have not been able to complete this thesis. Thank you for keeping me sane and grounded and always cheering me on. I am eternally grateful to have you in my life. This work is dedicated to you.